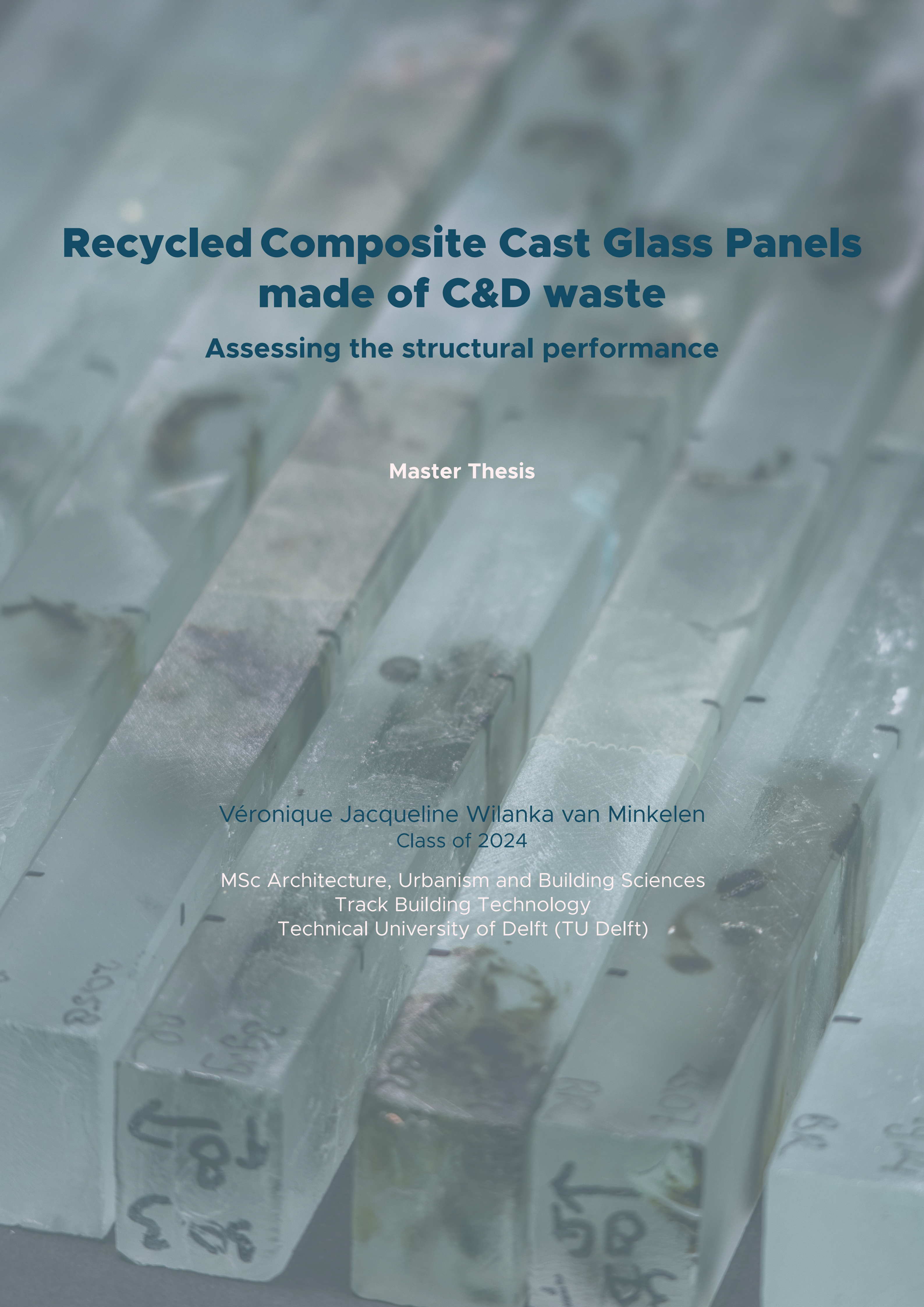

Recycled Composite Cast Glass Panels made of C&D waste

Assessing the structural performance

Master Thesis

Véronique Jacqueline Wilanka van Minkelen
Class of 2024

MSc Architecture, Urbanism and Building Sciences
Track Building Technology
Technical University of Delft (TU Delft)

Recycled Composite Cast Glass Panels made of C&D waste
Assessing the structural performance

Building Technology Graduation Project
MSc Architecture, Urbanism and Building Sciences
Technical University of Delft (TU Delft)

[Author]
Véronique Jacqueline Wilanka van Minkelen
4552156
June 16, 2024

[1st mentor]
Faidra Oikonomopoulou
Structural Design
TU Delft

[2nd mentor]
Marcel Bilow
Chair Building Product Innovation
TU Delft

TU Delft

ACKNOWLEDGEMENT

What an experience was this master's thesis! I have spent the last year writing my master's thesis, which has been the most difficult and thrilling experience I have had at TU Delft. I can say that this journey broadened my horizons as I now stand at the nexus of the architectural and engineering fields, marking the end of an intense and incredibly enriching years of the Building Technology track. I discovered how much I enjoy the circularity industry thanks to this thesis.

I wasn't sure which track I wanted to pursue for my master's degree—track Architecture or track Building Technology. I therefore choose to do both. I followed the Architecture Engineering studio after beginning with Architecture. I became interested in finding ways to incorporate more circularity into the built environment. I discovered that my passion was material science and their behaviour, particularly in terms of structural performance.

During my Building Technology Journey, I chose to join the study board, take on the role of chair of events, and get a lot of experience in event management—skills that proved to be very useful throughout the thesis. One of the hardest things to do in the lab is still managing your time.

I acquired a special set of abilities throughout the Building Track that I could apply to my thesis. For my thesis, the Glass Technology course from the first year was especially crucial. I've already learnt a little bit about the fascinating potential in the glass sector from this course.

Throughout my master's thesis research, I had a lot of assistance, direction, and support from a variety of people. First and foremost, I want to sincerely thank Faidra Oikonomopoulou and Marcel Bilow, my supervisors, for their important advice and criticism over the entire thesis process. I appreciate all of the meetings, the useful advice, and the way you always made each meeting fun. This thesis was made much more enjoyable by the two of you.

I want to sincerely thank Telesilla Bristogianni for all the guidance she provided while I was writing my thesis. I greatly appreciate your assistance in the Civil Engineering lab and in using the microscope to examine my findings. I am grateful that you allowed me to pursue my ambitious projects in the lab. I couldn't have accomplished as much without your support and guidance.

I also want to sincerely thank Fred Veer for his invaluable assistance and advice with all four of the four-point bending examinations in Mechanical Engineering. Additionally, I am deeply grateful to Menandros Ioannidis for his guidance in the Civil Engineering lab, for helping me with my first four-point bending tests, for assisting me in creating a prototype and most of all, for answering all my questions. Furthermore, I would like to thank Wilfried Damen for his help during the first four-point bending test and for his positive feedback throughout my thesis.

But without my friends' and family's support, this adventure would not have been the same. Fred and Anja, my parents, have always been interested in my thesis and have made an effort to fully comprehend it. Motivating me to work as hard as I could and taking pride in every constructive feedback session or presentation I gave.

It was a long year for me in the lab. I would want to express my gratitude to Anna, Lucy, Nils and Ramya for adding enthusiasm to those lab days. It was a long journey, but we succeeded. In addition, I want to thank my friends from JC Mazzel, for their study participation and interest in my thesis. I'd want to express my gratitude to my former roommates for their unwavering happiness and keen interest in my thesis. I would especially like to thank Iris, for all her support during this thesis time, for helping me rehearse for

my presentations, and for listening to my struggles.
Finally, I would want to express my gratitude to my BK friends: Joël, Joost, Kuba, Lotte, Lyonne and Maaike. Thank you for all your advice and for making this thesis more joyful. My BK journey would not have been the same without you guys. I am especially grateful to Lotte for her constant encouragement and for creating the most amazing pictures for my thesis research.

Thank you!

Véronique

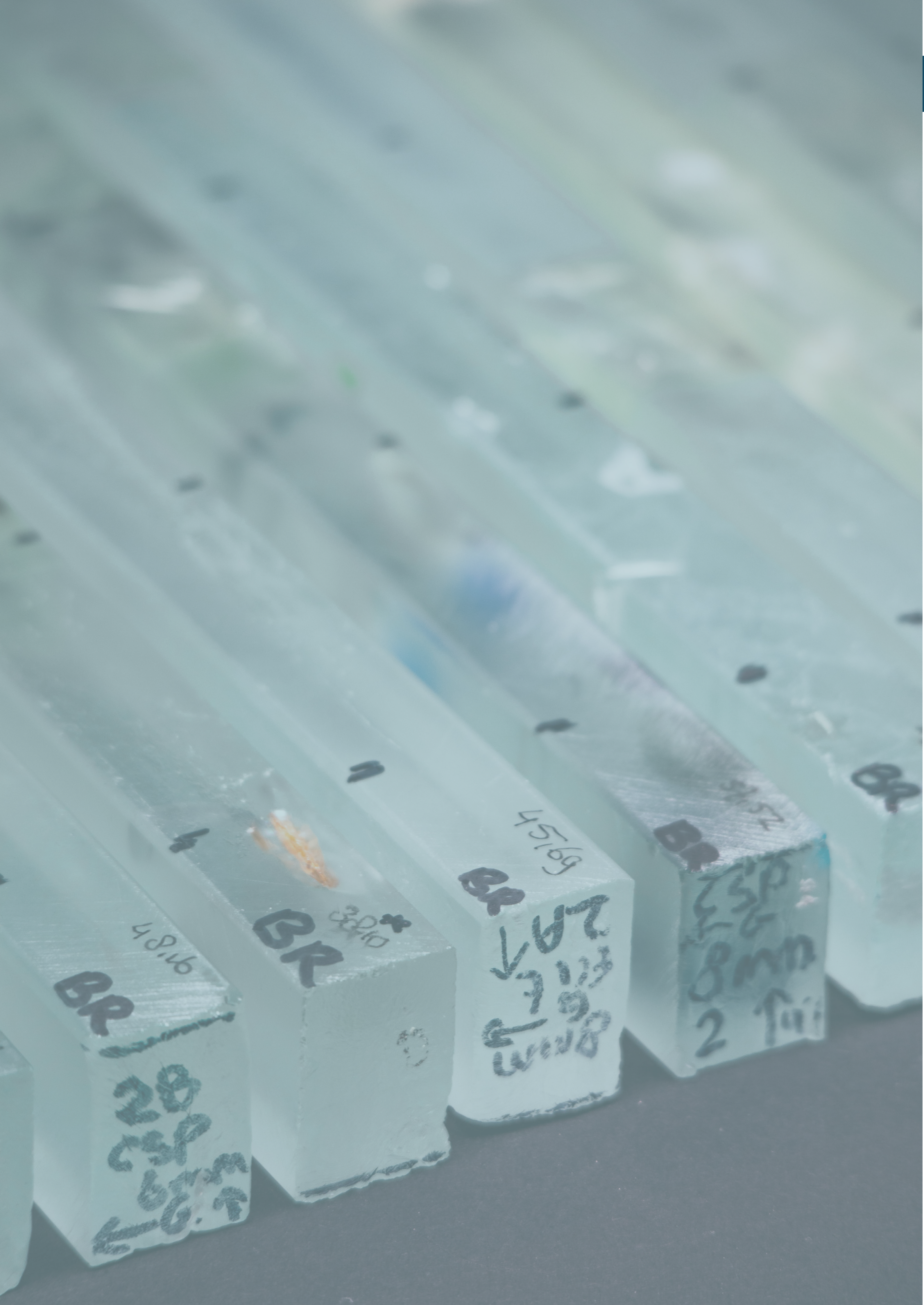

ABSTRACT

Glass is a material that is used in many different industries nowadays, including digitalisation, telecommunications, transportation, and architecture. Despite being widely used, the manufacture of flat glass presents serious environmental issues because to its energy-intensive methods, such as the Float method.

Glass recycling and reuse have been explored to mitigate these environmental impacts. Incorporating cullet, or recycled glass, into manufacturing processes has shown substantial reductions in energy consumption and CO2 emissions (Bristogianni & Oikonomopoulou, 2023a). However, challenges such as financial, infrastructural, and technical limitations hinder the increased use of cullet, especially from post-consumer sources. (Bergmann, 2020).

Creative thinking is essential to overcome these challenges. In line with the EU's zero C&D waste goals, researchers aim to maximise the use of recycled glass in building construction through experimental testing and analysis (Geboes et al, 2023). Various approaches to reusing waste glass in construction are under investigation by research organisations like Delft University of Technology (Inano et al., 2023). Methods such as casting allow for volumetric designs and can accommodate higher levels of impurities and contaminants. Since Float glass typically breaks due to surface imperfections and flaws, enhancing surface quality is crucial while the bulk can tolerate lower quality. This concept has led to the development of composite panels, where the surface contains higher purity cullet and the bulk contains lower purity cullet (Bristogianni & Oikonomopoulou, 2023a). Composite constructions enhance structural performance by integrating purer pre-consumer glass on the surface with post-consumer glass in the bulk (Matskidou, 2022).

Despite these advancements, there is still a significant gap in understanding the optimal ratio between the surface and bulk layers to achieve the best structural performance while maximising recyclability. Furthermore, the specific material compositions for both the surface and bulk layers remain unknown. Current research aims to address this gap by investigating the impact of various factors, including glass material composition and the thickness of both surface and bulk layers, on the performance of composite glass panels. (Bristogianni & Oikonomopoulou, 2023a).

Research on glass casting and recycling is essential for sustainable development since it presents viable answers to environmental problems facing the building industry. This study focuses on experimental methods that are essential to the advancement of casting and glass recycling.

The research aims to increase glass recycling operations through investigations into experimental variables using cast glass recycled beams, conducting mechanical and microscopic tests, and optimising mechanical behaviour. To better understand structural behaviour, the experimental methodology includes testing both homogeneous and composite glass beams. In order to maximise surface-to-bulk ratios, various material compositions of surface and bulk and layering techniques are investigated. Techniques for both mechanical and microscopic validation are used to assess beam performance and to understand variables affecting structural integrity.

Recycled Composite Cast Glass Panels made of C&D waste are an example of a new solution for sustainable building applications that can be produced by improving beam configurations and understanding material behaviour. This helps the building construction industry make the shift to a circular economy.

In conclusion, recycling and reusing glass are essential steps toward building a sustainable future. The industry can overcome current obstacles and maximise the potential of recycled glass to mitigate environmental impacts and promote circularity in glass production and consumption through innovative technologies and research initiatives such as recycled cast glass composites. (Oikonomopoulou et al., 2023).

Keywords:

- Glass recycling
- Casting techniques
- Composite glass beams
- Circular economy
- Innovative recycled building application

TABLE OF CONTENTS

ACKNOWLEDGEMENT **5**
ABSTRACT **7**
LIST OF ABBREVIATIONS **12**
KEY TERMS AND DEFINITIONS **13**

PART 1: INTRODUCTION TO THE RESEARCH 14

01 | INTRODUCTION TO THE RESEARCH **16**
1.1 Background 16
1.2 Problem statement 18
1.3 Research question 21
1.3.1 Main research question 21
1.3.2 Sub questions 21
1.4 Objective and boundary conditions 21
1.4.1 Boundary conditions 21
1.4.2 Design objectives 21
1.4.3 Overall goal 22
1.5 Methodology 22
1.5.1 Part 1 Introduction 22
1.5.2 Part 2 Theoretical framework 23
1.5.3 Part 3 Design and experimental validation of cast glass made of C&D waste 23
1.5.4 Part 4 Design Application 23
1.5.5 Part 5 Integrated discussion of the research results 23
1.6 Planning 23
1.7 Relation to Building Technology 23
1.8 Societal relevance and scientific relevance 24
1.8.1 Social relevance 24
1.8.2 Professional and scientific relevance 24

PART 2: THEORETICAL FRAMEWORK 26

02 | BACKGROUND OF GLASS **28**
2.1 Glass definition 28
2.2 Glass families 28
2.3 Production techniques 30
2.3.1 Glass manufacturing process overview 30
2.3.2 Float line 30
2.3.3 Annealing 32
2.3.4 Casting 33

03 | MECHANICAL BEHAVIOUR OF GLASS **36**
3.1 Structural usage of glass in buildings 36
3.2 Brittleness and fracture behaviour 36
3.3 Structural properties 37
3.3.1 The theoretical strength of glass 37
3.3.2 The flexural strength of glass 38
3.3.3 Strength of cast glass beams 38
3.4 Elastic properties 38
3.4.1 Deflection 39
3.4.2 Stress 40
3.5 Thermal properties 40
3.6 Flaw categories 40
3.6.1 Crystalline inclusions 41
3.6.2 Glassy Inhomogeneities 41
3.6.3 Gaseous Inhomogeneities 41
3.7 Increasing safety in glass 42
3.7.1 Annealed glass 43
3.7.2 Heat strenghtened glass 43
3.7.3 Tempered glass 43

04 | GLASS RECYCLING **44**
4.1 Service life & end-of-life of glass units 44
4.1.1 Service life and reasons for replacement 44
4.1.2 Environmental and economic implications 44
4.2 Glass recyclability 45
4.2.1 Necessity of glass recycling 45
4.2.2 Barriers and opportunities in glass recycling 45
4.2.3 Current status of glass recycling 46
4.2.4 End-of-life strategy 46
4.3 C&D glass waste treatment 46
4.3.1 Difficulties in C&D waste treatment 46
4.3.2 Innovations in C&D waste management 48
4.4 Cullet utilisation 49
4.4.1 Cullet definitions 49
4.4.2 Cullet classifications 49
4.4.3 Usage of cullet in glass production 51
4.4.4 Contamination problems 52

05 | TU DELFT CASTING RESEARCH **54**
5.1 Restruct cast glass 54
5.2 Innovations and challenges in glass casting 55
5.2.1 The development of glass casting processes 55
5.2.2 Barriers and opportunities in glass casting 55
5.3 Composite cast glass 57
5.3.1 Concept of composite cast glass panels 57
5.3.2 Manufacturing process 58
5.3.3 Applications and functionalities 59
5.3.4 Prior research findings 59
5.3.5 Research gap 59

PART 3: DESIGN AND EXPERIMENTAL VALIDATION OF CAST C&D WASTE 60

06 | EXPERIMENTAL METHODOLOGY **62**
6.1 Experimental variables 62
6.1.1 Literature review on recycled cast glass 62
6.1.2 Experimenting with homogeneous and composite beams 63
6.1.3 Further analysis 64
6.2 Mould preparation 66
6.3 Cullet preparation 67
6.4 Fire Rounds 68
6.4.1 Set-up of the Fire Rounds 68
6.5.2 Name of the Fire Rounds 68
6.5.3 Fire Round 1A, Homogeneous beams, behaviour of one single pollutant 69
6.5.4 Fire Round 1B, Homogeneous beams, behaviour of one single pollutant 69
6.5.5 Fire Round 1C, Homogeneous beams, behaviour of one single pollutant 70
6.5.6 Fire Round 1D, Homogeneous beams, behaviour of one single pollutant 70
6.5.7 Fire Round 2A, Composite beams, Influence of the ratio between surface and bulk 70
6.5.8 Fire Round 2B, Composite beams, Influence of the ratio between surface and bulk 72
6.5.9 Fire Round 2C, Composite beams, Influence of the ratio between surface and bulk, higher temperature 72

TABLE OF CONTENTS

6.5.10 Fire Round 2D, Composite beams, Influence of the ratio between surface and bulk 72
6.5.11 Fire Round 3A, Composite beams, Influence of the bulk material 72
6.5.12 Fire Round 4A, Composite beams, Influence of the surface material 72
6.6 Feasibility validation 74
6.6.1 Fire Round 1A, Homogeneous beams, behaviour of one single pollutant 74
6.6.2 Fire Round 1B, Homogeneous beams, behaviour of one single pollutant 76
6.6.3 Fire Round 1C, Homogeneous beams, behaviour of one single pollutant 76
6.6.4 Fire Round 1D, Homogeneous beams, behaviour of one single pollutant 76
6.6.5 Fire Round 2A, Composite beams, Influence of the ratio between surface and bulk 76
6.6.6 Fire Round 2B, Composite beams, Influence of the ratio between surface and bulk 80
6.6.7 Fire Round 2C, Composite beams, Influence of the ratio between surface and bulk,higher temperature 80
6.6.8 Fire Round 2D, Composite beams, Influence of the ratio between surface and bulk 80
6.6.9 Fire Round 3A, Composite beams, Influence of the bulk material 83
6.6.10 Fire Round 4A, Composite beams, Influence of the bulk material 83
6.7 Discussion and conclusion 86
6.7.1 Results homogeneous beams 86
6.7.2 Results composite beams- Ratios 88
6.7.3 Results composite beams- Bulk 90
6.7.4 Results composite beams- Surface 92

07 | MECHANICAL TESTS 94
7.1 Preparation for structural performance tests 94
7.1.1 Cutting of the beams 94
7.1.2 Polishing of the beams 94
7.1.3 Identifying of each beams 94
7.1.4 Four-point bending test process 95
7.1.5 Planning of the four-point bending tests 96
7.2 Four point bending test results 96
7.2.1 General overview 96
7.2.2 Structural performance- Homogeneous beams 99
7.2.3 Structural performance- Composite beams 101
7.3 Discussion and conclusion 108
7.3.1 Homogeneous beams 108
7.3.2 Composite beams 108

08 | MICROSCOPIC VALIDATION 110
8.1 Crack patterns 110
8.1.1 Theory behind cracks 110
8.1.2 Shape of the crack patterns 112
8.1.3 Origin of the fracture 113
8.2 Microscopic evaluation 113
8.2.1 Flaw types 114
8.3 Stress in flaw categories 119
8.4 Discussion and conclusion 122
8.4.1 Crack patterns 122
8.4.2 Flaw types 123

09 | MECHANICAL BEHAVIOUR OPTIMISATION 126
9.1 Influence of cullet selection 126
9.1.1 Contaminants on the cullets 126
9.1.2 Tiles with contaminants 126
9.1.3 Feasibility evaluation – Tiles 127
9.1.3 Stress in pollutants 128
9.2 Influence of a higher temperature schedule 131
9.2.1 Fire Round 2C, Composite beams, Influence of the ratio between surface and bulk, higher temperature . 131
9.2.2 Feasibility evaluation- Fire Round 2C 132
9.2.3 Structural performance- Fire Round 2C 135
9.2.4 Microscopic validation of Fire Round 2C 137
9.3 Discussion and conclusion 139

PART 4: DESIGN APPLICATION 140

10 | DESIGN APPLICATION 142
10.1 Introduction to the design application 142
10.1.1 Introduction to the case study 142
10.1.2 Introduction to the Recycled Composite Cast Glass Panels made of C&D waste 142
10.2 The design application 142
10.2.1 Design principle 142
10.2.2 Manufacturing of the panels 142
10.2.3 Aesthetics of the panels 144
10.2.4 Connections and details 144

PART 5: INTEGRATED DISCUSSION OF THE RESEARCH RESULTS 148

CONCLUSION 150
RECOMMENDATION 158
REFLECTION 160
REFERENCES 164
LIST OF FIGURES 168
LIST OF GRAPHS 174
LIST OF TABLES 176
APPENDIX A 178
A- Time planning for thesis 178
APPENDIX B 179
B- Amount of glass weight per mould 179
APPENDIX C 180
C- Overview beams with dimensions- Four point bending test I 180
C- Overview beams with dimensions- Four point bending test II 180
C- Overview beams with dimensions- Four point bending test III 182
C- Overview beams with dimensions- Four point bending test IV 182
APPENDIX D 184
D- Overview beams with photos- Four point bending test I 184
D- Overview beams with photos- Four point bending test II 188
D- Overview beams with photos- Four point bending test III 192
D- Overview beams with photos- Four point bending test IV 194
APPENDIX E 196
E- Overview beams with structural performance- Four point bending test I, II, III and and IV 196
APPENDIX F 200
F- Overview beams with failure analysis- Four point bending test I 200
F- Overview beams with failure analysis- Four point bending test II 204
F- Overview beams with failure analysis- Four point bending test III 206
F- Overview beams with failure analysis- Four point bending test IV 210
APPENDIX G 212
G- Overview beams with microscopic analysis- Four point bending test I 212
G- Overview beams with microscopic analysis- Four point bending test II 218
G- Overview beams with microscopic analysis- Four point bending test III 224
G- Overview beams with microscopic analysis- Four point bending test IV 230

LIST OF ABBREVIATIONS

Abbreviation	Definition
C&D	Construction and Demolition
CCF	Closed cavity facade
CO_2	Carbon dioxide
eq	equivalent
EU	European Union
GWP	Global Warming Potential
kg	kilogram
IGUs	Insulated Glass Units
PVB	Polyvinyl butyral
CSP	Ceramic, stones and porcelain

KEY TERMS AND DEFINITIONS

Key term	Definition
Cullet	Broken or waste glass suitable for remelting.
Recycling	The collection and often reprocessing of discarded materials for reuse. Recycled materials include those used in manufacturing processes and those used in consumer products. The recycled material is often degraded somewhat by use or processing and therefore must be converted to another purpose.
Upcycling	To process (used goods or waste material) so as to produce something that is often better than the original.
Downcycling	To process (used goods or waste material) in order to produce something of lesser quality because the original material cannot be recycled into something of the same or better quality.
Open-loop recycling	When recyclable materials are recycled and then converted into new raw materials and products.
Closed-loop recycling	Closed-loop systems are developed so that all of the materials in manufactured goods can be recycled, usually for use in the same type of product.
Flat glass	A type of glass that is produced in flat form, with smooth and parallel surfaces. It is commonly used in windows, doors, and architectural applications.
Float glass	A type of flat glass produced by floating molten glass on top of molten tin, resulting in a uniform thickness and surface.
Cast glass	Cast glass is formed by pouring molten glass into a mold and allowing it to cool and solidify. This process allows for the creation of intricate shapes and textures
Contamination	Contamination refers to the presence of unwanted or harmful substances in a material. In the context of glass, contamination can include impurities such as metals, organic compounds, or other foreign materials that affect its quality and properties.
Internal glass	Internal glass is produced inside the glass producing facility.
Pre-consumer glass	Glass waste generated during the manufacturing process. This type of glass waste is typically recycled within the manufacturing facility.
Post-consumer glass	Glass waste generated by end-users after they have served their intended purpose.
Poisson ratio	The Poisson ratio is a measure of the deformation behaviour of a material when subjected to stress. It is defined as the ratio of transverse strain to longitudinal strain in the direction of the applied force.
Flexural strength	Stress at failure in bending
Stress	The measure of an external force acting over the cross sectional area of an object. Stress has units of force per area: N/m2

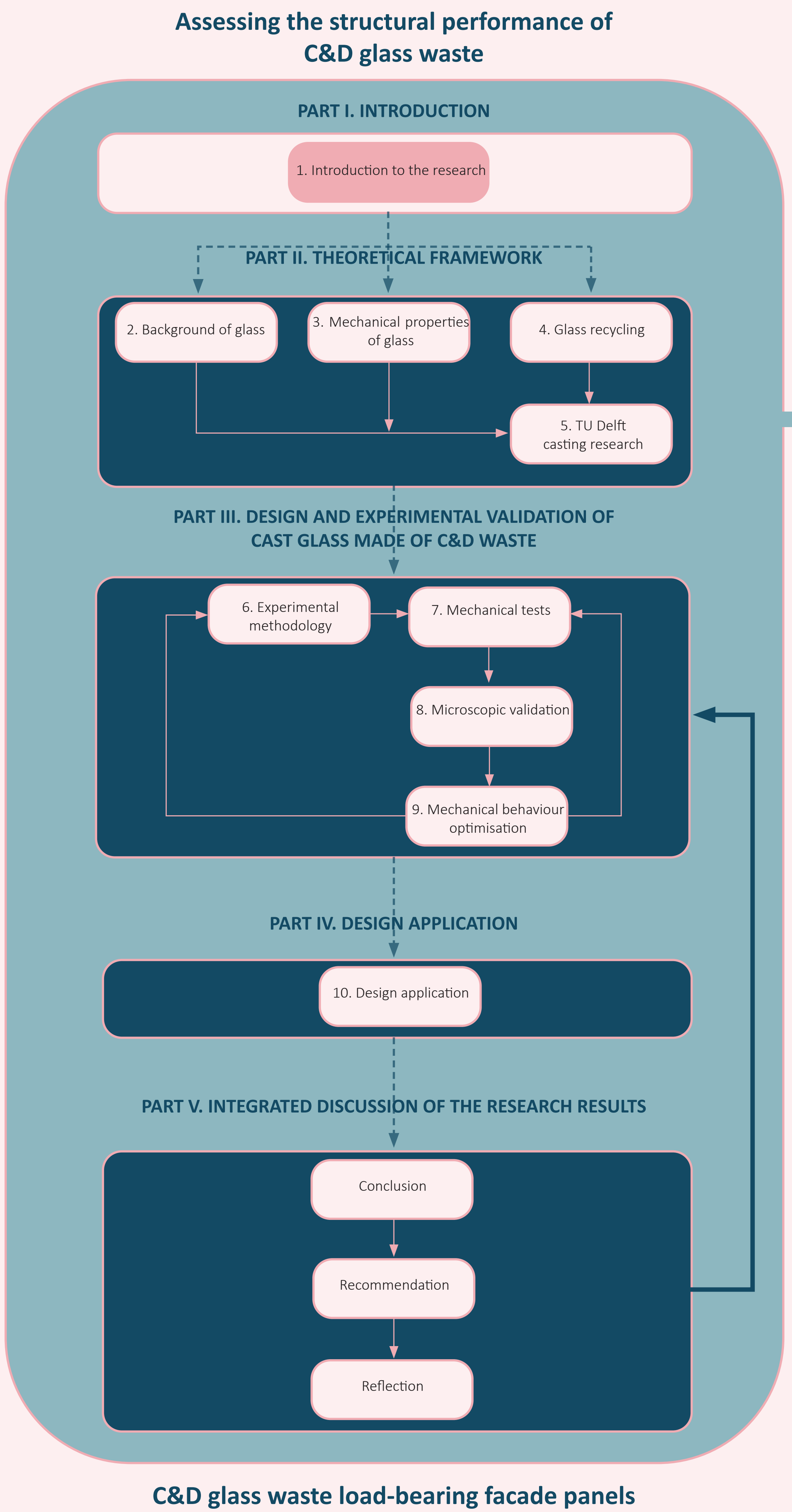

PART 1

INTRODUCTION TO THE RESEARCH

01 | INTRODUCTION TO THE RESEARCH

1.1 Background

Glass, an essential component of contemporary life, is widely used in many different industries, including digitalisation, telecommunications, transportation, and architecture. It benefits both high-tech uses and reasonably priced mass-produced goods. Designating 2022 as the 'International Year of Glass', the UN recognised the significance of glass and its role in a sustainable future (Oikonomopoulou et al, 2023).

According to Hubert (2019), in "Industrial Glass Processing and Fabrication," the output of flat glass worldwide reached 44 million tonnes in 2007, with architectural flat glass accounting for 70% of this total. Lendager and Pederson (2020) draw attention to the tendency of replacing end-of-life glazing with contemporary IGUs in order to comply with energy regulations. This has resulted in a notable rise in the amount of glass used in each window. (Geboes et al, 2023).

A GWP of 1.13 kg CO2-eq is produced during the manufacturing of flat glass, particularly through the energy-intensive Float process, which uses 1.2 kg of raw materials for every kilogramme of glass produced. The complex production process and the large supply of raw materials are to blame for this significant environmental effect. Adding cullet to the melting batch, however, greatly lessens this effect. Cullet usage maintains natural resources and lowers energy use and emissions at production facilities by saving 1.2 tonnes of raw materials and 0.3 tonnes of CO2 emissions per tonne utilised (Bristogianni & Oikonomopoulou, 2023a; Glass for Europe, 2013). Moreover, 3% less energy might be used during the melting process if 10% cullet is added (Bergmann, 2020; Geboes et al., 2023).

According to Hartwell et al. (2023), using cullet in place of all primary raw materials in the manufacture of flat glass might result in a 27% overall energy savings and a 41% decrease in emissions, from the procurement of raw materials to the manufacturing of uncoated flat glass. But at the moment, just a third of the batch used to produce flat glass is made up of secondary raw materials, mostly leftover from internal manufacturing. (Geboes et al, 2023).

Even though glass is highly recyclable, in the Netherlands, only 9.3% of collected Float glass is successfully recycled back into the original product. This draws attention to a big problem: Glass waste from consumers is still a significant problem that has to be addressed. (Vlakglas Recycling Nederland, 2022).

Glass is 100% recyclable in reality, although recycling rates are actually far lower (Figure 04). The majority of glass items, such as glass used in architecture, are either recycled or end up in landfills. In the Float glass business, closed-loop recycling is mostly restricted to pre-consumer cullet. The chances of recycling glass back into glass grow more difficult after it is sold to consumers. When a glass approaches the end of its lifespan, it usually ends up in a container (Figure 05). (Oikonomopoulou et al., 2023).

Glass companies have set goals to become carbon neutral by 2050 (Rijksoverheid, 2023a, 2023b; Schuttelaar & Partners, 2018). However, obstacles like limited infrastructure, different glass compositions, and degradation of thin-walled glass products during recycling still need to be addressed (Bristogianni &

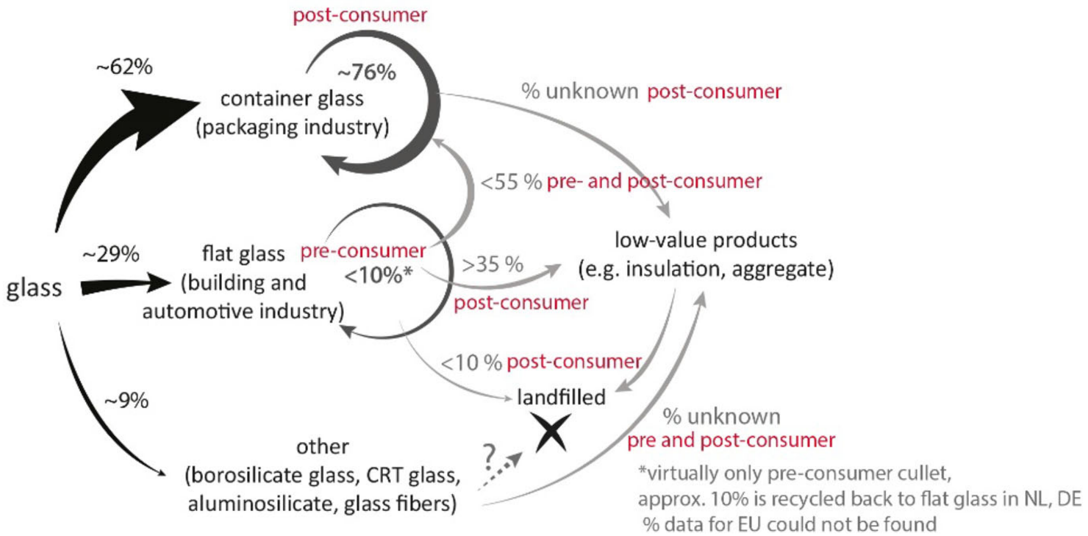

Figure 04: Illustration of the production and glass cullet in EU28 in 2017 (Bristogianni & Oikonomopoulou, 2023)


(a) (b)

Figure 05: (a), (b) Glass waste from Octatube was being placed in a container

Oikonomopoulou, 2010). It is clear that circularity is essential to the manufacture of glass. Reusing glass that has been used previously, especially if it has a good surface quality, seems like a potential (Rota et al.,2023). Investigating the world of reuse options becomes more crucial given the complex difficulties involved in recycling glass. As a result, well-known organisations like Delft University of Technology are taking action early. To determine whether various waste glass types—from borosilicate to soda-lime silica—are viable as building materials, they are closely analysing them. (Inano et al., 2023)

Glass is completely recyclable in theory, but its widespread usage for building purposes is limited by difficult disassembly processes and adhesive and coating contamination. Furthermore, most facilities only handle container glass, leaving Float glass in need of proper facilities for collection and treatment. Although glass may be recycled indefinitely in theory without losing quality, this is not always the case in practice. Recyclers mostly come from specialised businesses and only very little gets recycled. Because cast glass units can handle larger impurities and use waste glass as a raw material, they're offering a solution. (Bristogianni et al., 2019).

A interesting possibility for local recycling is casting, which enables small-scale glass casting businesses to get involved without having to make major changes to their current setup. This strategy takes care of CO2 emissions, waste collection, transportation, and related expenses. (Bristogianni & Oikonomopoulou, 2023a).

Effective recycling and reuse are severely weakened by the glass's linear lifespan, which includes difficulties with contamination and difficulties returning components to their original location. Findings by Datsiou and Overend (2017), which point to a decline in old glass's strength that is specifically connected to surface degradation, intensify this condition even more. Furthermore, studies by Rodichev and Veer (2010) and Afolabi et al. (2016) delve further into the relationship between weathering and glass strength, demonstrating a significant variation across various types of glass. While these studies provide insight into the nuance of glass degradation, differences in sample quantities and testing protocols might make direct comparisons difficult. (Rota et al, 2023).

Together, these components highlight how difficult it is to recycle and reuse glass in an effective way. This circumstance highlights the need for comprehensive strategies to address these complex issues and highlights the need for creative and comprehensive solutions in the area of glass recycling and reuse. (Bristogianni, 2022)

01 | INTRODUCTION TO THE RESEARCH

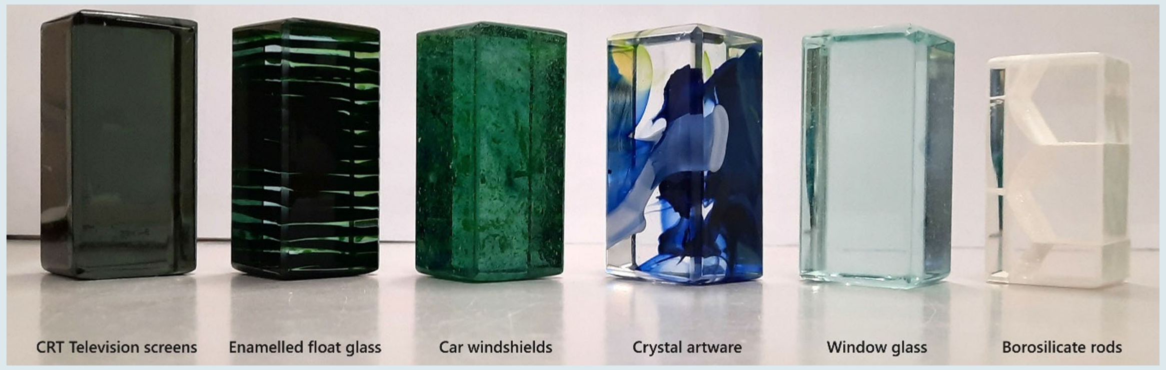

Figure 06: Wide range of kiln-cast glasses evolved from the recycling of various different glass waste streams. (Bristogianni & Oikonomopoulou, 2023)

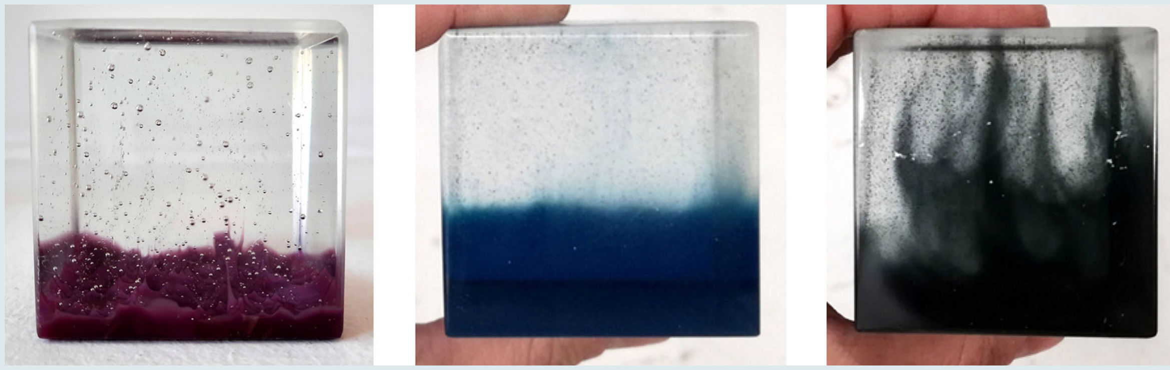

Figure 07: Composite kiln-cast components showing abrupt and gradient transitions between opaque or dark tinted and clear glass. (Bristogianni & Oikonomopoulou, 2023)

1.2 Problem statement

Building material production in the construction sector uses a lot of energy and raw materials, which has a big impact on the environment and produces a lot of CO2 emissions. According the European Commission, Graeme DeBrincat (2023) highlights the environmental and waste management problems faced by the C&D sector by pointing out that it is one of the largest and most voluminous waste streams in the EU.

In response to environmental issues, mainly the need to cut CO2 emissions, the EU is moving closer to a closed-loop economy and a zero-waste building sector. Significant legal changes are taking place in parts of Belgium, such as Flanders, with the goal of moving away from traditional waste management and towards sustainable material utilisation by 2025. According to Geboes et al. (2023), the building industry accounts for 20–30% of all waste produced in Europe, making it a key player in this transformation. In accordance to the European Commission, this change is in line with the EU's goal of becoming carbon neutral by 2050 and the European Green Deal. The significance of Bristogianni & Oikonomopoulou (2023a) and Rijksoverheid (2023a) efforts for sustainable growth in the building sector is highlighted.

Glass is becoming a crucial component in the EU's efforts to create a closed-loop economy and a zero-waste construction sector. The material's potential stems from its predicted ability to be recycled indefinitely into new glass products with no material loss and substantial energy benefits (Oikonomopoulou et al., 2023). Using cullet, or recycled glass, results in significant cost savings since less energy and raw materials are required:

- Using cullet reduces the amount of waste that accumulates and the requirement to extract new raw materials. Remarkably, 1.2 tonnes of raw materials are saved for every tonne of cullet utilised, including 850 kg of sand (DeBrincat & Babic, 2023; Surgenor et al., 2018).
- The energy consumption for glass production drops by 2.5–3% for each 10% addition of cullet incorporated into the melting batch. Additionally, the CO2 emissions associated with melting the glass are reduced by 300 kg for every tonne of cullet used (Hartwell et al, 2023).
- Because the batch is less corrosive and requires lower melting temperatures, glass melting furnace lifespans can be increased by up to 30%. This increases the furnace's durability and efficiency.

These advantages demonstrate glass's value and sustainability (Bristogianni & Oikonomopoulou, 2023a).

There are many obstacles facing the glass recycling industry today, especially in the flat glass sector that includes automotive and architectural glass. Once on the market, architectural glass is rarely recycled into other items of a comparable nature. Rather, it's frequently disposed away in a landfill or down-cycled into less valuable materials (Oikonomopoulou et al., 2023). An explanation of this problem is provided in paragraph 4.2, "Glass recyclability."

Only 10–25% of cullet, mainly internal or pre-consumer, is usually used by flat glass makers in the UK; post-consumer flat glass accounts for less than 1% of new output. Flat glass recycling needs to be free of contaminants; DeBrincat et al. (2018) and Geboes et al., (2023) have drawn attention to this difficulty, pointing out that even little amounts of contamination can result in large production losses. According to Bergmann (2020), recycling is more difficult when coatings or lamination are used, even though production waste can be readily reintroduced.

These difficulties are increased by coated glass, which is recyclable, and laminated glass, which needs the layers to be separated for recycling. As noted by Graeme DeBrincat (2023), glass is currently kept out of the recycling loop by ceramic frits. Additionally, problems with glass waste management are made worse by public ignorance of recyclable glass products.

Cullet utilisation in flat glass production is limited by technical, infrastructural, and financial constraints because just a small percentage is recycled back into the production of flat glass, suggesting a considerable gap in completing a closed-loop system. Sustainable recycling is made more difficult by the industry's unwillingness to use external, post-consumer glass cullet, primarily because of strict quality criteria. Bergmann (2020) highlights that in order to guarantee sustainability and environmental considerations from the beginning, an end-of-life strategy must be implemented throughout the product development stage.

The difficulties in recycling glass that have been brought to light underscore the need for creative, worldwide appropriate solutions that can handle compositional changes and increased contamination levels. The utilisation of glass waste as a main component for final products is essential to this. This endeavour is led by TU Delft's research on volumetric glass components cast from waste glass (Figure 06). This adaptable method works well for recycling post-consumer glass, providing thick-walled, solid, or durable components even in cases when contamination levels are higher. It uses glass that has been recycled "as-is" from consumer products, saving labour and energy in the process of treating it or removing unnecessary materials. (Bristogianni, 2022; Bristogianni & Oikonomopoulou, 2023a; Bristogianni et al., 2018).

Significant benefits of the casting technique are its adaptability, its ability to include various glass compositions, and its higher failure tolerance. The Four-point bending test is a technique used in TU Delft's research to provide a thorough understanding of the flexural behaviour of different glass specimens. It entails investigating cast glass's advantages in terms of both structure and aesthetics. Figures 06 and 07 show how it is configured. (Bristogianni et al., 2021). Although kiln-casting post-consumer glass yields lesser quality, it can be improved by using composite techniques (see "TU Delft casting research" in Chapter 5, which goes into additional depth). (Bristogianni & Oikonomopoulou, 2023a).

Matskidou (2022) suggests casting C&D glass waste into composite glass components as a way to use it. These parts are intended to be composed of a higher-quality glass surface and a core made of lower-grade post-consumer glass waste. Remarkably, there is a noticeable difference in bulk between the outside and inside of every single glass fragment. The bulk acts as a kinetic barrier to prevent crystal formation since it has a high viscosity and generally stays cooler. On the other hand, the outside heats up more quickly, which causes a decrease in viscosity that makes fusion with nearby shards easier. The observed crystallisation in these places can be explained by the fact that the reduced viscosity facilitates the production of crystals. (Bristogianni et al., 2018)

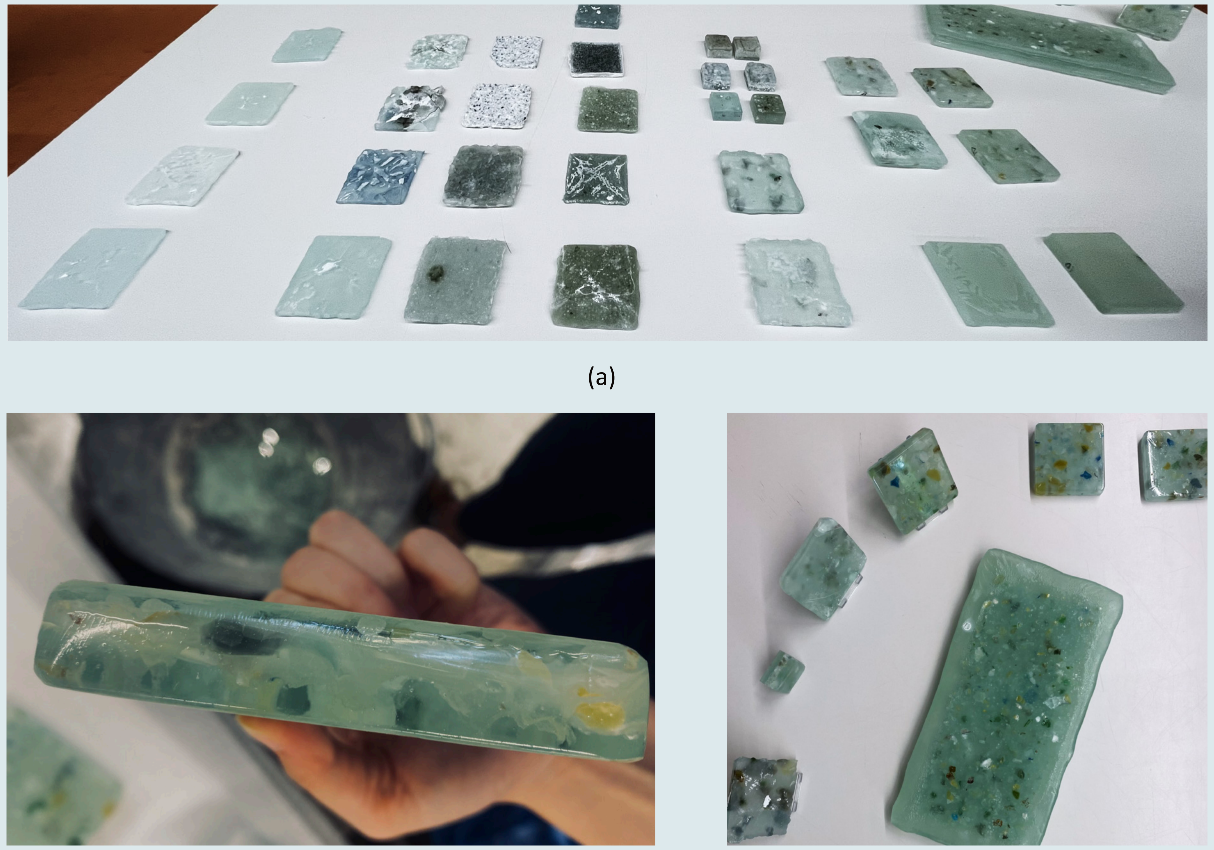

(a) (b) (c)

Figure 08: Tiles made of C&D waste during the thesis of Isidora Matskidou (Matskidou, 2022)

Shelby (2005) pointed out that glasses' fracture strengths usually fall short of their theoretical values. It is more helpful to think of fracture strength as a distribution function as opposed to a single characteristic value for a given glass composition. The primary cause of this decrease in strength is surface imperfections that seriously jeopardise the glass's integrity.

Matskidou's research (Figure 08) looks at different waste combinations, sizes and types of cullet, mould technologies, and firing schedules. According to the studies, these composite panels need impact testing is advised to learn more about their mechanical characteristics (Matskidou, 2022). While this strategy seems promising, there is still a lack of comprehensive knowledge on how it affects structural performance, especially when it comes to the geometry and the material compositions. The ratio between the surface, which has a higher purity of cullet, and the bulk, which has a lower purity of cullet, is unknown. Additionally, the material composition of both the surface material and the bulk material is unknown.

The structural performance of composite glass panels generated from C&D glass waste has been found to be poorly understood. This study attempts to fill this knowledge gap by focusing on the impact of geometrical parameters, such as layer thickness, and material compositional parameters in the core and at the surface. According to Matskidou (2022), this field is important but has not received enough attention, particularly in view of the EU's zero-waste building objectives. This study uses a Four-point bending machine for mechanical testing in an effort to improve the strength of recycled post-consumer glass that is kiln-cast. To test the structural performance, multiple cast beams of C&D waste will be produced. In order to assess the impact of these variables on the mechanical properties of the beams, the experimental approach described in Chapter 6.1: Experimental variables, will primarily focus on varying the ratio of post-consumer to pre-consumer glass and layer thicknesses. The work of Bristogianni and Oikonomopoulou (2023a) is incorporated into this study.

1.3 Research question

The primary goal of this thesis is to advance a sustainable building construction application that is in line with the EU's circular economy and zero waste aims. This study intends to investigate the feasibility and effectiveness of implementing C&D waste glass in the manufacturing of structural glass panels (to test the structural performance, beams will be used) given the underutilised potential of recycled glass, especially from flat glass used in building. In order to comply with the circularity requirements of the EU and aid in the decrease of CO2 emissions and energy usage, the following research issue will be investigated in this study:

1.3.1 Main research question

"What is the effect of the different parameters in respect to the geometry and glass composition of composite cast glass beams to their overall structural performance made out of C&D flat glass waste?"

Sub-questions that explore into the different aspects of recycling flat glass for building construction usage will be investigated in order to fully address the thesis's main research question:

1.3.2 Sub questions

1. What are the main practical implications and limitations of recycling C&D glass elements?
2. How can casting be utilised in the manufacturing of glass panels for built environment applications, specifically in transforming C&D glass waste into reusable cast glass products for facade envelopes, and what are the advantages and limitations of this method?
3. Which glass composition family group is the most promising in the creation of recycled glass beams?
4. How does a composite C&D beam compare with a homogeneous C&D beam of similar external glass quality in terms of structural performance?
5. How do variations in geometrical parameters, specifically the surface-bulk thickness, affect the structural performance of recycled composite C&D cast beams?
6. How does temperature affect the homogeneity and structure of the composite panel, particularly regarding the viscosity of molten glass, the cooling process, and the annealing schedule?
7. How do different flaws/defects in glass, such as inclusions, crystallization, infolds and machining manifest in the beams created from recycled glass, and how do they impact the structural performance?
8. What information does the crack pattern provide about the properties of the glass beam?
9. How can recycled C&D waste beams be optimised using experimental research?
10. Is there an optimum balance between class B and C waste for achieving structural performance while maximising material recyclability?
11. How should a created panel be reintegrated into the building market after its production from recycled materials?

The purpose of these sub questions is to provide insight into the complicated workings of glass recycling in the building industry with a focus on structural, practical, and environmental factors.

1.4 Objective and boundary conditions

1.4.1 Boundary conditions

This thesis examines the structural performance of a novel recycled cast glass panel that is made entirely of C&D (float) glass waste and is designed to be used in load-bearing façades. The main goal of this research is to make closed-loop recycling possible. The study will take place at the Stevin Lab II glass lab facilities, where many C&D (float) glass waste beams will be produced and put through a series of tests in order to assess structural performance criteria.

1.4.2 Design objectives

- Creation of recycled glass panel:
  - Focusing on the possibility of closed-loop recycling, develop and produce recycled cast glass beams from C&D (float) glass waste.
- Testing parameters:
  - Perform comprehensive Four-point bending tests on the produced C&D glass cast beams in order to:
    1. Evaluate the structural equilibrium between minimising material degrading to landfills and performance.
    2. Examine the differences in structural performance between a homogeneous cast beam and a composite beam.

3. Examine the effects of changing geometrical parameters between the different glass grades (B and C) in the composite beam, such as the bulk-surface ratio.
4. Assess how the structural integrity of the recycled glass material is affected by intrinsic flaws.
5. Examine how the structural performance is affected by a different temperature schedule.

- Integration of class C cullet:
    - Examine the feasibility and advantages of incorporating larger amounts of class C cullets into newly manufactured cast glass panels in order to support a more circular economy in glass recycling methods.
- Mechanical and microscopic evaluation:
    - Examine structural variations using a four-point bending machine to understand the structural performance differences between beams of homogeneous and composite cast glass, and then subject them to the cast glass at a microscopic level.

1.4.3 Overall goal

This study's main goals are to identify the mechanical and microscopic differences in structural behaviour and to thoroughly assess how composite cast glass beams affect structural performance. The goal of this research is to promote a more sustainable and circular economy in (float) glass recycling procedures while offering insights into how to improve the acceptability of recycled cast glass panels for loadbearing façade applications.

1.5 Methodology

In order to accomplish its main goals and respond to the research questions identified, this thesis uses a mixed-methods methodology. The approach is divided into five main stages, each of which is vital to the direction of the investigation. The coming sections go into detail about these stages. In addition, the overall research framework is depicted in Figure 10.

1.5.1 Part 1 Introduction

An thorough summary of the research is given in this part, starting with the background information on glass recycling. It presents the problem statement, emphasising the obstacles that still need to be overcome before glass may be fully recycled. This is used to identify the research gap, which then helps to formulate the main research question and any related sub-questions. After that, the study's goals and limitations are outlined. A thorough description of the technique that outlines the sequential processes needed for the research follows here. This is followed by an overview on how the research is planned. The study's societal and scientific importance is finally discussed.

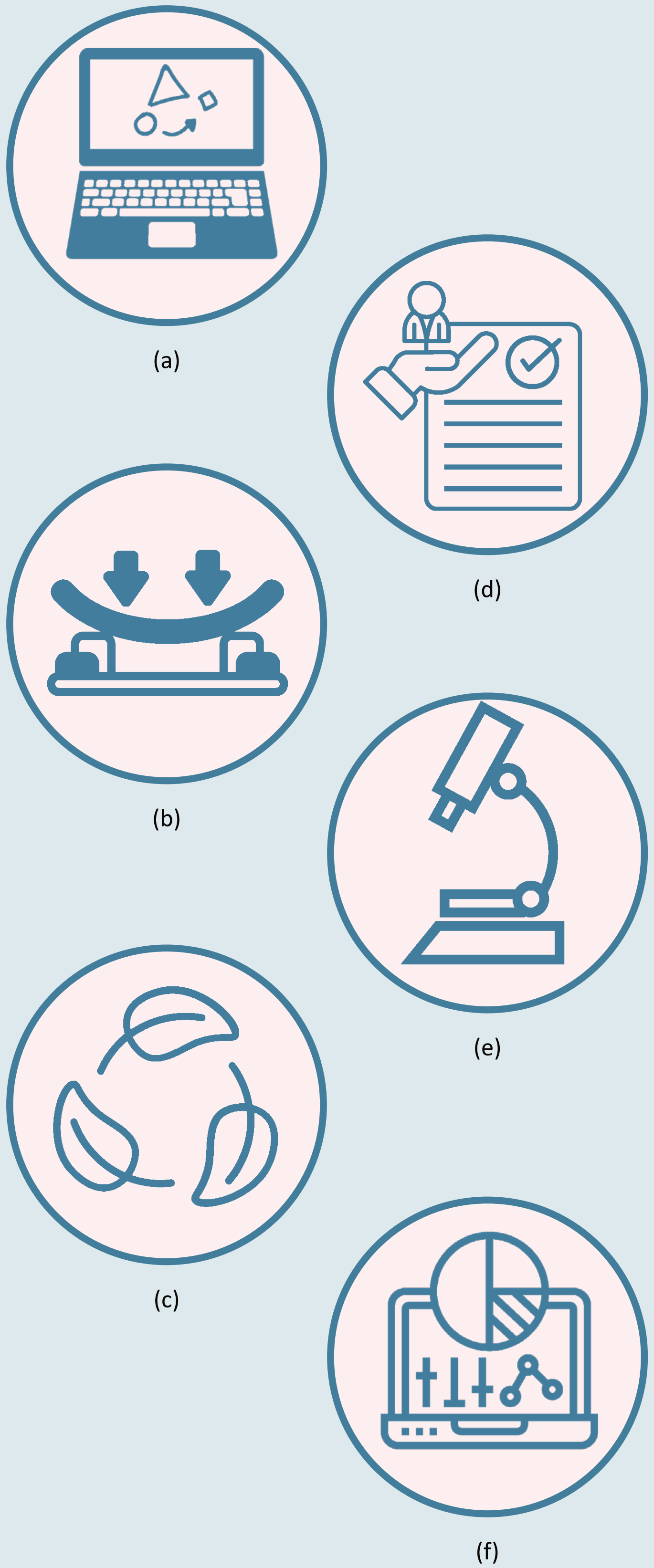

Figure 09: Design objectives: (a) creation of recycled glass panel, (b) Four-point bending tests on the manufactured C&D glass cast beams, (c) contributing to a more circular economy in glass recycling practices, (d) mechanical evaluation of the bending strength, (e) microscopic evaluation and (f) Overall goal, optimisation of the structural performance.

1.5.2 Part 2 Theoretical framework

A thorough explanation of glass is given in this part, covering its common types, behaviours, and manufacturing techniques. After that, the topic of glass's mechanical characteristics is covered. The discussion next turns to the glass units' service life and end-of-life issues, and then it looks into the possibility of recycling glass. After highlighting the situation of glass recycling at the moment, the treatment procedures for C&D glass waste are looked at. There is additional information on the uses and possibilities of glass cullet.

This section's last chapter examines how casting techniques might improve glass's capacity to be recycled. This contains a summary of the casting projects that TU Delft has completed thus far. The benefits of use casting to recycle C&D glass waste are then discussed. The potential of composite cast glass is finally highlighted, underscoring its importance in relation to glass recycling.

1.5.3 Part 3 Design and experimental validation of cast glass made of C&D waste

The experimental methodology is presented in this section, along with a thorough explanation of the variables used in the study, the fabrication of the moulds and usage of the cullets, fire round schedules, and the protocols used in the Stevin Lab II glass lab facilities. Class B and C cullets, each containing specific pollutants, are used in the research. The paper will go into further detail about these classes' distinctions later on.

The process involves producing the required prototypes and assessing the beams according to structural feasibility standards such compatibility, transparency, and absence of visible fractures. It should be mentioned that the beams' results are unpredictable; therefore, depending on the oven's output, the feasibility standards could need to be adjusted. The study then involves mechanical testing of the beams using a four-point bending machine and data analysis. The study also includes microscopic analysis of beam cracks to identify material impurities.

This section will conclude with an explanation of an experimental study that aims to optimise the mechanical behaviour of glass waste beams through a combination of prior findings and experimental work. The material type, the temperature schedule, and the ratio of surface to bulk material are the main optimisation factors.

1.5.4 Part 4 Design Application

This section examines the potential uses of cast glazed panels made from C&D glass cullet. Connection details are explained to showcase the simplicity of integrating this system. Case studies using plastic panels and concrete panels are included to demonstrate how these new cast glass panels can be used. The importance of recycled cast glass panels will also be elaborated upon.

1.5.5 Part 5 Integrated discussion of the research results

An in-depth evaluation of the study and experimentation is provided in the last part. It contains the study's conclusions, thoughts on the design and manufacture of recycled glass panels cast from recycled glass, and an evaluation of the structural performance. There are suggestions for more research at the end of this section.

1.6 Planning

Table 01 provides a detailed overview of this thesis's planning, which is systematically divided into the same five parts as outlined in the methodology section. Table 01 can be found at Appendix A.

1.7 Relation to Building Technology

The MSc AUBS program's Building Technology Master track combines engineering and architectural design to address interdisciplinary problems and promote creative solutions. Its concentration is on a broad variety of technical and architectural skills that are essential for the development of innovative and sustainable building components that are incorporated into the built environment, as well as future sustainable design practices.

In this thesis, façade, product, and structural design are integrated with building technology. With a focus on circular building products, the goal is to do to a material research and to produce a novel building envelope and project.

By lowering waste and CO2 emissions, the study intends to investigate how cast glass made of C&D waste could support sustainable development. Studying

01 | INTRODUCTION TO THE RESEARCH

glass's mechanical characteristics, examining (float) glass recycling procedures, carrying out independent experimental research, and improving techniques through mechanical testing are all part of this. The objective is to create a closed-loop recycling system, develop recycled cast glass panels from C&D glass waste, and assess the panels' suitability for load-bearing façade applications by researching the structural performance of the cast C&D waste beams.

In order to maximise structural performance and minimise materials that end up in landfills, the study involves the production and optimisation of multiple cast beams created from C&D debris, with a preference for constructing a closed-loop system.

1.8 Societal relevance and scientific relevance

1.8.1 Social relevance

Glass's expanding social significance is reflected in the structural designs that use it more and more. Glass was formerly thought to be brittle and opaque, but thanks to its special combination of transparency and high compressive strength, it has become a material that is optically clear, and strong in structure. This development emphasises glass as a pioneering material in the construction sector and signals a dramatic change in architectural and structural applications. It is the perfect material to use for making translucent structural elements because of its capacity to promote light transmittance. Compared to other materials, glass is relatively new in structural contexts, yet it provides revolutionary possibilities that could completely change how the building industry, architectural engineering, and structural engineering approach their work in the future.

1.8.2 Professional and scientific relevance

One of the biggest problems nowadays is glass waste, especially Float glass from the C&D industry. Glass cullet frequently ends its career in landfills because to a lack of an efficient recycling mechanism for this kind of waste, which is intensified by quality standard failures brought on by contamination from coatings, lamination, adhesives, or recipe incompatibilities. Because it investigates the possibility of recycling C&D glass, this study has a great deal of scientific value. This thesis attempts to increase trust among engineers, architects, designers, and the general public in both cast glass as a structural material and glass casting as a feasible production technology by examining the viability of employing cast glass in architectural applications. The study offers crucial information that can direct the industry in the recycling-by-casting process, such as the kinds of waste glass that can be used, the amounts to be used, and the required fire schedules. Additionally, TU Delft's research on waste streams and the potential for (float) flat glass recycling emphasises the need for more investigation in this field, especially with regard to the repurposing of Float glass waste in structural cast glass applications, about which there is currently an absence of thorough information.

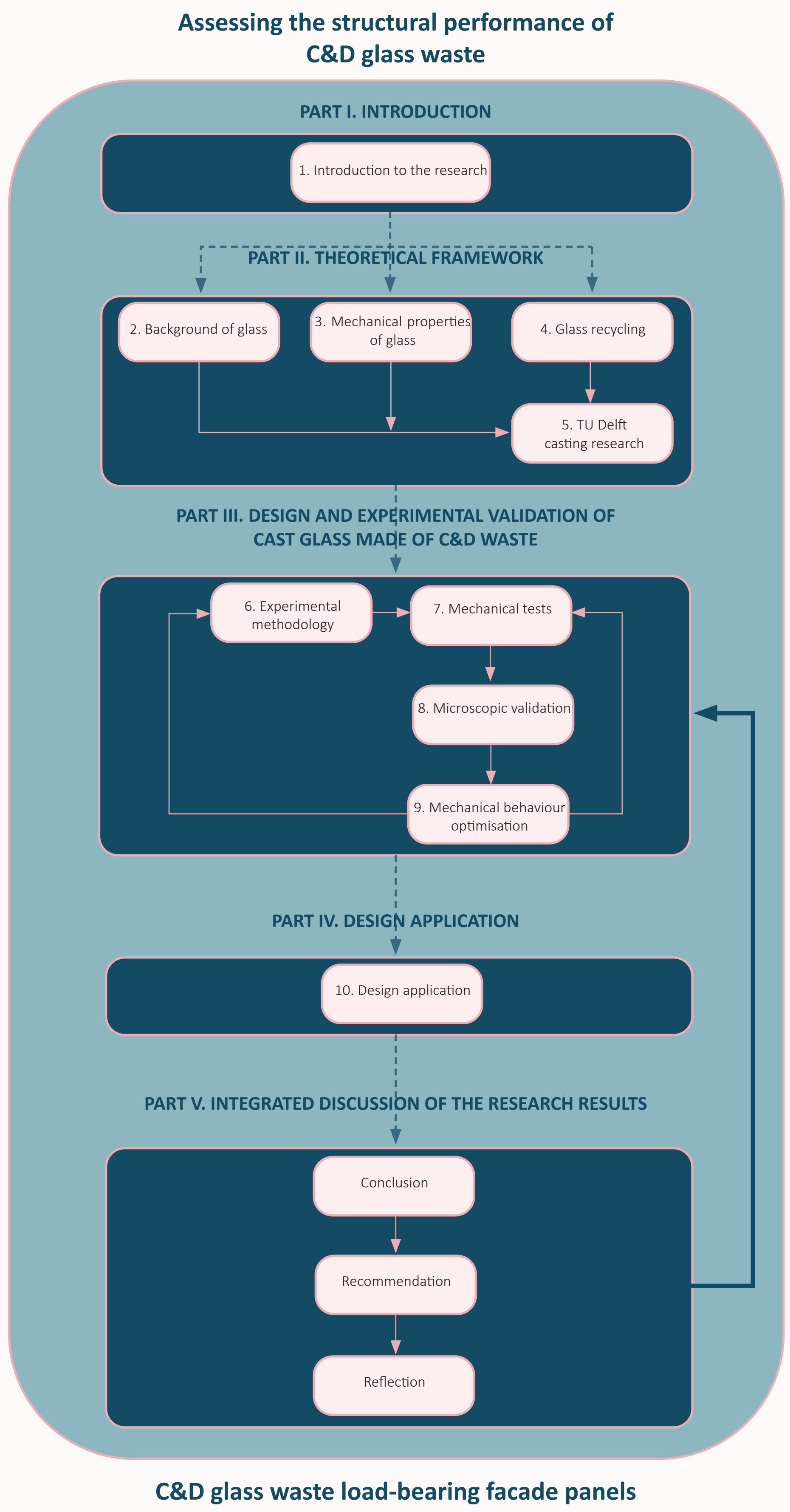

Figure 10: Illustration of the research framework, the framework is devided into 5 parts

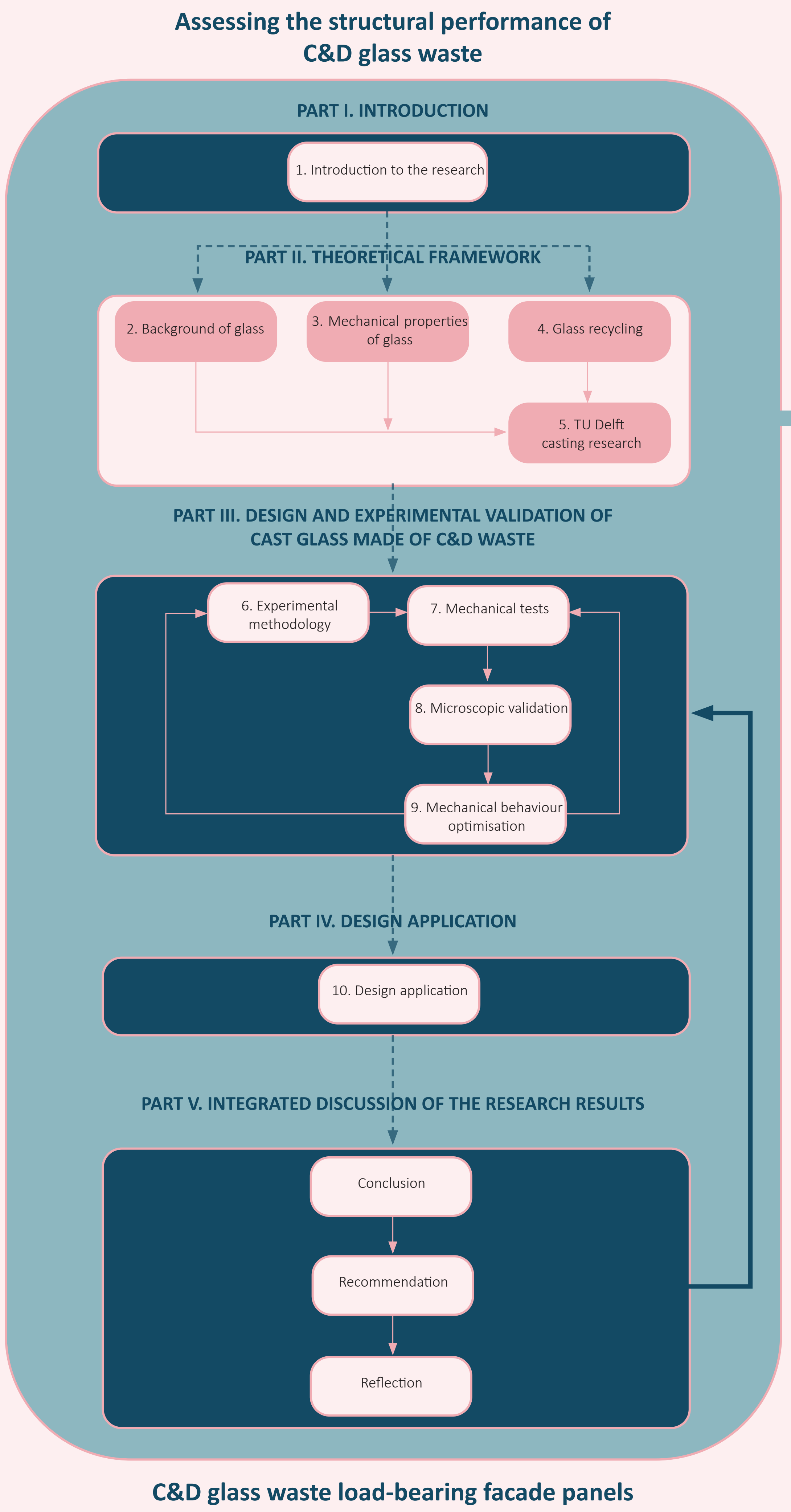

PART 2

THEORETICAL FRAMEWORK

02 | BACKGROUND OF GLASS

2.1 Glass definition

Glass is a material that we use on a daily basis and is present in many facets of our life. Glass is everywhere: in our buildings' windows, in the glasses we drink from, and in the oven doors we look through while our food cooks. Its growing use in a variety of disciplines emphasises how important technology is to modern life. However, what exactly is glass?

According to Shelby, there are two basic characteristics shared by all known glasses. First off, none exhibit a constant, organised atomic structure. Second, as Graph 01 (2005) illustrates, all varieties of glass exhibit time-dependent changes. These changes usually occur within a temperature range referred to as the glass transformation zone.

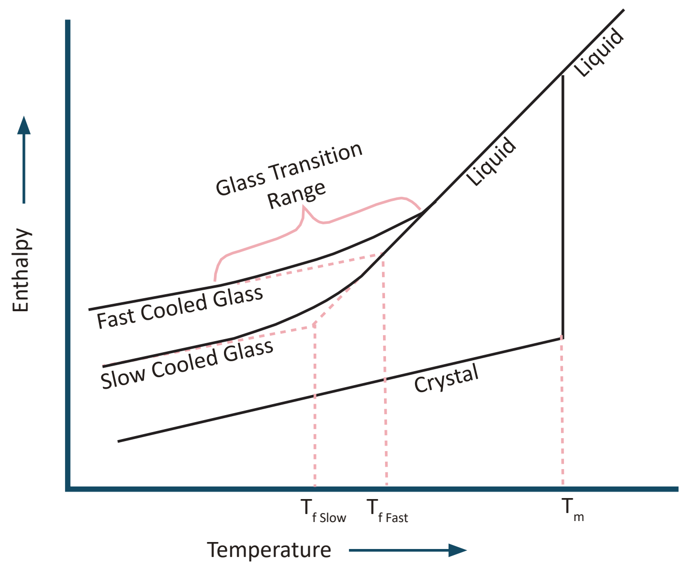

Graph 01: Effect of temperature on the enthalpy of glass forming melt (Shelby, 2005)

According to scientific definitions, glass is an inorganic solid substance that is characterised by hardness, brittleness, transparency or translucence, and resistance to environmental factors. It is created by quickly cooling molten substances, such as silica sand, so that no visible crystals can form (Britannica, 2023). Silicon dioxide (SiO_2), or silica, is a common element in nature and the foundation of most commercially significant glasses. It is particularly found in quartz and beach sands. Vitreous silica or silica glass is made entirely of silica. On the other hand, the commonly used "soda-lime" glasses are mostly made of lime (calcium oxide, CaO) and soda (sodium oxide, Na_2O).

According to Varshneya (2016), glass is a solid material with a liquid atomic structure. This is the understanding

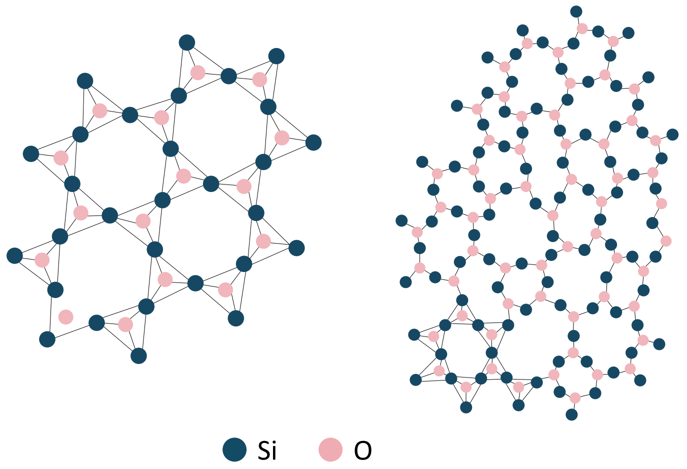

Figure 11: Two molecule structures, left Crystalline SiO_2 (Quartz), right Amorphous SiO_2 (Glass) (Ortiz, 2007)

of modern science. Structured solids called crystals are made up of molecules arranged in a repeating organised pattern. Glasses, on the other hand, are amorphous, or extremely disorganised materials that lack long-range molecular organisation (Ortiz, 2007). Figure 11 provides an illustration of this variation.

Glass's atomic structure and chemical composition greatly influence its characteristics, with the exception of its solid state's elastic and strength behaviour (Varshneya, 2016). A few essential elements are vital to the production of glass. The quality of glass can be drastically changed by contamination, either during the melting process or from the materials used. The homogeneity and internal tension of the glass are influenced by the thermal history, specifically the firing schedule. The final qualities of the glass are also influenced by the casting process. (Bristogianni, 2022).

2.2 Glass families

Every type of glass is a member of a particular family with distinctive compositions, each having advantages and limitations specific to the purposes for which it is designed. The six primary families of commercial glass are: 96% silicate, soda-lime, borosilicate, lead, aluminosilicate, and fused silica (quartz) glass. Oikonomopoulou (2019) goes into detail on this classification.

The chemical composition of glass affects its properties. In its purest form, glass is made up of a molecular structure made completely of silica oxide. Its attributes can change when further elements are added. Temperature-related characteristics such as viscosity, thermal expansion, and operating temperature are significantly influenced by composition (Oikonomopoulou, 2019).

Among them, automated blown, mouth-blown, and Float glass are the three divisions based on the manufacturing process for soda-lime silica glass, which is particularly used in the building industry. According to Bristogianni (2022), these subdivisions are essential since the production process has a big impact on the basic soda-lime silica composition.

Table 02 illustrates that soda-lime glass is the most cost-efficient option and that it is frequently utilised in the building industry because of its affordability and durability. However, borosilicate glass, which has at least 5% boric oxide, shows less thermal expansion, improving its resistance to thermal shock and requiring less time to anneal (Oikonomopoulou, 2019). A thorough summary of the physical characteristics of the materials mentioned in Table 02 is given in Table 03. But soda lime needs a longer annealing period than other glass compositions, such as borosilicate glass, and is less able to withstand rapid temperature swings that could result in thermal shock.

Because soda-lime silica glass is widely used in the building industry and is reasonably priced, it was chosen for prototype manufacture in this study. It is utilised in C&D waste. Soda-lime glass is more cost-effective than borosilicate glass because it has a lower melting point, which lowers production energy costs, as well as higher demand and greater availability (Oikonomopoulou, 2019). Furthermore, it is possible to forecast the mechanical, optical, and thermal properties of the finished goods using the information in Table 03 (Bristogianni, 2022).

Glass type	Approximate Composition	Observations	Typical applications
Soda-lime (window glass)	73% SiO_2 17% Na_2O 5% CaO 4% MgO 1% Al_2O_3	Durable. Least expensive type of glass. Poor thermal resistance. Poor resistance to strong alkalis e.g. wet cement)	Window panes Bottles Façade glass
Borosilicate	80% SiO_2 13% B_2O_3 4% Na_2O 2.3% Al_2O_3 0.1% K_2O	Good thermal shock and chemical resistance. More expensive than sodalime and lead glass.	Laboratory glassware Household ovenware Lightbulbs Telescope mirrors
Lead silicate	63% SiO_2 21% PbO 7.6% Na_2O 6% K_2O 0.3% CaO 0.2% MgO 0.2% B_2O_3 0.6% Al_2O_3	Second least expensive type of glass. Softer glass compared to other types. Easy to cold-work. Poor thermal properties. Good electrical insulating properties.	Artistic ware Neon-sign tubes TV screens (CRT) Absorption of X-rays (when PbO % is high)
Aluminosilicate	57% SiO_2 20.5% Al_2O_3 12% MgO 1% Na_2O 5.5% CaO	Very good thermal shock and chemical resistance. High manufacturing cost.	Mobile phone screens Fiber glass High temperature thermometers Combustion tubes
Fused-silica	99.5% SiO_2	Highest thermal shock and chemical resistance. Comparatively high melting point. Difficult to work with. High production cost.	Outer windows on space vehicles Telescope mirrors
96% silica	96% SiO_2 3% B_2O_3	Very good thermal shock and chemical resistance. Meticulous manufacturing process and high production cost.	Very good thermal shock and chemical resistance. Meticulous manufacturing process and high production cost.

Table 02: Approximate chemical compositions and typical applications of the different glass types (Shand,Armistead 1958; Oikonomopoulou, 2019)

02 | BACKGROUND OF GLASS

Glass type	Mean melting Point at 10 Pa.s*	Softening Point	Annealing Point	Strain Point	Density	Coefficient of Expansion 0°C - 300°C	Young's Modulus 0°C - 300°C
	[°C]	[°C]	[°C]	[°C]	Kg/m³	10^{-6}/°C	[°C]
Soda-lime (window glass)	1350-1400	730	548	505	2460	8.5	69
Borosilicate	1450-1550	780	525	480	2230	3.4	63
Lead silicate	1200-1300	626	435	395	2850	9.1	62
Aluminosilicate	1500-1600	915	715	670	2530	4.2	87
Fused-silica	>>2000	1667	1140	1070	2200	0.55	69
96% silica	>>2000	1500	910	820	2180	0.8	67

Table 03: Approximate properties of the different glass types of Table 02 based on (Shand, Armistead 1958)*. Mean Melting Point at 10 Pa.s as stated by (Martlew 2005).

*These values are only given as a guideline of the differences between the various glass types. In practice, for each glass type there are numerous of different recipes resulting into different properties.

2.3 Production techniques

Nowadays, there are many different ways to produce glass, each suited to a particular purpose depending on the intended use, ideal shape, and raw material composition. Drawing, blowing, pressing, floating, casting, and extraction are some of these techniques. Various combinations of these techniques can give the finished glass product unique qualities. The two biggest segments of the global glass industry, accounting for roughly 45–50% and 30% of the weight produced, respectively, are container and flat glass (Hubert, 2019).

2.3.1 Glass manufacturing process overview

The selection and preparation of raw materials, batch preparation, melting, batch to melt conversion, fining of the melt, conditioning, shaping, annealing, and post-processing including inspection are some of the crucial phases in the manufacturing of glass (Hubert, 2019). The process of batching includes choosing the raw materials, figuring out how much of each ingredient to use, weighing, blending, and occasionally adding liquids. In batch melting, the raw components are broken down to start the melting process, and the temperature and air quality are controlled during the liquid formation process (Shelby, 2005).

Glass can be formed into solid, extruded, or flat parts for use in the construction sector. Of these techniques, Float glass (to create flat glass) is the most widely used in the construction sector, and 3D printing is an emerging technique in the context of research (Oikonomopoulou, 2019). An overview of several glass production techniques is shown in Figure 12, along with information on the processing steps and the products that can be made with these procedures.

Products go through an automated quality inspection process at the end of the glass production line. Currently, 15% or more of flat glass could be found to be deficient, mostly because of intolerable optical flaws. These broken glass fragments, also known as internal cullet, may be recycled and used to make new glass products (Hartwell et al., 2022).

2.3.2 Float line

Float glass production technique

Over 90% of flat glass produced worldwide is currently produced using the Float glass method, a revolutionary invention by Pilkington Brothers in 1959. This process is highly regarded because to its affordability, capacity to create glass with exceptional optical quality, ability to make big panels, and general accessibility (Luible et al., 2008). A thorough description of the 'Floating' production method is shown in Figure 13. This diagram shows in detail how molten glass is formed into flat sheets by floating it on top of a bed of molten tin. This process is known for yielding smooth, even sheets of glass.

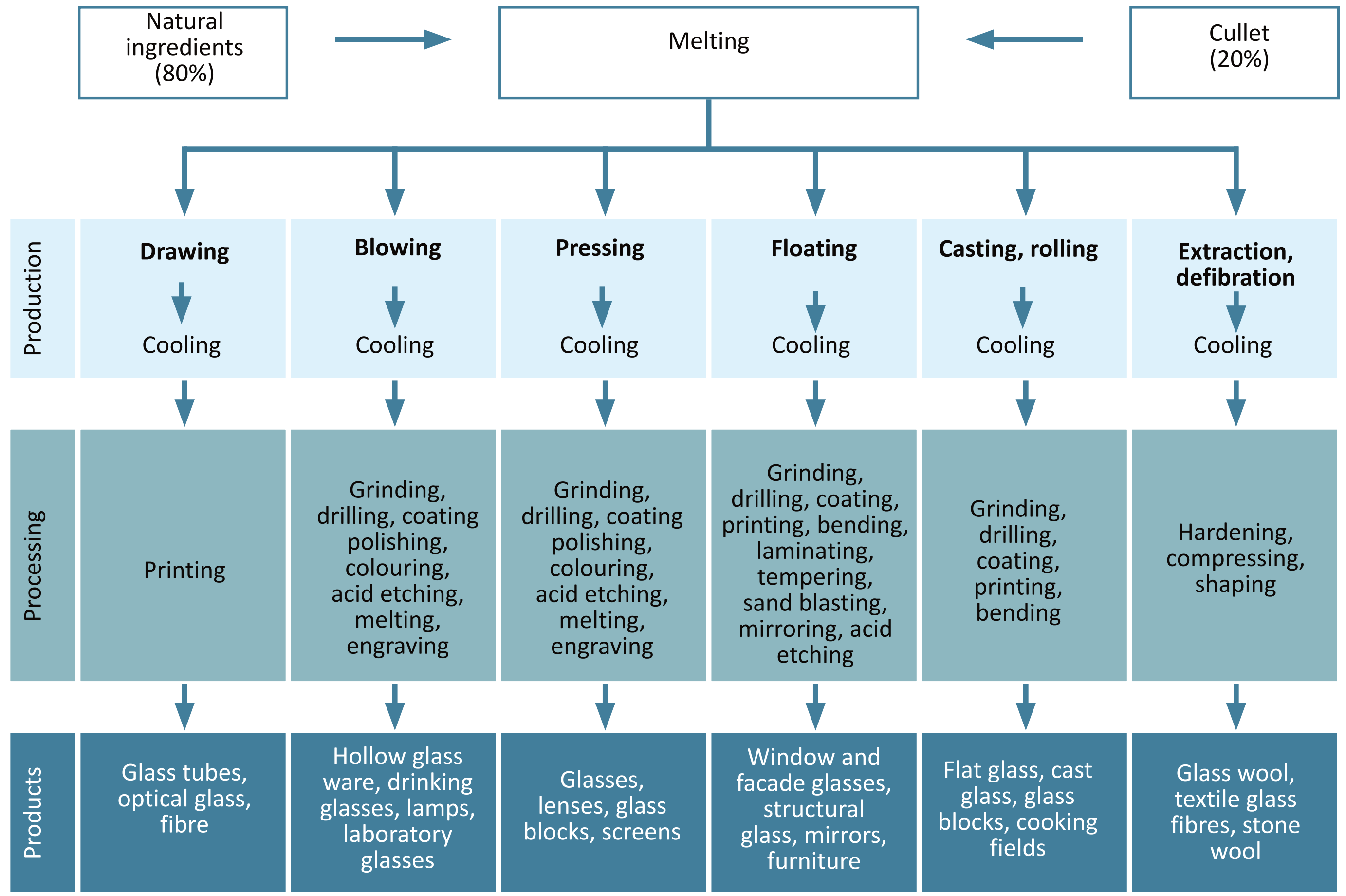

Figure 12: Glass production techniques. (Luible et al., 2008)

Initial production steps

Edgar (2008) provides a full description of the method, which starts with feeding a mixture of recycled glass and raw materials into a furnace that reaches temperatures of 1,600°C. The combination is melted by this extreme heat, turning it into a fluid state appropriate for additional processing.

Formation of glass panel

After melting, the glass is gently poured over a tin bath that has also melted. The glass's thickness can be adjusted using top rollers, enabling conventional thickness ranges of 2 to 25 mm. This stage is crucial for the production of the glass panel (Oikonomopoulou, 2019). The production of a continuous panel with unusually smooth surfaces is made possible by the smooth surface of the molten tin and the difference in density between glass and tin. This procedure guarantees excellent quality and consistent thickness (Hubert, 2019).

Annealing and final processing

The glass panel needs to be annealed before it can be used after formation. More information about the annealing process will be provided in the next paragraph, 2.3.3 Annealing. This step, which is critical for reducing internal temperature-related tensions, entails progressively chilling the glass panel in a regulated setting. This step is crucial, as noted by Edgar (2008) and Bricknell (2009). It entails warming the glass and closely monitoring its cooling cycle. By preventing residual stresses from developing, this regulated cooling maintains the safety and structural integrity of the glass.

The viscosity of the glass at its melting temperature and working point, its shape, its mass distribution, and the unique features of the annealing temperature, among other factors, are critical in determining how effective this process is (Martlew, 2005). When the glass is annealed, it is then put through an automated quality control inspection process. Finally, it is cut to final sizes using precise instruments like diamond wheels (Oikonomopoulou, 2019)

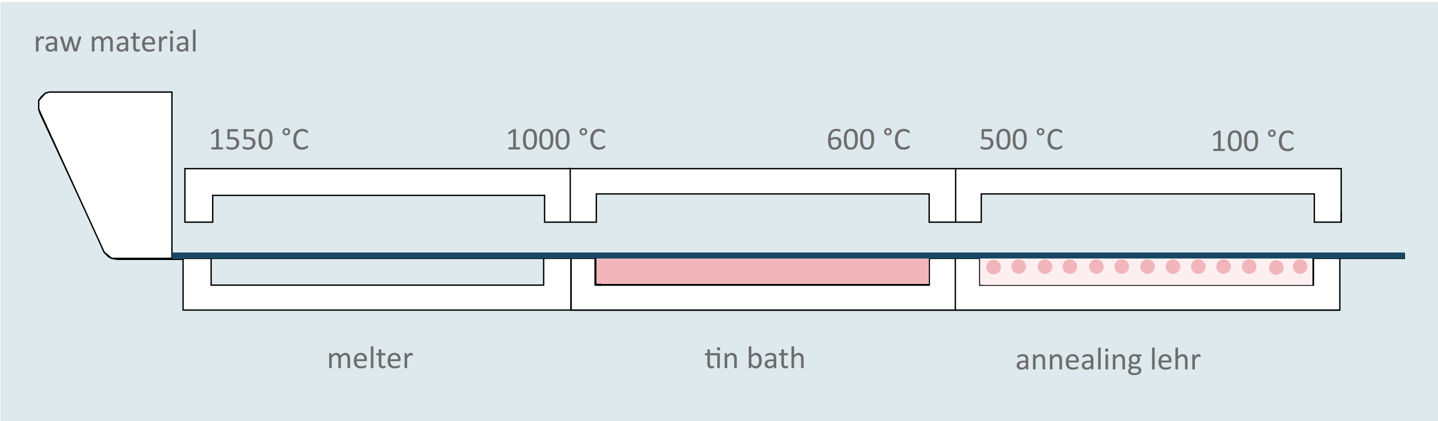

Figure 13: Production process for Float glass.(Luible et al., 2008)

2.3.3 Annealing

As previously mentioned, an important step in the production of glass is annealing, which guarantees the material's safety and structural integrity. The goal of this procedure is to reduce internal tensions brought on by abrupt temperature variations that occur during the forming process. Glass items can break or split if they are not properly annealed, especially when they are subjected to mechanical stress or temperature changes. Glass must be kept melted within a specific temperature range (Graph 02) during the annealing process in order to remove strain and avoid residual tension from forming when the element cools down further. (Oikonomopoulou, 2019). A recommended annealing schedule is shown in Graph 03 and Table 04.

Process details

Quenching (A): To stop the production of a crystallisation, it is essential to make sure that the temperature of the glass drops below its softening point during this quick cooling phase, also known as quenching. The object's weight and thickness are two parameters that affect this process (Oikonomopoulou, 2019). Any produced thermal stress can quickly relax to a tolerable level because of the glass's comparatively low viscosity during quenching (Shelby, 2005).

Anneal Soak (B): Internal stresses are successfully decreased by keeping the glass at a particular temperature between its annealing and strain points. By allowing internal tensions to release, this procedure stabilises the glass (Hubert, 2019). As soon as the glass melt reaches the softening point, the annealing process starts. The glass's enough viscosity at this temperature allows for molecular rearrangement, which reduces stress inside the element (Oikonomopoulou, 2019). Float glass is annealed in an annealing lehr, a specialised chamber, to relieve these stresses. The glass must be cooled progressively during this operation from 600°C to 60°C (Hartwell et al., 2022).

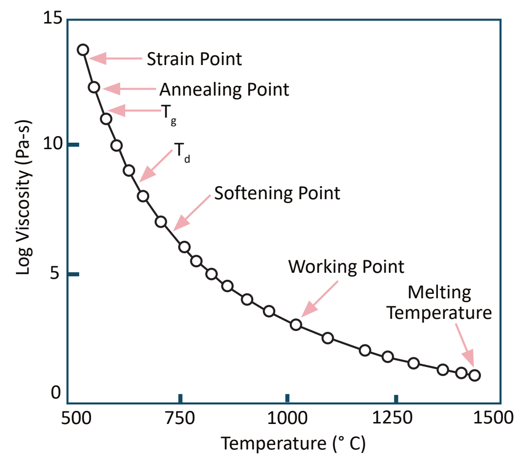

Graph 02: Typical curve for viscosity as a function temperature for a soda-lime-silica (Shelby, 2005)

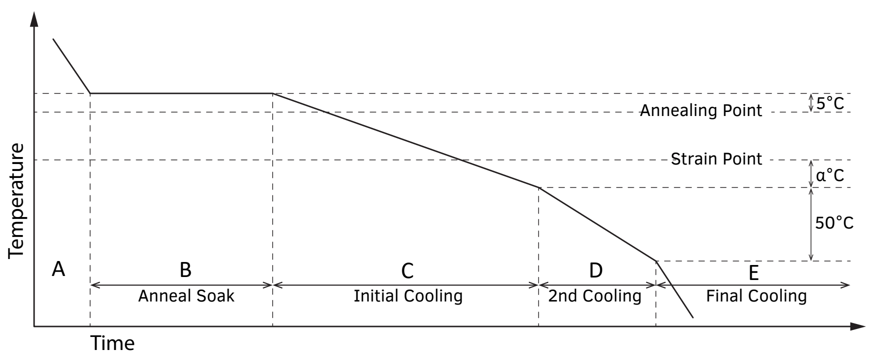

Graph 03: Typical annealing scheme for commercial soda-lime glasses. (Oikonomopoulou, 2019)

Initial Cooling (C): According to Oikonomopoulou (2019), this stage usually entails cooling the glass just below its softening point, which is the essential point at which the glass begins to distort under its own weight. Faster cooling is feasible as the element's temperature falls below the strain point, but it must still be done slowly enough to reduce the chance of thermal shock.

2nd Cooling (D): After the first cooling, the glass is cooled under regulated conditions so that internal strains can gradually release. The glass's viscosity at this point, which must be both fluid to allow for molecular rearrangements and solid to preserve its shape, is taken into consideration while regulating the rate of cooling (Martlew, 2005; Shelby, 2005).

Final Cooling (E): During this stage, the glass is cooled to room temperature.

Annealing time

The annealing time required increases exponentially with the component's size. As an example, an identical piece of flat glass placed on a kiln shelf with one side exposed requires twice as much annealing time as the same piece placed on the shelf with both sides exposed (Oikonomopoulou, 2019).

Choosing the right annealing time for a glass object is a difficult process that depends on a lot of variables (Oikonomopoulou et al., 2018). The annealing process is affected by a number of factors, including the mass distribution and model shape, the surface area exposed to cooling, the presence of other thermal masses in the oven, and the characteristics of the oven itself. Although extant literature endeavours to furnish exact directives for annealing, those materials frequently depend on implicit presumptions and particular situations that might not be broadly relevant (Watson, 1999).

2.3.4 Casting

On the other hand, one can make entirely transparent structures with almost infinite form freedom using cast glass (Oikonomopoulou, 2019). The material is heated to a liquid state first, and then it is poured into a mould to take on the desired shape. The substance is then allowed to cool and solidify inside the mould before being removed (Hubert, 2019).

Glass casting is an old craft; evidence of its application by Roman glassmakers dates to the first century AD. These ancient craftsmen made flat glass panels and containers by casting molten glass onto slabs of flat stone. This ancient method, which was attested to by discoveries in Pompeii and Herculaneum, usually generated glass that was translucent because of its large thickness (Hubert, 2019).

Projects like the Atocha Memorial, the Optical House, the Crystal Houses façade, and the Crown Fountain have demonstrated its possibilities.

Expansion Coef. of Glass per °C	Glass Thickness [mm]	Cooling on one side					Cooling on two sides				
		B	C		D	E	B	C		D	E
		Anneal soak	Initial cooling (annealing)		2nd cooling	Final cooling	Anneal soak	Initial cooling (annealing)		2nd cooling	Final cooling
		Time [min]	Temp. [°C]	Cool rate [°C/min]	Cool rate [°C/min]	Cool rate [°C/min]	Time [min]	Temp. [°C]	Cool rate [°C/min]	Cool rate [°C/min]	Cool rate [°C/min]
33*10-7	3.2 6.3 12.7	5 15 30	5 10 20	12 3 0.8	24 6 1.6	130 30 8	5 15 30	5 10 20	39 12 3	78 24 6	400 130 30
50*10-7	3.2 6.3 12.7	5 15 30	5 10 20	8 2 0.5	16 4 1	85 21 5	5 15 30	5 10 20	26 8 2	52 16 4	260 85 21
90*10-7	3.2 6.3 12.7	5 15 30	5 10 20	4 1 0.3	8 2 0.6	50 11 3	5 15 30	5 10 20	14 4 1	28 8 2	140 50 11

Table 04: Typical annealing scheme for commercial soda-lime glass (Oikonomopoulou, 2019)

02 | BACKGROUND OF GLASS

Figure 14: Casting of soda-lime glass blocks at Poesia Factory in Italy. (Oikonomopoulou, 2019)

Figure 15: Kiln-casting (Oikonomopoulou, 2019)

Contemporary casting methods

Primary casting: In this process, raw ingredients are melted to create molten glass. The glass is poured into a mould while it is still liquid (Figure 14). Several sizes and shapes can be produced with this method, all of which are customised to meet certain design specifications. Large, solid glass components with sizable cross-sections are best created using the main casting technique, which offers some design and application flexibility (Oikonomopoulou, 2019).

Secondary casting: This technique, on the other hand, entails remelting cullet—previously created solid glass shards (Figure 15). Usually by kiln-casting, the cullet is heated to a temperature at which it becomes flexible and may be moulded into the required shape. Compared to primary casting, this process requires lower operating temperatures, which makes it generally more energy-efficient. In secondary casting, a single kiln is used for both melting and annealing. The glass pieces are placed in a holder so that, when heated sufficiently, the molten glass can pour into the moulds. When using pre-existing solid parts, lower temperatures are required. It is the recommended procedure for customised components because of this and the need for only one furnace (Oikonomopoulou, 2019).

In order to prevent surface irregularities or structural weaknesses in the finished product caused by the temperature differential between the molten glass and the mould, both processes require precise temperature management and specific mould preparation (Bristogianni et al., 2018; Oikonomopoulou, 2019). It is noteworthy that the surface that is exposed to the top air cools considerably faster than the surfaces that are in contact with the mould (Oikonomopoulou, 2019). A comparison of some of the key distinctions between the Float line and casting processes is shown in Table 05.

Mould types

As was previously said, the selection of a mould is essential for all casting processes, including kiln-casting and hot-forming. This selection is greatly influenced by a number of factors, including the volume of production, the desired precision of the glass product, and time and cost restrictions. (Oikonomopoulou, 2019). Figure 16 shows an overview of the mould types. Table 06 shows the characteristics per mould type.

Glass process	Optical Characteristics	Main type of glass applied	Standard size [mm]	Thickness [mm]
Float	Smooth Transparent	Soda-lime	3210 x 6000[a]	2-25
Cast	Smooth Transparent	Soda-lime Borosilicate Lead	currently up to 20000 kg[b]	n/a

Table 05: Overview of existing glass fabrication methods for building components and their current size limitations. (Oikonomopoulou, 2019)

a. The max. panel size is continuously stretching. At present, up to 20 m long panels have been produced.
b Weight of the Hale Telescope monolithic glass blank.

Characteristics	Mould type						
Reusability	Disposable		Permanent				
Material	Silica Plaster	Alumina-silica fiber	Steel/ Stainless steel			Graphite	
Adjustability	-	-	Adjustable	Fixed	Pressed	Adjustable	Fixed
Production method	Investment casting/ lostwax technique	Milling	Milling/cutting and welding			Milling/ grinding	
Manufacturing costs	Low	High	Moderate to high			High	
Top temperature	900 - 1.000 °C	≈ 1.650 °C	≈ 1.200 °C/1.260 °C			unknown	unknown
Glass annealing method	Mould not removed for annealing		Mould usually removed for annealing but can also remain if high accuracy is required			Mould removed for annealing	
Release method	Immerse in water	Water pressure	Release coating necessary (ex. Boron Nitride)			Release coating necessary	
Level of precision	Low/moderate	High	Moderate/ High	High	Very high	Moderate/ High	High
Finishing surface	Translucent/ rough	Translucent/ rough	Glossy. Surface chills may appear if the mould is not properly pre-heated			Glossy with surface chills	
Post-processing requirements	Grinding and polishing required to restore transparency and increase accuracy		Minimum or none post-processing required			Minimum to moderate post-processing required	
Applicability	Single component/low volume production		High volume production			High volume production	

Table 06: Characteristics of prevailing mould types for glass casting (Oikonomopoulou, 2019)

Permanent moulds

Permanent moulds composed of steel or graphite are the preferable material for circumstances when serial production is required. When it comes to pressed moulds, permanent moulds—especially those made of graphite—can greatly improve dimensional accuracy. Only steel moulds can achieve the crucial requirement of keeping the mould in place throughout the annealing process in order to preserve dimensional stability. For the glass components to release easily from the steel mould, a release agent coating is essential. As long as the moulds are properly heated prior to casting, items made from permanent moulds often have smooth, shiny surfaces and require little post-processing. (Oikonomopoulou, 2019).

Disposable moulds

Because disposable moulds are less expensive than permanent moulds, they are better suited for single components or small batch castings. The highest melting temperatures and degrees of precision offered by these moulds vary. For example, low-cost silica-plaster moulds are appropriate for castings at temperatures lower than 1,000 °C, and milled alumina-silica fibre ceramics provide the best results. But no matter what kind of material is used, glass surfaces that come into touch with disposable moulds often take on a translucent, coarse texture that requires post-processing to achieve a transparent finish. They are frequently utilised in kiln-casting applications because of their brittle character, which makes cooling using disposable moulds problematic (Oikonomopoulou, 2019).

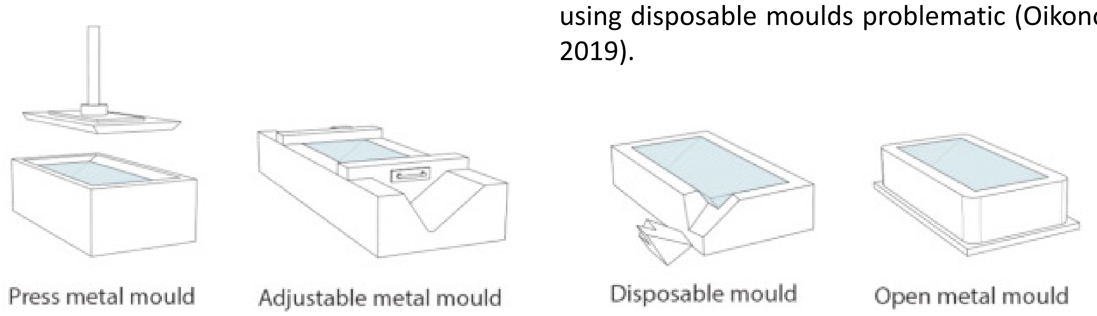

Figure 16: Illustration of the most common mould types (Oikonomopoulou, 2019)

03 | MECHANICAL BEHAVIOUR OF GLASS

3.1 Structural usage of glass in buildings

Because of its translucency, high compressive strength, longevity, and weather resistance, glass is frequently used in architecture. It is completely elastic, isotropic, and brittle, which sets it apart from traditional building materials like steel and wood (Kozłowski, 2019). When it comes to building construction, glass is a material of choice for both practical and aesthetic applications (Figure 17). It is capable of supporting large weights due to its remarkable compressive strength. Many examples demonstrate its structural feasibility, most notably the creative glass structures designed by Eckersley O'Callaghan (EOC).

Glass has a strong compressive strength, but its structural applications are limited by its poor tensile strength. The primary cause of this constraint is the intrinsic brittleness of the material. When glass reaches its tensile limitations, it tends to fracture abruptly, in contrast to ductile materials that flex before failing. Surface imperfections are the cause of the difference in its theoretical and practical tensile strength (Kozłowski, 2019). These defects, which might be the result of environmental damage or manufacturing errors, concentrate stress and greatly lower the strength of the glass under tension. Expanding the use of glass in structural applications requires an understanding of these faults.

3.2 Brittleness and fracture behaviour

According to Shelby (2005), one of the most well-known characteristics of glass is its brittleness, which is greatly influenced by surface and edge treatment and the surrounding chemical environment. These components have a significant effect on the bond strength inside the vitreous network of glass, which in turn affects the glass's fracture strength. For example, the surface treatment of glass can have a major impact on the strength of these connections under stress, strengthening or weakening the glass structure. Likewise, the chemical environment surrounding the glass may influence its structural integrity on a microscopic level.

As was covered in paragraph 2.1, "Glass definition," glass is an amorphous substance, which means that it lacks a crystalline structure at the molecular level. Because of its amorphous structure, glass is not flexible. resulting in a brittle substance that will abruptly give way without exhibiting plastic behaviour. Moreover, glass cannot lessen local peak pressures because it lacks malleable behaviour (Oikonomopoulou, 2019).

Figure 17: (a) The Apple Store in New York by EOC Engineers (EOC Engineers, 2006), (b) The Crystal Houses façade in Amsterdam by MVRDV Architects, made of adhesively bonded glass blocks. (Scagliola & Brakke, 2016) and (c) Markthal in Rotterdam by Octatube (Octatube, 2014)

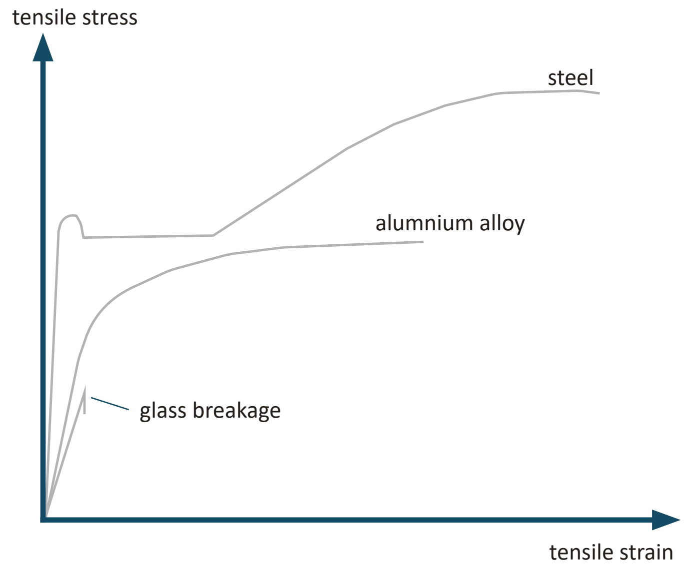

Graph 04: Stress-strain behaviour of glass, steel and aluminium alloy (Buildings Department, 2018)

In addition, glass has a distinct behaviour under tension that sets it apart from materials like steel and aluminium alloy. Graph 04 provides an illustration of this phenomenon by showing the relationship between tensile strain and tensile stress as a graph. Because of its imperfect and asymmetrical atomic structure, glass is especially prone to the spread of cracks. Its stress-strain behaviour makes this clear; glass lacks the yield point and large deformation capability of ductile materials, which allow for significant deformation before breakdown. Glass fails suddenly because it cannot withstand the growth of preexisting faults when it is under tension. This conduct emphasises how crucial it is to comprehend and take these material features into consideration in applications where glass is employed (Buildings Department, 2018).

3.3 Structural properties

3.3.1 The theoretical strength of glass

Orowan's stress formula can be used to determine the theoretical strength of glass, which is believed to be between 6000 and 10000 MPa (Haldimann et al., 2008). In essence, the interatomic binding forces define the strength of glass. Utilising Orowan's stress formula, the material's failure stress σm can be determined as follows

$$\sigma m = \sqrt{\frac{E_Y}{r_0}}$$

E = Young's modulus
γ = fracture surface energy
r0 = equilibrium spacing of the atoms

Formula 1: Orowan's stress

Compressive strength of glass

The material's compressive strength is remarkable. Although Orowan's equation from 1934 suggests that typical silica glass may potentially reach a strength of 32 GPa (Shelby, 2005), practical strength values for common glass products range from 14 to 70 MPa, with glass fibres reaching a maximum of 2.1 GPa (Varshneya, 2013). To put it straightforwardly, ordinary commercial glass breaks under tension at much lower stress values than 1000 MPa. Therefore, a primarily compressive loading state that inhibits bond breakdown and network opening is indicated by the term "high compressive strength". It is reasonable to anticipate high (compressive) strength under low tensile stresses (Bristogianni, 2022).

However, because of structural flaws and material imperfections that cause stress concentrations and significantly reduce glass's structural performance, obtaining this strength is rarely realised. (Oikonomopoulou, 2019). Paragraph 3.6: Flaw categories will go into additional detail about these weaknesses. In addition to significant defects that cause a considerable strength drop of up to 75%, specific chemical compositions that are useful to performance are emphasised (Bristogianni et al., 2020). A comprehensive list of the different mechanical qualities and their related values is given in Table 07.

Mechanical property	Value
Young's modulus, E	70 GPa
Shear modulus, G	28.7 GPa
Poisson's ratio, υ	0.22
Density, ρ	2500 kg m^{-3}
Characteristic tensile strength	45 Mpa
Coefficient of thermal expansion,	9×10^{-6} K^{-1}
Thermal conductivity	1 $W\times m^{-1}K^{-1}$

Table 07: Basic properties of soda-lime-silicate glass based on (Achintha, 2016) and (Kozłowski, 2019)

Tensile strength of glass

As a result, the tensile strength of glass is not constant but rather depends on a number of variables, including surface and edge quality, glass element size, loading history (both duration and intensity), residual stress quantity, and environmental parameters. Accordingly, the effective tensile strength is decreased by greater loads, longer times, deeper initial surface defects, or unfavourable environmental circumstances (Haldimann et al., 2008). Glass has a far higher compressive strength than tensile strength because faults cannot spread or fail under just compressive force. Nevertheless glass's structural applications are not primarily determined by its compressive strength; rather, glass usually fails because local tensile stresses are reached. Peak tensile stresses appear even under compression loading, well in advance of compressive strength, as a result of buckling or Poisson's ratio effect (Oikonomopoulou, 2019).

3.3.2 The flexural strength of glass

Because it shows isotropy and linear-elastic behaviour, glass is particularly durable when used in building. Its long-term dependability is, however, compromised by stress corrosion cracking, often known as "static fatigue," which occurs when surface imperfections enlarge under tensile stress in humid environments (Achintha, 2016).

Because of static stress, glass strength tends to deteriorate over time. Higher failure strengths are observed with quickly increasing loads, and dynamic fatigue occurs under changing load conditions (Shelby, 2005). Surface imperfections and stress concentrations affect the tensile strength of Float glass, causing brittle failure behaviour and making it uncommon to use in load-bearing structures. On the other hand, glass varieties that are laminated and hardened are recommended for these kinds of applications (Achintha, 2016; O'Regan, 2014). Glass's strength is greatly impacted by its surface condition, particularly the direction and location of flaws (Bedon et al, 2018)

"We never test the strength of glass; all we test is the weakness of its surface," highlighted Littleton. He conducted an experiment in which he removed surface microcracks from glass beams by etching them in hydrofluoric acid. The result was glass specimens with high tensile strength values that were stronger than nickel steel (Preston 1942). The nominal flexural strength formula was used to determine flexural strength in accordance with failure load and geometry: Four-point bending can be used to test it in-plane until failure happens. (Bristogianni, 2022).

$$\sigma = \frac{3 \cdot F \cdot (L - L_i)}{2 \cdot b \cdot d^2}$$

F = Maximum load
L = Support span
Li = Load span
b = Beam's width
d = Beam's height

Formula 2: The nominal flexural strength

It's important to note that due to fixed loading pins, a systematic positive error may arise due to frictional constraint (μ·F/2) at each pin, where μ is the coefficient of friction, μ = 0,3 (Quinn et al., 2009). However, the actual failure strength of glass consistently refers to its tensile strength, which is linked to bond strength and inherent flaws, thus the above equation should be rewritten as:

$$\sigma = \frac{3 \cdot F \cdot (L - L_i - \mu \cdot d)}{2 \cdot b \cdot d^2}$$

F = Maximum load
L = Support span
Li = Load span
b = Beam's width
d = Beam's height

Formula 3: The nominal flexural strength with coefficient of friction

3.3.3 Strength of cast glass beams

Research on the structural behaviour of cast glass beams has already been done by TU Delft. Flexural strength range of 9-73MPa has been demonstrated by four-point bending studies on kiln-cast specimens 30x30x240mm (Bristogianni et al., 2020) and 20x30x350mm (Bristogianni et al., 2021b) and industrially fabricated reference beams. Because there aren't many specimens evaluated for each kind, this range should only be regarded as suggestive. Variables like composition, defect type, cooling rate, surface quality, and specimen size can all affect this range. These four-point bending test setups will be used in the approach in a following section, Chapter 7, Mechanical tests.

A Zwick Z10 displacement-controlled universal testing machine is used to test the specimens at a speed of 0.2 mm per minute in a laboratory atmosphere. The four-point bending fixtures have fixed loading pins with a 10mm diameter, and a 110mm span for the loading rollers and a 220mm span for the support rollers. They are attached to the four-point bending machine to provide for some support. (Figure 18)

3.4 Elastic properties

Solids are differentiated from liquids by elastic characteristics. It is important to comprehend the elastic properties of glass since most glass products behave in ways that are strongly dependent on their solid-like qualities. The semi-experimental method of investigating solid elasticity mostly relies on findings from a range of engineering material studies. Three main stress states are experienced by solids: pure shear, triaxial stress, and uniaxial stress. (Quinn et al., 2009)

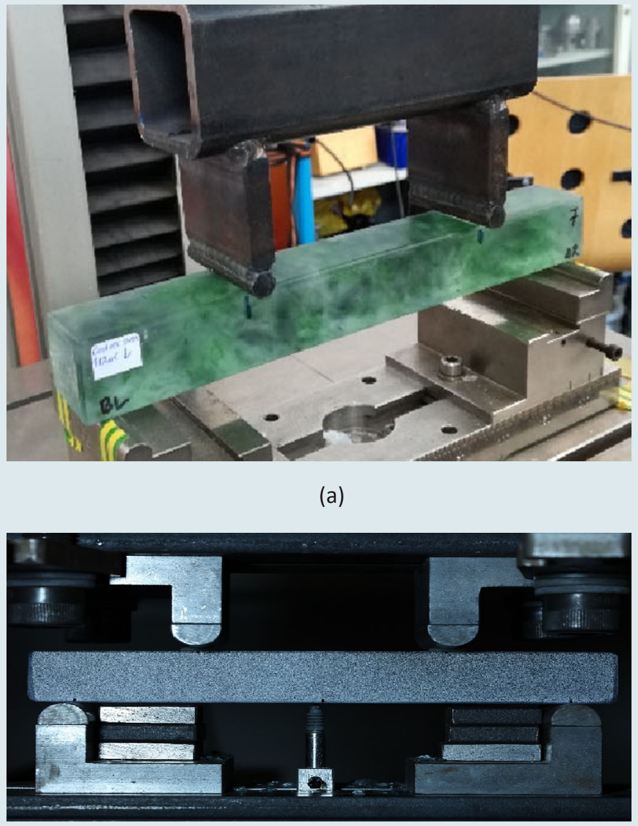

(a)

(b)

Figure 18: (a) Set-up for of 1st series of four-point bending experiment at the TU Delft, for investigating glass waste its flexural strength and (b) set up for 2nd series of four-point bending experiment at the TU Delft. (Bristogianni, et al., 2021b)

The Young's modulus, denoted as E or sometimes as Y, represents the ratio of linear stress to linear strain

$$\sigma_x = Eex$$

E = Young's modulus
e = axial strain

Formula 4: Compressive stress

There are three primary types of methods for determining the elastic moduli of glasses: stress-strain curve methods, ultrasonic wave propagation methods, and natural frequency estimation methods. Among these, a mechanical testing equipment is typically used to apply uniaxial tension and record the specimen's change in length as the load increases in order to determine the Young's modulus (Quinn et al., 2009). A four-point bending test can be used to achieve this.

3.4.1 Deflection

In a four-point bending test, the centre of the beam's deflection is determined using the following formula:

$$\delta = \frac{F(L_1 - L_2)(2L_1^2 + 2L, L_2^2 - L_2^2)}{9bEI}$$

F = Maximum load
L1 = The separation between the outer support pegs
L2 = The separation between the inner support pegs
b = Beam's width
E= Young's Modulus
I = Moment of Inertia

Formula 5: Deflection of the centre of a beam

Shear deflection should be taken into account for the four-point bending test. According to Bristogianni (2022), the total vertical deflection should take shear deflection into consideration. The following formulas can be used to determine the bending and shear deflection at mid-span:

$$\Delta l_{shear\_mid} = \frac{\Delta F \cdot \left(\frac{L - L_i}{2}\right)}{2 \cdot G \cdot b \cdot d}$$

F = Maximum load
L = The separation between the outer support pegs
L1 = The separation between the inner support pegs
b = Beam's width
d = Beam's height

Formula 6: Shear deflection at mid-span

$$G = \frac{E}{2 \cdot (1 + v)}$$

E = Young's Modulus
v = poisson ratio = 0,22

Formula 7: Shear modulus

Where v for soda-lime silica glass equal 0.22. Variations in this value between the tested glasses by about ±0.02 hardly affect the results. It can be ascertained by summing the two vertical deflection segments and calculating the Young's modulus:

$$E = \frac{\Delta F}{\Delta l_{shear\_mid}} \cdot \left(\frac{11 \cdot \left(\frac{L - L_i}{2}\right)^3}{2 \cdot b \cdot d^3} + \frac{(L - L_i) \cdot (1 + v)}{2 \cdot b \cdot d} \right)$$

F = Maximum load
l = Deflection
L = The separation between the outer support pegs
L1 = The separation between the inner support pegs
b = Beam's width
d = Beam's height
v = poisson ratio = 0,22

Formula 8: Young's Modulus formula

3.4.2 Stress

A cast glass beam is tested using a four-point bending test to determine its flexural strength, which is essentially a measurement of how much the beam can bend and withstand internal stresses before breaking. Important information on the material's structural integrity and ability to withstand applied loads is provided by this test. The distribution of stresses present in a four-point bending test is shown in Figure 19. Compressive stress is a sign of compression at the top of the beam. Tensile stress, on the other hand, is predominant towards the bottom and indicates the tension in the material. The neutral axis, where neither compressive nor tensile stress predominates, is located within the midpoint of the beam. The tension stress zone, which is mostly found around the bottom of the beam, is very concerning. This is the most critical area since glass is vulnerable to breaking under tension.

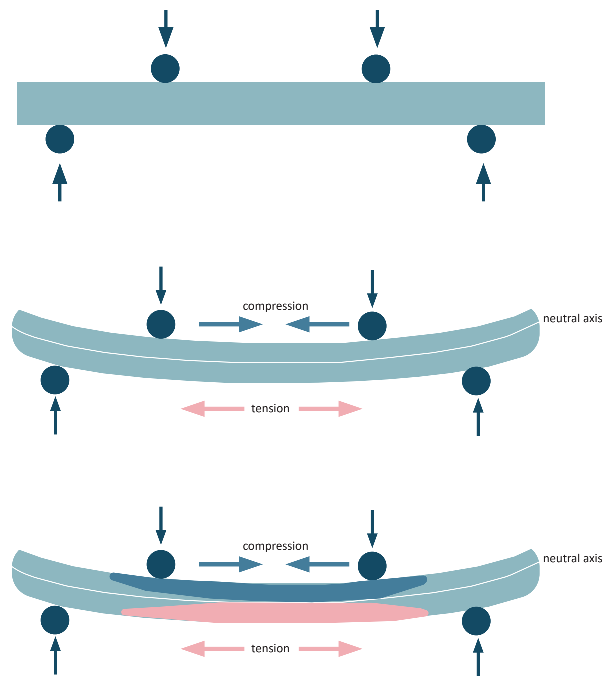

Figure 19: Tensile and compressive stress areas visualised in a beam

3.5 Thermal properties

The thermal characteristics of soda-lime glass, such as its specific heat and expansion coefficients, reduce the strength of the glass in comparison to materials like steel or concrete. Surface coatings can improve this property, though (Achintha, 2016). Soda-lime glass can react to temperature changes more quickly because to its reduced thermal mass, which is useful in some architectural applications but can also present problems with thermal stress and management. Surface coatings can be applied to modify these characteristics, improving the glass's resilience to external influences and thermal performance. Nonetheless, variations in the thermal expansion coefficients of different kinds of glass provide difficulties. This variation may cause differential expansion in the presence of heat stress, which could lead to cracks and reduced structural integrity. (Anagnia et al., 2020; Shelby, 2005).

Furthermore, the liquidus point of glass also affects its thermal behaviour. Glasses with a lower liquidus point, which melt at lower temperatures, can have more uniform surfaces and fewer stone formations or heating defects. This characteristic is especially helpful in procedures such as kiln-casting, where quality and usefulness depend heavily on the homogeneity of the glass surface and the reduction of flaws (Bristogianni et al., 2020). Higher quality and more dependable glass products for architectural and other purposes can result from these techniques being able to generate a more homogenous melt at lower temperatures.

3.6 Flaw categories

As stated in paragraph 3.3: Structural properties, flaws in cast glass components seriously damage their structural integrity. Common material defects and irregularities include bubbles, internal tensions, crystallised interfaces, stones, cord, and surface damage from machining (surface and edge treatment) and moulding, among other stages. The influence of these faults on structural performance is more noticeable, especially when they are at the surface-level (Bristogianni, 2022). An overview of the cast glass faults is shown in Figure 20. This graphic illustrates how a high tensile stress will develop in a cast glass beam at or near the surface when it is subjected to pressure. However, the tensile stress will be minimal in the bulk.

Float glass, which is thin-walled, can't have any impurities. While cast glass is more tough to faults like bubbles and inclusions than Float glass, these flaws can nonetheless decrease or affect the cast glass's aesthetic appeal

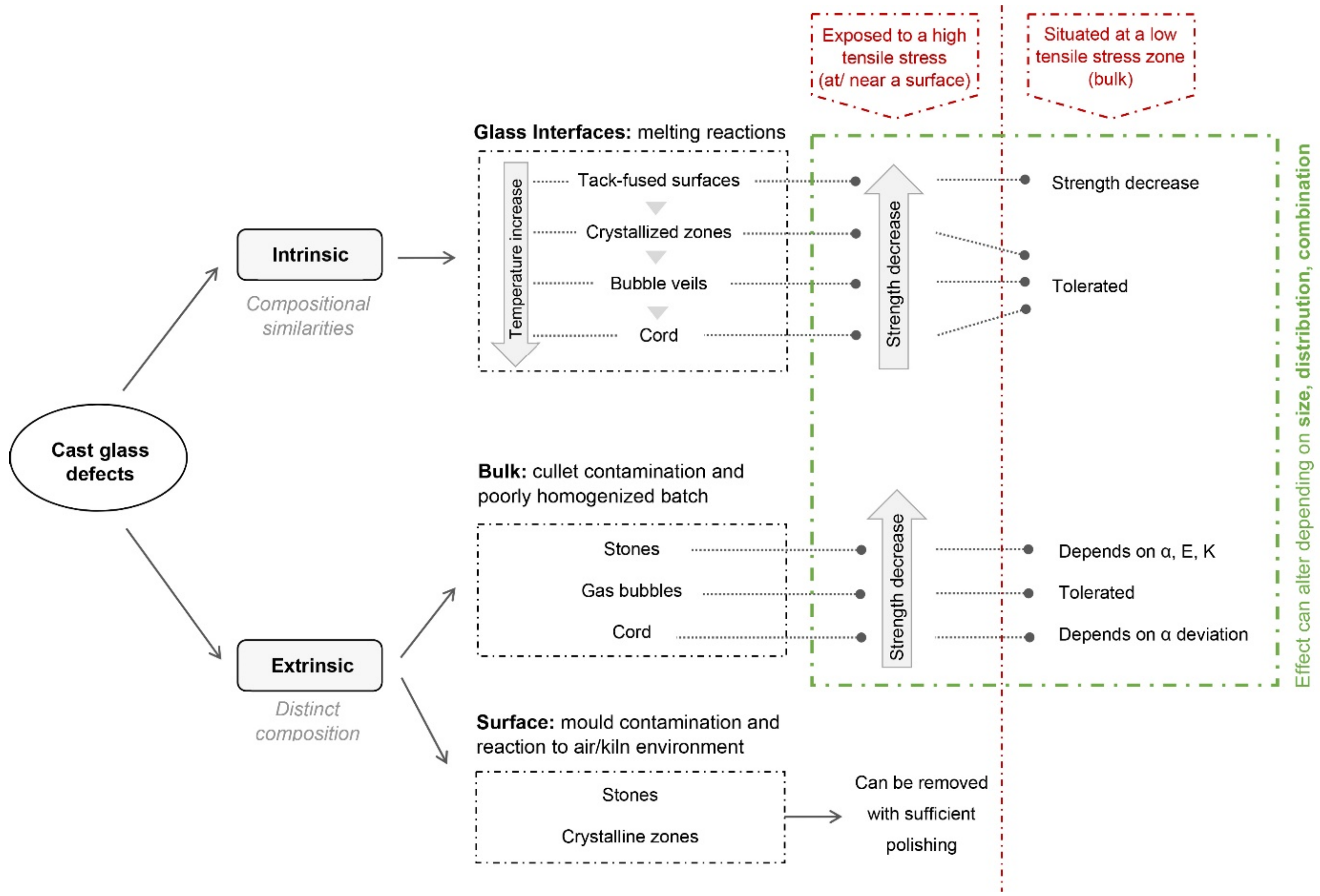

Figure 20: Classification of casting defects and assessment of their severity based on their characteristics and location in the glass specimen. (Bristogianni, 2022)

(Bristogianni et al., 2018b). Testing the surface and edge quality have a significant impact on the flexural strength of Float glass (Bristogianni et al, 2020; Veer & Rodichev, 2011). Cast glass is volumetric and more vulnerable to manufacturing faults, which makes homogeneity control difficult. The distribution and type of flaws are used to categorise them, and digital microscopy and stress analysis are used to help with identification.

Specimens of kiln-cast glass frequently have a variety of defects that come from different phases of the manufacturing process (Figure 21). Defects related to casting, like bubbles and stones, are closely associated with the parameters used during the casting process and can appear on the surface or in the bulk of glass beams. On the other hand, surface imperfections such as scratches and chippage/ infolds are caused by handling and post-processing. These can be caused by the fragility of some varieties of glass as well as the accuracy of the machinery and polishing materials.

3.6.1 Crystalline inclusions

Crystalline inclusions are a complex problem. These could result from mould growth, thermal history effects, or cullet contamination, each of which has a different effect on the integrity of the glass. Notably, visible undissolved particles—also called stones—often lead to the rejection of commercial glass (Bristogianni et al, 2021b).

3.6.2 Glassy Inhomogeneities

Glassy inhomogeneities encompass variations in glass cullet, impartially molten contaminations, and element volatilisation. Cord-like inclusions and coloured streaks typify these variations (Bristogianni et al, 2021b).

3.6.3 Gaseous Inhomogeneities

In kiln-cast specimens, gaseous inhomogeneities, especially bubbles, are common and can be caused by a variety of factors, including as air entrapment, chemical reactions during cullet bonding, and responses

03 | MECHANICAL BEHAVIOUR OF GLASS

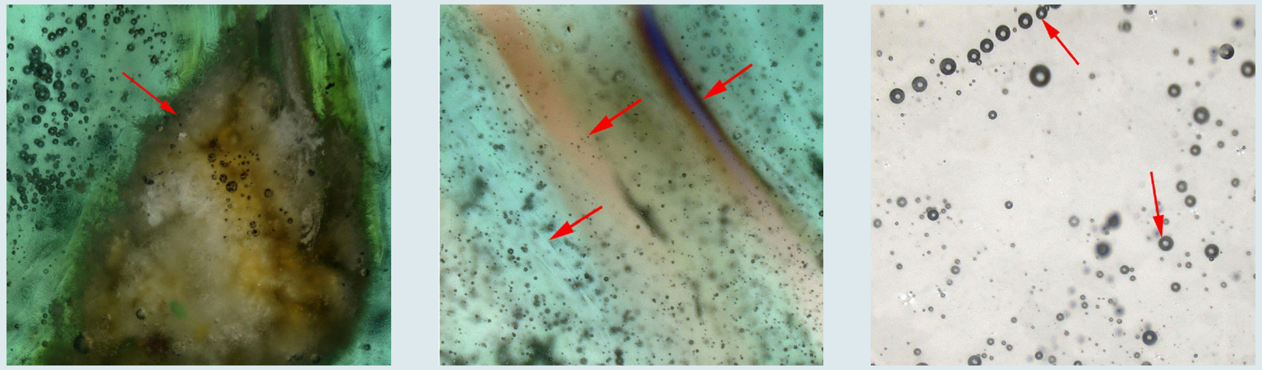

(a)

a. Cullet contamination
b. Thermal history
c. Mould contamination

(b)

a. Glass cullet variations
b. Impartially molten contaminants
c. Element volatilisation
d. Composite glasses

(c)

a. Air-entrapment between cullet
b. Chemical reactions
c. Reaction to contaminants

Figure 21: Flaw categories in kiln-cast specimens. (a) Crystalline inclusions, (b) Glassy inhomogeneities and (c) Gaseous inhomogeneities (Bristogianni, et al., 2021b)

to impurities and melted inclusions. Exposure at the object's surface can seriously reduce strength, although small bubble clusters within the bulk may have no effect on the final component's strength. However, in the molten stage, bubbles might be advantageous since they facilitate convection and homogenisation variations. (Bristogianni et al, 2021b).

Bubbles are created and removed via intricate systems. These could involve physically capturing ambient gases during the first stages of batch melting or batch component breakdown. Notably, bubbles can be removed by rising to the surface physically or by dissolving chemically into the surrounding melt. (Shelby, 2005).

3.7 Increasing safety in glass

Different types of glass fracture in different ways: tempered glass fractures into smaller cubes due to residual tension, earning it the name "safety glass," while annealed Float glass shatters into huge, sharp shards (Haldimann et al., 2008). Improved post-breakage performance is offered by laminated glass with a PVB interlayer because it keeps broken fragments together and preserves structural integrity even after severe breakage (Achintha, 2016). Figure 22 provides a thorough comparison of the impact resistance and structural performance of fully tempered glass, heat-strengthened glass, and annealed glass. It also shows the relationship between the frequency of cracks in each type of glass and the structural capacity that remains after breakage. This graphic illustration highlights the connection between increased residual structural integrity and a decreased risk of cracks, providing important information about the strength and safety features of these various kinds of glass.

It is advised to use laminated glass for load-bearing components like balustrades and roofs. It is recommended to utilise laminated or tempered glass for building façades that act as protective barriers. Particular recommendations are given regarding the size of the panels and the height of installation when using tempered glass in façades (Buildings Department, 2018).

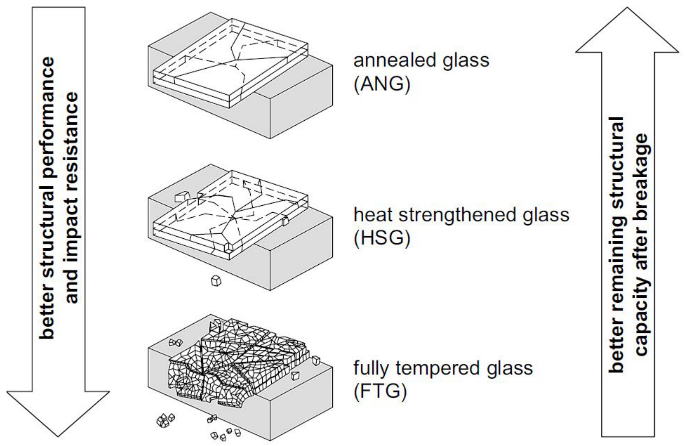

Figure 22: Post breakage behaviour of laminated glasss made of different glass types (Hubert, 2019)

3.7.1 Annealed glass

The basic product created by the Float process is referred to as annealed glass, and it is treated with an annealing process to relieve internal stresses (Buildings Department, 2018).This treatment is widely used since it is clear and reasonably priced, and it comprises a controlled cooling procedure that lowers residual tensions.

3.7.2 Heat strenghtened glass

Heat-strengthened glass is made from annealed glass and goes through a certain thermal cycle. In this cycle, the glass is heated above its annealing temperature and then rapidly cooled through air quenching. The glass produced by this method is not as strong as tempered glass, but it is stronger than annealed glass. Heat-strengthened glass is particularly resistant to thermal stress, which makes it ideal for areas with temperature swings. On the other hand, heat-strengthened glass offers more flexibility in terms of post-production modifications yet being more durable than annealed glass. The choice between the two types of glass is usually based on particular criteria for applications involving strength, safety, and temperature requirements.

3.7.3 Tempered glass

The cooling techniques used in each type of glass are the primary differences between tempered and heat-strengthened glass. Rapid quenching is used in the making of tempered glass, which results in high internal tensile stresses and surface compressive stresses (Buildings Department, 2018). Because of this process, tempered glass is around four times stronger than annealed glass, which makes it the best option for safety applications. It's crucial to remember that once tempered glass is formed, it becomes difficult to cut or adjust.

To further, the stress profile in tempered glass is shown in an illustrated detail in Figure 23. Understanding the distribution and strength of stresses within glass—especially under different conditions—is made easier with the aid of this graphic representation. Furthermore, Table 08 provides important information on the ultimate design strength under short-term load duration for Float (annealed), heat-strengthened, and fully toughened glass. The relative strength and resilience of various glass kinds under various loading scenarios are provided by this table. To further support this, Table 09 lists the typical bending strengths of several kinds of glass.

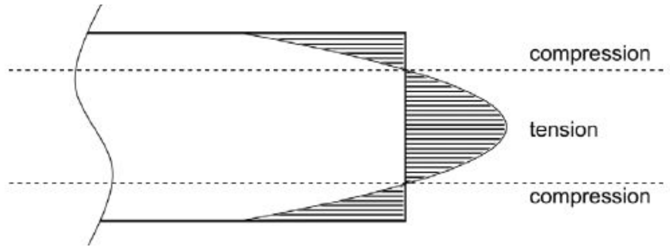

Figure 23: Stress profile in tempered glass (Buildings Department, 2018)

Type of glass	Ultimate design strength (p_y) under short-term load duration (MPa)
Float (annealed)	20
Heat strengthened	40
Fully toughened	80

Table 08: Ultimate design strength (p_y) for different glass types under short-term load duration (Buildings Department, 2018)

Type of glass	Characteristic bending strength (MPa)
Float (annealed)	45
Heat strengthened	70
Fully toughened	120

Table 09: Characteristic bending strength of different glass types (Luible et al., 2008)

04 | GLASS RECYCLING

4.1 Service life & end-of-life of glass units

IGUs and CCFs are essential to modern architecture because of their ability to reduce noise and provide thermal insulation. Nevertheless, the effects of their service life and end-of-life management on the environment and the economy are often overlooked. This section explores the lifetime of IGUs and CCFs, explaining why they need to be replaced after a given amount of time, the typical lifespan of glass in buildings, and the techniques used to remove and recycle them.

4.1.1 Service life and reasons for replacement

IGUs should expect a technical life of roughly 25 to 30 years on average, according to findings from Saint-Gobain (2023) and Hartwell et al. (2023). Since the glass panels can hold their original condition for a longer period of time, the degradation of components like sealants have a greater impact on this length of the service life than the glass itself. While the glass panels may survive much longer, the breakdown of polymer edge seals is the primary cause of the IGUs' shorter service life. According to Mohamed (2020), the main cause of IGU replacement is component failure, which results in reduced thermal performance and possible condensation problems. An IGU being removed is seen in Figure 24. Although the glazing industry is creating new techniques to get around this limitation, it will likely take some time for double and triple glazed units to become outmoded. Triple glazing will probably become more common as thermal performance standards grow (DeBrincat & Babic, 2023).

According to Glass for Europe (2020), industrial advancements are made to extend the lifespan of high-performance IGUs, which will decrease the amount of raw materials and energy used during the duration of a building's lifetime. The development of glazing goods that are stronger, lighter, and thinner supports this goal. These products not only require less raw material but also make installation easier and reduce the carbon footprint associated with transporting glass. Initiatives like "design for recycling" are examined to improve the end-of-life handling of these units. Bergmann (2020) discusses how the industry is looking into ways to increase the service life of IGUs and improve their end-of-life management. Geboes et al. (2023) note that there is still a gap between potential and reality in the practical use of reusing post-consumer IGUs. The difference offers the sector opportunities and challenges for innovation.

4.1.2 Environmental and economic implications

IGU lifecycles have important economic and environmental implications. As Worrell et al. (2008) note out, the use of cullet in glass manufacturing can result in significant cost savings by lowering the requirements for both energy and raw materials. Because of the lower melting temperatures and less harmful batches, this procedure also increases the service life of glass melting furnaces. According to Saint-Gobain (2023), the glazing sector needs to adopt more sustainable methods because replacing IGUs during a façade's lifetime adds to the structure's embodied carbon. Glass has a notably lower environmental impact than steel and concrete. In particular, the carbon footprint and embodied energy of Float glass are 0.232 kg CO2/kg and 15 MJ/kg, respectively. This is more than reinforced concrete, at 1.39 MJ/kg and 0.057 kg CO2/kg, but lower than steel, which has values of 24.6 MJ/kg and 0.466 kg CO2/kg. The high temperatures needed for glass's manufacturing account for a sizable amount of its embodied energy and carbon impact. Moreover, compared to Float glass, toughened glass, which is heated one more time, has a higher embodied energy and carbon footprint (23.5 MJ/kg and 0.346 kg CO2/kg) (Achintha, 2016).

Figure 24: Facade Glass Removal & Replacements (Glass Hoppers, 2021)

Market impact

According to estimates from Kellenberger et al. (2007) and Hartwell et al. (2023), IGUs make up 40–50% of the mass market for architectural glazing. There are large Float glass outflows from the manufacture and final disposal of these units. Edgar (2008) projects a significant rise in waste Float glass, estimating 160k–250k tonnes annually as a result of the ageing of the initial double-glazing generation. This emphasises how critical it is to have efficient recycling plans and handle glass trash.

4.2 Glass recyclability

4.2.1 Necessity of glass recycling

The single Float glass production process is notable for its high energy consumption, leading to CO2 emissions. Edgar (2008) points out that melting glass requires a significant amount of energy, with a large furnace needing about 4 GJ of energy for every tonne of molten glass. This emphasises how crucial recycling is to cutting down on energy use. These emissions originate from two primary sources: firstly, the generation of electricity or the burning of natural gas needed to heat the furnace, and secondly, the chemical reactions involved in glassmaking. In these reactions, CO2 is emitted as a byproduct when carbonate raw materials—specifically soda ash (sodium carbonate), limestone (calcium carbonate), and dolomite (calcium magnesium carbonate)—are processed in the melting tank (DeBrincat & Babic, 2023).

In an effort to save resources and lower CO2 emissions, the flat glass business is actively working to improve glass collection, sorting, and recycling. Setting up systems for removing, gathering, and classifying glass from buildings both before and after demolition is necessary for effective recycling (Glass for Europe, 2013). This is best demonstrated by Saint-Gobain (2023) with their cullet programme, which recycles more than 55,000 tonnes of glass annually and significantly lowers emissions and the need for raw materials.

According to Bristogianni et al. (2019), very little glass is recycled, mostly for use in the Float and packaging industries, even though it has the ability to be remelted indefinitely without losing quality. According to Hartwell et al. (2023), less than 1% of end-of-life Float glass products are recycled back into the market, making up around 10% of new manufacturing.

4.2.2 Barriers and opportunities in glass recycling

Barriers in glass recycling

Limited collaboration in the IGU recycling supply chain creates problems like lack of storage space, logistical constraints, and insufficient time for collection, particularly in smaller-scale initiatives. It is essential to improve local glass collecting networks.

Glass recycling and removal from structures are highly regulated processes. According to Vlakglas Recycling Nederland (2022), environmental parks and demolition businesses play a vital role in gathering Float glass for recycling purposes. In order to facilitate recycling, the Bouwbesluit of 2014 requires that Float glass be separated from other construction waste while buildings are being demolished.

A number of logistical considerations are necessary for effective glass recycling, including the distance between disassembly factories and service sites, the energy required for disassembly and remanufacturing, and the quantity of glass panels that may be reused. The continuous yield of glass that is unsuitable for remanufacturing and the secondary product end-of-life chain, which includes spacers and sealants, must also be addressed (Rota et al.,2023). Moreover, increasing reprocessing yield rates and optimising the quality of returning cullet would require the development of refining techniques to improve the efficiency of sorting and reprocessing flat glass products containing adherent polymers/sealants (Hartwell et al., 2023).

Opportunities in glass recycling

By implementing a recycling cost on IGUs, this programme encourages network coordination and selective collection (Vlakglas Recycling Nederland, 2022). By allowing participation in different IGU lifecycle stages, deconstruction contractors' dynamic role—from destruction to reclaiming and reselling IGUs—supports the circular economy. Furthermore, producers are investigating take-back programmes, which provide advantages including lower energy usage, financial savings, and a decreased reliance on raw resources (Hartwell et al., 2023).

4.2.3 Current status of glass recycling

It is not unusual for end-of-life building glass to be recycled into new, lower-quality consumer glass goods like glass fibre or bottles, container glass. Nevertheless, it is rare to recycle end-of-life building glass back into Float glass, which frequently results in landfill disposal. Despite obstacles caused by the characteristics of the building glass, efforts are being made to increase recycling rates and resource efficiency in the glass recycling industry for building. This project supports Europe's objectives for sustainable, low-resource buildings (Oikonomopoulou et al., 2023a).

Container glass, characterised by its a straightforward composition is practically mono material (metal lids/ caps can be removed with a magnet, labels are burnt), facilitating its recycling process greatly. It doesn't contain contaminations such as plastics, making recycling easy. This simplicity allows container glass to be frequently recycled back into similar products, a practice well-established in the industry (Oikonomopoulou et al., 2023a). The process is supported by the relatively less binding quality standards and a well-developed infrastructure for collection and recycling of container glass. Typically, container glass is recycled in a closed-loop system, where the recycled glass is reused to create similar products. In contrast, the Float glass industry predominantly operates in an open-loop recycling system. Unlike container glass, Float glass used in architectural and automotive applications includes additional materials like coatings and frits, complicating its recycling process. This complexity necessitates specialised separation and treatment procedures, making recycling more challenging (Hartwell et al., 2023). This system is further elaborated in Figure 25.

4.2.4 End-of-life strategy

As highlighted by Bergmann (2020), an end-of-life strategy is crucial and should be considered at the initial stages of glass production development. This approach underscores that sustainability should be an integral part of the production development process, ensuring that the environmental impact is considered right from the beginning. Figure 26 illustrates the current linear treatment of glass. In 2022, Vlakglas Recycling Nederland

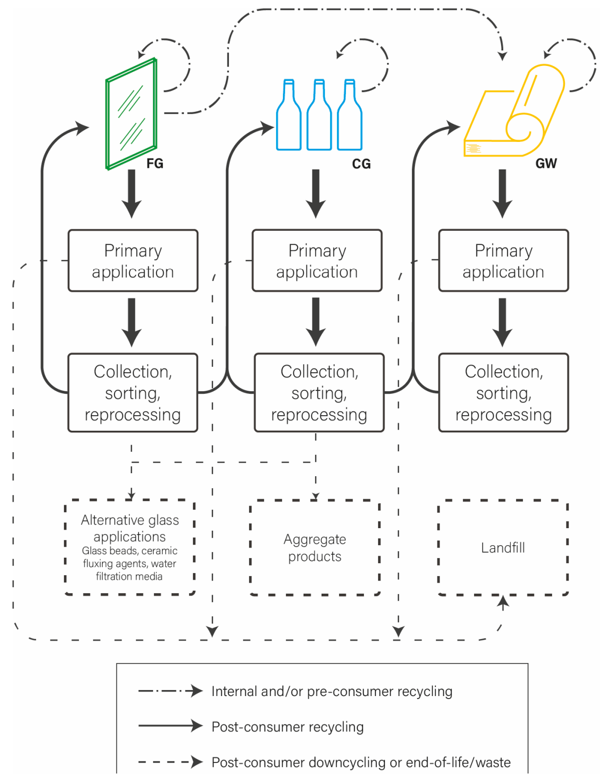

Figure 25: Schematic representation of the excisting recovery routes for flat glass (FG), container glass (CG) and glass wool (GW) and glass wool (GW) in the UK. (Hartwell et al., 2022)

managed to collect and prepare approximately 80,000 tonnes of flat glass. Despite these efforts, the proportion of glass recycled back into the flat glass manufacturing process was only about 9.3% in 2022, indicating a significant gap in achieving a closed-loop recycling system for this material (Vlakglas Recycling Nederland, 2022) Rota et al. (2023) emphasise the construction sector's high energy use and the need for circular practices, such as design for disassembling. It is crucial for effective material recovery and recycling, particularly for difficult materials like construction glass. Additionally, Geboes et al. (2023) report that a considerable 54% of C&D waste is still sent to landfills, highlighting a significant potential for enhancing waste management in construction. Therefore, this thesis will concentrate on glass from C&D waste, aiming to investigate and establish sustainable methods for handling glass waste, specifically in the context of recycled panels for load-bearing facade applications.

4.3 C&D glass waste treatment

4.3.1 Difficulties in C&D waste treatment

The construction sector has a large environmental impact, mostly due to its high CO2 emissions and production of building and demolition debris. With an emphasis on sustainable material use, the EU is moving towards a

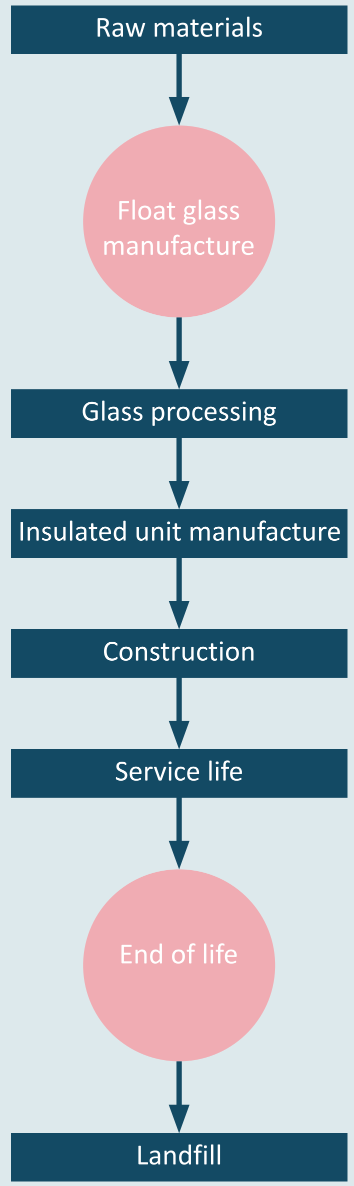

Figure 26: Linear life-cycle of glass manufacturing and processing. (DeBrincat & Babic, 2023)

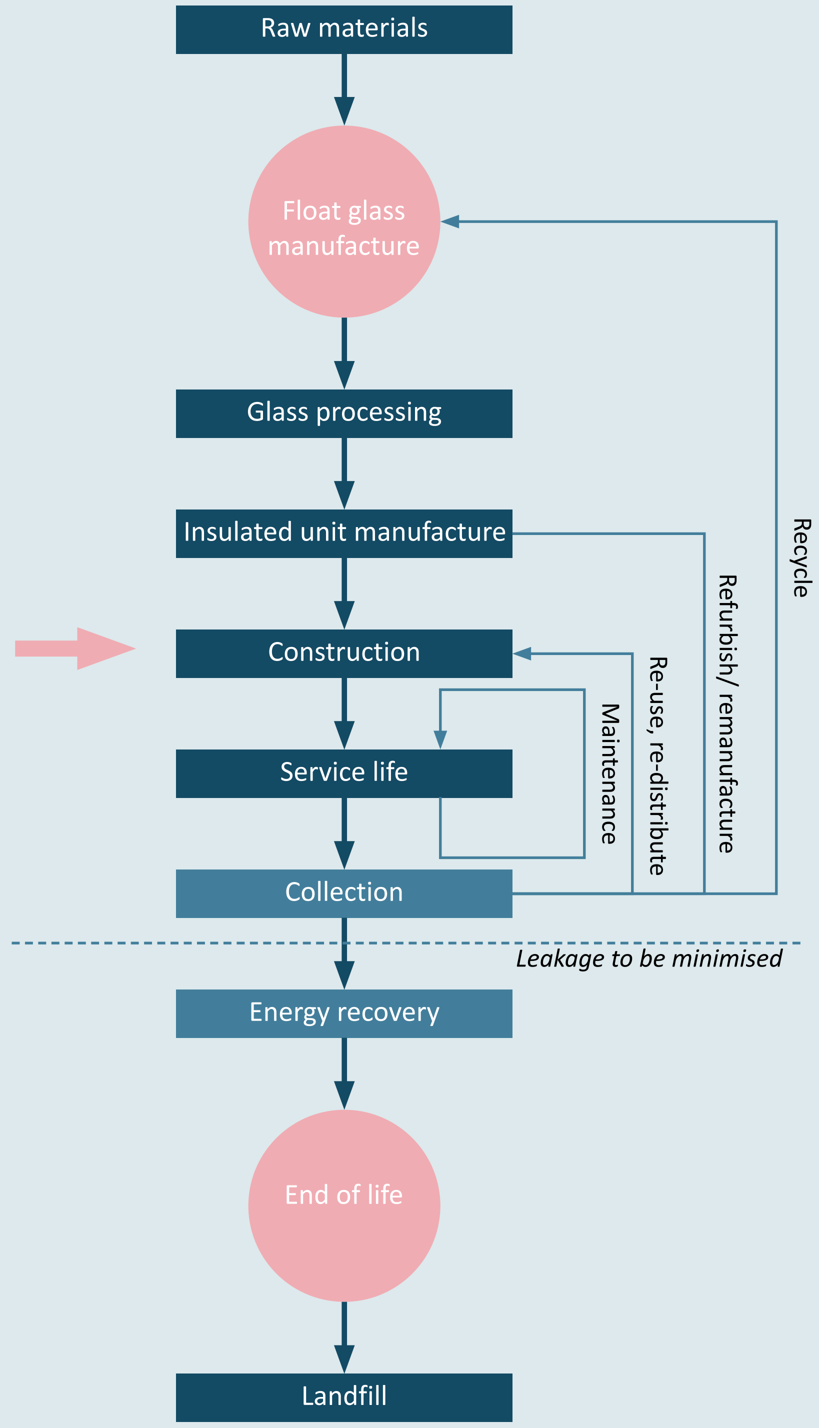

Figure 27: Circular economy diagram adopted for glass industry. (DeBrincat & Babic, 2023)

zero-waste building industry with the goal of becoming climate neutral by 2050 as part of the European Green Deal. Researchers like DeBrincat (2023), Geboes et al. (2023) and Bristogianni & Oikonomopoulou (2023), and also Rijksoverheid (2023) emphasise the significance of this goal for environmentally friendly building practices. In recent years, the management of C&D glass waste has received a lot of attention from the scientific and industrial communities. This interest is a result of realising that despite advancements, the sector still faces many obstacles and unrealised potential. Understanding glass in its current state (Figure 26) and seeing its potential in the future (Figure 27) are the first steps in the recycling process.

The greatest obstacle to efficient glass waste management continues to be the general lack of knowledge about which products can and which cannot be recycled. This indicates a discrepancy between the material's potential and current use, along with the short service life of insulating glass units (double and triple glazing) (Oikonomopoulou et al., 2023).

According to Bristogianni et al. (2019), research efforts are increasingly focused on recycling consumer glass, which is a common glass waste. But as Glass for Europe (2020) notes, the industry standard technique is a high-volume, capital-intensive process, particularly in the manufacture of Float glass. The fact that these plants run constantly to reduce expenses and energy consumption makes it difficult to integrate new recycling technology because they only permit restricted updates.

The findings of Geboes et al. (2023), note that the reuse of pre-consumer IGUs is small and accounts for only a percentage of the total collected pre-consumer waste, further highlight this potential gap. According to the Flemish Living Lab study (Galle et al., 2019), Figure 28's Sankey diagram shows that 92 kilotons of pre-consumer flat glass trash were recycled mostly in 2015. 35 kilotons were recycled openly into items like glass wool insulation and container glass, and the remaining 57 kilotons were recycled closed-loop for high-value applications.

The necessity for space and resources for storage and remanufacturing is impeding efforts to repurpose post-consumer IGUs, which range from being integrated into furniture to being utilised in greenhouses (Geboes et al., 2023). Figure 29's Sankey diagram illustrates the post-consumer flat glass journey in Flanders, including its sources, collection techniques, and applications (Geboes et al., 2023).

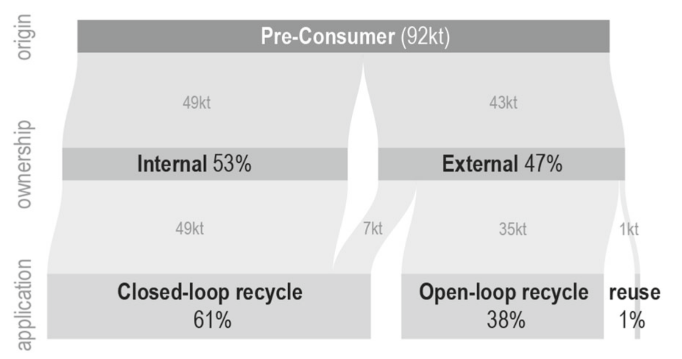

Figure 28: Sankey diagram of the pre-consumer flat glass flow per origin, ownership, and application in Flanders, expressed in kilotonnes (reference year 2015). Results from and figure based on Debacker et al. (2021.). (Geboes et al., 2022)

4.3.2 Innovations in C&D waste management

Even though architectural glass makes up just around 0.66% of C&D trash, Bergmann (2020) claims that the amount of end-of-life glass generated from this waste is substantial. This emphasises how important it is to manage these resources effectively. Modifications to EU waste legislation are upcoming, which presents an opportunity chance to boost building glass recycling in Europe, as pointed out by Glass for Europe (2014).

While end-of-life building glass contains a high percentage of recyclable materials, it is frequently not recycled into new glass products. Instead, it is often crushed and disposed of in landfills alongside other construction materials or recovered together with C&D waste (Glass for Europe, 2014).

There are numerous potential advantages to increasing the use of recycled glass. For example, according to Glass for Europe (2020), increasing the use of recycled glass might result in a 7% decrease in CO2 emissions. The collection and recycling of waste glass, especially from windows and other end-of-life construction materials, still faces significant challenges. Glass recycling is still far from reaching its full potential, even with the continent's high recycling average of 61% (FEVE, 2021) and the UK's growing trend (Edgar, 2008).

To address these challenges, a coordinated plan is essential. The primary focus of the supply-chain barrier lies in the logistics aspects of gathering, handling, and recycling exterior glass cullet. This underscores the necessity of well-organised collection, sorting, treatment, and recycling programs, particularly for glass types other than soda-lime glass (Bristogianni & Oikonomopoulou, 2023a).

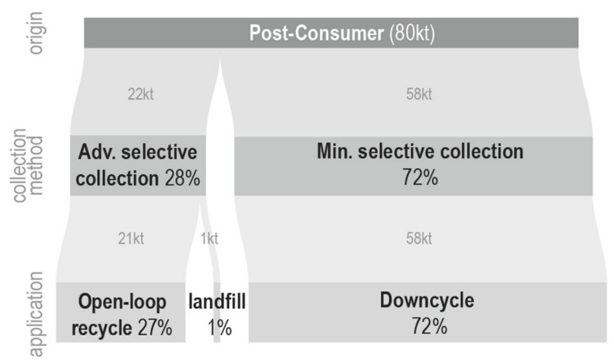

Figure 29: Sankey Diagram of the post-consumer flat glass flow per origin, ownership, and application in Flanders, expressed in kilotonnes (reference year 2015). Results from and figure based on Debacker et al. (2021) . (Geboes et al., 2022)

The problem of glass waste can be effectively resolved by establishing international and national recycling standards as well as providing governmental incentives for the use of recycled materials (Bristogianni & Oikonomopoulou, 2023a). According to Graeme DeBrincat (2023), there is a market for waste management companies that handle framed windows and IGUs, and this industry is expanding, providing a strong financial motivation for recycling glass.

In conclusion, recycling of architectural glass and CO2 emission reductions in the glass industry have improved, but much more needs to be done. The future of C&D glass waste treatment depends on resolving issues with awareness, legislation, and logistics. The industry may be pushed towards a more sustainable and effective use of glass by utilising recycling technologies. This will have a major positive impact on the development of a circular economy.

4.4 Cullet utilisation

4.4.1 Cullet definitions

Three types of cullet exist in the production of glass: internal, pre-consumer and post-consumer cullet. When a product has been modified or glass failed to meet the quality requirements, internal cullet is generated within the glass producing facility as a result. Pre-consumer cullet is waste that is produced during the later stages of the production of glass products, before it is consumed (Hartwell et al., 2022). It's critical to distinguish between glass waste that comes from pre- and post-consumer sources. Pre-consumer cullet, which comprises leftovers from productions like the creation of jumbo sheet glass, is produced during the making of glass products. This kind of cullet is frequently recycled or utilised again in high-value applications; it is never sold to consumers (Geboes et al., 2023; Hartwell et al., 2022).

Conversely, post-consumer cullet is glass waste from items that have been used by customers and have come to the end-of-life. The strength values of post-consumer glass can be comparable to those of pre-consumer glass, indicating that it can be reused in a variety of applications (Rota et al., 2023). However, because contaminants like silicone or butyl must be treated, returning post-consumer glass to the Float factory is frequently more complicated and costly than dumping of it in a landfill (Geboes et al. 2022). As has been said, there are difficulties with this kind of cullet, like contamination and difficult recycling procedures. The procedure gets more complicated after coatings, laminations, or other treatments are done and the glass is put on the market. During glass its service life, estimating contamination levels in glass becomes increasingly challenging, thereby complicating recycling efforts. Bergmann (2020).

Presently, post-consumer cullet lacks a worldwide standard or specification. The European Commission's Joint Research Centre (JRC) (2011) guidance document describes the end-of-waste standards for reprocessed cullet. It was created by analysing an extensive amount of literature and consulting technical specialists in the European glass sector. An overview of the minimum quality standards for "furnace-ready" cullet is provided in this guidance, along with the maximum amounts of common contaminants from metals, organic, and inorganic components that are permitted for the container glass, flat glass, and glass wool sub-sectors (Hartwell et al., 2022).

4.4.2 Cullet classifications

According to Arup, the glass recycling sector has created three main types of glass cullet. (Figure 30):

Class A Cullet: The best grade, Class A cullet is highly prised for direct use in the manufacturing of new glass since it is uncontaminated. There is potential to increase the amount of Class A cullet collected from post-consumer sources, however the majority currently originates from pre-consumer sources (DeBrincat & Babic, 2023). Class A cullet is glass that is cut or drilled.

Class B Cullet: Generally used for applications such as coloured container glass or glass wool insulation, Class B is a mixed quality cullet that may contain certain impurities. Continuous attempts are being made to advance technology such that Class B cullet might potentially be utilised in the production of Float glass (DeBrincat & Babic, 2023). Class B cullet is glass that is coated, laminated, tinted or printed

Class C Cullet: This is contaminated glass that shouldn't be remelted and is frequently utilised for other purposes like aggregate or road paint. (DeBrincat & Babic, 2023). Class C cullet is glass that is heat treated or chemical treated and also the glass from IGUs containing metal spacers.

Apart from these divisions, it's crucial to recognise the various kinds of cullets. For example, clear cullet is made up of clean off-cuts of flat glass, and mixed cullet includes all clean off-cuts of standard flat glass. Items that need to be properly segregated include sealed units, mirrored glass, tinted glass, laminated glass, wired glass, and printed glass (Surgenor et al., 2018). The acceptable requirements for mixed cullet and clear cullet are summarised in Table 10.

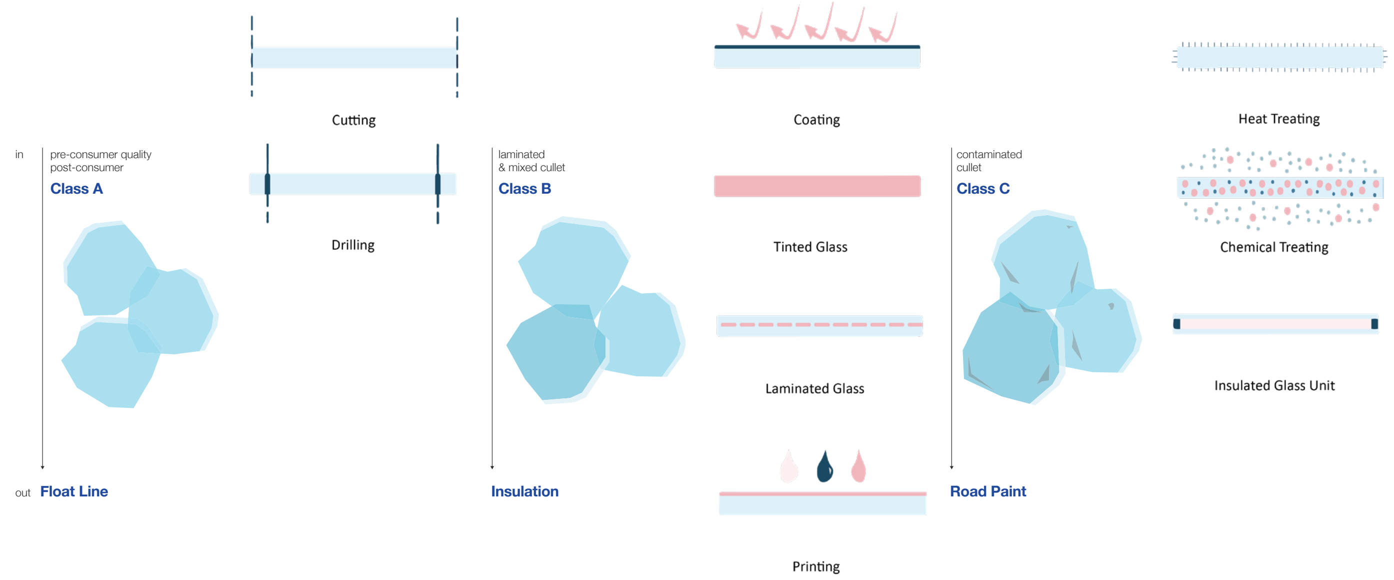

Figure 30: Grades of cullet. (DeBrincat & Babic, 2023) and added illustrations of the classification types

Clear cullet				
Off-cuts of clear flat glass only. The following are not permitted:				
Heat resistant glass	Laminated fire glass	Other glass	Metals	Other waste
BoroFloat Pyran Robax Cran	Pyrostop Pyrodur Pyroguard	Sealed units Mirrored Laminated Windscreen Wired	Drink cans Spacer bars Cutting blades	Foam spacers Paper Plastics Cutting disks Stones
Mixed cullet				
All clean off-cuts of standard flat glass should be placed in a clear cullet bin/skip				
Only: - Sealed units - Mirrored glass - Tinted glass - Laminated glass - Wired glass - Printed glass				
The following are not permitted:				
Heat resistant glass	Laminated fire glass	Metals	Other waste	
BoroFloat Pyran Robax Cran	Pyrostop Pyrodur Pyroguard	Drink cans Cutting blades	Foam spacers Paper Plastics Cutting disks Stones	

Table 10: Specifications for clear and mixed cullet: a comparative overview (Surgenor et al.,2018)

4.4.3 Usage of cullet in glass production

Advantages in the manufacturing process

For environmental and economic reasons, the use of glass cullet in the manufacturing process has grown in importance. Cullet use in glass batches has increased significantly in recent years, from 20% to 26% (Glass for Europe, 2020). Utilising cullet lowers the requirement for raw materials while also reducing energy use and CO2 emissions. According to Surgenor et al. (2018), specifically, 1.2 tonnes of raw materials are saved for every tonne of cullet used, reducing the need for mining of raw materials. Hartwell et al. (2023) also point out that using 100% post-consumer cullet in place of 100% original raw material saves 27% energy and 41% of CO2 emissions, demonstrating the significant environmental advantages of cullet utilisation. The possible reductions in emissions that can be achieved by using cullet at different phases of the flat glass manufacturing process are illustrated in Figure 31 and Figure 32.

Furthermore, using cullet has three advantages. First, when you increase the same quantity of raw materials by a factor of roughly 1.2, there is a reduction in the energy and emissions related to their obtaining and processing. The breakdown losses sustained during the melting process of the carbonate primary raw materials during stage 2 are the cause of the 20% variation in the total mass input needed. Second, for every 10% increase in cullet, it permits the glass furnace to run at a lower temperature, which subsequently lowers the energy consumption of the main processing stage by 2.5–3.0% (Beerkens et al., 2011). Consequently, Figure 31's highlighted related combustion emissions are decreased. Lastly, by using cullet that has already experienced thermal breakdown in place of carbonate raw materials that require calcination, process emissions are decreased. The relative CO2 emissions savings from using cullet at each stage of the glass production process are displayed in Figure 32 (Hartwell et al., 2022). However, the transportation and treatment costs associated with recycling waste flat

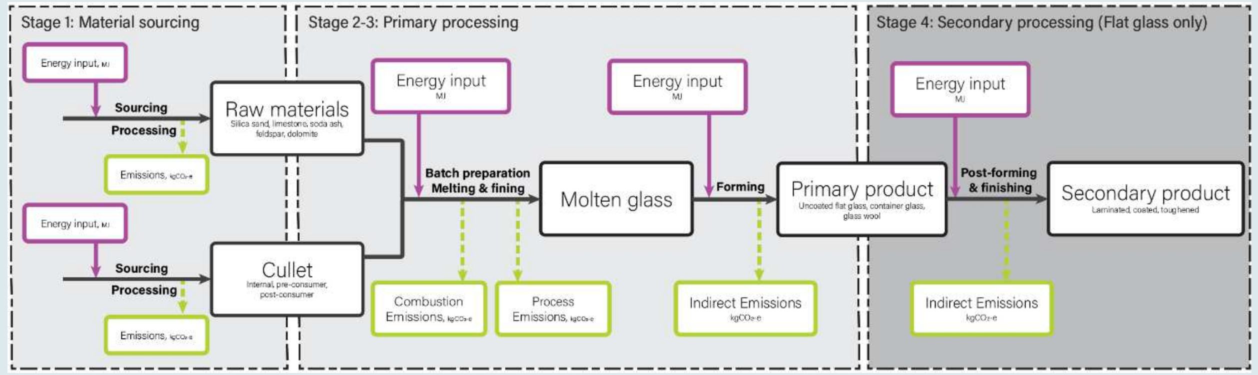

Figure 31: Energy inputs and corresponding emissions associated with glass products including: raw material sourcing and processing (stage 1), primary glass production (stage 2-3) and secondary flat glass processing (stage 4). (Hartwell et al., 2022)

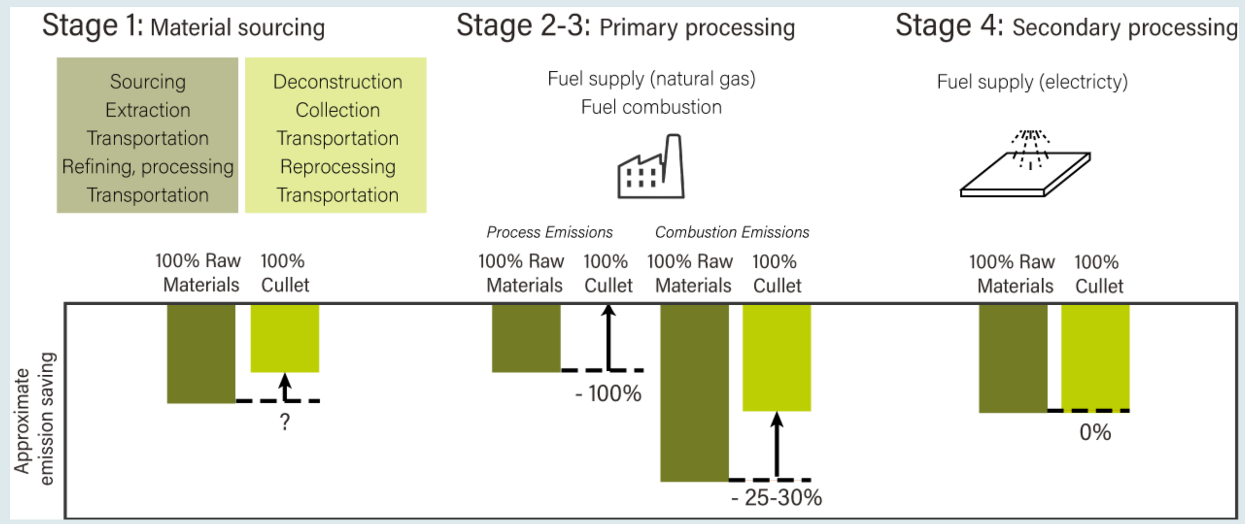

Figure 32: Schematic of emission savings potential from the use of cullet t each stage of flat glass production. (Hartwell et al., 2022)

glass into cullet are high. Considering these costs, Inano et al. (2023) emphasise the need for stronger financial encouragement to increase the growth of glass recycling.

Types of cullets used in the glass production

DeBrincat and Babic (2018) state that producers of flat glass frequently incorporate 10–25% cullet into their new glass manufacturing process. There is very little post-consumer waste, estimated to be less than 1% in the UK. The challenge of effectively gathering clean, flat glass cullet is the primary barrier to higher post-consumer recycling rates (JRC European Commission, 2011) (Hartwell et al., 2022). Closed-loop recycling is hindered by large-scale flat glass companies' unwillingness to use external, post-consumer glass cullet, particularly for architectural glass. This hesitation is a result of the strict requirements for quality that flat glass products have to achieve. Because of this, the recycling process is usually restricted to internal cullet or flat glass that has not been altered or contaminated—mostly pre-consumer glass.

External cullet, or post-consumer waste, on the other hand, usually ends up in open-loop recycling since it doesn't fit the requirements for closed-loop recycling. This involves recycling waste glass into various products, such as foam glass, glass wool insulation, and container glass. This division of the recycling procedures draws attention to the obstacles and constraints that the glass recycling industry faces in achieving a closed-loop system (Geboes et al., 2023).

4.4.4 Contamination problems

Flat glass must be free of impurities such as metals, organic compounds, glass ceramic, stones, porcelain, and hazardous elements in order to be recycled. These contaminants may come from IGU components or other building materials. According to DeBrincat et al. (2018), even minimal pollution levels in a furnace can result in several days of production loss, outweighing the financial and environmental advantages of recycling. Significant harm may result from this contamination (Geboes et al, 2023). The impact of the different contaminations on the structural performance of glass is illustrated in Figure 33.

To meet quality standards, flat glass must have a total of 0.5 g/tonne (0.5 ppm) or less non-ferrous impurities (Hartwell et al., 2022). For instance, reprocessing and recycling clean, tempered glass that has been recovered without interface parts into "furnace-ready" cullet is a straightforward operation. Nevertheless, recycling ceramic-Fritted glass creates difficulties since ceramics have a high melting point and can contain ceramic particles in the final product. Additional difficulties arise when laminated glass is reintroduced directly into the Float glass tank because the PVB interlayer has the potential to alter the controlled redox state of the glass (Beerkens, 1999; Beerkens et al., 2011; Hartwell et al., 2022).

Table 11 provides an overview of the recyclability of various glass processing steps. Recycled glass that has been laminated presents additional difficulties due to the need for separating the layers and removing the laminate layer. Glass coatings burn off during remelting and do not impede recycling. On the other hand, glass cannot currently be recycled again because of ceramic frit (DeBrincat & Babic, 2023). The recycling potential of glass is not adversely affected by heat strengthening or toughening procedures.

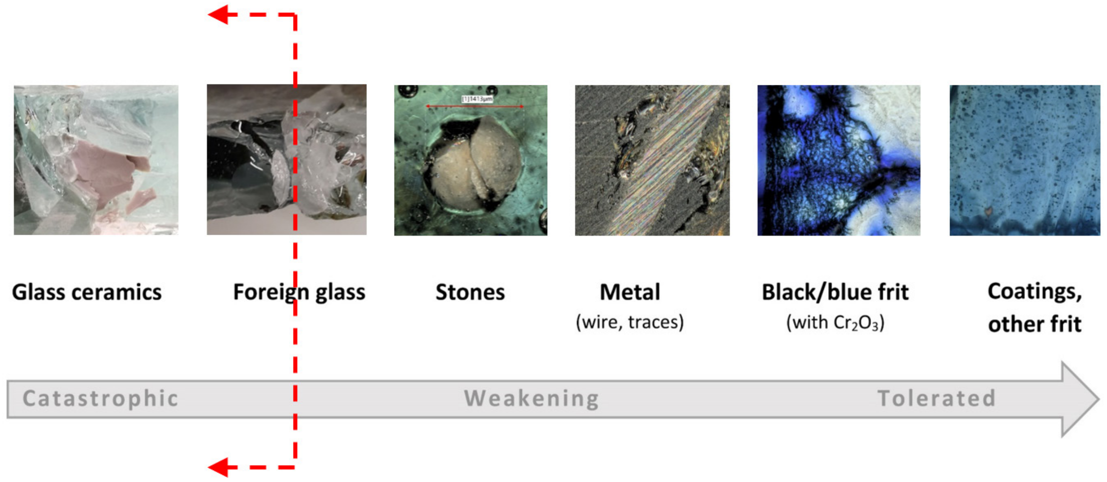

Figure 33: Ranking of the impact each type of flaw may have on the hosting glass network (Bristogianni, 2022)

Glass process	Stage	Recyclability to			Remarks
		Float	Container	Mineral wool	
Annealing	Internal	x	-	-	Internal cullet—readily recyclable
Cutting and edge processing	Internal	x	-	-	Internal cullet is recycled almost at 100% internally. Cullet from cutting lines of building and car glazing production are generally not contaminated. Glasses of different colors have to be separated to be recycled to Float glass manufacture
	Pre-consumer	x	x		
Tempering	Internal/ pre-consumer	x	-	-	No effect on recyclability if internal process
Laminating	Pre-consumer	-	x	x	Delamination (separating glass and foil) is technically feasible, but related to high expense. The resulting glass cullet usually contains less than 0.1% by weight of PVB
Coating (hard/soft), Mirroring	Pre-consumer	x	-	-	Coatings can be burnt off in the remelting process, so they can be mostly recycled. Metal contamination (e.g. silver from mirrors) can be absorbed in an internal recycling process when it is known and calculable. Once considered post-consumer the same material is down-cycled to other products
	Post-consumer	-	x	x	
Ceramic printing and fritting, enamel	Pre-consumer	-	-	-	Recycling of such glass is currently not possible (e.g. ovendoors, enamelled windscreens, architectural glass)
Wired-glass	Pre-consumer	-	-	-	Recycling of such glass is currently not possible
Insulating glass units (assembled, multi-material)	Post-consumer	-	x	x	Requires removal of the spacer bars and edge seals. Danger of contamination due to traces of adhesive or metals and due to differences in chemical composition (colour contamination) renders its recycling back to Float glass particularly challenging
Automotive glass (assembled, multi-material)	Post-consumer	-	x	x	Requires challenging and expensive logistics linked to the separation and treatment processes due to variety of colours, contamination by foreign matters, lamination, black enamel, use of different types of glass, which renders such cullet more expensive than new raw materials

Table 11: Principal recyclability streams of flat glass according to processing steps based on (Surgenor et al. 2018) and (Kasper 2006)

05 | TU DELFT CASTING RESEARCH

5.1 Restruct cast glass

Glass's involvement in the developing field of sustainable design is quite significant and has a lot of promise, especially when it comes to waste management and recycling. As demand increases for the exploration and utilisation of Float glass waste, current research and experimental data serve as a starting point toward developing innovative recycling techniques for architectural applications. The investigation into glass recyclability isn't solely about adopting a circular approach; it signifies a transformative shift in how we utilise glass in contemporary architecture. (Bristogianni & Oikonomopoulou, 2023).

The specialists from the Restruct group, well-known for their expertise in structural mechanics, materials, and design, are in charge of this expedition. The Restruct Group's team for Glass and Transparency and the team for Sustainable Structures are depicted in Figure 34. Their work with glass, a material embodying both aesthetics and sustainability, is central to their pursuit of innovative, eco-friendly, and visually appealing architectural solutions. One of their most notable projects, the Amsterdam Crystal Houses façade by MVRDV Architects, is a prime example of this forward-thinking methodology. This project combines the inventiveness of contemporary glass technology with classical masonry. Here, the façade is a transparent copy of a 19th-century masonry elevation, thanks to the use of cast glass bricks (Bristogianni et al., 2019). Figure 35 displays pictures taken at various phases of the design process. The completed glass bricks are shown in Figure 35a; a mechanical test on the glass brick wall is shown in Figure 35b; and the ultimate product, a cast glass brick façade, is shown in Figure 35c.

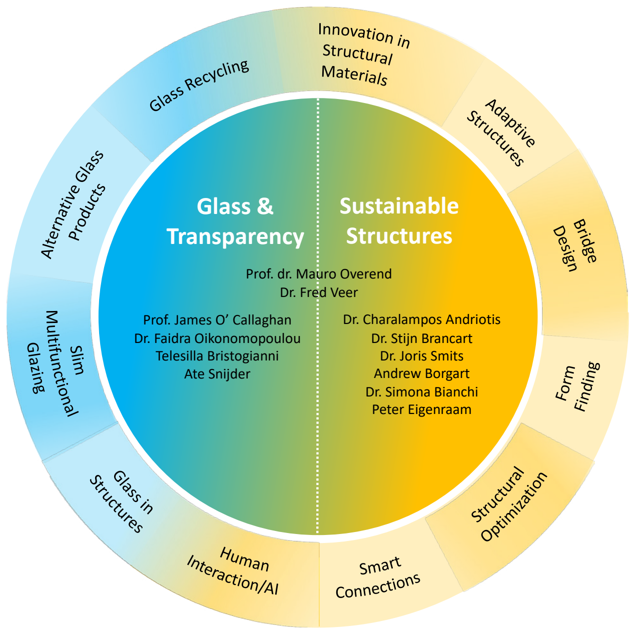

Figure 34: Restruct Group and their specification (Restruct TU Delft, 2024)

Unfortunately architectural design is severely constrained by the Float glass industry's present dominance. The potential forms and shapes of all-glass constructions are limited by the industry's emphasis on planar, two-dimensional glass components. This creates a major barrier to sustainable glass design, along with the difficulties in recycling and reusing architectural glass because of difficult disassembly and contaminants from coatings and adhesives. One possible answer to these problems turns out to be cast glass. Its capacity to go beyond the two-dimensional limitations of Float glass creates new opportunities. It is possible to create solid, three-dimensional glass components that have larger cross-sections and practically any form by pouring molten glass into moulds. By using the entire compressive strength of glass, these monolithic components may be made to interlock and form massive, simply constructed structures without the need for adhesives (Bristogianni & Oikonomopoulou, 2023). The Restruct group has been exploring several options, as shown in Figures 36 and 37, which show how glass waste cullet may be used to make cast glass elements.

Furthermore, cullets may be used into cast glass as a perfect medium because of its larger cross-section, which permits a higher degree of impurities. Cast glass works well with mixed or imperfect glass. This feature is very important when discussing sustainability since it offers a chance to reintegrate leftover glass into the supply chain, directly addressing the problem of glass waste. This innovative approach can be observed in TU Delft's pioneering work in this domain, especially in their Re3 Glass project. By investigating the creation of volumetric cast glass components, the project seeks to push the limits of conventional Float glass. In doing so, it opens up new possibilities for using glass in buildings, where innovative design, reusability, and recycling, moving towards a circular economy.

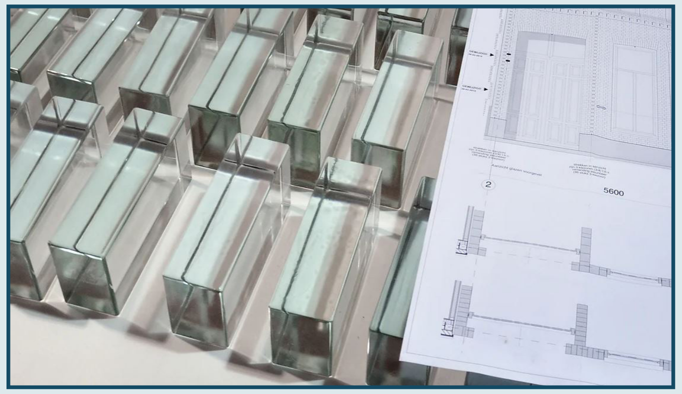

(a)

(b)

(c)

Figure 35: (a) Glass bricks used for the facade of Crystal Houses, (b) Mechanical tests conducted to verify the structural integrity of the building facade with glass bricks and (c) The final appearance of the glass brick facade. (Restruct TU Delft, 2024)

5.2 Innovations and challenges in glass casting

5.2.1 The development of glass casting processes

Expanding on the initial work of the Re3 Glass project, this thesis delves deeper into the investigation of glass casting as a transforming factor in recycling, as well as specific architectural applications. The innovative approaches shown here are redefining how waste glass is used, turning obstacles in the recycling process into chances for the glass industry's circular growth.

Innovative glass recycling techniques that are primarily flexible are urgently required. These techniques need to be able to manage changes in the composition of glass and withstand increased levels of contamination in the end products. One innovative approach, as previously mentioned, involves casting volumetric glass components from glass waste. It is particularly useful for recycling post-consumer glass with little to no pre-processing because of its adaptability and capacity to handle a wide range of glass compositions and high contamination levels (Bristogianni, 2022; Bristogianni & Oikonomopoulou, 2023a, 2023b; Bristogianni et al., 2018a).

Furthermore, research at TU Delft examines the advantages of cast glass components from a structural standpoint. (Bristogianni et al., 2020). Figure 38 shows the quality grading of various types of glass waste based on the strength of castings made just above their liquidus point. (Bristogianni & Oikonomopoulou, 2022). This figure shows that Float combo is initially unsuitable, but removing the critical contaminants will increase its structural performance.

5.2.2 Barriers and opportunities in glass casting

Opportunities in glass casting

The adaptability of the glass casting technique is one of casting its main advantages. It makes it possible to utilise several glass recipes in the same moulds and furnace, preserving efficiency during each cycle of annealing. A significant benefit over thin-walled alternatives, Float glass, is this flexibility. Volumetric glass components, can be recycled in a closed loop in their as-received form, minimising the requirement for treatment and purification. It is expected that volumetric glass components will withstand a significantly higher contamination rate than thin-walled glass. (Bristogianni & Oikonomopoulou, 2023a, 2023b; Bristogianni et al., 2021b; Bristogianni et al., 2020).

The TU Delft Glass & Transparency Lab's experimental testing on cast glass components shows that a small number of air bubbles or inclusions (such as ceramic stones) within the bulk of the cast glass components—which don't exceed a millimetre in diameter—do not significantly affect the structural performance (Bristogianni et al., 2018b).

05 | TU DELFT CASTING RESEARCH

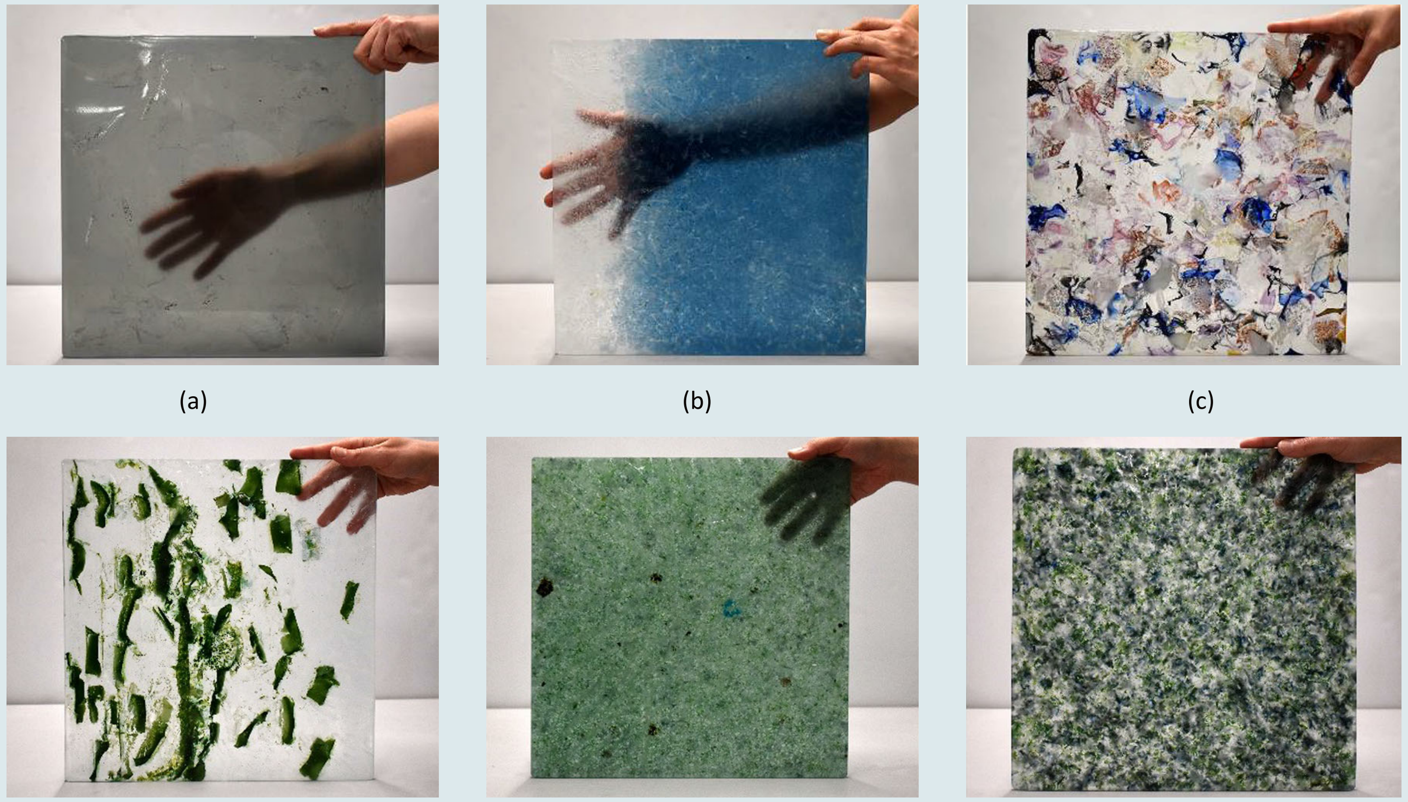

(a) (b) (c)

(d) (e) (f)

Figure 36: (a) Glass kiln-cast panels (350*350*10 mm) made at TU Delft from glass waste cullet, namely Cathode-Ray Tube (CRT) front screen, (b) transition Float glass from clear to blue, (c) CRT back screen and crystal coloured glass, (d) enamel Float glass, (e) automotive glass and (f) oven doors. (Bristogianni & Oikonomopoulou, 2023)

(a) (b) (c)

(d) (e) (f)

Figure 37: (a) Interlocking waste glass component, (b) Interlocking waste glass component, (c) Structural cast glass components out of different glass waste streams, to be used in an interlocking wall system, (d) Structural cast glass components out of different glass waste streams, to be used in an interlocking wall system, (e) Re3 casted component and (f) Re3 casted component. (Restruct TU Delft, 2024)

Barriers in glass casting

However, similar bubbles or stones in a 6/8 mm thick glass panels would significantly reduce both the product's strength and aesthetic appeal. These flaws need to be addressed in the glass casting process, especially since impurities and inclusions with different thermal expansion rates can lead to fractures. Additionally, while colour changes are generally undesirable to customers and the industry for aesthetic reasons, they can add value in cast glass elements (Bristogianni et al., 2020).

Ensuring the quality of recycled glass requires careful attention to the post-processing, surface and edge treatment, phase. The thoroughness of the recycling process is further emphasised by the necessity of this step in correcting surface imperfections (Bristogianni et al., 2020).

Cast glass offers a lot of promise for a variety of load-bearing architectural applications. Glass may be fully utilised for its stated compressive strength by creating volumetric glass components by casting. Unfortunately, cast glass lacks engineering, production, and quality control standards, and its mechanical properties are unclear due to a variety of chemical compositions and a lack of knowledge about the impact of flaws in the bulk of the glass. These factors prevent cast glass from being widely used (Bristogianni et al., 2021b).

5.3 Composite cast glass

Recent years have witnessed remarkable progress in the production and recycling of glass, especially in the area of cast glass panels. TU Delft researchers have made significant contributions to this field by creating composite cast glass panels that include different types of glass waste. This paragraph explains the fundamental ideas, working methods, and uses of these cast composite waste glass panels, based on current studies.

5.3.1 Concept of composite cast glass panels

When inspecting cast glass components for quality control with a microscope, the most common flaws found are inclusions, crystallised interfaces, bubbles, infolds, internal strains, and surface damage from machining, post-processing, and mould contact. The severity of these defects depends on various factors, such as their location within the cast component (whether on the surface or within the bulk), their association with other flaws, and their specific characteristics relative to the properties of the glass matrix (material composition, toughness, elastic modulus, size of the panel, thickness of the panel). Intrinsic and extrinsic defects are differentiated, with the extrinsic defects potentially being more critical due to differences in thermal expansion between the defect and the glass composition. The distinction between the inclusion and the material composition of the glass is crucial, but occasionally, differences in the thermal expansion coefficient lead to strains that cannot be eliminated after annealing, thereby impacting the strength of the glass. Variations in thermal expansion can result in glass fracture during cooling (Figure 39).

Unsuitable	Weak	Moderate	Strong
Float combo*	Lead silicate	Float, dark frit	C-glass
Float metal*	CRT screen & funnel	Refrigerator glass	Float (standard, tinted, coated, light frits)
Borosilicate mix (automated)*	E-fibers	Oven Doors	Ba/Sr silicate (CRT screen)
Microwave*	Wired glass		Borosilicate (pure, mix/manual)
	Automotive glass*		

Figure 38: Quality grading of tested glass waste types, based on the strength obtained for castings performed slightly above the glasses' liquidus point (Bristogianni & Oikonomopoulou, 2023)

* Status obtained due to the precence of external contaminants (e.g. glass ceramics). Removal of these critical contaminants would automatically increase the strength of the recycled glass

	Glass ceramics	Borosilicate	Terracotta	Lead crystal	Soda lime silica	Steel	Aluminium
α at 20°C (10^{-6} K^{-1}):	0	3	5	8	9	12	22
K_{Ic} (MPa√m):	2.3	0.65-0.73	0.7-0.85	0.6	0.75	>50	>20
E (GPa):	95	63	45	69	72	210	70

Figure 39: The extent of difference in thermal expansion in combination with the size of a contaminant play the most crucial role in the probability of fracture of the glass matrix (Bristogianni, 2022)

Typical materials that can be traced in a recycled soda lime silica (SLS) cullet provided by the glass recycling industry, and their approximate thermal expansion coefficient (α), fracture toughness (KIc) and Young's modulus (E) in relation to SLS.

In the bulk, meso-level flaw structures are often tolerated. However, when these flaws are exposed at the surface and interact with other defects, they may reduce the glass's strength. This suggests the idea of a composite panel, whereby glass with a higher purity and fewer contaminants should be positioned at the surface, while glass with a lower purity and more contaminants should be placed in the bulk. (Bristogianni, 2023).

TU Delft's research on composite cast glass panels offers an innovative method for using glass waste. The basic concept entails building a three-layered structure (Figure 40):

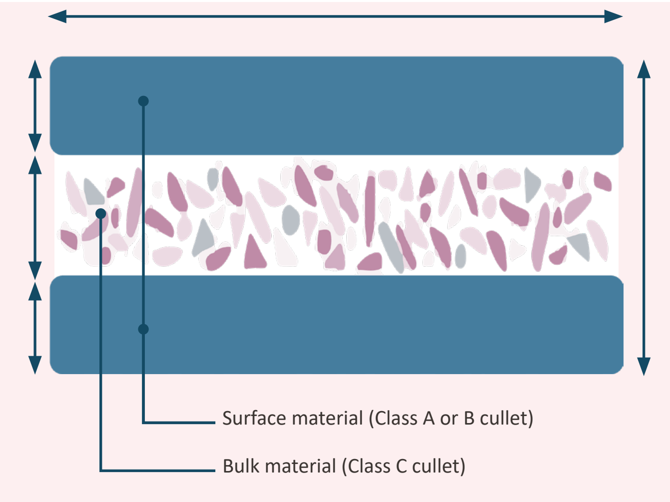

Figure 40: Ilustration of the principle of a composite cast glass panel

- **Bulk material**: In the bulk, glass with lower purity is used, containing more impurities and contaminants. This includes glass that has undergone heat treatment, chemical treatment, or glass from IGUs. Due to the high level of contaminants in post-consumer glass cullet, it is primarily used for the bulk of these panels. The glass used for the bulk is classified as C cullet glass.

- **Surface material**: On the surface, glass with higher purity is utilised, containing no impurities or contaminants such as cut or drilled glass. This corresponds to class A type cullets. Additionally, glass with minimal contaminants, such as coated, tinted, fritted, or laminated glass, is used, classified as class B cullet. Pre-consumer glass will be used for the surface.

Bristogianni and Oikonomopoulou (2023) highlight that surface imperfections/ flaws often constitute the primary cause of failure in Float glass and (large) cast glass components. Therefore, by employing higher-quality glass on the surface to compensate for the weaker quality of glass in the bulk, this composite structure aims to enhance the strength and durability of the glass.

5.3.2 Manufacturing process

These composite panels are created using the kiln-casting method. To begin, moulds are produced, and different layers are stacked on top of each other. The process starts with a sheet of class A or class B cullet, representing the higher purity layer. Next, cullets of type C are placed in the bulk, followed by another sheet of type A or type B cullet on top. This composite structure results in different quality zones within the glass. Several crucial elements contribute to this, including the size of cullets in the bulk (ranging from fine to large shards), viscosity variations between the surface and the bulk, as well as differences between various cullets and other contaminants in the bulk. These factors affect material differentiations and differences in thermal expansions, leading to stress and eventual fractures. Lastly, the forming temperature plays a significant role, as cullets may have different melting temperatures, influencing the outcome. (Bristogianni & Oikonomopoulou, 2023a).

5.3.3 Applications and functionalities

Beyond its structural purposes, composite cast glass panels find extensive use in fields such as interior and architectural design. These composite glass panels can provide:

- **Aesthetics**: According to Bristianogianni & Oikonomopoulou (2023a the ability to transition between opaque, translucent, and transparent states, as well as between dark and clear hues, through the use of mirrors, metallic elements, or tinted glass, allows for a diverse range of design applications that address privacy or shade requirements. Each panel will have an unique aesthetic characteristic.

- **Strength in diversity**: These cast glass composites can be customised for a wide range of architectural applications, catering to various strength requirements. They can be used for lower-strength purposes, such as bathroom tiles, or for high-strength needs in structural components like cladding for load-bearing facade applications, depending on the types of waste glass utilised (material composition) and the ratio between the surface and the bulk (the geometrical composition). (Bristogianni & Oikonomopoulou, 2023a).

5.3.4 Prior research findings

Important information on the creation and possibilities of these composite cast glass panels is supplied by Matskidou (2022). Important conclusions consist of:

- **Impact of cullet characteristics**: The material composition, contamination rates, and particle size of the cullet utilised have a major impact on the performance of composite specimens.

- **Stress generation and fracture patterns**: The way these composites behave under stress is an interesting feature.

The primary factors influencing the flexural strength of cast glass are its material composition and surface defect. Unless a significant defect is present at the surface, inhomogeneities or flaws in the bulk rarely impact the structural performance. Instead, the quality of the surface is of most importance for the structural performance. This means that surface engineering in composite glasses enhances both the flexural strength and fracture resistance of cast glass

5.3.5 Research gap

Studies from TU Delft already looked a bit into this topic. However, a lot is still unknown about the optimal geometry and parameters of these composite panels The ratio of the low quality cullet in the bulk to the high quality cullet at the surface is unknown. Also the material composition of the low quality bulk and high quality surface is unknown. Which leads to the research gap of this thesis. To address this gap the main research question will be answered as stated:

"What is the effect of the different parameters in respect to the geometry and glass composition of composite cast glass beams to their overall structural performance made out of C&D flat glass waste?"

Experiments will be conducted at the glass lab facilities at Stevin Lab II at Civil Engineering. Beams will be produced instead of panels for two main reasons: firstly, it is easier to test the structural performance of beams, and secondly, less material is required. If the concept of the beams proves successful, panels can be made using this principle.

Moulds for the cast beams will be produced at the Stevin Lab. The beams will be manufactured through several firing rounds and will undergo surface and edge treatments before undergoing a four-point bending test at the mechanical engineering department to assess their flexural strength. Subsequently, the beams will be analysed for crack patterns and the fracture origin, providing insights into their structural performance. Flaws will be investigated using a microscope to determine their impact on structural performance, focusing on whether they are located in the bulk or on the surface. Finally, experimental work will be conducted to improve and optimise the structural performance of the beams.

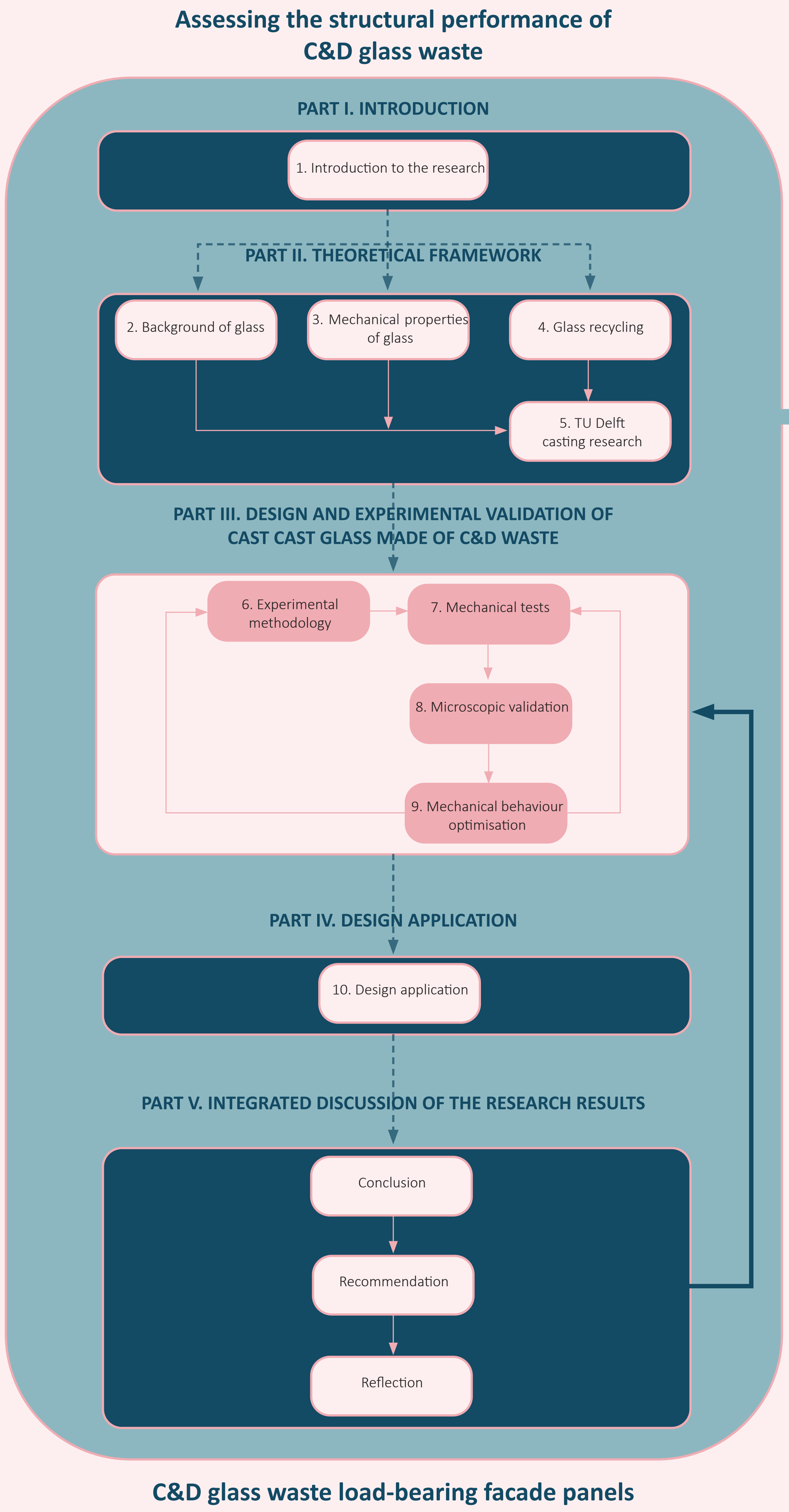

PART 3

DESIGN AND EXPERIMENTAL VALIDATION OF CAST GLASS MADE OF C&D WASTE

06 | EXPERIMENTAL METHODOLOGY

6.1 Experimental variables

This section thoroughly describes the experimental techniques necessary to understand the fields of glass recycling and casting research. It covers the experimental setup of all tests, including the preparation of the moulds and the selection of the cullets. This is followed by an explanation of the different fire rounds used to produce the beams. Afterward, a feasibility analysis of each beam is provided to determine their suitability for testing structural performance. The results are then discussed, and general overview tables are created to draw conclusions about the feasibility of different cast glass beams made from C&D waste. In summary, this section expands on the basic knowledge regarding the current and potential future states of glass recycling established in previous chapters.

6.1.1 Literature review on recycled cast glass

As discussed in paragraph 4.4.4: Contamination problems, contaminants on glass pose a major issue for recycling. These contaminants can be classified based on their impact on structural performance. They manifest as flaws either on the surface or within the bulk of the glass. Figure 20 illustrates the classification of casting defects and assesses their severity based on their characteristics and location within the glass specimen. The defects are divided into two categories: intrinsic and extrinsic. Intrinsic defects result from melting reactions, such as surface crystallization. Extrinsic defects arise from cullet contamination, including coatings and adhesives, or from poorly homogenised batches, leading to inclusions in the bulk, such as ceramics.

The quality of the C&D waste in the buckets is affected by contaminants. Some contaminants, like stones, can be removed more easily. However, removing contaminants such as coatings or laminated glass is still difficult and costly. Since this thesis focuses on assessing the structural performance of C&D waste cast glass beams, it is important to consider the influence of different flaws in the specimens, as visualised in Figure 33. Glass ceramics and foreign glass are particularly catastrophic to the beams because, as shown in Figure 39, the thermal expansion between the glass and these materials differs significantly, resulting in localised stress.

Furthermore, while larger stones weaken the glass, smaller ones are acceptable. Metallic pollutants such as wires weaken the glass under stress rather than causing it to shatter instantly. As shown in Figure 33, these types of flaws weaken the structural performance. Dark-coloured frits produce flakes that weaken the glass when they come into contact with the mold during casting. In contrast, light-coloured frits and properly applied coatings have little impact. As shown in Figure 33, these types of flaws are tolerated (Bristogianni & Oikonomopoulou, 2023a).

Numerous factors affect the quality of cast glass. It is essential to remember that each factor has the potential to impact the overall quality of recycled kiln-cast glass components. This is well illustrated in Figure 41, which explains how the quality grade of the beams is affected by cullet characteristics such as material composition, size, contaminants, thermal history (specifically the temperatures used in the firing schedules), and the type of defects, whether they induce stress or reduce strength.

The theoretical framework of this thesis will greatly assist in this part of the research. It will aid in the analysis of different contaminants and the evaluation of various cullet quality grades. This thesis primarily focuses on type B and type C cullet, as these two grades are the most challenging to recycle. Grade A cullet is not the main emphasis because it generally does not present significant obstacles in the recycling process. However, type A cullet will also be used as a help tool for the composite beams.

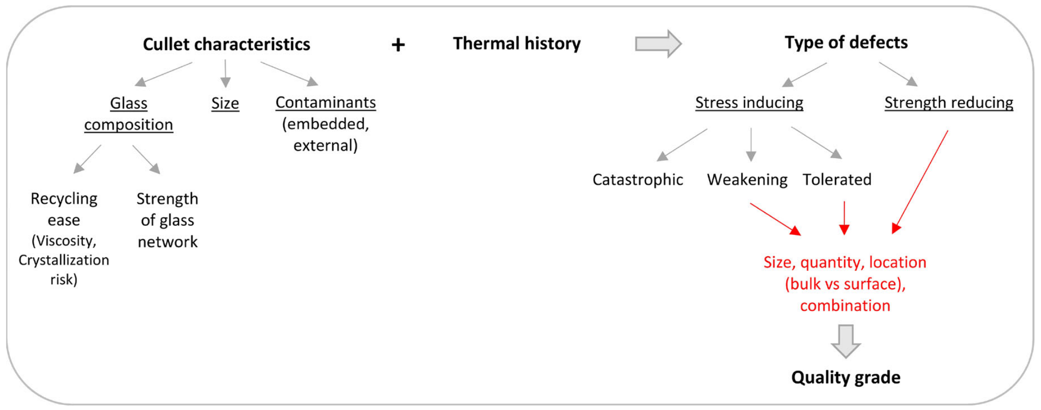

Figure 41: Parameters affecting the quality grade of the recycled kiln-cast glass component. (Bristogianni & Oikonomopoulou, 2023)

6.1.2 Experimenting with homogeneous and composite beams

The experiments were being conducted in the glass lab at Stevin Lab II in the Civil Engineering department. Various types of beams were being produced. It is essential at this stage to understand the impacts of temperature on the beams, the material composition of the cullets, and the influence of the mould designs. To achieve this, several experiments are proposed to closely examine how the behaviour of the cullets varies. For the setup of this research, four types of experiments are outlined, as depicted in Figure 42.

- **Homogeneous beams**: These beams serve as a reference group for comparison with the composite beams. They allow for an investigation into the influence of employing a composite strategy with higher quality glass on the surface.
- **Composite beams with different surface-bulk ratios**: These experiments aim to find the optimal ratio between the surface and bulk materials and to observe how this ratio affects structural performance.
- **Composite beams with different bulk materials**: These tests explore the impact of various bulk materials on the overall structural performance.
- **Composite beams with different surface materials**: These experiments analyse how different surface materials affect the overall structural performance.

Experiment type 1: Homogeneous beams

This experiment will conduct a comprehensive analysis of three different types of homogeneous beams. The types of cullets used for these tests are explained in paragraph 6.3, Cullet preparation.

- **Class A Cullet Beams**: These beams will involve testing with Float glass.
- **Class B Cullet Beams**: This will include testing glass with black frit and soft coatings. Two different types of coatings were investigated.
- **Class C Cullet Beams**: This category will examine glass with more harmful flaws. Beams with HR glass, beams with CSP pollutants, and beams with metallic pollutants (wires and traces) were investigated.

Experiment type 2: Composite beams finding the optimal ratio between surface and bulk

One of the primary objectives of this research is to examine how different types of recycled glass waste in a composite composition affect structural performance. To investigate this, the research closely examined several compositions where the ratio between the surface and bulk varied. As explained in paragraph 3.4.2 Stress, when testing the mechanical behaviour of glass, a four-point bending test is used. Pressure is applied to four different points, with compression occurring at the top of the beams and tension at the bottom. Since glass typically fails under tension, this research will focus on the two lower layers, which contain the tensile stress area. For the final product, a composite panel, a three-layer system will be utilised again.

Four different types of ratios between surface and bulk will be investigated for the experimental setup. The surface consists of type A cullet, specifically Float glass, while CSP pollutants are utilised for the bulk.

- **Surface: 6 mm and Bulk: 15 mm**
- **Surface: 8 mm and Bulk: 13 mm**
- **Surface: 10 mm and Bulk: 11 mm**
- **Surface: 12 mm and Bulk 9 mm**

The aim of these various setups during the experiment is to determine the optimal ratio of surface to bulk. It involves determining the thickness of the surface layer in millimetres at which flaws in the bulk become noticeable and start to impact structural performance.

Experiment type 3: Composite beams finding the influence of the bulk material

For this experiment, metallic pollutants will be used in the bulk instead of CSP pollutants. The objective is to determine whether the structural performance will be affected by the presence of different bulk materials. The surface consists of type A cullet, specifically Float glass, while Metallic pollutants are utilised for the bulk.

- **Surface: 8 mm and Bulk: 13 mm**
- **Surface: 10 mm and Bulk: 11 mm**

Experiment type 4: Composite beams finding the influence of the surface material

For this experiment, Fritted glass (type B cullet) will be used on the surface instead of Float glass (type A cullet). If the structural performance results of type B cullet on the surface do not differ significantly from those of type A cullet, it may indicate the potential to recycle more material for the composite beams.

- **Surface: 8 mm and Bulk: 13 mm**: CSP Pollutants are in the bulk
- **Surface: 8 mm and Bulk: 13 mm**: Metallic Pollutants are in the bulk

6.1.3 Further analysis

Mechanical validation

After the beams are produced, they need to be manufactured and prepared for the structural performance test. Surface and edge treatment must be carried out for each beam. The structural performance of each beam will be assessed using a four-point bending machine. According to this section of the research, beams constructed entirely of Class B cullet will be stronger than those constructed entirely of Class C cullet. Since composite beams will incorporate stronger glass (type A cullet) on the surface, they will be stronger than homogeneous beams.

Microscopic validation

After the structural performance test, the beams will be evaluated for their crack patterns, and the origin of the fracture will be analysed. This analysis is conducted using a microscope. The flaws are examined and investigated to determine which ones have the most harmful effect on structural performance. Additionally, the location of these flaws on the beam—whether at the surface or within the bulk—is analysed

Structural performance optimisation

To optimise the structural performance of the beams, experimental tests are conducted. The selection of cullets for the beams is optimised while analysing the influence of specific cullets. Additionally, the effect of temperature on the composite beams is examined to understand whether higher temperatures affect the compatibility between the cullets and between the bulk and surface.

Experiment type 1: Homogeneous beams

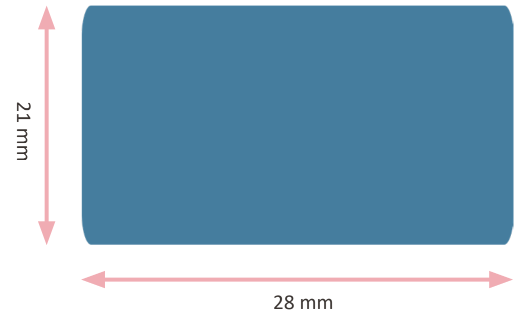

(a)

A homogeneous beam comprising type A glass cullet. This implies conducting tests using Float glass

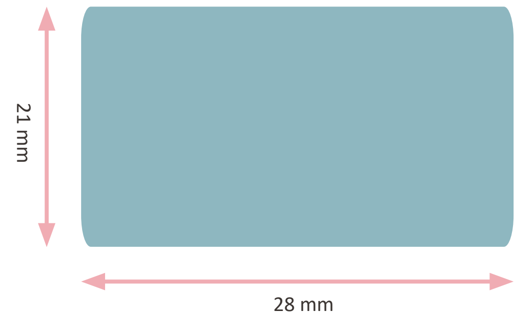

(b)

A homogeneous beam comprising type B glass cullet. This implies conducting tests using glass that is either coated or fritted.

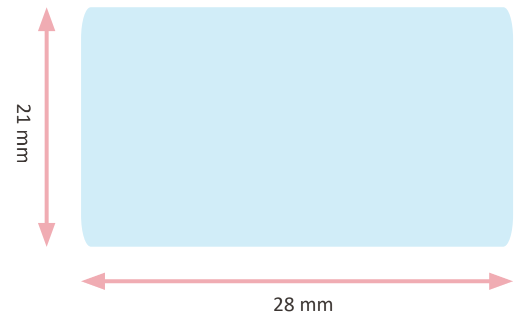

(c)

A homogeneous beam comprising type C glass cullet. This implies conducting tests using glass that is containing HR glass, CSP pollutants or metallic pollutants.

Figure 42: Experimental setup, (a) homogeneous beams with cullet type A, (b) homogeneous beams with cullet type B, (c) homogeneous beams with cullet type C , (d) composite beams ratio between surface and bulk variant A (6 mm Float glass), (e) composite beams ratio between surface and bulk variant B (8 mm Float glass), (f) composite beams ratio between surface and bulk variant C (10 mm Float glass), (g) composite beams ratio between surface and bulk variant D (12 mm Float glass), (h) composite beams with different bulk material variant A (8 mm Float glass), (i) composite beams with different bulk material variant B (10 mm Float glass), (j) composite beams with different surface material variant A (CSP Pollutants), (k) composite beams with different surface material variant B (Metallic Pollutants)

Experiment type 2: Composite beams finding the optimal ratio between surface and bulk

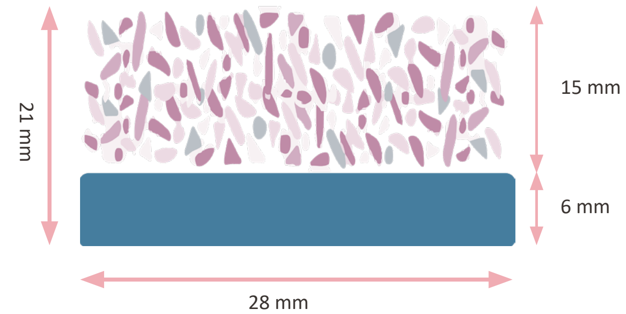

(d)

A composite beam featuring type A cullet on the surface and type C cullet in the bulk. It undergoes a ratio of 6 -15 mm.

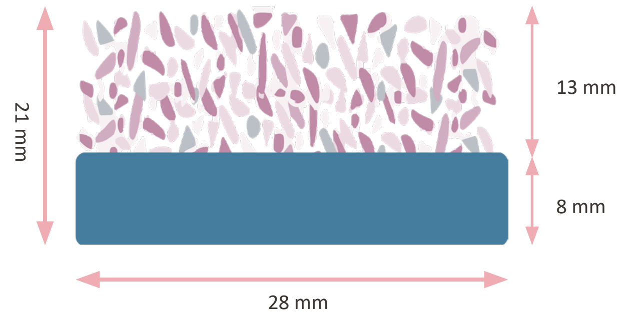

(e)

A composite beam featuring type A cullet on the surface and type C cullet in the bulk. It undergoes a ratio of 8 -13 mm.

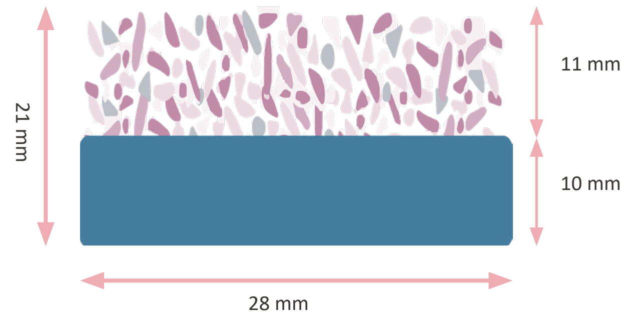

(f)

A composite beam featuring type A cullet on the surface and type C cullet in the bulk. It undergoes a ratio of 10 -11 mm.

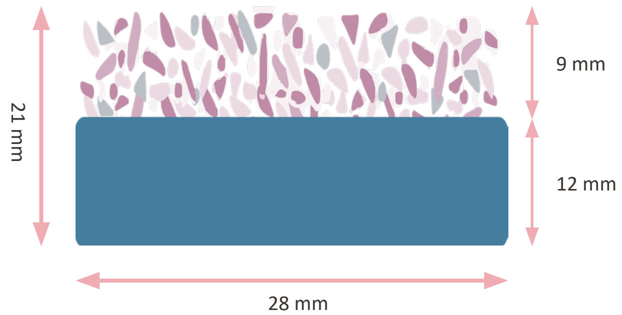

(g)

A composite beam featuring type A cullet on the surface and type C cullet in the bulk. It undergoes a ratio of 12 -9 mm.

Experiment type 3: Composite beams finding the influence of the bulk material

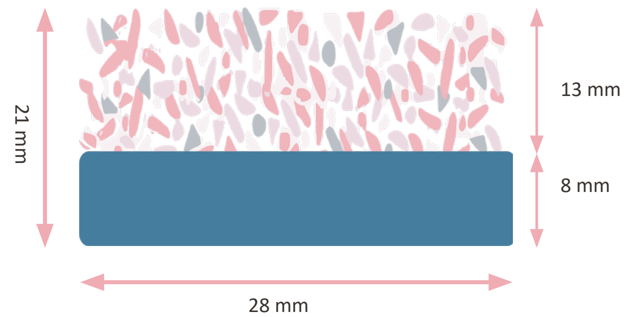

(h)

A composite beam with type A cullet on its surface and type C cullet in its bulk. The testing focuses on the bulk, containing metallic pollutants

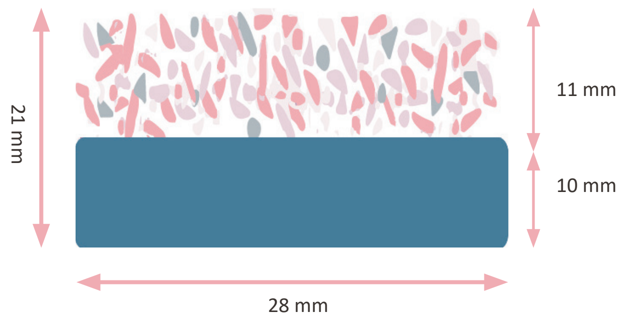

(i)

A composite beam with type A cullet on its surface and type C cullet in its bulk. The testing focuses on the bulk, containing metallic pollutants

Experiment type 4: Composite beams finding the influence of the surface material

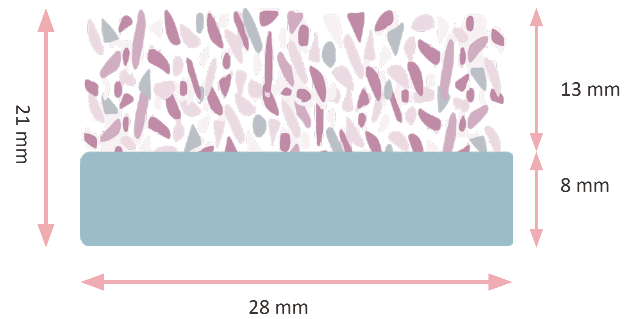

(j)

A composite beam with type B cullet on its surface and type C cullet (CSP) in its bulk. The testing focuses on the surface type containing Fritted glass

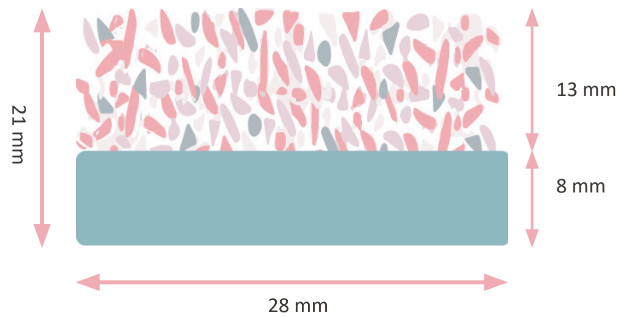

(k)

A composite beam with type B cullet on its surface and type C cullet (Metallic) in its bulk. The testing focuses on the surface type containing Fritted glass

6.2 Mould preparation

Making the moulds is a crucial step in the casting process, as emphasised in section 2.3.4: Casting. Various types of moulds can be used, including disposable and permanent moulds, which are listed in Table 06. Due to its low manufacturing costs and ease of production, the disposable mould was chosen for this thesis. Given the relatively low production volume, a disposable mould is suitable. However, for higher production volumes, permanent moulds would be recommended.

Since disposable moulds were chosen, a new mould needed to be created for each beam. In total, 58 moulds were produced for the beams. The procedure began with constructing a glass reservoir and a 3D-printed element shaped as a rectangular beam, based on the research of Bristogianni et al. (2021b). The reservoir is necessary due to the change in volume of the glass cullets before and after melting, caused by trapped air between the cullets. Its precise measurements are 21 mm in width, 28 mm in height, and 350 mm in length.

The following steps are the stages involved in producing a mould (Figure 43):

1. Place the 3D printed beam at a position that is acceptable for it and has enough room surrounding it.
2. Use clay to anchor the beam to the surface along its edges.
3. Because clay dries quickly, make sure it stays wet by misting it with a cleaner.
4. To make the model's release from the mould easier, lightly coat the model's exterior with petroleum jelly.
5. Build a wooden box around the 3D printed part, allowing a two-centimeter overhang on all sides. Maintain a consistent clearance by ensuring that the gap between the 3D printed part and the wooden planks is uniform on all sides. Fix the wooden planks to create a box and fasten them tightly
6. Use clay to seal the wooden box's edges to stop leaks when the liquid plaster is poured in.
7. In this phase, the silica plaster mixture is ready to be cast for the beams. The silica plaster that is used is Crystalcast M2482 containing 73% silica powder (cristobalite, quartz), 23% calcium sulphate (gypsum), and 1% organics (Goodwin Refractory Services 2003, 2019). One litre of water is added to every 2.8 kg of Crystalcast to make the mixture. The mixture is made by gradually adding Crystalcast to the water until a creamy consistency is reached.
8. The wooden box is then filled with the creamy plaster mixture. To make sure there are no trapped air bubbles, it is crucial to verify the depth after pouring—ideally, it should be at least 2 cm in the centre of the wooden box. In addition, any trapped bubbles can be released by lightly tapping at the surface of each wooden board. After that, the mould is given at least an hour to dry. Every mould used in this thesis is given a minimum of 75 minutes to dry.
9. After the mould is completely dry, the 3D printed part is removed, cleaned, and prepared for the next mould, starting again from step 1. Any clay that had not dried is reused once the mould itself has been cleaned. The beam is then washed with warm water to remove any residual petroleum jelly and left to dry completely for at least a day before it is used in the oven.

(a)

(b)

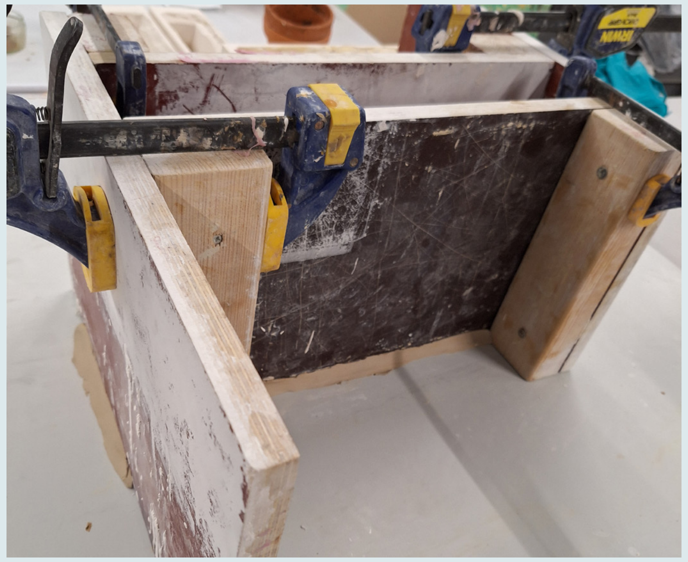

(c)

(d)

(e)

Figure 43: Preparation of the crystal silica moulds for the beams. (a) step 1, (b) step 5, (c) step 6,(d) step 7 and (e) step 8

6.3 Cullet preparation

The cullets used for these experiments are based on previous research, including Matskidou's 2022 thesis. She analysed the effects of different quality grades of cullets. The following selection of cullets was made with the help of her observations and conclusions (Matskidou, 2022):

- Float glass containing CSP pollutants, which is a grade C cullet, offers the most promising results for composite panels. Even with heavy contamination, homogeneity and high compatibility can be achieved through effective remelting.
- For cullet size, shard shape is chosen. This shape inhibits bubble formation, allowing remelting at a lower temperature (1070°C) and for a shorter duration, resulting in a more translucent product.
- It is advised to further investigate the compatibility between the layers in the composite.
- There is a direct connection between the type of flaws and cullet contamination, composition, and annealing schedules.

Following an examination of all the tiles created throughout her investigation, the following criteria were used to select the cullets: compatibility, transparency, mould response, presence of cracks, breakage, and bubble level. Since the main goal of this thesis is to create recycled cast glass panels from C&D waste, structural performance is evaluated. The focus is on the presence of fractures, breakage, and bubbles in the tiles. If fractures are discovered before the beam is tested for structural performance, the beam is not suitable for the end application.

An overview of the chosen cullets used in this experiment is provided in Table 12.

Type B cullet		Type C cullet	
Name	Type of contamination	Name	Type of contamination
Coating SNX 60/28 (Guardian)	Soft coating	Combi HR Float (Maltha)	Heat resistant glass
SunGuard Solar Light Blue 52 (Guardian)	Soft coating	Combi CSP Float (Maltha)	CSP pollutants
Lacobel LT Black (AGC)	Fritted glass	Combi HR float, metallic pollutants (Maltha)	Metallic pollutants

Table 12: Overview of used cullets during experiments

A weight list had to be made in order to prepare the beams. This may be seen in Appendix B. The amount of weight that each kind of cullet required to be put into the moulds.

6.4 Fire Rounds

6.4.1 Set-up of the Fire Rounds

The temperatures used for the production of the beams are carefully discussed with Dr. Bristogianni each time. Generally, the homogeneous beams are heated to a maximum temperature of 1120°C, while the composite beams are heated to a maximum temperature of 1070°C. The higher maximum temperature for the homogeneous beams ensures greater homogeneity, as they consist of a single type of cullet that can fully mix. For the composite beams, a slightly lower temperature is chosen to ensure that the layered system remains intact.

Both the homogeneous and composite beams are annealed at around 580°C. They are heated at a rate of 50°C per hour until reaching the desired maximum temperature. Subsequently, they are cooled down to a temperature 20°C above the annealing point at a rate of -160°C per hour. They anneal for an additional ten hours, followed by five hours of gradual cooling to the annealing point at a rate of -3°C per hour. After this, they are gradually cooled to the strain point at the same rate before being quickly cooled to room temperature.

This heating and cooling process replicates the methodology Dr. Bristogianni employed in her investigation of the flexural strength and stiffness of cast glass (Bristogianni et al., 2021b).

6.5.2 Name of the Fire Rounds

As previously mentioned in paragraph 6.1.2 Experimenting with homogenous and composite beams, the setup of this research involves four types of experiments. The name of each fire round corresponds to the type of experiment being conducted.

- **Fire Round 1**: Based on experiment type 1, involves homogeneous beams containing type A, B, or C cullet.
- **Fire Round 2**: Based on experiment type 2, involves composite beams with different surface-bulk ratios.
- **Fire Round 3**: Based on experiment type 3, involves composite beams with different bulk materials.
- **Fire Round 4**: Based on experiment type 4, involves composite beams with different surface materials.

Some fire rounds include multiple sub-rounds, which are categorised with letters (A, B, C, etc.).

For example, Fire Round 2A refers to a fire round for composite beams with different surface-bulk ratios, and it is the first sub-round.

Names of composite compositions

Each composition is assigned a specific name. The name starts with the number of the fire round (1, 2, 3, or 4) followed by a letter indicating the thickness of the surface material:

A = 6 mm, B = 8 mm, C = 10 mm, D = 12 mm

When the bulk or surface material changes, a Roman numeral (I, II, III) can be added to the name.

6.5.3 Fire Round 1A, Homogeneous beams, behaviour of one single pollutant

- Cullet type:
  - Grade C Cullet: HR glass
  - Grade C Cullet: CSP Pollutants
- Temperature: 1120 degrees

Six beams were set up inside the oven for the first fire schedule. Three beams had HR glass; the other three beams had CSP pollutants. The cullets in this fire round were cleaned, but no pollution of any kind was eliminated. The objective of this experiment was to determine the impact of the CSP pollutants and the HR cullets in a cast beam arrangement. The organisation of the Fire Round is depicted in diagram in Figure 44. An illustration of the beam placement in the oven may be found in Figure 45.

6.5.4 Fire Round 1B, Homogeneous beams, behaviour of one single pollutant

- Cullet type:
  - Grade B Cullet: Fritted glass
  - Grade B Cullet: Soft coated glass
  - Grade C Cullet: HR glass
- Temperature: 1120 degrees

Six beams were placed into the oven during this fire round. Three beams were made of black Fritted glass, two beams had a soft coating, and one beam had HR glass. Since silicone and ceramics within the composition caused all of the HR beams to shatter during Fire round 1A, it was decided that for this round these elements were removed.

This test was set-up to determine the impact of one specific contamination. The organisation of the fire round is depicted in diagram in Figure 46. An illustration of the beam placement in the oven may be found in Figure 47.

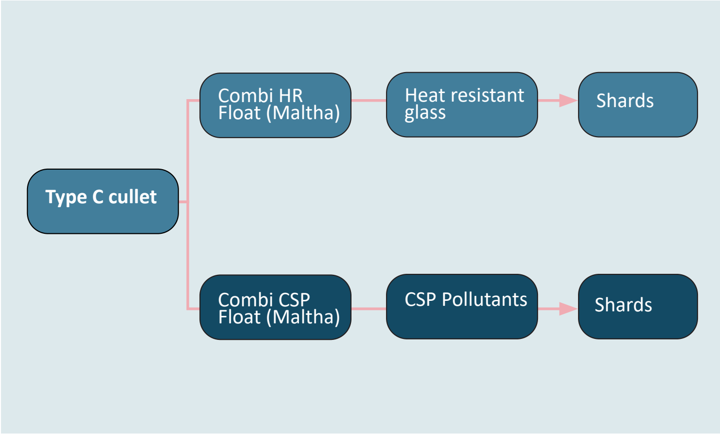

Figure 44: Ilustratic diagram of Fire Round 1A

Figure 45: Fire Round 1A placed in the oven

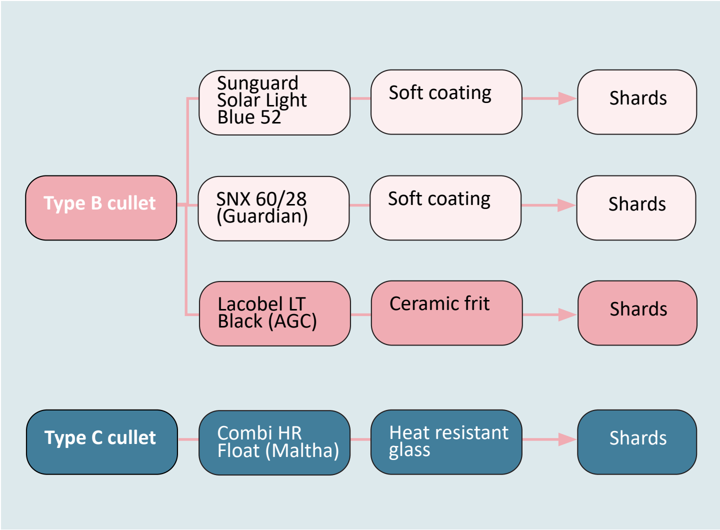

Figure 46: Illustratic diagram of Fire Round 1B

Figure 47: Fire Round 1B placed in the oven

6.5.5 Fire Round 1C, Homogeneous beams, behaviour of one single pollutant

- Cullet type: • Grade C Cullet: Met. Pollutants
- Temperature: 1070 degrees

A lower temperature is used here so that the three beams can be placed in the same oven as the composite beams. This decision was made for logistical reasons.

Three beams were made of glass with metallic pollutants. This test was designed to determine the impact of a particular parameter. The organisation of the fire round is depicted in diagram in Figure 48. An illustration of the beam placement in the oven may be found in Figure 49.

6.5.6 Fire Round 1D, Homogeneous beams, behaviour of one single pollutant

- Cullet type: • Grade A Cullet: Float glass
- Temperature: 1070 degrees

Three beams were made of Float glass to determine the influence of the composite beams compared to the homogeneous Float glass beams. This test aims to see if there is an optimal configuration for the composite beams that allows them to achieve structural performance comparable to that of the fully Float glass beams. The organisation of the fire round is depicted in the diagram in Figure 50, and an illustration of the beam placement in the oven can be found in Figure 51.

6.5.7 Fire Round 2A, Composite beams, Influence of the ratio between surface and bulk

- Bulk • Grade B Cullet: Fritted glass
  • Grade C Cullet: CSP Pollutants
- Surface • Grade A Cullet: Float glass
- Temperature: 1070 degrees

This fire round marked the first placement of composite compositions. Seven beams were produced for this fire round. Six beams contain CSP pollutants in the bulk, and one beam contains Fritted glass in the bulk. First, the beams with CSP pollutants will be discussed, followed by the beam with Fritted glass. Three beams have a composition of 2B, and three beams have a composition of 2C. The beam with Fritted glass in the bulk has a composition of 3B-I. This experiment was designed to discover out how a composite composition affects the structural performance. The organisation of the fire round is depicted in diagram in Figure 52. An illustration of the beam placement in the oven may be found in Figure 53.

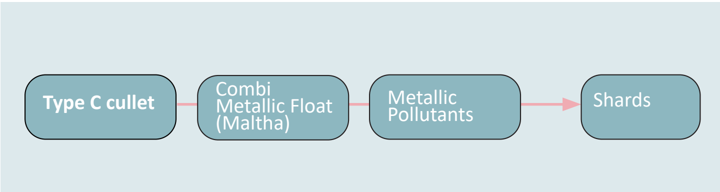

Figure 48: Illustratic diagram of Fire Round 1C

Figure 49: Fire Round 1C placed in the oven

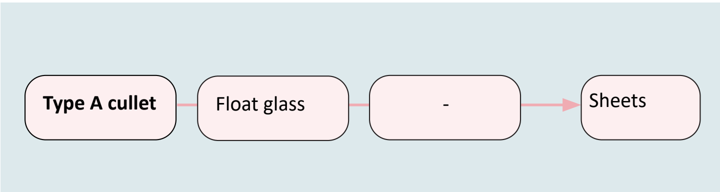

Figure 50: Illustratic diagram of Fire Round 1D

Figure 51: Fire Round 1D placed in the oven

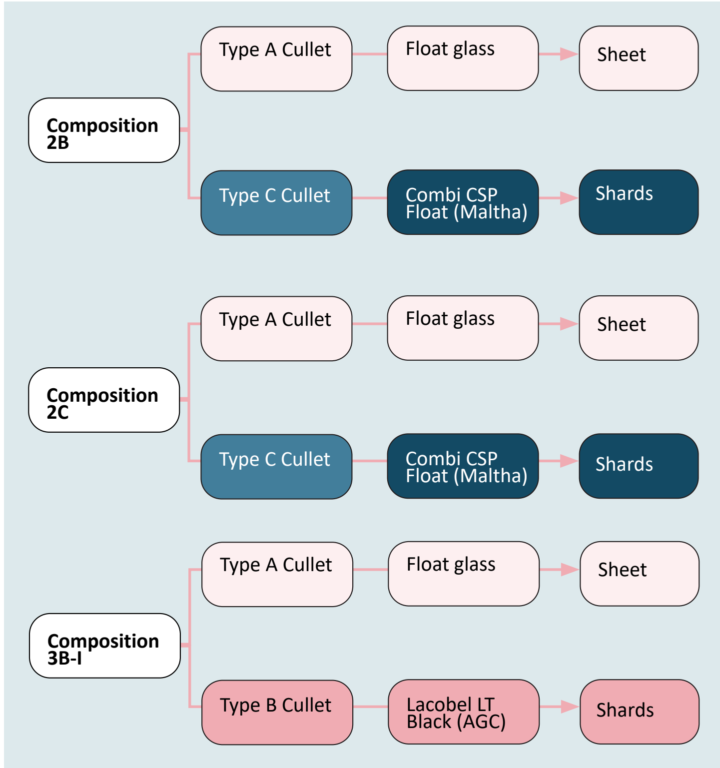

Figure 52: Illustratic diagram of Fire Round 2A

Figure 53: Fire Round 2A placed in the oven

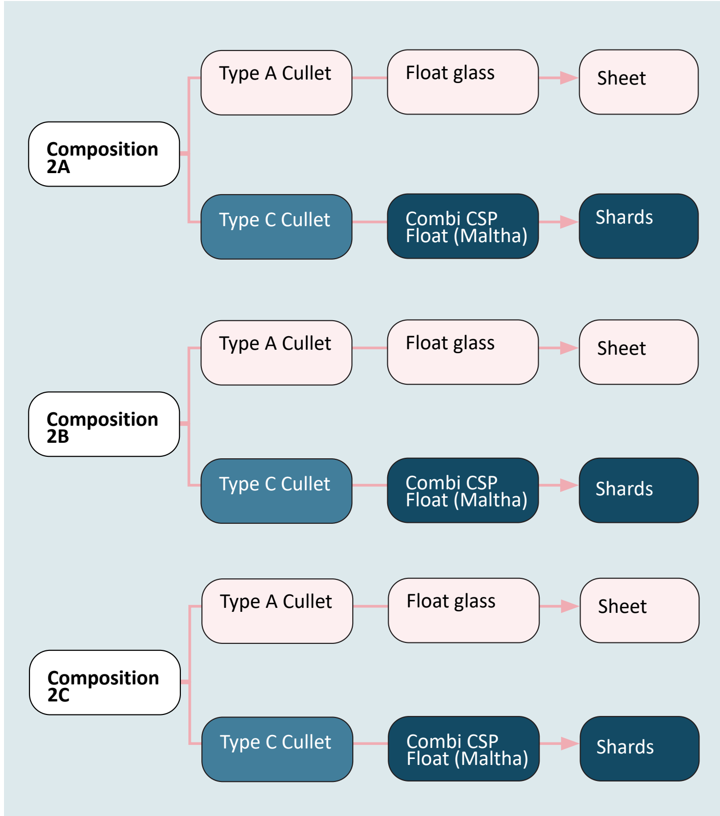

Figure 54: Illustratic diagram of Fire Round 2B

Figure 55: Fire Round 2B placed in the oven

6.5.8 Fire Round 2B, Composite beams, Influence of the ratio between surface and bulk

- Bulk — Grade C Cullet: CSP Pollutants
- Surface — Grade A Cullet: Float glass
- Temperature: 1070 degrees

In this fire round, six beams were arranged: two beams with composition 2A, two beams with composition 2B, and two beams with composition 2C. However, due to multiple beams breaking during the previous fire round, fire round 2A, an additional safety check was conducted on this bulk. Silicone and ceramic inclusions were removed. The goal of this fire round was to examine the effects of different ratios between surface and bulk and to observe the effect of removing inclusions in the bulk. The organisation of the fire round is depicted in the diagram in Figure 54. An illustration of the beam placement in the oven can be found in Figure 55.

6.5.9 Fire Round 2C, Composite beams, Influence of the ratio between surface and bulk with higher temperature

To determine whether the relationship between the surface and bulk would change at higher temperatures, a different temperature schedule was used in this fire round. The connection between the bulk and surface is expected to be more important. This is explained in more detail in Chapter 9: Mechanical behaviour optimisation.

6.5.10 Fire Round 2D, Composite beams, Influence of the ratio between surface and bulk

- Bulk — Grade C Cullet: CSP Pollutants
- Surface — Grade A Cullet: Float glass
- Temperature: 1070 degrees

For this fire round, the last few composite compositions were placed in the oven. There was one beam with composition 2A, two beams with composition 2B, one beam with composition 2C, and three beams with composition 2D. However, the Float glass was cut in half for one beam of composition 2B and one of composition 2C to observe the influence of the tinted side of the Float glass. The goal of this fire round was to investigate the different surface-to-bulk ratios. A diagram showing how the fire schedule is organised is displayed in Figure 56, while Figure 57 illustrates the arrangement of beams in the oven.

6.5.11 Fire Round 3A, Composite beams, Influence of the bulk material

- Bulk — Grade C Cullet: Met. Pollutants
- Surface — Grade A Cullet: Float glass
- Temperature: 1070 degrees

Six beams are manufactured during this fire round. Three beams contain the 3B-II composition, and three beams contain the 3C composition. The objective of this fire round was to examine the effects of using a different bulk type, other than cullets with CSP contaminants. Additionally, it aimed to observe if the structural performance varies when the bulk and surface ratios of cullets containing metallic contaminants are different. The organisation of the fire round is depicted in the diagram in Figure 58, and Figure 59 provides an illustration of the beam placement in the oven.

6.5.12 Fire Round 4A, Composite beams, Influence of the surface material

- Bulk — Grade C Cullet: CSP Pollutants
- Grade C Cullet: Met. Pollutants
- Surface — Grade B Cullet: Fritted glass
- Temperature: 1070 degrees

Six beams are manufactured during this fire round. Three beams contain the 4B-I composition, and three beams contain the 4B-II composition. The goal of this fire round is to determine whether the composition would be affected by another surface material with a lower cullet quality grade. The schematic presented in Figure 60 shows how the fire round is organised, and Figure 61 shows how the oven's beam placement is done.

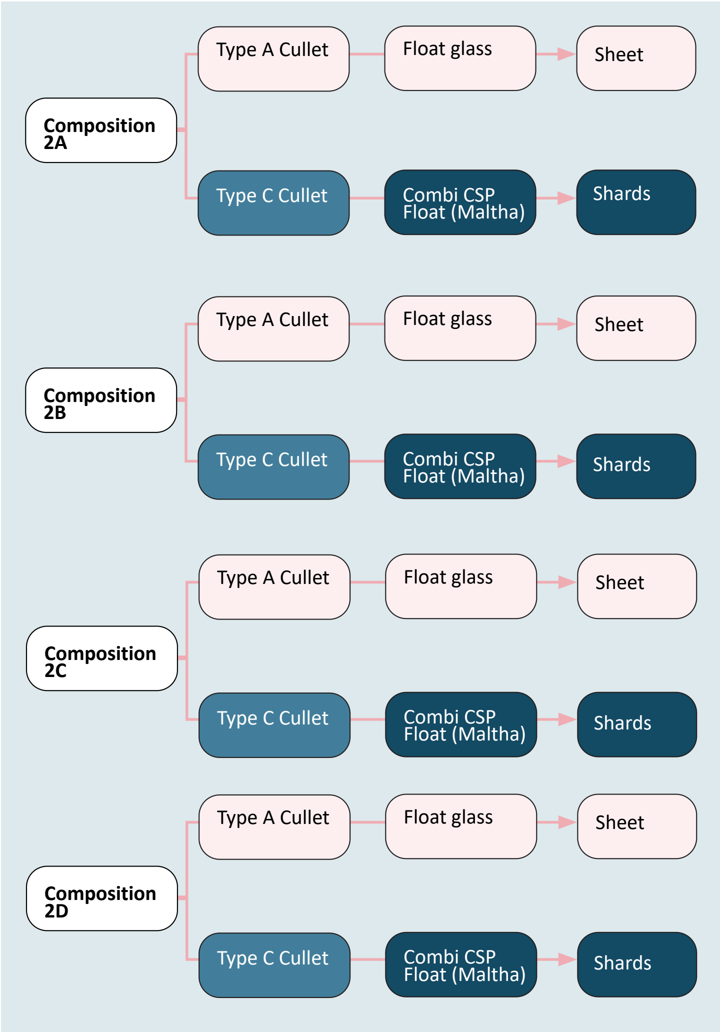

Figure 56: Illustratic diagram of Fire Round 2D

Figure 57: Fire Round 2D placed in the oven

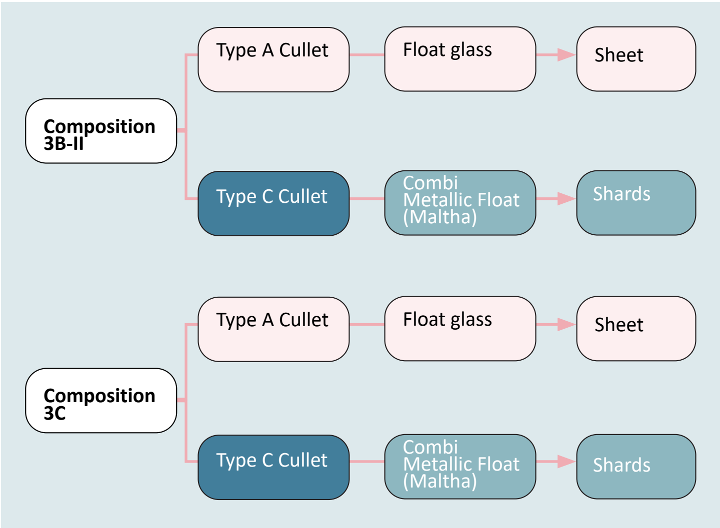

Figure 58: Illustratic diagram of Fire Round 3A

Figure 59: Fire Round 3A placed in the oven

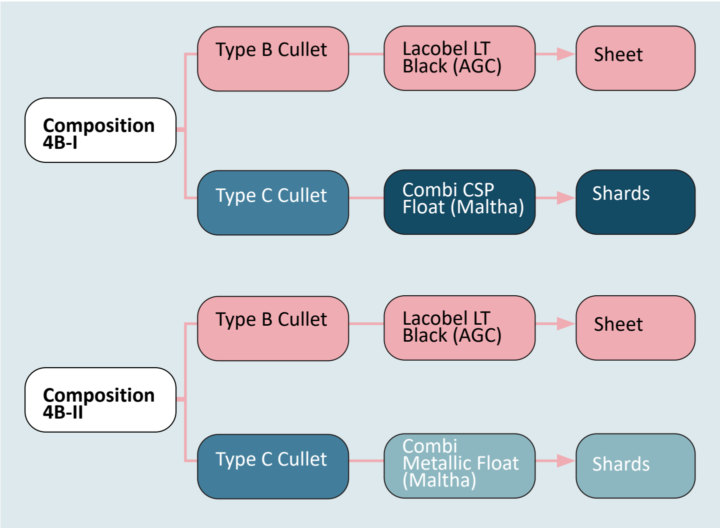

Figure 60: Illustratic diagram of Fire Round 4A

(a) (b)

Figure 61: Fire Round 4A placed in the oven, (a) CSP Pollutants, (b) Metallic Pollutants

6.6 Feasibility validation

Following that, the beams were created in the oven, and the mould for the cast glass beams had to be carefully removed. Each beam had to be examined to determine its feasibility for the structural performance test. Each beam is evaluated based on several characteristics: compatibility, transparency, mould reaction, presence of cracks, breakage, and level of bubbles. Additionally, the end criteria determine whether the beam succeeded or failed the structural performance test.

Names of cast glass beams

To evaluate each beam, the beams should be coded so that they can be easily recognised.

{Name Researcher} – {Name Fire Round} – {Type of Beam} – {Bulk type} – {Number in this batch}
Name researcher: Véronique (V)
Name Fire Round: 1A, 1B, 1C, 2A, 2B, 2C, 2D, 3A or 4A
Type of beam: Homogeneous (H) or Composite (C)
Surface thickness: 6 (mm), 8 (mm), 10 (mm) or 12 (mm). Generally, this is Float glass. When an "R" is added, it indicates Fritted glass instead of Float glass.
Bulk type: Float glass (Fl), CSP pollutants (C), HR glass (HR), Metallic pollutants (M), Fritted glass (F), Soft coated glass: SNX 60/26 (S)or Solar light Blue (B)

Example 1:
V – 1A – H – C – 1

This beam is created in Fire Round 1A. It is homogeneous, meaning that the majority of the cullets are CSP pollutants. And it is the first beam of this set.

Example 2:
V-2D-C8-C-2

This beam is created in Fire Round 2D. It is a composite beam, 8 mm Float glass and with CSP Pollutants in the bulk. And it is the second beam of this set.

Example 3:
V-4A-CR8-C-2

This beam is created in Fire Round 4a. It is a composite beam, 8 mm Fritted glass and with CSP Pollutants in the bulk. And it is the second beam of this set.

6.6.1 Fire Round 1A, Homogeneous beams, behaviour of one single pollutant

- Homogeneous beams with CSP Pollutants (Figure 62)
- Homogeneous beams with HR glass (Figure 63)

Six beams were being created in Fire Round 1A. Unfortunately, four beams failed during this fire round due to the presence of ceramic and silicone traces. As illustrated in Figure 39, there is a significant difference in thermal expansion between silicone and glass ceramics compared to soda lime glass. When the thermal expansion of these materials varies too much, it creates tension between two spots, leading to stress, cracks, and ultimately, beam breakage. Since these beams have

Homogeneous beams: CSP Pollutants

	Beam V-1A-H-C-1	Beam V-1A-H-C-2	Beam V-1A-H-C-3
	Material characteristics	**Material characteristics**	**Material characteristics**
The product:	Combi CSP Float (Maltha)	Combi CSP Float (Maltha)	Combi CSP Float (Maltha)
Cullet grade:	Class C	Class C	Class C
Contamination:	CSP Pollutants	CSP Pollutants	CSP Pollutants
Cullet Type:	Small shards	Small shards	Small shards
Forming temperature:	1120 °C	1120 °C	1120 °C

(a) (b) (c)

	Feasibility characteristics	**Feasibility characteristics**	**Feasibility characteristics**
Compatibility:	high	high	high
Transparency:	translucent	translucent	translucent
Mould reaction:	absent	absent	present
Cracks presence:	present	present	present
Breakage:	absent	absent	present
Bubbles level:	medium	low	medium
Structural performance:	succeeded	succeeded	failed

Figure 62: Feasibility validation of Fire Round 1A, Beams with CSP pollutants. (a) beam V-1A-H-C-1, (b) beam V-1A-H-C-2 and (c) beam V-1A-H-C-3

Homogeneous beams: HR glass

	Beam V-1A-H-HR-1	Beam V-1A-H-HR-2	Beam V-1A-H-HR-3
	Material characteristics	**Material characteristics**	**Material characteristics**
The product:	Combi HR Float (Maltha)	Combi HR Float (Maltha)	Combi HR Float (Maltha)
Cullet grade:	Class C	Class C	Class C
Contamination:	HR glass	HR glass	HR glass
Cullet Type:	Small shards	Small shards	Small shards
Forming temperature:	1120 °C	1120 °C	1120 °C

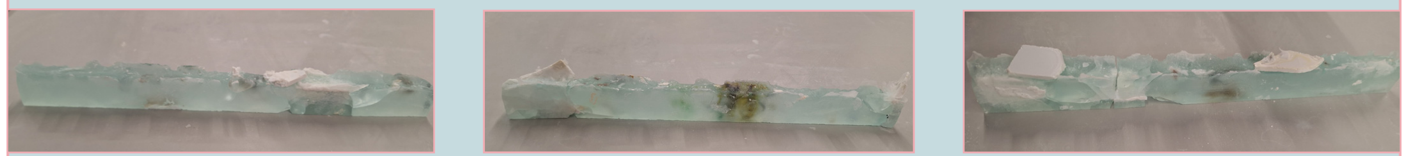

(a) (b) (c)

	Feasibility characteristics	**Feasibility characteristics**	**Feasibility characteristics**
Compatibility:	low	medium	low
Transparency:	translucent	translucent	opaque
Mould reaction:	absent	absent	present
Cracks presence:	present	present	present
Breakage:	present	present	present
Bubbles level:	low	low	low
Structural performance:	failed	failed	failed

Figure 63: Feasibility validation of Fire Round 1A, Beams with HR glass. (a) Beam V-1A-H-HR-1, (b) beam V-1A-H-HR-2 and (c) Beam V-1A-H-HR-3

already failed, they cannot be tested during the four-point bending test.

Regarding the beams with CSP pollutants, silicone traces caused Beam V-1A-H-C-3 to fracture. All of the homogenous HR Glass beams shattered. Large fractures began to form in beam V-1A-H-HR-3, and the ceramics in the middle caused the beam to break. Additionally, the ceramics caused large cracks in the middle. Beam V-1A-H-HR-2 almost survived, but unfortunately, it had ceramics at the edge.

6.6.2 Fire Round 1B, Homogeneous beams, behaviour of one single pollutant

- Homogeneous beams with Fritted glass (Figure 64)
- Homogeneous beams with HR glass (Figure 65)
- Homogeneous beams with soft coating SNX 60/28 (Figure 66)
- Homogeneous beams with soft coating blue solar (Figure 67)

Six beams were being created in this fire round. Three beams contain black Fritted glass. It was intriguing to observe throughout this test whether the black frit would retain its colour or fade due to the high temperature of the oven. What happened was that the black hue disappeared in the oven. It cannot be directly compared to the black frit utilised in Dr. Bristogianni's 2022 research due to its different composition. Bristogianni's PhD composition included chromium(III) oxide, a molecule with a very high melting point (2435 degrees), which did not melt in the oven. After conducting an XRF test at Mechanical Engineering, it can be confirmed that chromium(III) oxide is absent from the new mixture. The black hue of the frit is caused by the presence of two molecules: MgO (magnesium oxide) and Fe2O3 (iron(III) oxide).

In Fire Round 1A, all the beams containing HR glass failed due to ceramic traces. For this fire round, one beam with HR glass was made without these traces. As a result of the removal of these pollutants, the HR glass did not break. Lastly, two beams with a soft coating were constructed for this test. SunGuard Solar Light Blue 52 was present in one beam, while SunGuard eXtraSelective SNX 60/28 was present in the other. There was no sign of silicone on the Sunguard Solar Light. However, for the beam containing SunGuard eXtraSelective SNX 60/28, the silicone was held to the glass, and there was no way to remove the traces, which undoubtedly impacted the beam's performance, since this beam failed.

6.6.3 Fire Round 1C, Homogeneous beams, behaviour of one single pollutant

- Homogeneous beams with Metallic pollutants (Figure 68)

Three beams with metallic pollutants are being created in this fire round. All the beams passed the structural performance test. However, the metal traces began to interfere with the mould, resulting in mould reactions in all the glass beams. Blue traces are also appearing in these compositions, suggesting that some mirror fragments were mistakenly added, assuming they were metal.

6.6.4 Fire Round 1D, Homogeneous beams, behaviour of one single pollutant

- Homogeneous beams with Float glass (Figure 69)

Three beams made of Float glass are being created in this fire round. All the beams passed the structural performance test, demonstrating high compatibility. The beams are translucent, but they become transparent when water is applied to the glass.

6.6.5 Fire Round 2A, Composite beams, Influence of the ratio between surface and bulk

Surface: Float glass. Bulk: CSP Pollutants

- Composite beams: Surface 8 mm and Bulk 13 mm (Figure 70)
- Composite beams: Surface 10 mm and Bulk 11 mm (Figure 71)

Surface: Float glass. Bulk: Fritted glass

- Composite beams: Surface 8 mm and Bulk 13 mm (Figure 72)

Seven beams were being formed during this fire round. Since the beams were only cleaned and no harmful pollutants were removed from the batch, many beams broke during this process. It turned out that some pollutants, particularly ceramics and silicone, damaged the beams due to the discrepancy in thermal expansion between ceramics, silicone, and glass. The beams display multiple colours from the tinted glass, with different coloured streaks appearing.

Homogeneous beams: Fritted glass

	Beam V-1B-H-F-1	Beam V-1B-H-F-2	Beam V-1B-H-F-3
Material characteristics		**Material characteristics**	**Material characteristics**
The product:	Lacobel LT Black (AGC)	Lacobel LT Black (AGC)	Lacobel LT Black (AGC)
Cullet grade:	Class B	Class B	Class B
Contamination:	Fritted glass	Fritted glass	Fritted glass
Cullet Type:	Small shards	Small shards	Small shards
Forming temperature:	1120 °C	1120 °C	1120 °C

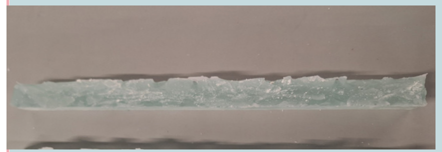
(a)

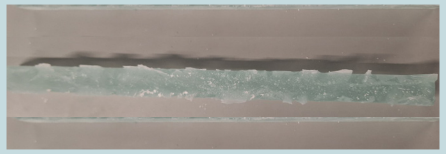
(b)

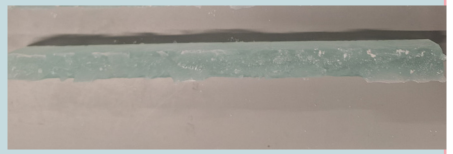
(c)

Feasibility characteristics		**Feasibility characteristics**	**Feasibility characteristics**
Compatibility:	high	high	high
Transparency:	translucent	translucent	translucent
Mould reaction:	absent	absent	absent
Cracks presence:	absent	absent	absent
Breakage:	absent	absent	absent
Bubbles level:	low	low	low
Structural performance:	succeeded	succeeded	succeeded

Figure 64: Feasibility validation of Fire Round 1B, Beams Fritted glass. (a) Beam V-1B-H-F-1, (b) Beam V-1B-H-F-2 and (c) Beam V-1B-H-F-3

Homogeneous beams: HR glass *SNX 60/28 coated glass* *Blue solar light coated glass*

	Beam V-1B-H-HR-1	Beam V-1B-H-S-1	Beam V-1B-H-B-1
	Material characteristics	**Material characteristics**	**Material characteristics**
The product:	Combi HR Float (Maltha)	SunGuard SNX 60/28 (Guardian)	SunGuard Solar Light Blue 52 (Guardian)
Cullet grade:	Class C	Class B	Class B
Contamination:	HR glass	Soft coated glass	Soft coated glass
Cullet Type:	Small shards	Small shards	Small shards
Forming temperature:	1120 °C	1120 °C	1120 °C


(a)


(c)


(b)

	Feasibility characteristics	**Feasibility characteristics**	**Feasibility characteristics**
Compatibility:	high	medium	high
Transparency:	translucent	translucent	translucent
Mould reaction:	absent	absent	absent
Cracks presence:	absent	present	absent
Breakage:	absent	present	absent
Bubbles level:	low	medium	low
Structural performance:	succeeded	failed	succeeded

Figure 65: Feasibility validation of Fire Round 1B, Beam V-1B-H-HR-1

Figure 66: Feasibility validation of Fire Round 1B, Beam V-1B-H-S-1

Figure 67: Feasibility validation of Fire Round 1B, Beam V-1B-H-B-1

06 | EXPERIMENTAL METHODOLOGY

Homogeneous beams: Metallic pollutants

	Beam V-1C-H-M-1 Material characteristics	Beam V-1C-H-M-2 Material characteristics	Beam V-1C-H-M-3 Material characteristics
The product:	Combi Mag. Float (Maltha)	Combi Mag. Float (Maltha)	Combi Mag. Float (Maltha)
Cullet grade:	Class C	Class C	Class C
Contamination:	Metallic Pollutants	Metallic Pollutants	Metallic Pollutants
Cullet Type:	Small shards	Small shards	Small shards
Forming temperature:	1070 °C	1070 °C	1070 °C

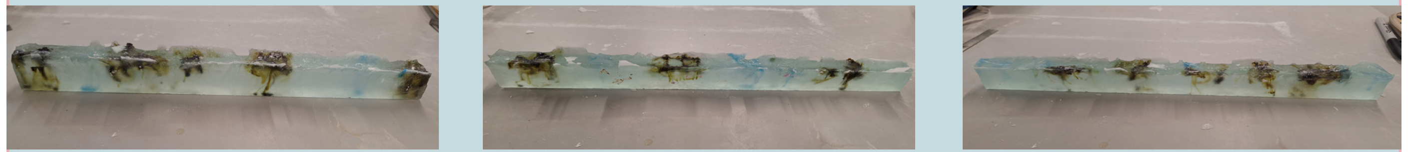

(a) (b) (c)

	Feasibility characteristics	Feasibilitycharacteristics	Feasibility characteristics
Compatibility:	high	high	high
Transparency:	translucent	translucent	translucent
Mould reaction:	present	present	present
Cracks presence:	present	absent	absent
Breakage:	absent	absent	absent
Bubbles level:	medium	high	medium
Structural performance:	succeeded	succeeded	succeeded

Figure 68: Feasibilty validation of Fire Round 1C, Beams Metallic pollutants. (a) Beam V-1C-H-M-1, (b) Beam V-1C-H-M-2 and (c) Beam V-1C-H-M-3

Homogeneous beams: Float glass

	Beam V-1D-H-FL-1 Material characteristics	Beam V-1D-H-FL-2 Material characteristics	Beam V-1D-H-FL-3 Material characteristics
The product:	Float glass (Pilkington)	Float glass (Pilkington)	Float glass (Pilkington)
Cullet grade:	Class A	Class A	Class A
Contamination:	-	-	-
Cullet Type:	Sheets	Sheets	Sheets
Forming temperature:	1070 °C	1070 °C	1070 °C

(a) (b) (c)

	Feasibility characteristics	Feasibilitycharacteristics	Feasibility characteristics
Compatibility:	high	high	high
Transparency:	translucent	translucent	translucent
Mould reaction:	absent	abesent	abesent
Cracks presence:	absent	absent	absent
Breakage:	absent	absent	absent
Bubbles level:	low	low	low
Structural performance:	succeeded	succeeded	succeeded

Figure 69: Feasibilty validation of Fire Round 1D, Beams with Float glass. (a) Beam V-1D-H-FL-1, (b) Beam V-1D-H-FL-2 and (c) Beam V-1D-H-FL-3

Composite beams: Surface: Float 8 mm, Bulk: CSP

	Beam V-2A-C8-C-1 Material characteristics	Beam V-2A-C8-C-2 Material characteristics	Beam V-2A-C8-C-3 Material characteristics
The product:	Float glass + Combi CSP Float (Maltha)	Float glass + Combi CSP Float (Maltha)	Float glass + Combi CSP Float (Maltha)
Cullet grade:	Class A + Class C	Class A + Class C	Class A + Class C
Contamination:	Float glass + CSP Pollutants	Float glass + CSP Pollutants	Float glass + CSP Pollutants
Cullet Type:	Sheet + Small shards	Sheet + Small shards	Sheet + Small shards
Forming temperature:	1070 °C	1070 °C	1070 °C

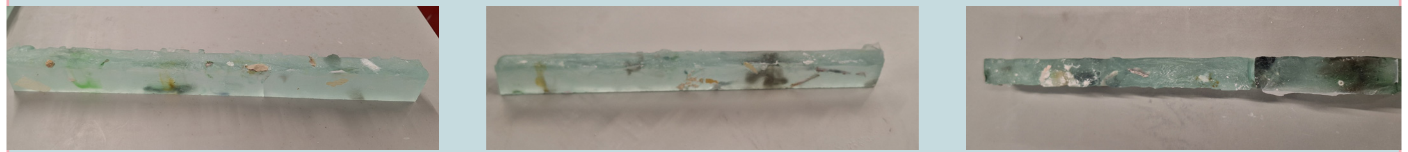

(a) (b) (c)

	Feasibility characteristics	Feasibility characteristics	Feasibility characteristics
Compatibility:	medium	medium	medium
Transparency:	translucent	translucent	translucent
Mould reaction:	absent	absent	absent
Cracks presence:	present	present	present
Breakage:	absent	present	present
Bubbles level:	medium	low	low
Structural performance:	succeeded	failed	failed

Figure 70: Feasibility validation of Fire Round 2A, (a) Beam V-2A-C8-C-1, (b) Beam V-2A-C8-C-2 and (c) Beam V-2A-C8-C-3

Composite beams: Surface: Float 10 mm, Bulk: CSP

	Beam V-2A-C10-C-1 Material characteristics	Beam V-2A-C10-C-2 Material characteristics	Beam V-2A-C10-C-3 Material characteristics
The product:	Float glass + Combi CSP Float (Maltha)	Float glass + Combi CSP Float (Maltha)	Float glass + Combi CSP Float (Maltha)
Cullet grade:	Class A + Class C	Class A + Class C	Class A + Class C
Contamination:	Float glass + CSP Pollutants	Float glass + CSP Pollutants	Float glass + CSP Pollutants
Cullet Type:	Sheet + Small shards	Sheet + Small shards	Sheet + Small shards
Forming temperature:	1070 °C	1070 °C	1070 °C

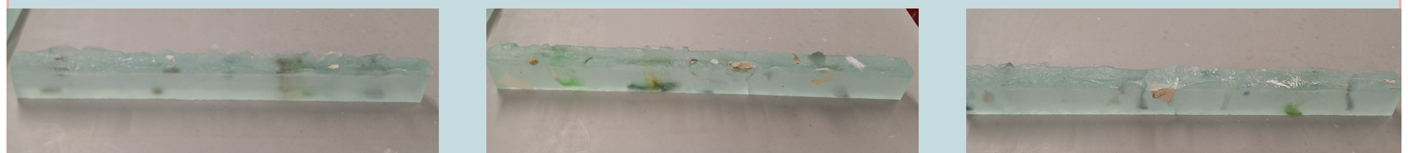

(a) (b) (c)

	Feasibility characteristics	Feasibility characteristics	Feasibility characteristics
Compatibility:	high	medium	high
Transparency:	translucent	translucent	translucent
Mould reaction:	absent	absent	absent
Cracks presence:	absent	present	present
Breakage:	absent	present	present
Bubbles level:	low	low	low
Structural performance:	succeeded	failed	failed

Figure 71: Feasibility validation of Fire Round 2A, (a) Beam V-2A-C10-C-1, (b) Beam V-2A-C10-C-2 and (c) Beam V-2A-C10-C-3

Composite beams: Surface: Float 8 mm, Bulk: Fritted glass

	Beam V-2A-C8-F-1
	Material characteristics
The product:	Float glass + Lacobel LT Black (AGC)
Cullet grade:	Class A + Class B
Contamination:	Float glass + Fritted glass
Cullet Type:	Sheet + Small shards
Forming temperature:	1070 °C

	Feasibility characteristics
Compatibility:	high
Transparency:	translucent
Mould reaction:	absent
Cracks presence:	absent
Breakage:	absent
Bubbles level:	low
Structural performance:	succeeded

Figure 72: Feasibility validation of Fire Round 2A, beam V-2A-C8-F-1

6.6.6 Fire Round 2B, Composite beams, Influence of the ratio between surface and bulk

Surface: Float glass. Bulk: CSP Pollutants

- Composite beams: Surface 6 mm and Bulk 15 mm (Figure 73)
- Composite beams: Surface 8 mm and Bulk 13 mm (Figure 74)
- Composite beams: Surface 10 mm and Bulk 11 mm (Figure 75)

As stated in paragraph 6.5.8, "Fire Round 2B, Composite beams: Influence of the ratio between surface and bulk," some pollutants, specifically ceramics and silicones, were removed. The contaminants that cause damage to the beams were manually selected and eliminated from the bulk material, as will be discussed in paragraph 9.1: "Influence of cullet selection." As a result, the beams from Fire Round 2B have high compatibility and all passed the structural performance test. No cracks or breakages were observed.

6.6.7 Fire Round 2C, Composite beams, Influence of the ratio between surface and bulk with higher temperature

For Fire Round 2C another temperature schedule was being used to try to optimise the mechanical behaviour of the beams. This will be explained in paragraph 9.2 influence of a higher temperature schedule.

6.6.8 Fire Round 2D, Composite beams, Influence of the ratio between surface and bulk

Surface: Float glass. Bulk: CSP Pollutants

- Composite beams: Surface 6 mm and Bulk 15 mm (Figure 76)
- Composite beams: Surface 8 mm and Bulk 13 mm (Figure 77)
- Composite beams: Surface 10 mm and Bulk 11 mm (Figure 78)
- Composite beams: Surface 12 mm and Bulk 9 mm (Figure 79)

The final composite beams, aimed at determining the ratio between surface and bulk, were completed during this fire round. As mentioned in paragraph 6.5.10, Fire Round 2D, Composite beams, influence of the ratio between surface and bulk, the Float glass was cut in half for one beam of composition 2B and one of composition 2C to observe the influence of the tinted side of the Float glass. At a temperature of 1070 degrees, no Voronoi pattern could be observed on the surface, nor was there any difference between the two sides. All the beams showed mould reactions. The cullets began to interfere with the mould, likely due to a coating.

Composite beams: Surface: Float 6 mm, Bulk: CSP

Composite beams: Surface: Float 8 mm, Bulk: CSP

	Beam V-2B-C6-C-1	**Beam V-2B-C6-C-2**	**Beam V-2B-C8-C-1**
	Material characteristics	**Material characteristics**	**Material characteristics**
The product:	Float glass + Combi CSP Float (Maltha)	Float glass + Combi CSP Float (Maltha)	Float glass + Combi CSP Float (Maltha)
Cullet grade:	Class A + Class C	Class A + Class C	Class A + Class C
Contamination:	Float glass + CSP Pollutants	Float glass + CSP Pollutants	Float glass + CSP Pollutants
Cullet Type:	Sheet + Small shards	Sheet + Small shards	Sheet + Small shards
Forming temperature:	1070 °C	1070 °C	1070 °C

(a)

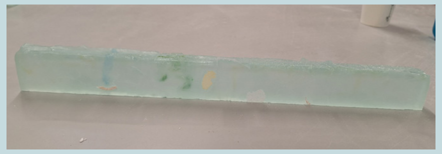

(b)

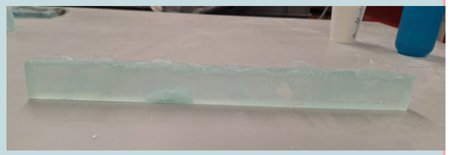

(a)

	Feasibility characteristics	**Feasibility characteristics**	**Feasibility characteristics**
Compatibility:	high	high	high
Transparency:	translucent	translucent	translucent
Mould reaction:	absent	absent	present
Cracks presence:	absent	absent	absent
Breakage:	absent	absent	absent
Bubbles level:	medium	medium	low
Structural performance:	succeeded	succeeded	succeeded

Figure 73: Feasibility validation of Fire Round 2B, (a) Beam V-2B-C6-C-1 and (b) Beam V-2B-C6-C-2

Composite beams: Surface: Float 10 mm, Bulk: CSP

	Beam V-2B-C8-C-2	**Beam V-2B-C10-C-1**	**Beam V-2B-C10-C-2**
	Material characteristics	**Material characteristics**	**Material characteristics**
The product:	Float glass + Combi CSP Float (Maltha)	Float glass + Combi CSP Float (Maltha)	Float glass + Combi CSP Float (Maltha)
Cullet grade:	Class A + Class C	Class A + Class C	Class A + Class C
Contamination:	Float glass + CSP Pollutants	Float glass + CSP Pollutants	Float glass + CSP Pollutants
Cullet Type:	Sheet + Small shards	Sheet + Small shards	Sheet + Small shards
Forming temperature:	1070 °C	1070 °C	1070 °C

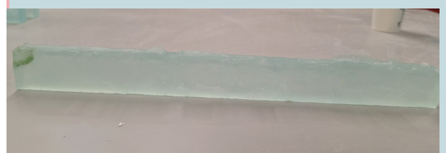

(b)

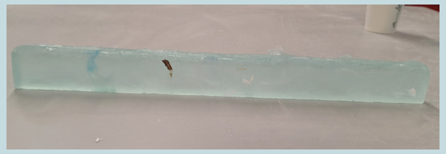

(a)

(b)

	Feasibility characteristics	**Feasibility characteristics**	**Feasibility characteristics**
Compatibility:	high	high	high
Transparency:	translucent	translucent	translucent
Mould reaction:	absent	absent	present
Cracks presence:	absent	absent	absent
Breakage:	absent	absent	absent
Bubbles level:	low	low	low
Structural performance:	succeeded	succeeded	succeeded

Figure 74: Feasibility validation of Fire Round 2B, (a) Beam V-2B-C8-C-1 and (b) Beam V-2B-C8-C-2

Figure 75: Feasibility validation of Fire Round 2B, (a) Beam V-2B-C10-C-1 and (b) Beam V-2B-C10-C-2

Composite beams: Surface: Float 6 mm, Bulk: CSP | *Composite beams: Surface: Float 8 mm, Bulk: CSP*

	Beam V-2D-C6-C-1	Beam V-2D-C8-C-1	Beam V-2D-C8-C-2
Material characteristics		**Material characteristics**	**Material characteristics**
The product:	Float glass + Combi CSP Float (Maltha)	Float glass + Combi CSP Float (Maltha)	Float glass + Combi CSP Float (Maltha)
Cullet grade:	Class A + Class C	Class A + Class C	Class A + Class C
Contamination:	Float glass + CSP Pollutants	Float glass + CSP Pollutants	Float glass + CSP Pollutants
Cullet Type:	Sheet + Small shards	Sheet + Small shards	Sheet + Small shards
Forming temperature:	1070 °C	1070 °C	1070 °C

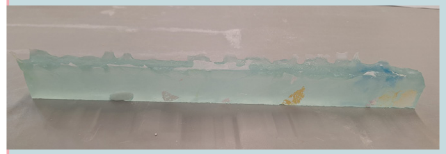
(a)


(a)

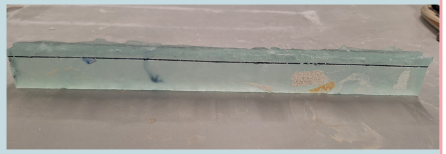
(b)

Feasibility characteristics		**Feasibility characteristics**	**Feasibility characteristics**
Compatibility:	**high**	**high**	high
Transparency:	**translucent**	**translucent**	translucent
Mould reaction:	**present**	**present**	present
Cracks presence:	**absent**	**present**	absent
Breakage:	**absent**	**absent**	absent
Bubbles level:	**low**	**low**	low
Structural performance:	**succeeded**	**succeeded**	succeeded

Figure 76: Feasibility validation of Fire Round 2D, Beam V-2D-C6-C-1

Figure 77: Feasibility validation of Fire Round 2D, (a) Beam V-2D-C8-C-1 and (b) Beam V-2D-C8-C-2

Composite beams: Surface: Float 10 mm, Bulk: CSP | *Composite beams: Surface: Float 12 mm, Bulk: CSP*

	Beam V-2D-C10-C-1	Beam V-2D-C12-C-1	Beam V-2D-C12-C-2
	Material characteristics	**Material characteristics**	**Material characteristics**
The product:	Float glass + Combi CSP Float (Maltha)	Float glass + Combi CSP Float (Maltha)	Float glass + Combi CSP Float (Maltha)
Cullet grade:	Class A + Class C	Class A + Class C	Class A + Class C
Contamination:	Float glass + CSP Pollutants	Float glass + CSP Pollutants	Float glass + CSP Pollutants
Cullet Type:	Sheet + Small shards	Sheet + Small shards	Sheet + Small shards
Forming temperature:	1070 °C	1070 °C	1070 °C


(a)

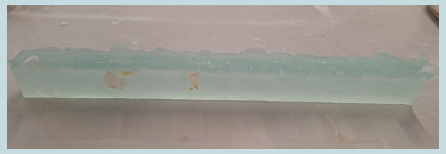
(a)


(b)

	Feasibility characteristics	**Feasability characteristics**	**Feasability characteristics**
Compatibility:	high	high	high
Transparency:	translucent	translucent	translucent
Mould reaction:	present	present	present
Cracks presence:	absent	absent	absent
Breakage:	absent	absent	absent
Bubbles level:	low	low	low
Structural performance:	succeeded	succeeded	succeeded

Figure 78: Feasibility validation of Fire Round 2D, (a) Beam V-2D-C10-C-1

	Beam V-2D-C12-C-3
Material characteristics	
The product:	Float glass + Combi CSP Float (Maltha)
Cullet grade:	Class A + Class C
Contamination:	Float glass + CSP Pollutants
Cullet Type:	Sheet + Small shards
Forming temperature:	1070 °C


(c)

Feasibility characteristics	
Compatibility:	**high**
Transparency:	**translucent**
Mould reaction:	**present**
Cracks presence:	**absent**
Breakage:	**absent**
Bubbles level:	**low**
Structural performance:	**succeeded**

Figure 79: Feasibility validation of Fire Round 2D, (a) Beam V-2D-C12-C-1, (b) Beam V-2D-C12-C-2 and (c) Beam V-2D-C12-C-3

6.6.9 Fire Round 3A, Composite beams, Influence of the bulk material

Surface: Float glass. Bulk: Metallic Pollutants

- Composite beams: Surface 8 mm and Bulk 13 mm (Figure 80)
- Composite beams: Surface 10 mm and Bulk 11 mm (Figure 81)

During Fire Round 3A, the focus was on examining the impact of using a different bulk material. In previous tests, cullets with CSP pollutants were placed in the bulk. In this fire round, however, cullets with metallic pollutants were used. Noteworthy, all the beams exhibited a clearly visible mould reaction. The metal began to interfere with the mould, and metal traces started to melt into the beam due to the higher density of the metal. The metal in the glass began to melt and interfere with it. All the beams showed high compatibility and overall passed the structural performance test. However, one beam, V-3A-C-M10-3, failed due to a small inclusion.

6.6.10 Fire Round 4A, Composite beams, Influence of the bulk material

Surface: Fritted glass. Bulk: CSP Pollutants

- Composite beams: Surface 8 mm and Bulk 13 mm (Figure 82)

Surface: Fritted glass. Bulk: Metallic Pollutants

- Composite beams: Surface 8 mm and Bulk 13 mm (Figure 83)

During Fire Round 4A, the focus was on examining the influence of using a different type of surface material. In the previous composite compositions, Float glass was always used. For this fire round, the influence of using B cullet type on the surface was being tested. Three beams were being made with CSP pollutants in the bulk to compare the results with Fire Rounds 2A, 2B, and 2D, and three beams were being made with metallic pollutants in the bulk to compare with the results of Fire Round 3A.

For the beams with CSP pollutants in the bulk, the results varied. One beam, V-4A-CR8-C-1, broke due to a large ceramic inclusion in the middle. The other beams passed the feasibility validation. In all beams, the frit burned off, resulting in translucent beams.

For the beams with metallic pollutants in the bulk, the results were quite comparable to each other. They all showed moderate to high mould reactions, with the metal beginning to interfere with the mould. One beam broke after initially passing the structural performance test; it failed during polishing due to excessive stress at a peak point.

Composite beams: Surface: Float 8 mm, Bulk: Metallic

	Beam V-3A-C8-M-1	Beam V-3A-C8-M-2	Beam V-3A-C8-M-3
	Material characteristics	**Material characteristics**	**Material characteristics**
The product:	Float glass + Combi Mag. Float (Maltha)	Float glass + Combi Mag. Float (Maltha)	Float glass + Combi Mag. Float (Maltha)
Cullet grade:	Class A + Class C	Class A + Class C	Class A + Class C
Contamination:	Float glass + Metal.Pollutants	Float glass + Metal.Pollutants	Float glass + Metal.Pollutants
Cullet Type:	Sheet + Small shards	Sheet + Small shards	Sheet + Small shards
Forming temperature:	1070 °C	1070 °C	1070 °C

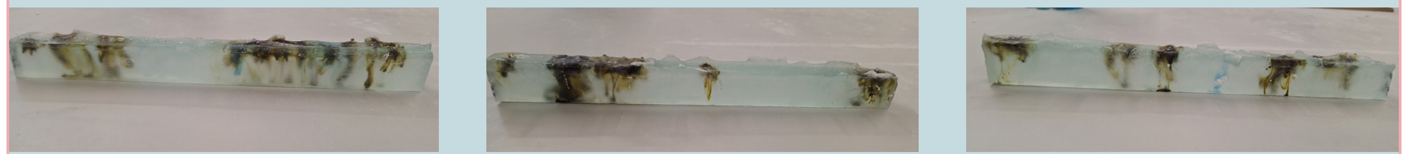

(a) (b) (c)

	Feasibility characteristics	Feasibility characteristics	Feasibility characteristics
Compatibility:	high	high	high
Transparency:	translucent	translucent	translucent
Mould reaction:	present	present	present
Cracks presence:	absent	absent	absent
Breakage:	absent	absent	absent
Bubbles level:	low	low	low
Structural performance:	succeeded	succeeded	succeeded

Figure 80: Feasibility validation of Fire Round 3A, (a) Beam V-3A-C8-M-1, (b) Beam V-3A-C8-M-2 and (c) Beam V-3A-C8-M-3

Composite beams: Surface: Float 10 mm, Bulk: Metallic

	Beam V-3A-C10-M-1	Beam V-3A-C10-M-2	Beam V-3A-C10-M-3
	Material characteristics	**Material characteristics**	**Material characteristics**
The product:	Float glass + Combi Mag. Float (Maltha)	Float glass + Combi Mag. Float (Maltha)	Float glass + Combi Mag. Float (Maltha)
Cullet grade:	Class A + Class C	Class A + Class C	Class A + Class C
Contamination:	Float glass + Metal.Pollutants	Float glass + Metal. Pollutants	Float glass + Metal.Pollutants
Cullet Type:	Sheet + Small shards	Sheet + Small shards	Sheet + Small shards
Forming temperature:	1070 °C	1070 °C	1070 °C

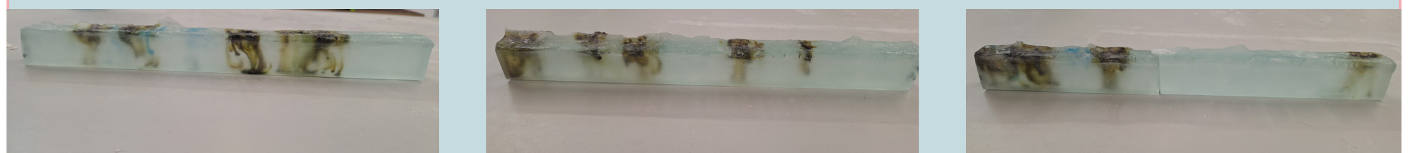

(a) (b) (c)

	Feasibility characteristics	Feasibiliy characteristics	Feasibility characteristics
Compatibility:	high	high	high
Transparency:	translucent	translucent	translucent
Mould reaction:	present	present	present
Cracks presence:	present	absent	present
Breakage:	absent	absent	present
Bubbles level:	medium	low	low
Structural performance:	succeeded	succeeded	failed

Figure 81: Feasibility validation of Fire Round 3A, (a) Beam V-3A-C10-M-1, (b) Beam V-3A-C10-M-2 and (c) Beam V-3A-C10-M-3

Composite beams: Surface: Fritted 8 mm, Bulk: CSP

	Beam V-4A-CR8-C-1	Beam V-4A-CR8-C-2	Beam V-4A-CR8-C-3
	Material characteristics	**Material characteristics**	**Material characteristics**
The product:	Fritted glass + Combi CSP Float (Maltha)	Fritted glass + Combi CSP Float (Maltha)	Fritted glass + Combi CSP Float (Maltha)
Cullet grade:	Class B + Class C	Class B + Class C	Class B + Class C
Contamination:	Fritted glass + CSP Pollutants	Fritted glass + CSP Pollutants	Fritted glass + CSP Pollutants
Cullet Type:	Sheet + Small shards	Sheet + Small shards	Sheet + Small shards
Forming temperature:	1070 °C	1070 °C	1070 °C

(a) (b) (c)

	Feasibility characteristics	Feasibility characteristics	Feasibility characteristics
Compatibility:	high	high	high
Transparency:	translucent	translucent	translucent
Mould reaction:	absent	absent	absent
Cracks presence:	present	present	absent
Breakage:	present	absent	absent
Bubbles level:	low	medium	low
Structural performance:	failed	succeeded	succeeded

Figure 82: Feasibility validation of Fire Round 4A,(a) Beam V-4A-CR8-C-1, (b) Beam V-4A-CR8-C-2 and (c) Beam V-4A-CR8-C-3

Composite beams: Surface: Fritted 8 mm, Bulk: Metallic

	Beam V-4A-CR8-M-1	Beam V-4A-CR8-M-2	Beam V-4A-CR8-M-3
	Material characteristics	**Material characteristics**	**Material characteristics**
The product:	Fritted glass + Combi Mag. Float (Maltha)	Fritted glass + Combi Mag. Float (Maltha)	Fritted glass + Combi Mag. Float (Maltha)
Cullet grade:	Class B + Class C	Class B + Class C	Class B + Class C
Contamination:	Frit glass + Metal.Pollutants	Frit glass + Metal.Pollutants	Frit glass + Metal.Pollutants
Cullet Type:	Sheet + Small shards	Sheet + Small shards	Sheet + Small shards
Forming temperature:	1070 °C	1070 °C	1070 °C

(a) (b) (c)

	Feasibility characteristics	Feasibility characteristics	Feasibility characteristics
Compatibility:	high	high	high
Transparency:	translucent	translucent	translucent
Mould reaction:	present	present	present
Cracks presence:	absent	present	absent
Breakage:	absent	present	absent
Bubbles level:	medium	medium	medium
Structural performance:	succeeded	failed	succeeded

Figure 83: Feasibility validation of Fire Round 4A, (a) Beam V-4A-CR8-M-1, (b) Beam V-4A-CR8-M-2 and (c) Beam V-4A-CR8-M-3

6.7 Discussion and conclusion

The following tables provide an overview of the structural feasibility validations for each beam. The beams are evaluated based on compatibility, transparency, mould reaction, cracks, breakage, bubbles level, and structural performance, as previously mentioned. The grading guidelines are displayed in Table 14. Before conducting the four-point bending tests, it is crucial to verify the values related to compatibility, cracks, breakage, and structural performance. If a beam fails under any of these conditions, it would not be suitable for use as a load-bearing façade cladding.

The results of the feasibility validation for the homogeneous beams are shown in Table 15. Tables 16, 17, and 18 present the results for the composite beams. Table 16 focuses on the optimal ratio between surface and bulk, featuring Float glass on the surface and CSP pollutants in the bulk. Table 17 examines the influence of the bulk material, with beams containing Float glass at the surface and metallic pollutants in the bulk. Table 18 investigates the influence of the surface material, using Fritted glass on the surface and CSP pollutants or metallic pollutants in the bulk.

6.7.1 Results homogeneous beams

For the homogeneous beams, the focus was on a single pollutant type. These tests were conducted over multiple fire rounds: Fire Round 1A, Fire Round 1B, Fire Round 1C, and Fire Round 1D. During these rounds, the quality grades of the following cullets were tested: Cullet Type A, Cullet Type B, and Cullet Type C. The results are presented in Table 15.

Class A Cullet

Three beams made from Class A cullet, containing only Float glass, were produced. These beams exhibit high compatibility and score well in all other characteristics. They serve as a reference group for comparing the structural performance with composite beams.

Class B Cullet

Beams with Fritted glass

During Fire Round 1B, homogeneous beams with Fritted glass were created. All these beams demonstrate high compatibility and are free from cracks and breakage. However, they do contain a small number of bubbles.

Beams with soft coated glass

During Fire Round 1B, homogeneous beams with soft coated glass were created. Beam V-1B-H-S-1 contained some silicone traces. While making this composition it was very difficult to remove the silicone traces. It can be helpful to be aware of this issue because, although everything is removed manually for this thesis, it would be extremely challenging to remove the silicone on a bigger scale. The thermal expansion mismatch between silicone and glass caused a few cracks in Beam V-1B-H-S-1, which caused it to break before the structural performance test. In the case of the beam V-1B-H-B-1, things were different. This beam turned out really good. Given that the coating melted entirely at 1120 degrees in the oven, it had a high compatibility.

Conclusions - Class B Cullet

- Similar results are obtained for beams with Fritted glass and the beams with a blue solar soft coating. Both show a high compatibility.
- At a temperature of 1120 degrees, the coatings and the frit burn and disappear.
- Almost all the beams contain white traces on top of the beam, containing a bit of surface crystallization.

Characteristics	Grading system			
	-	+	++	+++
Compatibilty		Low	Medium	High
Transparency		Opaque	Translucent	Transparant
Mould reaction	Present	Medium	Low	Absent
Cracks	Present	Medium	Low	Absent
Breakage	Present	Medium	Low	Absent
Bubbles level		High	Medium	Low
Structural performance	Failed			Succeeded

Table 14: Grading system of the feasibility validation of the created beams

Figure 84: Ceramic traces on cullets

Beam information						Feasibility characteristics						
Beam Name	The product	Cullet grade	Contamination	Cullet type	Forming temperature	Compatibility	Transparency	Mould reaction	Cracks	Breakage	Bubbles level	Structural performance
Homogeneous beams												
V-1A-H-C-1	Combi CSP Float (Maltha)	Class C	CSP Pollutants	Small Shards	1120 °C	+++	++	++	+	+++	++	+++
V-1A-H-C-2	Combi CSP Float (Maltha)	Class C	CSP Pollutants	Small Shards	1120 °C	+++	++	++	++	+++	+++	+++
V-1A-H-C-3	Combi CSP Float (Maltha)	Class C	CSP Pollutants	Small Shards	1120 °C	++	++	++	-	-	++	-
V-1A-H-HR-1	Combi HR Float (Maltha)	Class C	HR glass	Small Shards	1120 °C	+	++	+++	-	-	+++	-
V-1A-H-HR-2	Combi HR Float (Maltha)	Class C	HR glass	Small Shards	1120 °C	++	++	++	-	-	+++	-
V-1A-H-HR-3	Combi HR Float (Maltha)	Class C	HR glass	Small Shards	1120 °C	+	+	+	-	-	+++	-
V-1B-H-F-1	Lacobel LT Black (AGC)	Class B	Fritted glass	Small Shards	1120 °C	+++	++	+++	+++	+++	+++	+++
V-1B-H-F-2	Lacobel LT Black (AGC)	Class B	Fritted glass	Small Shards	1120 °C	+++	++	+++	+++	+++	+++	+++
V-1B-H-F-3	Lacobel LT Black (AGC)	Class B	Fritted glass	Small Shards	1120 °C	+++	++	+++	+++	+++	+++	+++
V-1B-H-HR-1	Combi HR Float (Maltha)	Class C	HR glass	Small Shards	1120 °C	+++	++	+++	+++	+++	+++	+++
V-1B-H-B-1	SunGuard Solar Light Blue 52 (Guardian)	Class B	Soft coated	Small Shards	1120 °C	+++	++	+++	+++	+++	+++	+++
V-1B-H-S-1	SunGuard eXtraSelective SNX 60/28 (Guardian)	Class B	Soft coated	Small Shards	1120°C	++	++	+++	+	-	++	-
V-1C-H-M-1	Combi Mag. Float (Maltha)	Class C	Metallic Pollutants	Small Shards	1070 °C	+++	++	+	++	+++	++	+++
V-1C-H-M-2	Combi Mag. Float (Maltha)	Class C	Metallic Pollutants	Small Shards	1070 °C	+++	++	+	+++	+++	+	+++
V-1C-H-M-3	Combi Mag. Float (Maltha)	Class C	Metallic Pollutants	Small Shards	1070 °C	+++	++	+	+++	+++	++	+++
V-1D-H-FL-1	Float glass (Pilkington)	Class A	-	Sheets	1070 °C	+++	++	+++	+++	+++	+++	+++
V-1D-H-FL-2	Float glass (Pilkington)	Class A	-	Sheets	1070 °C	+++	++	+++	+++	+++	+++	+++
V-1D-H-FL-3	Float glass (Pilkington)	Class A	-	Sheets	1070 °C	+++	++	+++	+++	+++	+++	+++

Table 15: Overview structural feasibility validation of the homogeneous beams with cullet grade A, B and C

Class C Cullet

Beams with HR glass

During Fire Round 1A, three homogeneous beams with HR glass were produced. Since no ceramic or silicone was removed from this batch, all the beams contained large cracks and fractures. The cullets that damaged these compositions are shown in Figure 84. For Fire Round 1B, one beam with HR glass was made. However, this beam did not contain these types of inclusions. As a result, no cracks were visible, and the compatibility increased from low to high.

Beams with CSP Pollutants

During Fire Round 1A, three homogeneous beams with CSP pollutants were constructed. The beams exhibited similar feasibility characteristics and contained several colour streaks, likely due to tinted glass in the batch. However, since the batch composition is unclear, it is impossible to determine which cullet originated in which part of the beam. Consequently, some cracks developed in these beams because the thermal expansion of specific cullets varied too much from one another. In the structural performance evaluation, beams V-1A-H-C-1 and V-1A-H-C-2 did not break. However, before the structural performance test, beam V-1A-H-C-3 broke due to an excessive number of cracks.

Beams with Metallic Pollutants

During Fire Round 1C, three homogeneous beams with metallic pollutants were created. The beams have similar characteristics and all exhibit medium to high mould reactions, with the metal starting to “eat” the mould. Additionally, these beams contain a medium to high level of bubbles, which is also noteworthy.

Conclusions - Class C Cullet

- Ceramic and silicone inclusions should be eliminated from the mixture. Beams with these traces fail for the structural performance.
- The compatibility increases from low to high when ceramic and silicone inclusions are eliminated from the HR glass composition.
- The CSP Pollutant mix provides a homogenised product with streaks of different colours in the glass composition. This composition, however, since the composition is unknown each time the result can vary meaning the composition can have varying results for the material composition.
- Almost all the beams contain white traces on top of the beam, containing a bit of surface crystallization.
- The Metallic Pollutant mix contains medium to high mould reaction since the metal started to react with the mould.

6.7.2 Results composite beams - Ratios

For the composite beams, the focus was on determining the optimal ratio between surface and bulk. These tests were conducted across multiple fire rounds: Fire Round 2A, Fire Round 2B, (Fire Round 2C), and Fire Round 2D. During these rounds, the following ratios between surface and bulk were tested: Surface 6 mm with a Bulk of 15 mm, Surface 8 mm with a Bulk of 13 mm, Surface 10 mm with a Bulk of 11 mm, and Surface 12 mm with a Bulk of 9 mm. The results are presented in Table 16.

Composite beams: Surface Float 6 mm, Bulk CSP

During Fire Round 2B, two composite beams with this composition were created. Beams V-2B-C6-C-1 and V-2B-C6-C-2 are very similar. Although they both received decent overall scores, their bubbles level scores are medium. The bubbles were found near the top of the beams. For the structural performance test, the bubbles will be visible from a side view, most likely the back. Another beam with this composition was being made during Fire Round 2D. Beam V-2D-C6-C-1 shows some mould reaction on the side due to an interaction between the cullets (probably due to a coating) and the mould.

Composite beams: Surface Float 8 mm, Bulk CSP

Multiple beams of this composition were being made over several fire rounds. During Fire Round 2A, three beams with this composition were made. The CSP Pollutant composition is the same as that used in the material batch of the CSP Pollutant Homogeneous beams. As mentioned previously, since the material composition of this batch is unknown, the results will vary each time. Two beams broke due to too many cracks and fractures: beam V-2A-C8-C-2 and beam V-2A-C8-C-3 failed the structural performance test. Beam V-2A-C8-C-1 passed the structural performance test; however, it also contained a few cracks and fractures on the side. Since the broken sections were outside the beam’s essential zone— the tension zone, as shown in Figure 19— this was not a problem.

As mentioned previously, some harmful pollutants were removed for Fire Round 2B (see paragraph 9.1: Influence of cullet selection). During Fire Round 2B, two beams of this new composition were produced: Beam V-2B-C8-C-1

Beam information						Feasibility characteristics						
Beam Name	The product	Cullet grade	Contamination	Cullet type	Forming temperature	Compatibility	Transparency	Mould reaction	Cracks	Breakage	Bubbles level	Structural performance
Composite beams - Ratios - I												
V-2A-C8-C-1	Float glass 8 mm + Combi CSP Float (Maltha)	Class A + Class C	Float glass + CSP Pollutants	Sheet + Small Shards	1070 °C	++	++	+++	+	+	++	+++
V-2A-C8-C-2	Float glass 8 mm + Combi CSP Float (Maltha)	Class A + Class C	Float glass + CSP Pollutants	Sheet + Small Shards	1070 °C	++	++	++	-	-	+++	-
V-2A-C8-C-3	Float glass 8 mm + Combi CSP Float (Maltha)	Class A + Class C	Float glass + CSP Pollutants	Sheet + Small Shards	1070 °C	++	++	++	-	-	+++	-
V-2A-C10-C-1	Float glass 10 mm + Combi CSP Float (Maltha)	Class A + Class C	Float glass + CSP Pollutants	Sheet + Small Shards	1070 °C	+++	++	+++	+++	+++	+++	+++
V-2A-C10-C-2	Float glass 10 mm + Combi CSP Float (Maltha)	Class A + Class C	Float glass + CSP Pollutants	Sheet + Small Shards	1070 °C	++	++	+++	-	-	+++	-
V-2A-C10-C-3	Float glass 10 mm + Combi CSP Float (Maltha)	Class A + Class C	Float glass + CSP Pollutants	Sheet + Small Shards	1070 °C	+++	++	+++	-	-	+++	-
V-2B-C6-C-1	Float glass 6 mm + Combi CSP Float (Maltha)	Class A + Class C	Float glass + CSP Pollutants	Sheet + Small Shards	1070 °C	+++	++	+++	+++	+++	++	+++
V-2B-C6-C-2	Float glass 6 mm + Combi CSP Float (Maltha)	Class A + Class C	Float glass + CSP Pollutants	Sheet + Small Shards	1070 °C	+++	++	+++	++	+++	++	+++
V-2B-C8-C-1	Float glass 8 mm + Combi CSP Float (Maltha)	Class A + Class C	Float glass + CSP Pollutants	Sheet + Small Shards	1070 °C	+++	++	+++	+++	+++	+++	+++
V-2B-C8-C-2	Float glass 8 mm + Combi CSP Float (Maltha)	Class A + Class C	Float glass + CSP Pollutants	Sheet + Small Shards	1070 °C	+++	++	+++	+++	+++	+++	+++

and beam V-2B-C8-C-2. Both beams exhibit excellent results, with no visible cracks or fractures, and show a high compatibility.

In Fire Round 2D, two more beams of the same composition as those in Fire Round 2B were being utilised. These beams also demonstrate good feasibility results. However, beam V-2D-C8-C-1 displays a severe perpendicular line in the middle, causing the Float glass to be cut in half. This line corresponds to the tensile area zone.

Composite beams: Surface Float 10 mm, Bulk CSP

Multiple beams of this composition were being produced over several fire rounds. During Fire Round 2A, three beams of this compositon were made. Beam V-2A-C10-C-1 showed great promise; it exhibits a high degree of compatibility and had not yet developed any cracks. However, the other two beams, V-2A-C10-C-2 and V-2A-C10-C-3, failed the structural performance test. Both of these beams contained too many cracks and fractures, likely due to the unknown material composition.

In Fire Round 2B, two new beams were created with a new material composition where harmful pollutants were removed. Beam V-2B-C10-C-1 and V-2B-C10-C-2 both passed the structural performance test and do not exhibit any cracks or fractures. However, these beams show some mould reaction on the side, likely due to a reaction between the cullets and the mould, possibly caused by a coating.

During the latest round, Fire Round 2D, another beam was fabricated, featuring the same material composition as in Fire Round 2B. This particular beam, named V-2D-C10-C-1, exhibits a severe perpendicular line in the middle, resulting in the Float glass was cut in half. This line aligns with the tensile area zone.

Composite beams: Surface Float 12 mm, Bulk CSP

During Fire Round 2D, three beams with this composition were in production. The beams exhibit good structural feasibility overall, displaying high compatibility and no cracks or fractures. However, they show some mould reaction on the side, likely resulting from the cullets with a coating reacting with the mould.

Conclusions - Composite beams ratio surface to bulk

- When the material composition of the bulk is unknow (Fire Round 2A), this has a negative influence on the overall structural feasibility.
- At a temperature of 1070 degrees, the surface (Float glass) and the bulk (cullets with CSP Pollutants) interfere well with each other.
- In some cases the cullets mixed more with the Float glass, this is because of their weight, which causes them to sink to the bottom due to gravity.
- Almost all the beams contain white traces on top of the beam, containing a bit of surface crystallization.
- Since composite beams (with CSP pollutants in the bulk) often have a high compatibility, a composite beam with CSP contaminants in the bulk is a promising option for a panel.

6.7.3 Results composite beams - Bulk

For the subsequent composite beams, the emphasis was on determining the impact of the bulk material. These tests were carried out over multiple fire rounds: Fire Round 2A and Fire Round 3A. During these rounds, the following bulk material compositions were examined: Surface 8 mm with a Bulk of 13 mm with Fritted glass, Surface 8 mm with a Bulk of 13 mm with Metallic Pollutants, and Surface 10 mm with a Bulk of 11 mm with Metallic Pollutants. The results are outlined in Table 17.

Composite beams: Surface Float 8 mm, Bulk Fritted glass

During Fire Round 2A, a single beam with this material composition was being fabricated. Beam V-2A-C8-F-1 achieved a high structural feasibility score. This beam demonstrated excellent compatibility, showed no cracks, and the black colour of the Fritted glass had completely vanished, aligning with the results of the homogeneous beams with Fritted glass.

Composite beams: Surface Float 8 mm, Bulk Metallic

During Fire Round 3A, three beams of this composition were made. All three beams demonstrated high compatibility and showed no cracks or breaks, suggesting strong feasibility for structural performance. However, a notable side effect was the presence of significant mould reactions on all beams. In particular, beam V-3A-C8-M-1 exhibited severe mould reactions, where the metal traces and the mould interacted with each other.

Composite beams: Surface Float 10 mm, Bulk Metallic

Three beams of this composition were made during Fire Round 3A. All three beams exhibited high compatibility. Additionally, these beams displayed mould reactions where the metal traces reacted with the mould. Beams V-3A-C10-M-1 and V-3A-C10-M-2 showed no cracks or breaks, indicating good structural feasibility. However, one beam, V-3A-C10-M-3, failed due to a ceramic inclusion. This occurrence is rare because extra attention was paid to removing ceramic inclusions during the composition process. It suggests that eliminating these inclusions is a challenging task, which is likely to pose difficulties on a larger scale.

Beam information						Feasibility characteristics						
Beam Name	The product	Cullet grade	Contamination	Cullet type	Forming temperature	Compatibility	Transparency	Mould reaction	Cracks	Breakage	Bubbles level	Structural performance
Composite beams - Ratios - II												
V-2B-C10-C-1	Float glass 10 mm + Combi CSP Float (Maltha)	Class A + Class C	Float glass + CSP Pollutants	Sheet + Small Shards	1070 °C	+++	++	++	+++	+++	+++	+++
V-2B-C10-C-2	Float glass 10 mm + Combi CSP Float (Maltha)	Class A + Class C	Float glass + CSP Pollutants	Sheet + Small Shards	1070 °C	+++	++	++	+++	+++	+++	+++
V-2D-C6-C-1	Float glass 6 mm + Combi CSP Float (Maltha)	Class A + Class C	Float glass + CSP Pollutants	Sheet + Small Shards	1070 °C	+++	++	++	+++	+++	+++	+++
V-2D-C8-C-1	Float glass 8 mm + Combi CSP Float (Maltha)	Class A + Class C	Float glass + CSP Pollutants	Sheet + Small Shards	1070 °C	+++	++	++	++	+++	+++	+++
V-2D-C8-C-2	Float glass 8 mm + Combi CSP Float (Maltha)	Class A + Class C	Float glass + CSP Pollutants	Sheet + Small Shards	1070 °C	+++	++	++	+++	+++	+++	+++
V-2D-C10-C-1	Float glass 10 mm + Combi CSP Float (Maltha)	Class A + Class C	Float glass + CSP Pollutants	Sheet + Small Shards	1070 °C	+++	++	+++	++	+++	+++	+++
V-2D-C12-C-1	Float glass 12 mm + Combi CSP Float (Maltha)	Class A + Class C	Float glass + CSP Pollutants	Sheet + Small Shards	1070 °C	+++	++	++	+++	+++	+++	+++
V-2D-C12-C-2	Float glass 12 mm + Combi CSP Float (Maltha)	Class A + Class C	Float glass + CSP Pollutants	Sheet + Small Shards	1070 °C	+++	++	++	+++	+++	+++	+++
V-2D-C12-C-3	Float glass 12 mm + Combi CSP Float (Maltha)	Class A + Class C	Float glass + CSP Pollutants	Sheet + Small Shards	1070 °C	+++	++	++	+++	+++	+++	+++

Table 16: Overview structural feasibility of the compostite beams, focus on ratio between surface and bulk

Beam information						Feasibility characteristics						
Beam Name	The product	Cullet grade	Contamination	Cullet type	Forming temperature	Compatibility	Transparency	Mould reaction	Cracks	Breakage	Bubbles level	Structural performance
Composite beams - Bulk												
V-2A-C8-F-1	Float glass 8 mm + Lacobel LT Black (AGC)	Class A + Class B	Float glass + Fritted glass	Sheet + Small Shards	1070 °C	+++	++	+++	+++	+++	+++	+++
V-3A-C8-M-1	Float glass 8 mm + Combi Mag. Float (Maltha)	Class A + Class C	Float glass + Metallic Pollutants	Sheet + Small Shards	1070 °C	+++	++	+	+++	+++	+++	+++
V-3A-C8-M-2	Float glass 8 mm + Combi Mag. Float (Maltha)	Class A + Class C	Float glass + Metallic Pollutants	Sheet + Small Shards	1070 °C	+++	++	++	+++	+++	+++	+++
V-3A-C8-M-3	Float glass 8 mm + Combi Mag. Float (Maltha)	Class A + Class C	Float glass + Metallic Pollutants	Sheet + Small Shards	1070 °C	+++	++	++	+++	+++	+++	+++
V-3A-C10-M-1	Float glass 8 mm + Combi Mag. Float (Maltha)	Class A + Class C	Float glass + Metallic Pollutants	Sheet + Small Shards	1070 °C	+++	++	++	++	+++	++	+++
V-3A-C10-M-2	Float glass 8 mm + Combi Mag. Float (Maltha)	Class A + Class C	Float glass + Metallic Pollutants	Sheet + Small Shards	1070 °C	+++	++	++	+++	+++	+++	+++
V-3A-C10-M-3	Float glass 8 mm + Combi Mag. Float (Maltha)	Class A + Class C	Float glass + Metallic Pollutants	Sheet + Small Shards	1070 °C	+++	++	++	-	-	+++	-

Table 17: Overview structural feasibility of the compostite beams, focus on different bulk material

Conclusions - Composite beams bulk material

- Nearly all the beams demonstrated high compatibility and feasibility for structural performance as they did not show any cracks or breaks.
- However, a notable side effect of this composition was the significant mould reactions observed in all the beams. This indicates a potential issue with the interaction between the metal traces and the mould.

6.7.4 Results composite beams - Surface

For the subsequent composite beams, the focus was on determining the impact of the surface material. This was tested during Fire Round 4A by using Fritted glass instead of Float glass for the surface. The following material compositions were investigated: Surface 8 mm with a Bulk of 13 mm with CSP, and Surface 8 mm with a Bulk of 13 mm with Metallic Pollutants. The results are presented in Table 18.

Beam information						Feasibility characteristics						
Beam Name	The product	Cullet grade	Contamination	Cullet type	Forming temperature	Compatibility	Transparency	Mould reaction	Cracks	Breakage	Bubbles level	Structural performance
Composite beams - Surface												
V-4A-CR8-C-1	Fritted glass 8 mm + Combi CSP Float (Maltha)	Class B + Class C	Float glass + CSP Pollutants	Sheet + Small Shards	1070 °C	+++	++	+++	-	-	+++	-
V-4A-CR8-C-2	Fritted glass 8 mm + Combi CSP Float (Maltha)	Class B + Class C	Float glass + CSP Pollutants	Sheet + Small Shards	1070 °C	+++	++	+++	++	+++	+++	+++
V-4A-CR8-C-3	Fritted glass 8 mm + Combi CSP Float (Maltha)	Class B + Class C	Float glass + CSP Pollutants	Sheet + Small Shards	1070 °C	+++	++	+++	+++	+++	+++	+++
V-4A-CR8-M-1	Fritted glass 8 mm + Combi Mag. Float (Maltha)	Class B + Class C	Float glass + Metallic Pollutants	Sheet + Small Shards	1070 °C	+++	++	++	+++	++	++	+++
V-4A-CR8-M-2	Fritted glass 8 mm + Combi Mag. Float (Maltha)	Class B + Class C	Float glass + Metallic Pollutants	Sheet + Small Shards	1070 °C	+++	++	+	-	-	++	-
V-4A-CR8-M-3	Fritted glass 8 mm + Combi Mag. Float (Maltha)	Class B + Class C	Float glass + Metallic Pollutants	Sheet + Small Shards	1070 °C	+++	++	+	+++	+++	++	+++

Table 18: Overview structural feasibility of the compostite beams, focus on different surface material

Composite beams: Surface Fritted 8 mm, Bulk CSP

Three beams were made with this composition. None of the beams experienced mould reactions. In terms of structural feasibility, one beam failed, namely beam V-4A-CR8-C-1. This failure was attributed to a large ceramic inclusion in the middle of the bulk. On the other hand, beams V-4A-CR8-C-2 and V-4A-CR8-C-3 both succeeded in terms of structural performance feasibility. Beam V-4A-CR8-C-3, in particular, is noteworthy as it contains no cracks, presenting an interesting outcome.

Composite beams: Surface Fritted 8 mm, Bulk Metallic

Three beams were made with this composition. One of the beams, beam V-4A-CR8-M-2, failed in terms of structural feasibility due to severe cracks. However, the other two beams succeeded. All beams exhibit medium to high mould reactions, similar to the beams from Fire Rounds 1C and 3A.

Conclusions - Composite beams surface material

- The black frit is totally vanished from the beams, and burned at a temperature of 1070 degrees which also already had been seen during Fire Round 2A.
- The line between the Fritted glass and the cullets is still remaining. So you can clearly see where the frit was located and where bulk composition
- All the beams contain a high compatibility
- No mould reaction has taken place on the beams with CSP Pollutants, however for the beams with Metallic Pollutants there is a high mould reaction for each beam.

07 | MECHANICAL TESTS

7.1 Preparation for structural performance tests

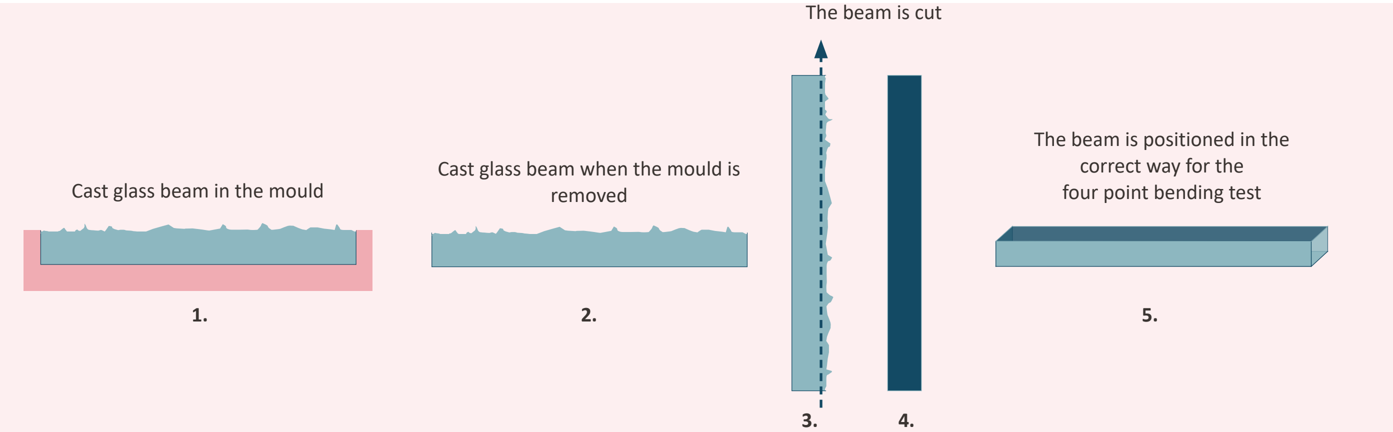

Figure 85: Illustration how to prepare the beams for structural analysyis

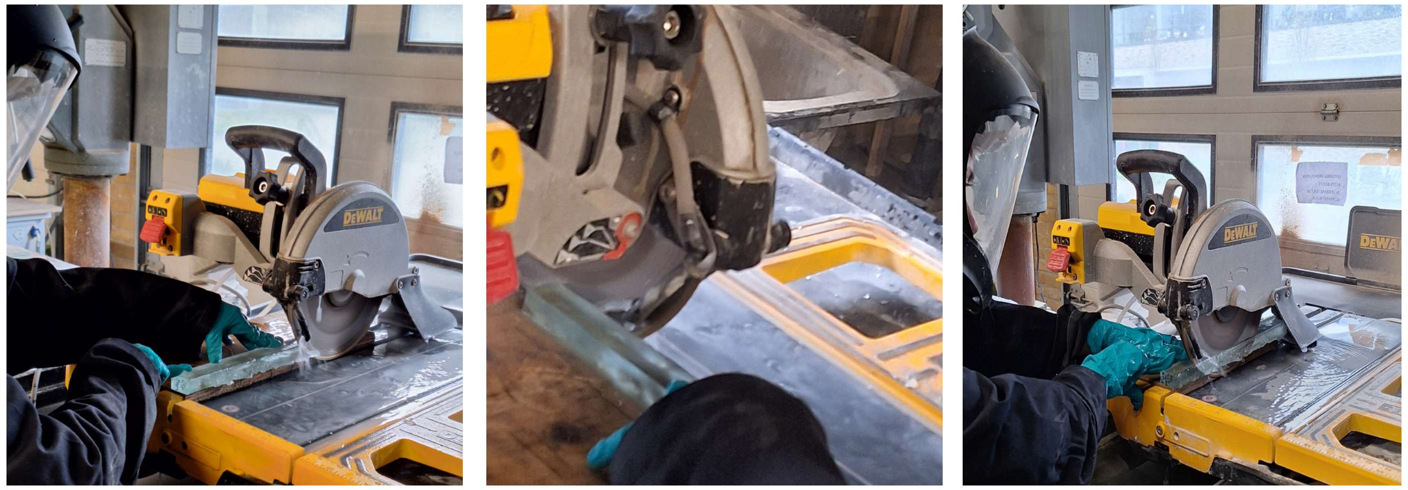

Figure 86: Cutting the beams with a diamond saw

7.1.1 Cutting of the beams

Before undergoing the four-point bending test, all beams had to undergo uniform surface and edge treatment. To ensure accurate comparison of results, beams were standardised to similar dimensions. The glass was set to a width of 29–30 mm using a diamond saw, as depicted in Figure 85 and Figure 86, illustrating the cutting procedure of the glass beams.

7.1.2 Polishing of the beams

After cutting the beams, each beam underwent polishing. The beams were arranged for a uniformity check using a 60 grit, aiming for a distance of approximately 28–29 mm. Once adjusted to 28 mm, the edges also received surface treatment. The beams were polished to a high smoothness level by starting with a 60 grit, followed by 120, 200, 400, and finally 600 grit. (Figure 87)

7.1.3 Identifying of each beams

Following polishing, the beams required additional inspection. The beams had to be reidentified before they could be subjected to the four point bending test. The beam's height is 21 mm, while its width is 28 mm. The most attractive surface needed to be chosen, and it was typically the one that measured 28 mm by 350 mm and was on the mould side rather than the cut side. Next, it was necessary to choose the surface that will be in front of the four-point bending test. This side, which measures 21 mm by 350 mm, is also the one that appears to be the most attractive or it may have an intriguing fracture or pollution on the front view. Once the beam was positioned appropriately, it needed to be identified. An overview of the name giving process is shown in Figure 88. Every beam's code was positioned in the left corner. The beam code is used as explained in paragraph 6.6 Feasibility validation – Names of cast glass beams. Following that, measurements of the beam's width and height were required. How the beam was measured is visualised in Figure 89. All of the measurements were entered into a table using this data. Appendix C: Overview beams with dimensions.

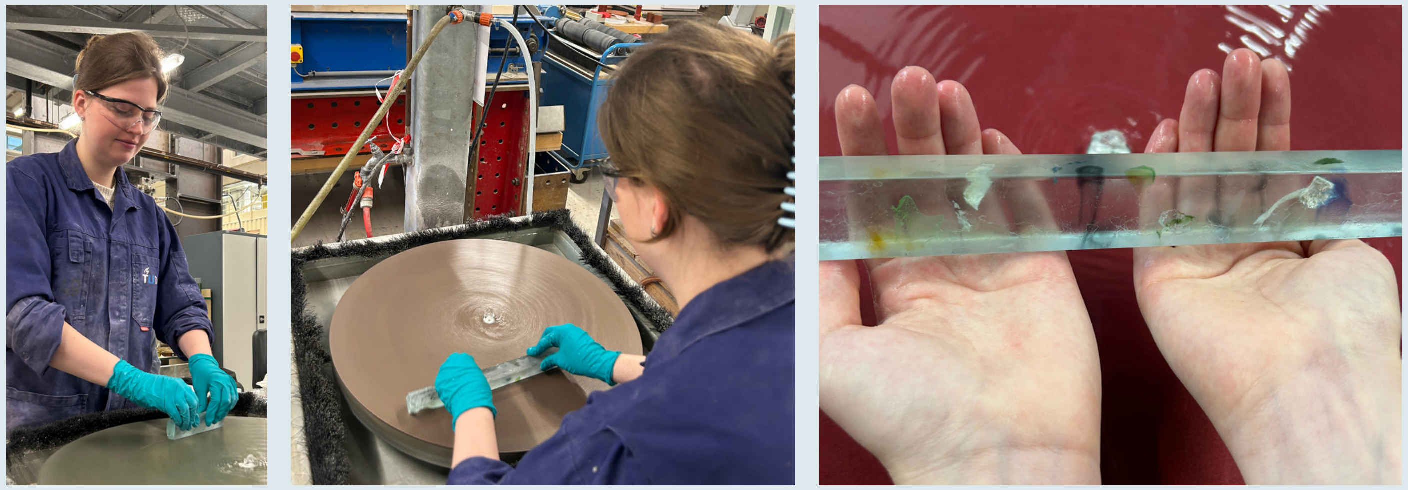

Figure 87: Polishing beams

Furthermore, it is important to provide a comprehensive visual assessment of each beam. Appendix D presents this overview, featuring photographs of each beam from various angles: front view, top view, back view, bottom view, and bird's-eye view.

7.1.4 Four-point bending test process

Under the guidance of Dr. Veer, the four-point bending tests were conducted. The beams were tested using a Zwick Z10 displacement-controlled universal testing machine in a laboratory air environment, at a rate of 0.1mm/min. The four-point bending fixtures featured a 140 mm span for the loading rollers and a 280 mm span for the support rollers, with 10 mm diameter fixed loading pins. These fixtures were loosely connected to the testing machine to allow some hinging. Figure 90 provides an overview of how the beams were positioned in the test setup.

During the tests, attention was given to several factors: the maximum load applied to the beam before failure, the location of failure (left, centre, or right), the distance

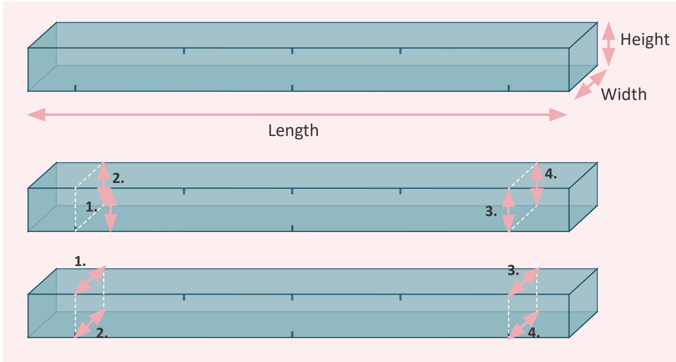

Figure 89: Illustration how to measure each beam for the structural performance test

of the fracture from the middle of the beam (to assess misalignments or torsion), the type of crack observed (low energy failure, medium-high energy failure, or high energy failure), and the location and shape of the crack, which provide information about the stress level. Lastly, the reason for the breakage, including any flaws causing the failure, was investigated under the microscope. The crack patterns and fracture analysis are further discussed in the next chapter, Chapter 8: Microscopic validation.

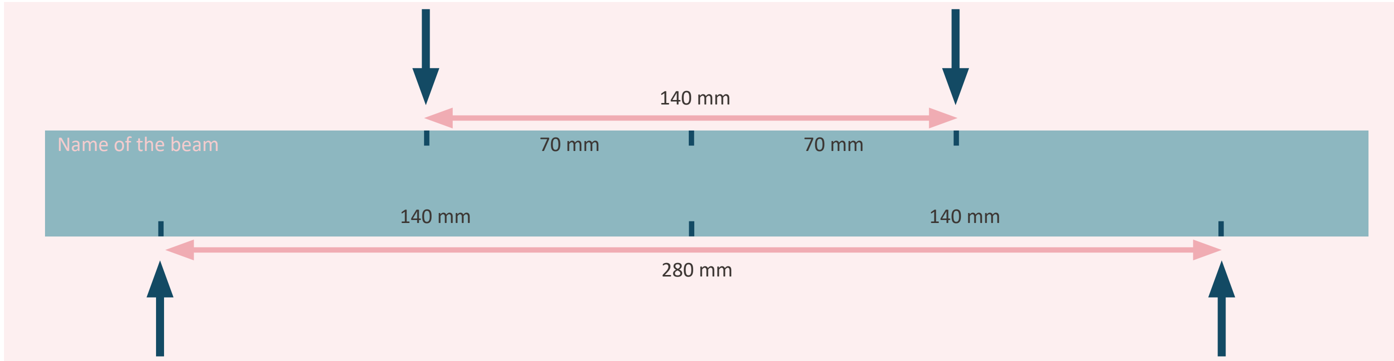

Figure 88: Illustration how to identify each beam for the structral performance test

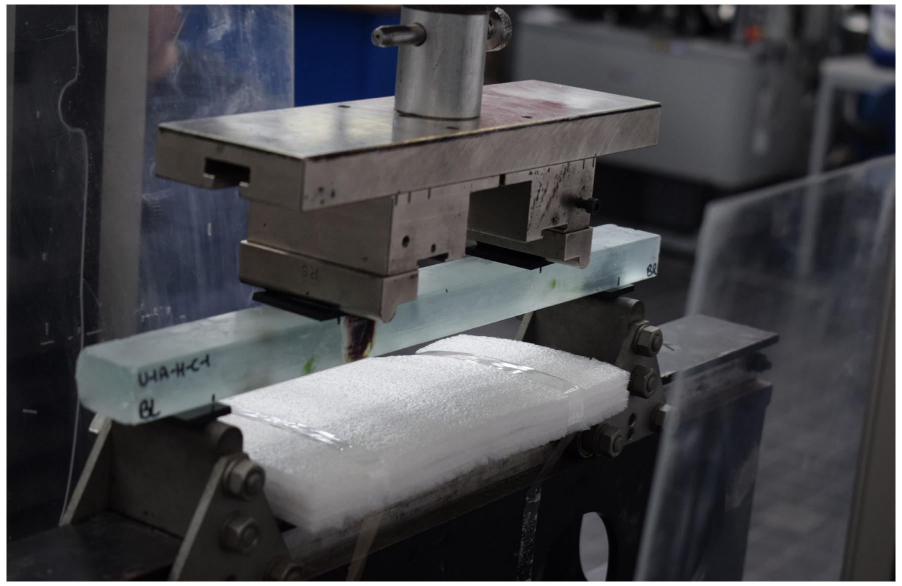

Figure 90: Photo of the test set-up of a four-point bending test

7.1.5 Planning of the four-point bending tests

For this thesis, four four-point bending tests were conducted. During Four-point bending test I, beams from Fire Rounds 1A, 1B, 2A, and 2B were tested. During Four-point bending test II, beams from Fire Rounds 2C, 2D, 3A, and 4A were investigated. During Four-point bending test III, beams from Fire Rounds 1C, 2D, and 4A were examined. Finally, during Four-point bending test IV, the beams from Fire Round 1D were studied.

7.2 Four point bending test results

The maximum load was measured during the four-point bending tests. The flexural strength of every beam could be determined by applying the calculations found in Chapter 3, "Mechanical behaviour of glass." Formula 2, which provides the nominal flexural strength, is used in this calculation. It also takes into account the coefficient of friction, which is explained in Formula 3. This Chapter ignores the elastic behaviour and deflection because these are not the main focus of this research. Moreover, the Young's modulus calculation produced false numbers; as a result, it has been disregarded.

The strength at the support formula is another value that is utilised for the calculations.

$$\sigma = \frac{3Pa}{bd^2}$$

P = Maximum load
a = Support span - Loadspan
b = Beam's width
d = Beam's height

Formula 10: Strength at support

The tables that show the outcomes of these computations can be found in Appendix E: Overview beams with structural performance - Four point bending test I, II, III and IV

7.2.1 General overview

Graph 05 provides a general overview of the flexural strength of each beam across the four four-point bending tests. The four experimental groups are as follows:

- Experiment Type 1 (blue): Homogeneous beams, tested with specimens 1.1-1.7, 3.1-3.3, and 4.1-4.3.
- Experiment Type 2 (pink): Composite beams, focusing on the optimal ratio between surface and bulk, tested with specimens 1.8, 1.9, 1.11-1.16, 2.8, 2.9, and 3.4-3.8.
- Experiment Type 3 (dark pink): Composite beams, examining the influence of bulk material, tested with specimens 1.10 and 2.10-2.14.
- Experiment Type 4 (light pink): Composite beams, investigating the influence of surface material, tested with specimens 2.15, 2.16, 3.9, and 3.10.

The graph reveals varying results. Further analysis, focusing on individual parameters, will provide more comprehensive conclusions. However, some general observations can be made. For Experiment Type 1, homogeneous beams with CSP Pollutants (type C cullet) perform the worst. Beams with Fritted glass also show comparable performance. The best-performing beam

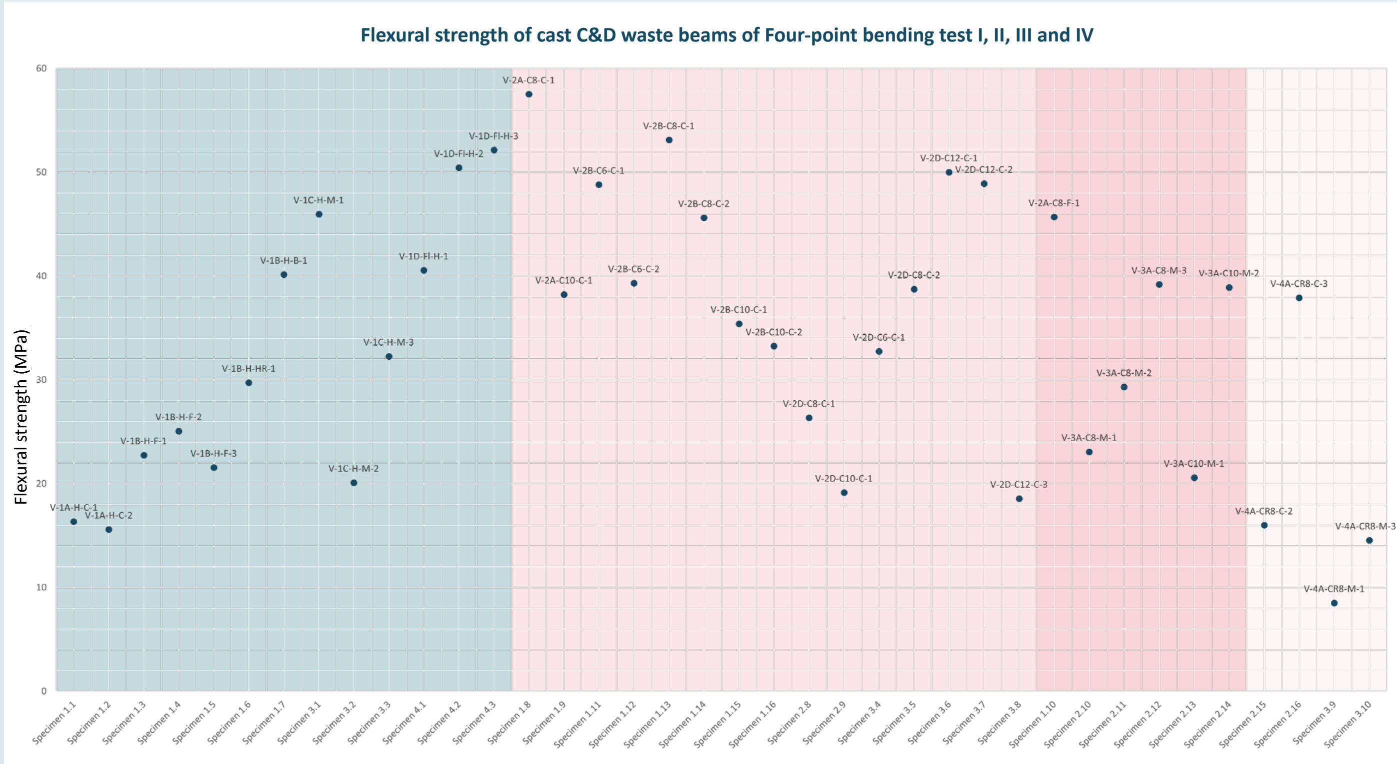

Graph 05: General overview of the flexural strength of all the beams during four-point bending test I, II, III and IV

The results from Fire Round 2C are not integrated in this graph, these will be explained in Chapter 9

Experiment type 1:
Homogeneous beams
Glass with A cullet

Float glass	V-1D-H-Fl-1, V-1D-H-Fl-2 and V-1D-H-Fl-3

Glass with B cullet

Fritted glass	V-1B-H-F-1, V-1B-H-F-2 and V-1B-H-F-3
Soft coating	V-1B-H-B-1

Glass with C cullet

CSP	V-1A-H-C-1 and V-1A-H-C-2
HR glass	V-1B-H-HR-1
Metallic	V-1C-H-M-1, V-1C-H-M-2 and V-1C-H-M-3

Experiment type 2:
Composite beams: Surface + Bulk
Float glass + CSP pollutants

6 mm + 15 mm	V-2B-C6-C-1 and V-2B-C6-C-2
8 mm + 13 mm	V-2A-C8-C-1, V-2B-C8-C-1, V-2B-C8-C-2, V-2D-C8-C-1 and V-2D-C8-C-2
10 mm + 11 mm	V-2A-C10-C-1, V-2B-C10-C-1, V-2B-C10-C-2, and V-2D-C10-C-1
12 mm + 9 mm	V-2D-C12-C-1, V-2D-C12-C-2 and V-2D-C12-C-3

Experiment type 3:
Composite beams: Surface + Bulk
Float glass + Fritted glass

8 mm + 13 mm	V-2A-C8-F-1

Float glass + Metallic pollutants

8 mm + 13 mm	V-3A-C8-M-1, V-3A-C8-M-2 and V-3A-C8-M-3
10 mm + 11 mm	V-3A-C10-M-1 and V-3A-C10-M-2

Experiment type 4:
Composite beams: Surface + Bulk
Fritted glass + CSP Pollutants

8 mm + 13 mm	V-4A-CR8-C-2 and V-4A-CR8-C-3

Fritted glass + Metallic Pollutants

8 mm + 13 mm	V-4A-CR8-M-1 and V-4A-CR8-M-3

overall is V-2A-C8-C-1, a composite beam with 8 mm Float glass and CSP Pollutants in the bulk.

In general, composite beams with Float glass and CSP Pollutants perform quite well, with the exception of beams V-2D-C8-C-1, V-2D-C10-1, and V-2D-C-12-3. These beams will be examined in more detail in Chapter 8: Microscopic validation, where microscopic analysis will pinpoint the defects causing their low-grade performance. Additionally, each beam's friction coefficient error is less than 5%, indicating that all the findings are statistically significant.

07 | MECHANICAL TESTS

Figure 91: Experiment Type 1: Homogeneous beams of Cullet Type A, Cullet Type B and Cullet Type C

Experiment type 1:
Homogeneous beams
Glass with A cullet

Fire Round 1D:	3 beams were made with the composition Float glass

Glass with B cullet

Fire Round 1B:	3 beams were made with the composition Fritted glass
Fire Round 1B:	2 beams were made with a soft coating, the blue solar light coating and the SNX 60/28 coating

Glass with C cullet

Fire Round 1A:	3 beams were made with the composition of HR glass
Fire Round 1B	1 beam was made with the composition of HR glass when harmful pollutants were removed
Fire Round 1A:	3 beams were made with CSP Pollutants in the bulk
Fire Round 1C:	3 beams were made with Metallic Pollutants in the bulk

Experiment type 1: **Total 18 beams**
Structural performance feasibility:
Succeeded: **13 beams**
Failed: **5 beams**

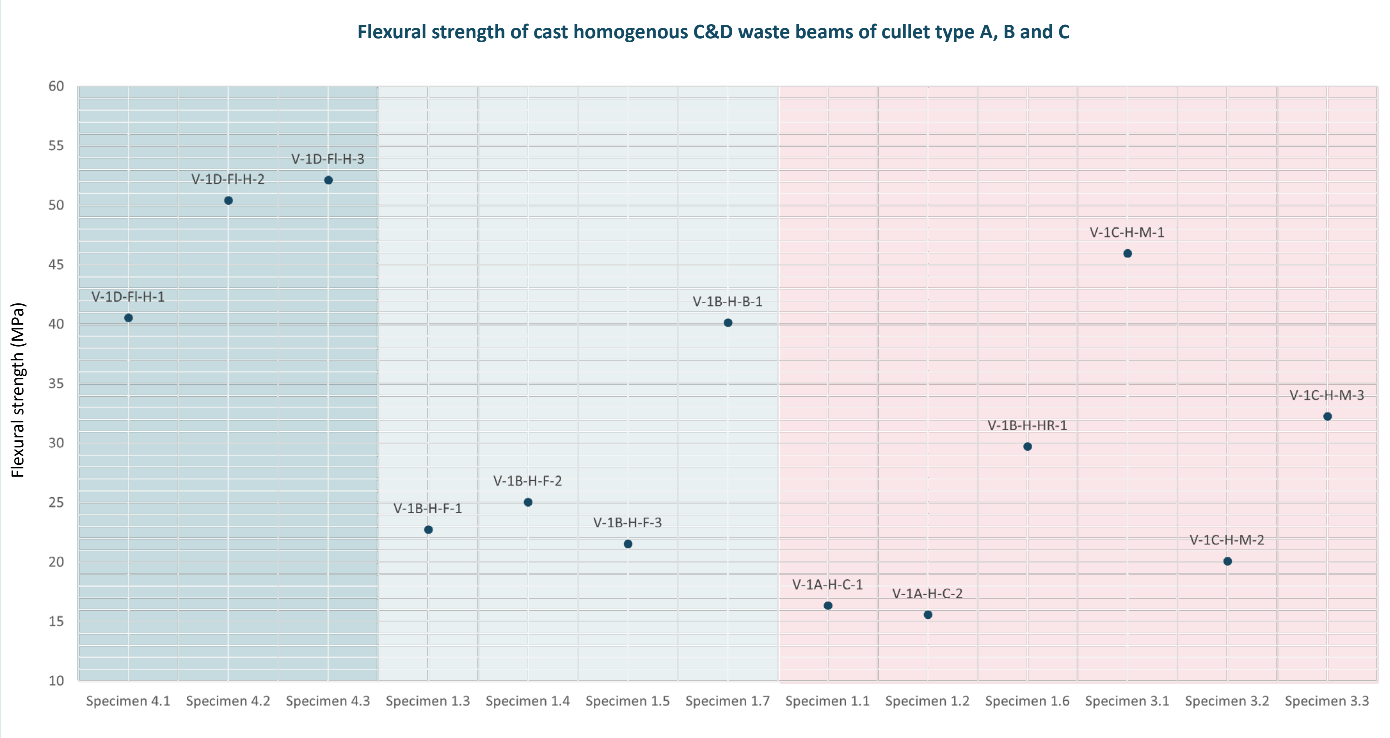

Graph 06: Flexural strength of all the homogeneous beams containing type A cullet, type B cullet and type C cullet

Experiment type 1:
Homogeneous beams
Glass with A cullet

Float glass	V-1D-H-Fl-1, V-1D-H-Fl-2 and V-1D-H-Fl-3

Glass with B cullet

Fritted glass	V-1B-H-F-1, V-1B-H-F-2 and V-1B-H-F-3
Soft coating	V-1B-H-B-1

Glass with C cullet

CSP	V-1A-H-C-1 and V-1A-H-C-2
HR glass	V-1B-H-HR-1
Metallic	V-1C-H-M-1, V-1C-H-M-2 and V-1C-H-M-3

7.2.2 Structural performance - Homogeneous beams

Graph 06 illustrates the structural performance of Experiment Type 1: Homogeneous beams. This graph includes homogeneous beams made from Cullet types A, B, and C.

- **Class A Cullet** (blue): Homogeneous beams with Float glass (specimens 4.1-4.3)
- **Class B Cullet** (light blue): Homogeneous beams with Fritted glass (specimens 1.3-1.5) and soft coated glass (specimen 1.7)
- **Class C Cullet** (pink): Homogeneous beams with CSP Pollutants (specimens 1.1 and 1.2), HR glass (specimen 1.6), and Metallic Pollutants (specimens 3.1-3.3)

The graph clearly shows that beams with Cullet Type A perform the best. Among Cullet Type B beams, the beam with soft coated glass (Beam V-1B-H-B-1) performs quite well, outperforming the beams with Fritted glass. There was also another soft coated beam, Beam V-1B-H-S-1, which failed before the structural performance test due to cracks and fractures caused by silicone inclusions. This indicates that removing silicone inclusions improves structural performance.

In general, Cullet Type B beams perform better than those with Cullet Type C. However, there is some variation in the performance of Cullet Type C beams. Beams with CSP Pollutants (Beams V-1A-H-C-1 and V-1A-H-C-2) perform the worst. The performance of beams with Metallic Pollutants varies significantly, with beam V-1A-H-M-1 performing quite well. One beam with HR glass (Beam V-1B-H-HR-1) had the ceramic removed, which improved its structural performance. When the ceramic is not removed, all beams fail, as observed during Fire Round 1.

07 | MECHANICAL TESTS

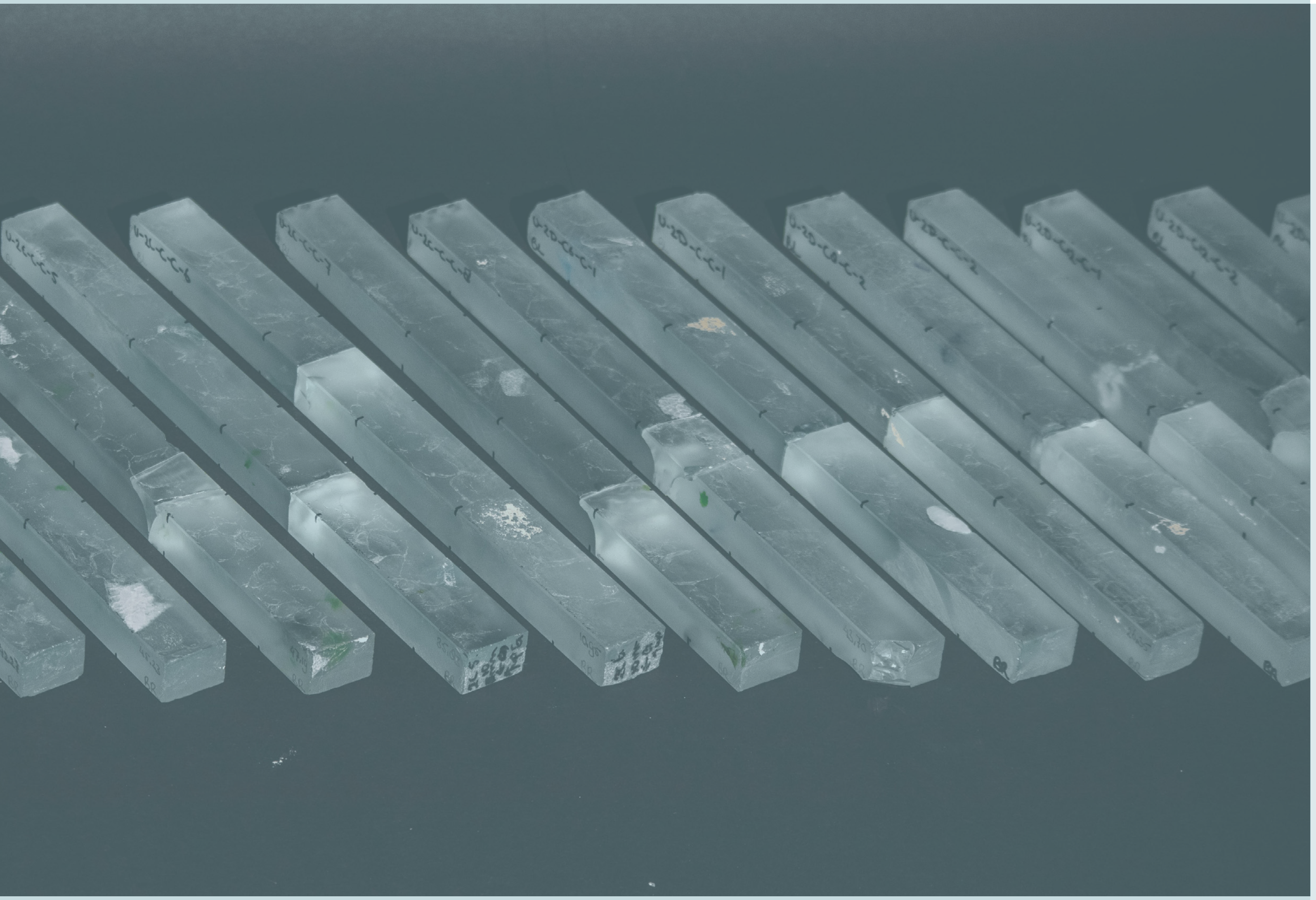

Figure 92: Experiment Type 2: Composite beams, focus on the optimal ratio between surface and bulk

Experiment type 2:
Composite beams: Optimal ratio between surface and bulk
6 mm Float glass + 15 mm CSP Pollutants in the bulk
Fire Round 2B: 2 beams were made with this composition
Fire Round 2C: 2 beams were made with this compostion with a higher temperature schedule
Fire Round 2D: 1 beams were made with this composition

8 mm Float glass + 13 mm CSP Pollutants in the bulk
Fire Round 2A: 3 beams were made with the composition back when harmful pollutants were still included
Fire Round 2B: 2 beams were made with this compostion
Fire Round 2C: 2 beams were made with this compostion with a higher temperature schedule
Fire Round 2D: 2 beams were made with this compostion

10 mm Float glass + 11 mm CSP Pollutants in the bulk
Fire Round 2A: 3 Beams were made with the composition back when harmful pollutants were still included
Fire Round 2B: 2 beams were made with this compostion
Fire Round 2C: 2 beams are made with this compostion with a higher temperature schedule
Fire Round 2D: 1 beams was made with this compostion

12 mm Float glass + 9 mm CSP Pollutants in the bulk
Fire Round 2C: 2 beams were made with this compostion with a higher temperature schedule
Fire Round 2D: 3 beams were made with this compostion

Experiment type 2: Total 27 beams
Structural performance feasibility:
Succeeded: 22 beams
Failed: 5 beams

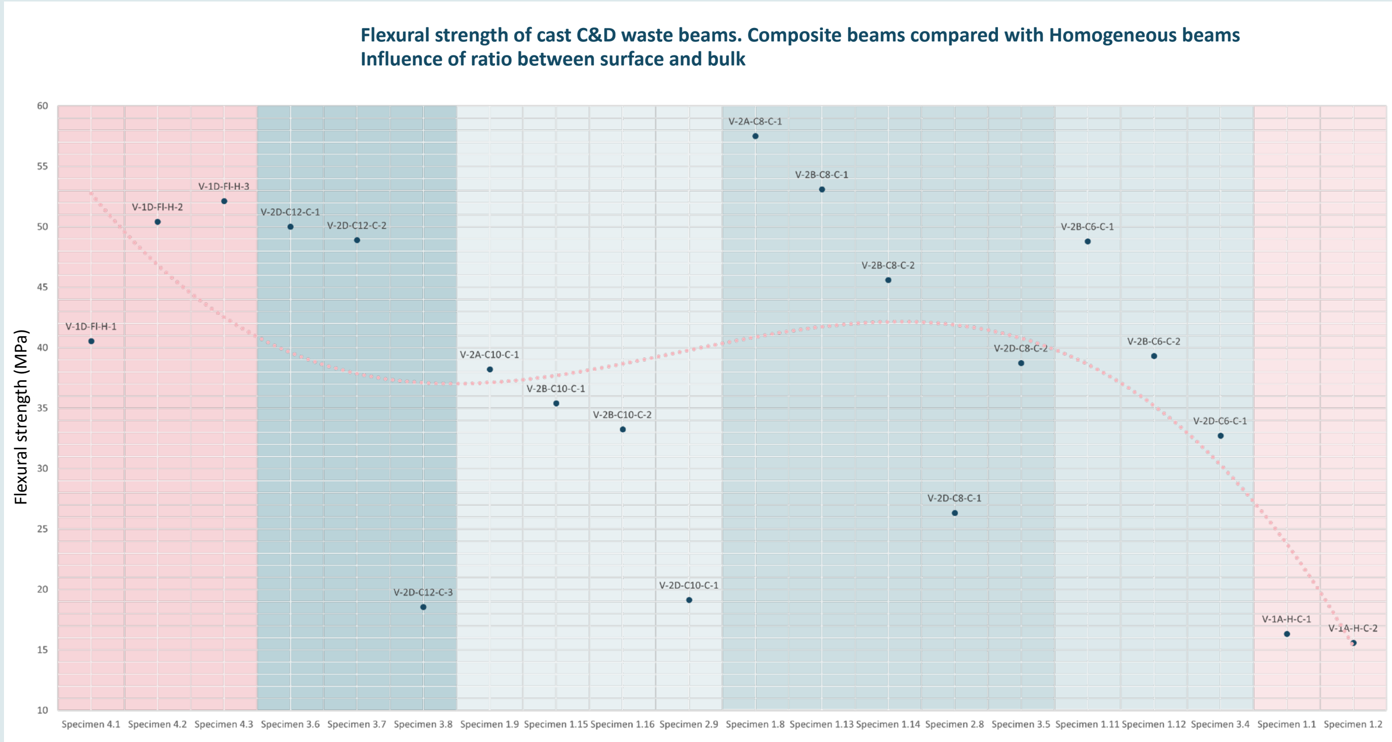

Graph 08: Composite beams relation between surface and bulk compared with homogeneous beams

The results from Fire Round 2C are not integrated in this graph, these will be explained in Chapter 9

Experiment type 2:
Composite beams: Surface + Bulk
Float glass + CSP pollutants
6 mm + 15 mm V-2B-C6-C-1, V-2B-C6-C-2 and V-2D-C6-C-1
8 mm + 13 mm V-2A-C8-C-1, V-2B-C8-C-1, V-2B-C8-C-2, V-2D-C8-C-1 and V-2D-C8-C-2
10 mm + 11 mm V-2A-C10-C-1, V-2B-C10-C-1, V-2B-C10-C-2, and V-2D-C10-C-1
12 mm + 9 mm V-2D-C12-C-1, V-2D-C12-C-2 and V-2D-C12-C-3

Experiment type 1:
Homogeneous beams
Glass with A cullet
Float glass V-1D-H-Fl-1, V-1D-H-Fl-2 and V-1D-H-Fl-3
Glass with C cullet
CSP V-1A-H-C-1 and V-1A-H-C-2

7.2.3 Structural performance - Composite beams

Influence of ratio between surface and bulk

The following results are based on Experiment Type 2 compared with Experiment Type 1. Before the structural performance tests were conducted, predictions were made on how the structural performance curve would proceed for the composite beams compared to the homogeneous beams (Graph 07). It was predicted that the beams with the highest amount of Float glass (homogeneous beams with Float glass) would perform the best, followed by composite beams with decreasing amounts of Float glass (12 mm, 10 mm, 8 mm, and finally 6 mm), all performing better than the homogeneous beams with CSP pollutants.

Graph 08 illustrates the actual results from the composite beams compared to the homogeneous beams.

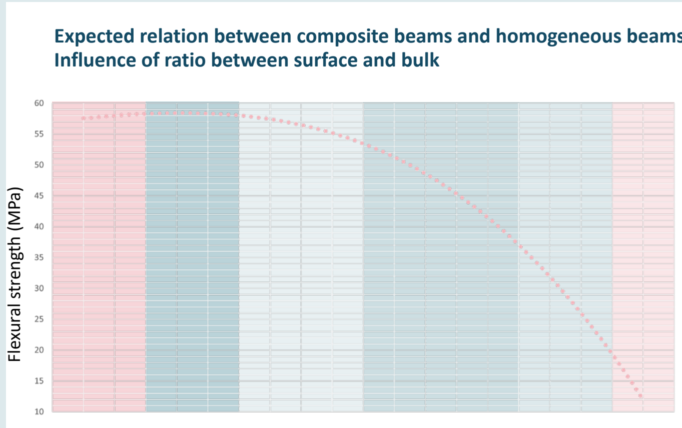

Graph 07: Expected curve for the relationship between composite beams and homogeneous beams

07 | MECHANICAL TESTS

- **Cullet Type A** (dark pink): Homogeneous beams with Float glass (specimens 4.1-4.3)
- **Composite beams** (dark blue): Composite beams with 12 mm Float glass and 9 mm bulk material with CSP Pollutants (specimens 3.6-3.8)
- **Composite beams** (light blue): Composite beams with 10 mm Float glass and 11 mm bulk material with CSP Pollutants (specimens 1.9, 1.15, 1.16, 2.9)
- **Composite beams** (blue): Composite beams with 8 mm Float glass and 13 mm bulk material with CSP Pollutants (specimens 1.8, 1.13, 1.14, 2.8, 3.5)
- **Composite beams** (lightest blue): Composite beams with 6 mm Float glass and 15 mm bulk material with CSP Pollutants (specimens 1.11, 1.12, 3.4)
- **Cullet Type C** (light pink): Homogeneous beams with CSP Pollutants (specimens 1.1 and 1.2)

It is interesting to compare the results of the composite beams with those of the homogeneous beams containing Float glass and CSP Pollutants. When testing the cast glass beams, failure always occurs in the tensile area, which is the part of the beam experiencing tension. In these four-point bending tests, the area above the neutral axis (the line within the beam that experiences no stress) is in compression and does not typically fail. Therefore, it is logical to expect that composite beams with a higher proportion of Float glass will perform similarly to homogeneous beams made entirely of Float glass, since both have strong tensile areas.

Furthermore, beam V-1D-H-Fl-1, V-1D-H-Fl-2, and V-1D-H-Fl-3 behave similarly to beams V-2D-C12-C-1 and V-2D-C12-C-2, as well as beam V-2A-C8-C-1 and V-2B-C8-C-1. However, the best-performing beam overall is not a homogeneous Float glass beam but beam V-2A-C8-C-1, a composite beam with 8 mm Float glass and CSP Pollutants in the bulk.

When comparing composite beams to homogeneous beams with CSP Pollutants, the composite beams generally perform better. However, a few composite beams perform poorly, specifically beams V-2D-C12-C-2, V-2D-C10-C-1, and V-2D-C8-C-1.

Comparing the actual results (Graph 08) with the expected results (Graph 07) shows that the composite beams with 10 mm Float glass did not behave as predicted. The rest of the compositions performed approximately as expected, with the 12 mm Float glass composition performing the best, except for the 10 mm composition. The 8 mm Float glass performed better than the 6 mm Float glass.

To investigate the behaviour of the 10 mm Float glass, an XRF test was conducted. It revealed that the material composition of the 10 mm Float glass differs from the 6 mm, 8 mm, and 12 mm Float glass. The 10 mm Float glass contains a lower amount of MgO (magnesium oxide), resulting in a lower melting point. This causes earlier surface crystallization in the 10 mm Float glass compared to other compositions. The effects of crystallization will be discussed further in Chapter 8: Microscopic validation.

The outcomes of composite beams versus homogeneous beams are shown separately in the following graphs. Graph 09 compares a composite beam with 6 mm Float glass to a homogeneous beam, Graph 10 compares an 8 mm Float glass composite beam to a homogeneous beam, Graph 11 compares a 10 mm Float glass composite beam to a homogeneous beam, and Graph 12 compares a 12 mm Float glass composite beam to a homogeneous beam.

All four graphs clearly show that using Float glass enhances structural performance compared to homogeneous beams. This means that having a purer cullet on the surface and a less pure cullet in the bulk improves structural performance compared to less pure homogeneous beams. Each graph includes a trend line to visualise the impact of having a stronger surface material.

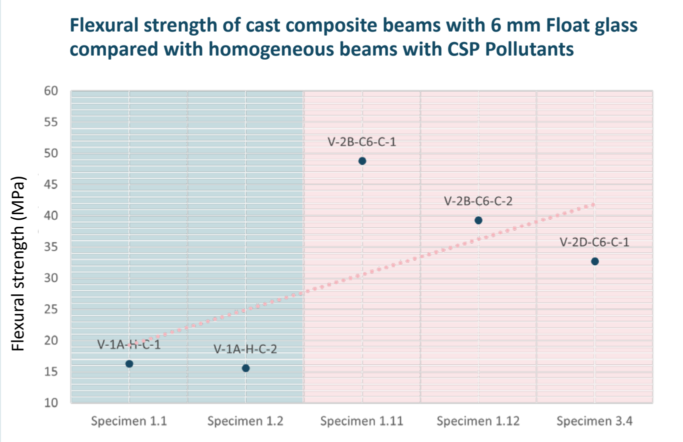

Graph 09: Comparison between a composite with 6 mm Float glass and a homogeneous beam

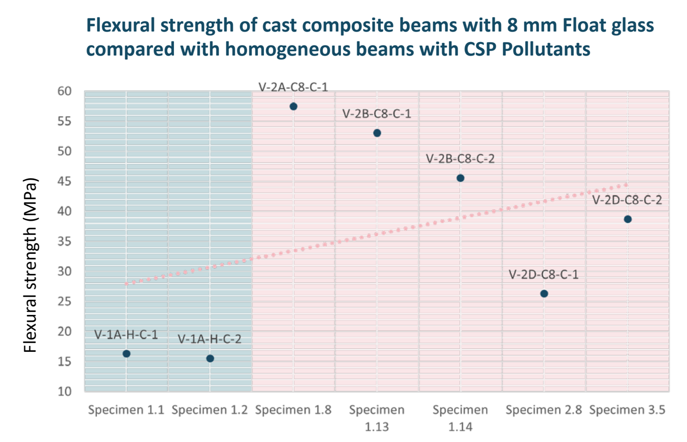

Graph 10: Comparison between a composite with 8 mm Float glass and a homogeneous beam

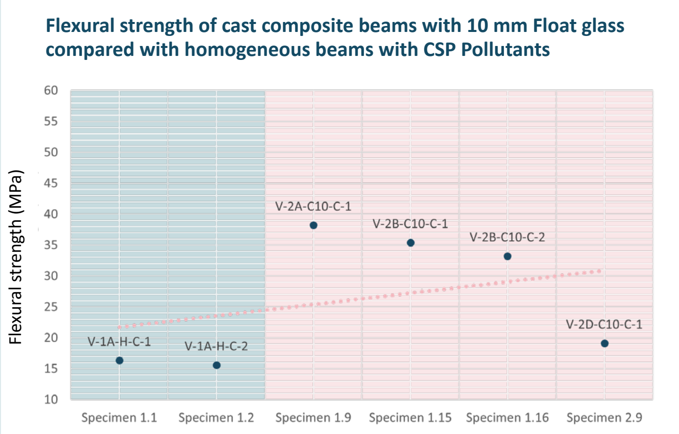

Graph 11: Comparison between a composite with 10 mm Float glass and a homogeneous beam

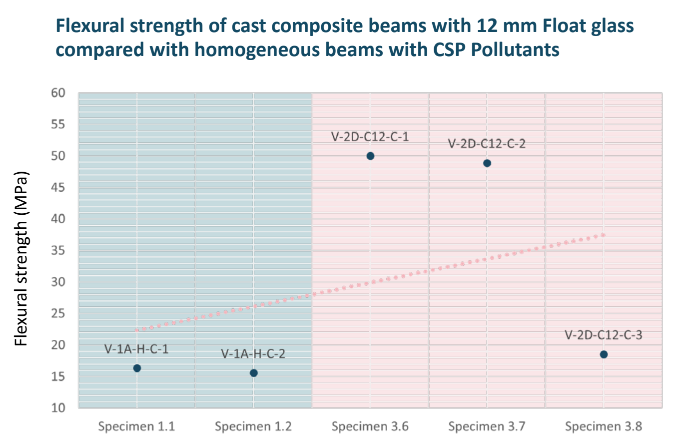

Graph 12: Comparison between a composite with 12 mm Float glass and a homogeneous beam

Experiment type 1:
Homogeneous beams
Glass with C cullet

CSP	V-1A-H-C-1 and V-1A-H-C-2

Experiment type 2:
Composite beams: Surface + Bulk
Float glass + CSP pollutants

6 mm + 15 mm	V-2B-C6-C-1,V-2B-C6-C-2 and V-2D-C6-C-1
8 mm + 13 mm	V-2A-C8-C-1, V-2B-C8-C-1, V-2B-C8-C-2, V-2D-C8-C-1 and V-2D-C8-C-2
10 mm + 11 mm	V-2A-C10-C-1, V-2B-C10-C-1, V-2B-C10-C-2, and V-2D-C10-C-1
12 mm + 9 mm	V-2D-C12-C-1, V-2D-C12-C-2 and V-2D-C12-C-3

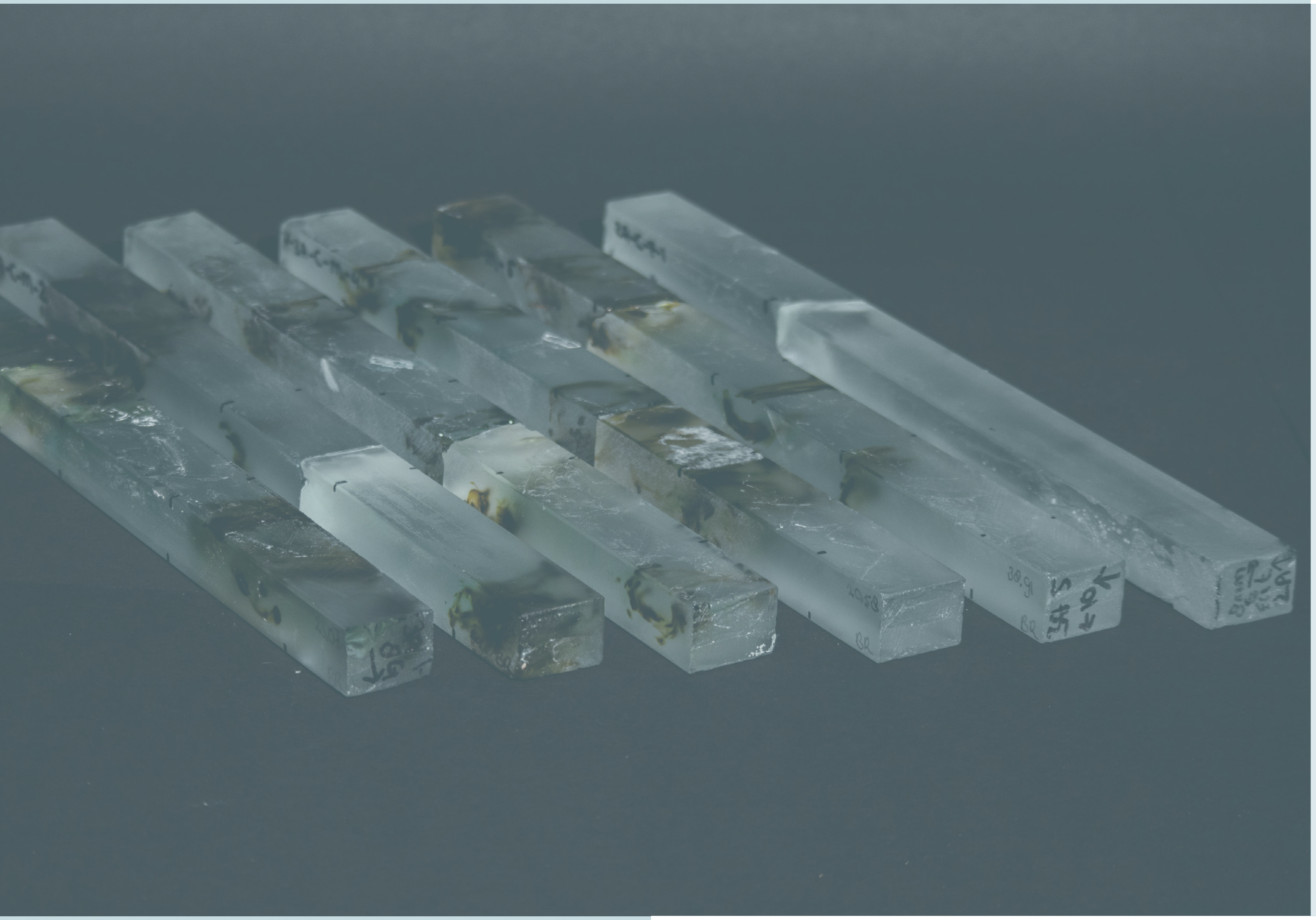

Figure 93: Experiment Type 3: Composite beams, focus on influence of the material composition of the bulk

Experiment type 3:
Composite beams: Influence of the material composition of the bulk
8 mm Float glass + 13 mm Fritted glass in the bulk
Fire Round 2A: 1 beams was made with this compostion

8 mm Float glass + 13 mm Metallic Pollutants in the bulk
Fire Round 3A: 3 beams were made with this compostion

10 mm Float glass + 11 mm Metallic Pollutants in the bulk
Fire Round 3A: 3 beams were made with this compostion

Experiment type 3: **Total 7**
Structural performance feasibility:
Succeeded: **6 beams**
Failed: **1 beams**

Influence of bulk material

The following results compare Experiment Type 3 with Experiment Type 2. In Experiment Type 2, CSP Pollutants were used as the bulk material, while Experiment Type 3 used a different bulk material.

- Composite beams with 8 mm Float glass and **Fritted glass** in the bulk (specimen 1.8)
- Composite beams with 8 mm Float glass and **Metallic Pollutants** in the bulk (specimens 2.10 – 2.12)
- Composite beams with 10 mm Float glass and **Metallic Pollutants** in the bulk (specimens 2.13 and 2.14)

Since the bulk of the beam is located in the compression area, it was interesting to analyse whether changing the bulk material would affect the overall structural performance.

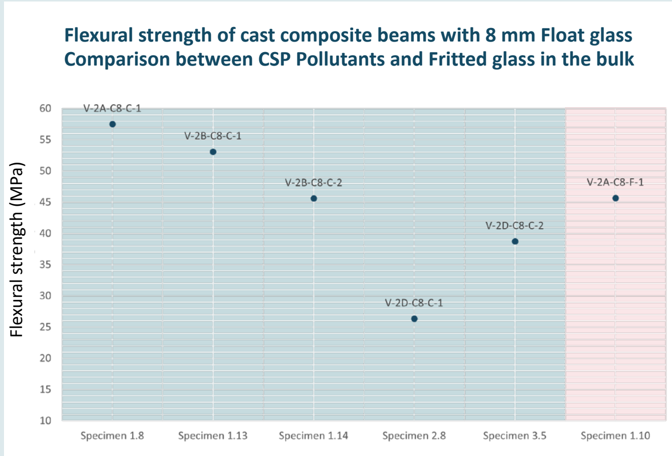

Graph 13: Overview of the difference between bulk CSP Pollutants and Fritted glass with 8 mm Float glass

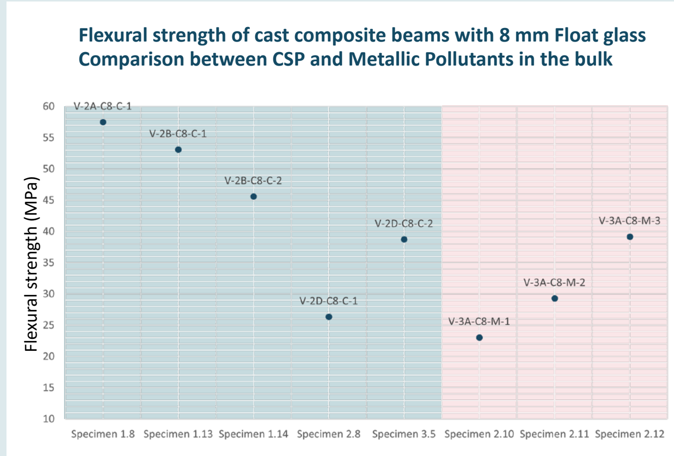

Graph 14: Overview of the difference between bulk CSP pollutants and bulk Metallic pollutants with 8 mm Float glass

Experiment type 2:
Composite beams: Surface + Bulk
Float glass + CSP pollutants
8 mm + 13 mm V-2A-C8-C-1, V-2B-C8-C-1, V-2B-C8-C-2, V-2D-C8-C-1 and V-2D-C8-C-2
10 mm + 11 mm V-2A-C10-C-1, V-2B-C10-C-1, V-2B-C10-C-2, and V-2D-C10-C-1

Experiment type 3:
Composite beams: Surface + Bulk
Float glass + Fritted glass
8 mm + 13 mm V-2A-C8-F-1
Float glass + Metallic pollutants
8 mm + 13 mm V-3A-C8-M-1, V-3A-C8-M-2 and V-3A-C8-M-3
10 mm + 11 mm V-3A-C10-M-1 and V-3A-C10-M-2

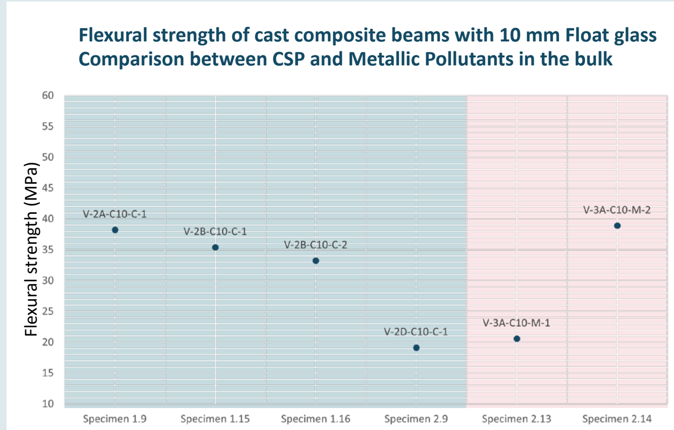

Graph 15: Overview of the difference between bulk CSP pollutants and bulk Metallic pollutants with 10 mm Float glass

Graph 13 compares Fritted glass and CSP Pollutants in the bulk. Fritted glass is considered a Class B cullet, while CSP Pollutants are considered a Class C cullet. Graph 06 already showed that homogeneous beams with Fritted glass performed better than those with CSP Pollutants. When comparing the composite beam with Fritted glass (Beam V-2A-C8-F-1) to composite beams with CSP Pollutants, the results vary significantly. With only one beam, the result is inconclusive.

Graphs 14 and 15 compare Metallic Pollutants and CSP Pollutants in the bulk. Generally, composite beams with CSP Pollutants perform better than those with Metallic Pollutants. This is quite interesting since homogeneous beams with Metallic Pollutants perform better than those with CSP Pollutants (Graph 06).

In Graph 14, composite beams with CSP Pollutants outperform those with Metallic Pollutants, except for beam V-2D-C8-C-1. This exception is due to a significant perpendicular surface flaw in the Float glass, drastically reducing structural performance. Further discussion is in Chapter 9: Microscopic validation.

Similar results are seen in Graph 15, where beams with CSP Pollutants outperform those with metallic pollutants, except for beam V-3A-C10-M-2, which was also the best performing 10 mm composite composition according to Graph 05.

07 | MECHANICAL TESTS

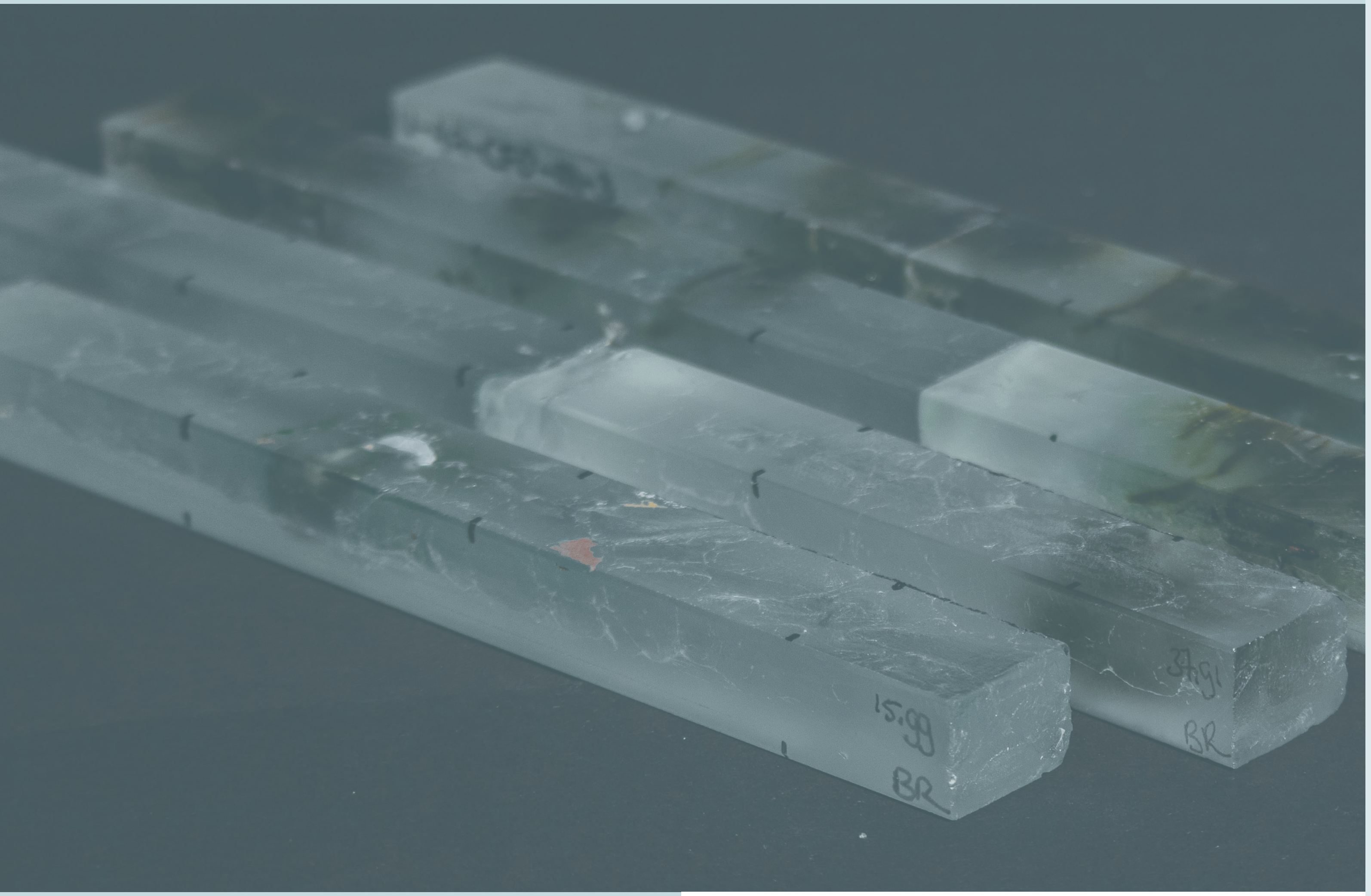

Figure 94: Experiment Type 4: Composite beams, focus on influence of the material composition of the surface

Experiment type 4:
Composite beams: Influence of the material composition of the surface
8 mm Fritted glass + 13 mm CSP Pollutants in the bulk
Fire Round 4A: 3 beams was made with this compostion

8 mm Fritted glass + 13 mm Metallic Pollutants in the bulk
Fire Round 4A: 3 beams was made with this compostion

Experiment type 4: Total 6
Structural performance feasibility:
Succeeded: 4 beams
Failed: 2 beams

Influence of surface material

The following results compare Experiment Type 4 with Experiment Types 2 and 3. In Experiment Type 2, Float glass was used on the surface with CSP Pollutants in the bulk. Experiment Type 4 used Fritted glass (a Class B cullet) on the surface and metallic pollutants in the bulk, instead of Float glass (a Class A cullet).

- Composite beams with 8 mm Fritted glass and CSP Pollutants in the bulk (specimens 2.15 and 2.16)
- Composite beams with 8 mm Fritted glass and metallic pollutants in the bulk (specimens 3.9 and 3.10)

Since the surface of the beam is located in the tension area, changing the surface material to a lower type of cullet would result in significant changes in structural performance. These differences are expected to be greater than those resulting from changing the bulk material.

This experiment focuses on comparing 8 mm Fritted glass with 8 mm Float glass, as 8 mm thickness generally performed best in previous experiments. Graph 16 shows the comparison for composite beams with CSP Pollutants in the bulk, and Graph 17 shows the comparison for composite beams with metallic pollutants in the bulk.
First, the beams with CSP Pollutants in the bulk will be discussed (Graph 16). The beams with Fritted glass (V-4A-CR8-C-2 and V-4A-CR8-C-3) perform worse than the beams with Float glass. Beam V-2D-C8-C-1 is an exception due to a surface flaw, as previously discussed. The structural performance of the two beams with Fritted glass differs significantly, with Beam V-4A-CR8-C-3 performing nearly identically to the beams with Float glass.

Next, we discuss the beams with Metallic Pollutants in the bulk (Graph 17). The beams with Fritted glass (Beams V-4A-CR8-M-1 and V-4A-CR8-M-3) perform significantly worse than those with Float glass on the surface.

To determine if creating a composite beam with Fritted glass improves the structural performance of homogeneous beams, the following graphs were created. Graph 18 shows the comparison between homogeneous beams of CSP Pollutants and composite beams with Fritted glass on the surface and CSP Pollutants in the bulk. This graph shows barely any difference between homogeneous beams and composite beams. Graph 19 compares homogeneous beams with Metallic Pollutants to composite beams with Fritted glass on the surface and Metallic Pollutants in the bulk. This graph indicates a decrease in structural performance when creating a composite beam.

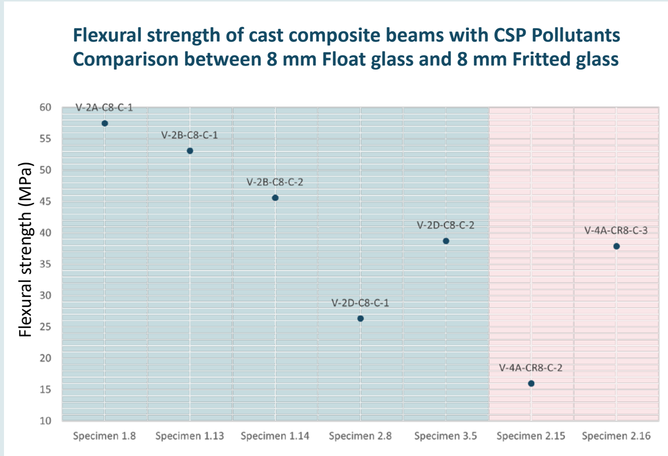

Graph 16: Overview of the difference between Float glass of 8 mm and Fritted glass of 8 mm at the surface with a bulk of CSP pollutants

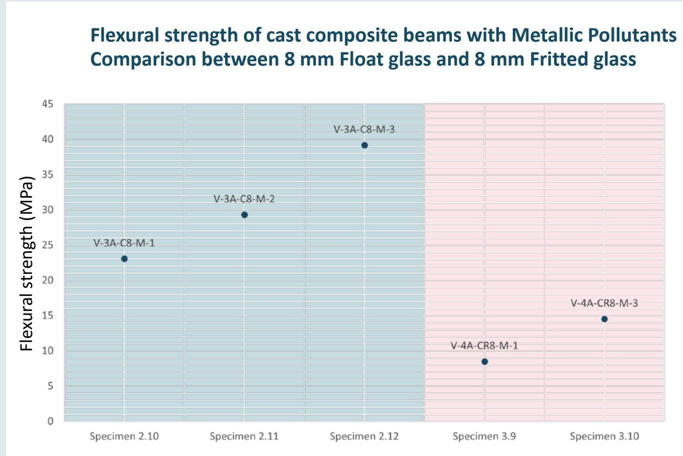

Graph 17: Overview of the difference between Float glass of 8 mm and Fritted glass of 8 mm at the surface with a bulk of Metallic pollutants

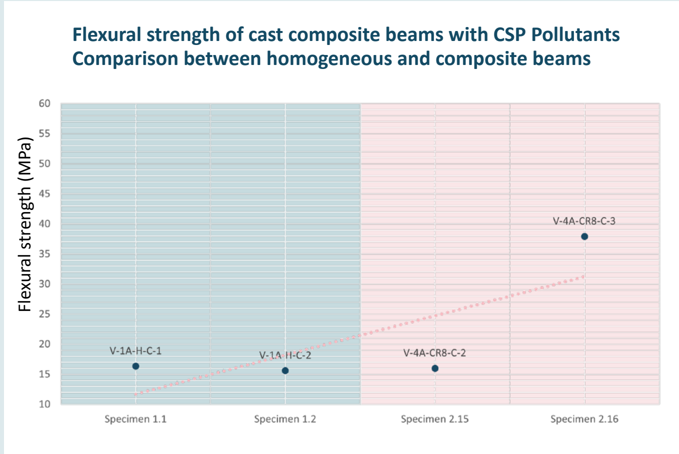

Graph 18: Overview of the difference between homogeneous beams with CSP Pollutants and composite beams with Fritted glass and CSP Pollutants in the bulk

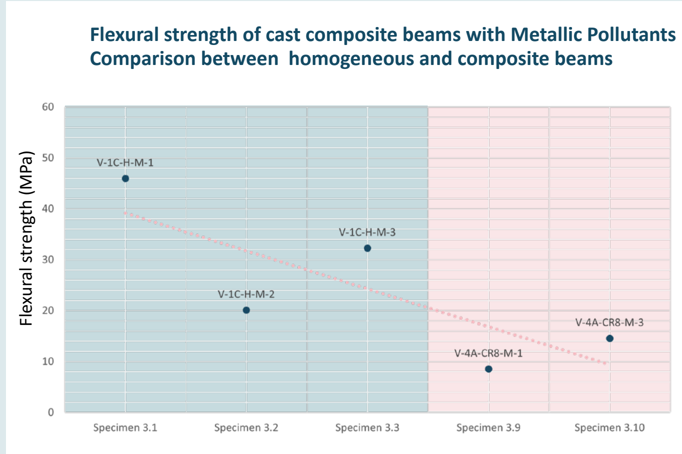

Graph 19: Overview of the difference between homogeneous beams with Metallic Pollutants and composite beams with Fritted glass and Metallic Pollutants in the bulk

Experiment type 1: Homogeneous beams
Glass with C cullet
CSP V-1A-H-C-1 and V-1A-H-C-2

Experiment type 2: Composite beams: Surface + Bulk
Float glass + CSP pollutants
8 mm + 13 mm V-2A-C8-C-1, V-2B-C8-C-1, V-2B-C8-C-2, V-2D-C8-C-1 and V-2D-C8-C-2

Experiment type 4: Composite beams: Surface matrial
Fritted glass + CSP Pollutants
8 mm + 13 mm V-4A-CR8-C-2 and V-4A-CR8-C-3
Fritted glass + Metallic Pollutants
8 mm + 13 mm V-4A-CR8-M-1 and V-4A-CR8-M-3

7.3 Discussion and conclusion

7.3.1 Homogeneous beams

- Beams with Cullet Type A exhibit the highest structural performance, followed by beams with Cullet Type B, and finally, beams with Cullet Type C.
- A beam's structural performance improves when ceramic and silicone inclusions are removed from its composition.
- Cullet Type C with CSP Pollutants has the lowest structural performance.
- Cullet Type C with Metallic Pollutants shows varying results.

7.3.2 Composite beams

Influence of ratio between surface and bulk

- Composite beams with Float glass on the surface and CSP Pollutants in the bulk show an improvement compared to homogeneous beams with CSP Pollutants.
- Homogeneous beams with Float glass perform similarly to composite beams with 12 mm Float glass and CSP Pollutants in the bulk.
- The relationship between composite beams and homogeneous beams is not as expected. The composition with 10 mm Float glass performs worse than expected, likely due to differences in material composition. The surface with 10 mm Float glass has less MgO.
- Among the four four-point bending tests, a composite beam with 8 mm Float glass on the surface and 13 mm CSP Pollutants in the bulk shows the best structural performance (Beam V-2A-C8-C-1).
- Using a higher purity cullet (Cullet Type A) on the surface and a lower purity cullet (Cullet Type C) in the bulk improves structural performance.

Influence of bulk material

- Composite beams with Fritted glass in the bulk do not show conclusive results compared to composite beams with CSP Pollutants in the bulk.
- Composite beams with Metallic Pollutants in the bulk perform worse than beams with CSP Pollutants in the bulk, which is interesting since homogeneous beams with Metallic Pollutants perform better than those with CSP Pollutants.
- The bulk material located in the compression zone also affects the overall structural performance of a beam.

Influence of surface material

- Since the surface of the beam is located in the tension area, changing the surface material to a lower type of cullet results in significant changes in structural performance. These differences are greater than those resulting from changing the bulk material.
- For composite beams with Float glass on the surface and CSP Pollutants in the bulk versus Fritted glass and CSP Pollutants in the bulk, the results vary too much.
- For composite beams with Float glass on the surface and Metallic Pollutants in the bulk comparing with Fritted glass and Metallic Pollutants in the bulk, the composite beams with Fritted glass perform much worse.
- Composite beams with Float glass on the surface perform better than those with Fritted glass on the surface because Float glass is a Type A cullet, whereas Fritted glass is a Type B cullet.
- There is barely any difference in structural performance between homogeneous beams with CSP Pollutants and composite beams with Fritted glass on the surface and CSP Pollutants in the bulk.
- Structural performance decreases when comparing homogeneous beams with Metallic Pollutants to composite beams with Fritted glass on the surface and Metallic Pollutants in the bulk.
- Creating a composite beam with Type B cullet on the surface and Type C cullet in the bulk does not improve the structural performance compared to homogeneous beams made of Type C cullet.

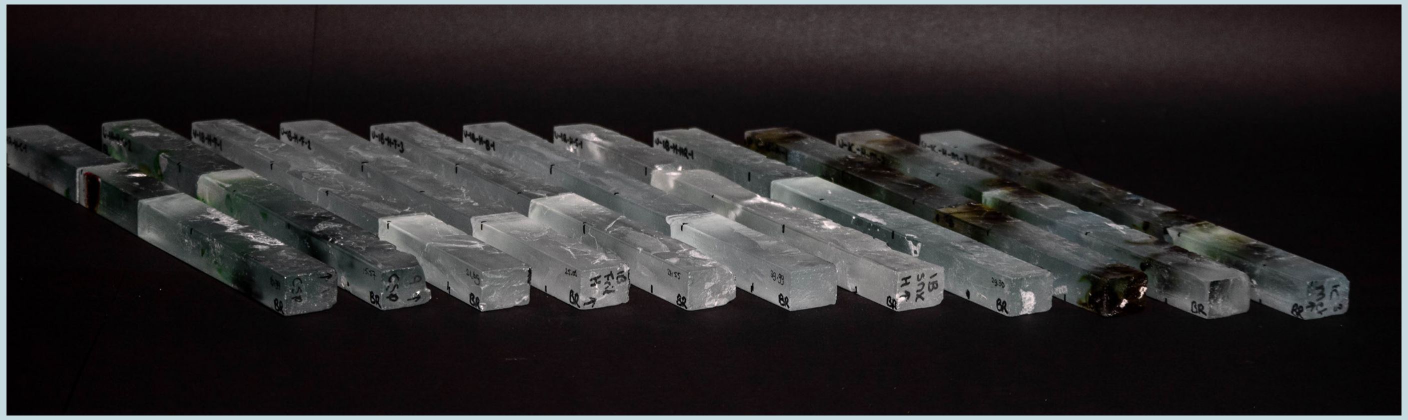

Figure 95: Experiment Type 1: Homogeneous beams of Cullet Type A, Cullet Type B and Cullet Type B

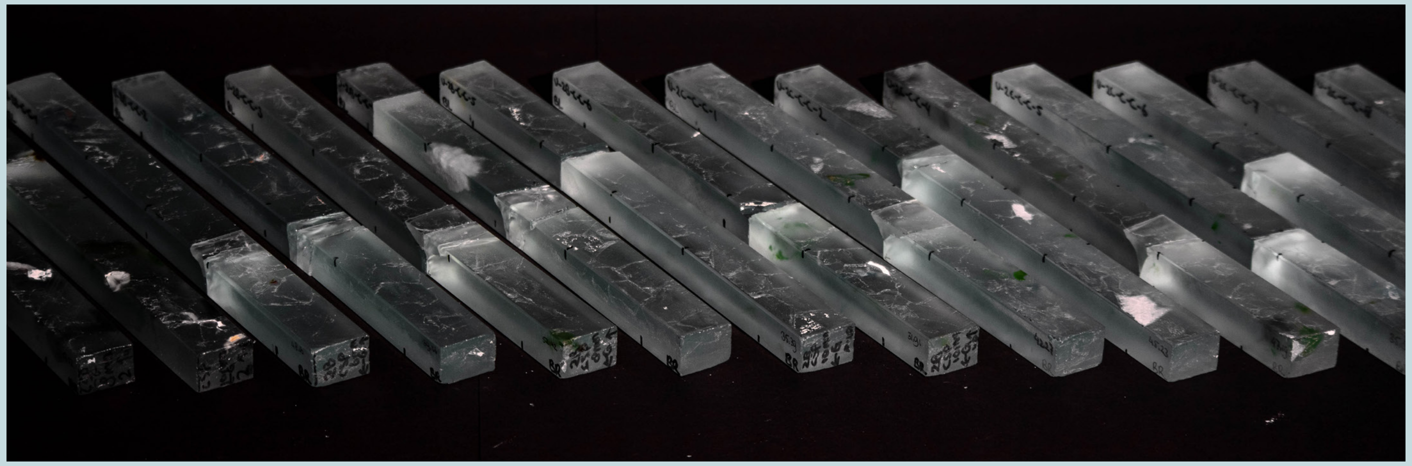

Figure 96: Experiment Type 2: Composite beams, focus on the optimal ratio between surface and bulk

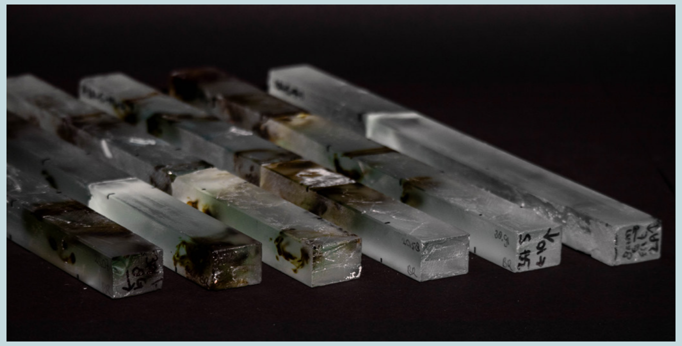

Figure 97: Experiment Type 3: Composite beams, focus on influence of the material composition of the bulk

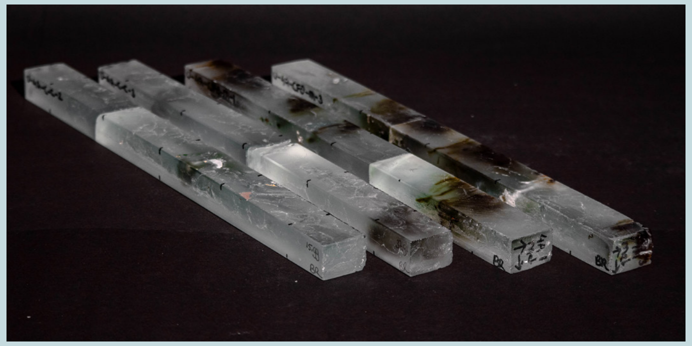

Figure 98: Experiment Type 4: Composite beams, focus on influence of the material composition of the surface

08 | MICROSCOPIC VALIDATION

The information presented in this chapter is based on George D. Quinn's book, Fractography of ceramics and glasses (Quinn, 2020). Dr. Bristogianni assisted with most of the microscopic testing and helped evaluate the results. Additionally, the inclusions are analysed using her articles on the features of inclusions. Information regarding the potential flaw categories investigated in this chapter is provided in paragraph 3.6, "Flaw categories."

8.1 Crack patterns

After the four-point bending tests, the beams were evaluated based on their fracture behaviour. Analysis focused on several key aspects: the crack pattern and its location, including whether it started directly under a load pin indicating misalignment; the vertical position of the fracture along the beam's height; whether the fracture occurred at the surface or within the bulk of the material; and its position on the surface, whether it occurred at an edge or in the centre of the surface.

The shape and location of the crack pattern provide valuable insights into the nature of the failure. Microscopic validation further refines these relationships. Appendix F presents a comprehensive failure analysis for each beam tested in the four-point bending tests. Specifically, Table 28 details the failure analysis for the beams tested in the first bending test, Table 29 for the second test, Table 30 for the third test, and Table 31 for the fourth test.

8.1.1 Theory behind cracks

In addition to indicating the origin of a fracture, the general patterns of crack extension and branching also provide insights into the stress level, energy level involved in the fracture, and its flaw source. Most brittle fractures originate from a single point and propagate outward. Both tensile stress and flaw categories significantly influence the likelihood of beam fracture. Figure 99 provides an illustrated overview of the theory behind crack patterns.

The law of normal crack propagation is a fundamental principle governing crack behaviour. According to this criterion, fractures propagate perpendicular to the maximum local tensile stress, or normal stress.

During the four-point bending test, a load is applied to the beam to determine its flexural strength. This test results in a stress distribution where the highest tensile stress occurs at the bottom of the beam, as discussed in Chapter 3: "Mechanical tests". Tensile stress decreases towards the interior of the beam, reaching zero at the neutral axis located at its centre. On the opposite side of the neutral axis, compressive stresses counterbalance tensile stresses. Understanding this balanced stress distribution is crucial for assessing the beam's structural integrity and performance under load.

Even minor misalignments in beam positioning under load or differences in elastic properties can cause tensile stresses that lead to fracture. Increased stress at the fracture point correlates with more noticeable fracture marks and higher stored energy in the beam, as shown in Figure 100. Conversely, interpreting weak sections with minimal stored energy can be challenging. When a beam fractures under low stress, it typically results in two fragments with relatively smooth fracture surfaces, as shown in Figure 101.

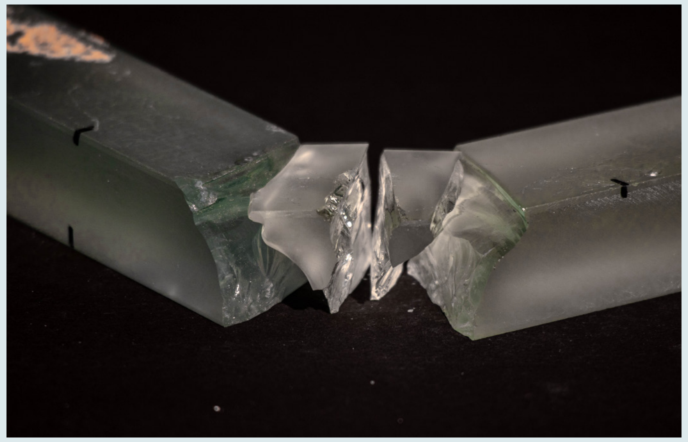

Figure 100: Beam with a high energy failure. This is a composite beam

Beam V-2D-C12-C-2

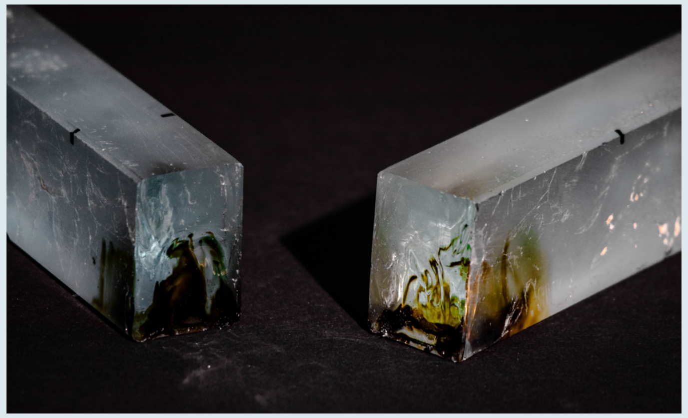

Figure 101: Beam with a low energy failure. This is a homogeneous beam with Metallic Pollutants

Beam V-1C-H-M-2

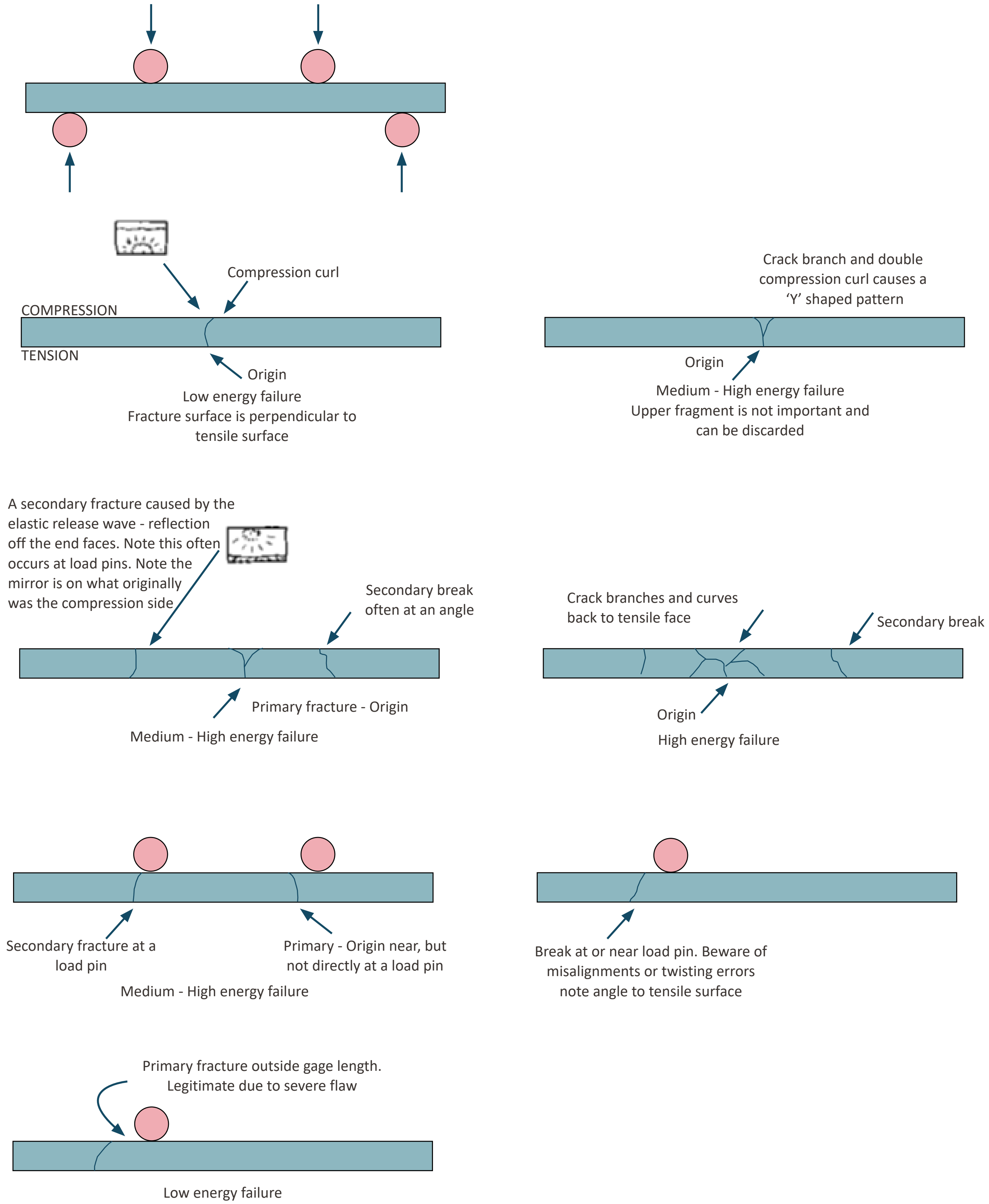

Figure 99: Illustratic overview of the theory of crack patterns (Quinn, 2020)

08 | MICROSCOPIC VALIDATION

The region where a crack extends from a fault at its origin is known as the fracture mirror. Fracture mirrors are valuable as they provide evidence of high-energy failure when well-defined boundaries are present, indicating significant stress in that area. Figure 102 illustrates a fracture resulting from high-energy failure. In contrast, a fracture with unclear boundaries suggests low-energy failure and minimal stress, often indicating a weak section, as shown in Figure 103. Typically, fracture mirrors for low-energy failures are ten to thirteen times larger than those for high-energy failures.

8.1.2 Shape of the crack patterns

The two most common shapes for crack patterns are compression curls and double compression curls. The compression curl, also known as the cantilever curl, has the following characteristics: the fracture originates exactly opposite the curl on the fracture surface. The concept here is straightforward: a beam exhibiting a compression curl experienced bending during loading. Compression curls typically occur in low-energy failure fractures and have big fracture mirrors. Figure 101 provides an example of a compression curl. To further clarify this concept, Figure 105 also depicts a compression curl.

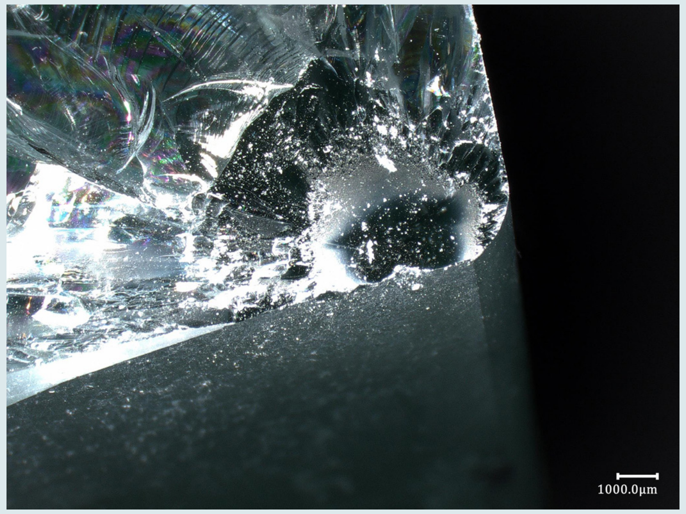

Figure 102: Beam with a high energy failure. A small mirror located at the fracture. This is a composite beam.

Beam V-2B-C6-C-1

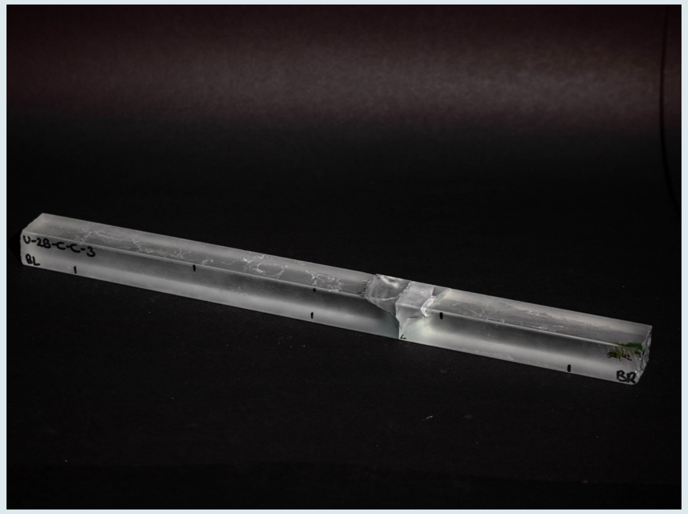

Figure 104: A double compression curl, a typical crack for composite beams

Beam V-2B-C8-C-1

Figure 103: Beam with a low energy failure. A big mirror located at the fracture. This is a compositie beam with Fritted glass.

Beam V-4A-CR8-C-3

Figure 105: A compression curl, a typical crack pattern for homogeneous beams

Beam V-1B-H-F-3

On the other hand, the double compression curl pattern appears when a beam withstands increased tension. These patterns are indicative of high-energy failures and feature smal(ler) mirrors. Figure 100 illustrates an example of a double compression curl. Additionally, Figure 104 depicts another example of a double compression curl.

As shown in Figure 99, secondary fractures may also occur. Reverberations and stress reflections at loading locations often lead to secondary fractures following the initial fracture. If the beam was unevenly loaded and the initial flaw causing the fracture is unclear, stress variations may occur. Secondary fractures tend to occur at a slight non-perpendicular angle to the specimen axis, as depicted in Figure 106.

A primary fracture perpendicular to the beam's centre is typically indicative of properly aligned specimens and fixtures, as illustrated in Figure 107.

8.1.3 Origin of the fracture

After analysing the location and shape of the crack, the next step is to determine the cause of the fracture — specifically, which flaw triggered the fracture. The investigated flaw categories include bulk flaws and surface flaws. As explained in Section 6.1.1 of the literature review on recycled cast glass, intrinsic defects stem from melting reactions, such as surface crystallization. Extrinsic defects result from cullet contamination, which includes coatings, adhesives, or poorly homogenised batches leading to bulk inclusions like ceramics.

Inclusions such as stones due to cullet contamination and poorly homogenised batches are examined as extrinsic factors. Infolds, caused by poorly interfered cullets resulting in small gaps, also influenced by gas bubbles, are considered intrinsic factors. Crystallization resulting from glass interfaces due to melting reactions in the oven is categorised as intrinsic. Lastly, machining surface flaws arise from surface and edge treatments using diamond saws for cutting beams or polishing, also categorised as intrinsic factors.

8.2 Microscopic evaluation

A summary of the microscopic analyses for each beam from the four four-point bending tests is available in Appendix G. This appendix contains four tables: Table 32 presents the results of the first four-point bending test, Table 33 presents the results of the second test, Table 34 presents the results of the third test, and Table 35 presents the results of the fourth test. These tables discuss and examine the observed problems (flaw categories). For each beam, the origin of the fracture is checked to determine if it stems from an inclusion, infold, crystallization, machining, or possibly a combination of these flaw categories. Three images in the microscopic photos depict these faults: a bottom-up view of the beam in the tension zone, an overview of the fracture's location, and a close-up of the fracture itself. This paragraph emphasises the most intriguing fractures discovered in the analyses.

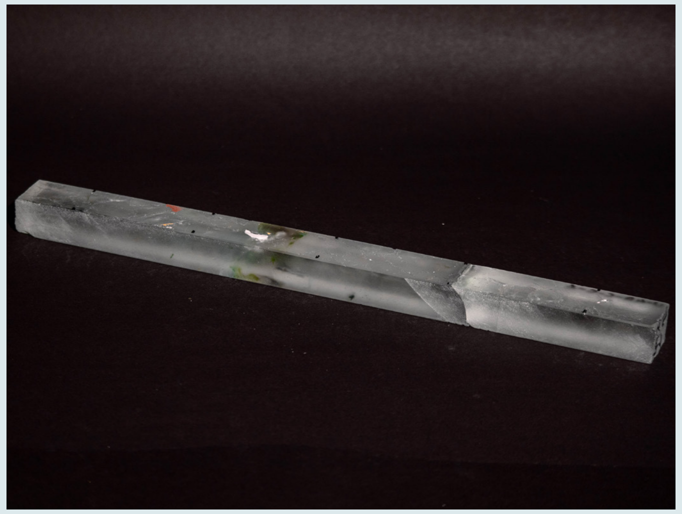

Figure 106: A non-perpendicular compression curl

Beam V4A-CR8-C-1

Figure 107: A perpendiculair compression curl

Beam V-2D-C8-C-1

8.2.1 Flaw types

Inclusions

Inclusions occur due to extrinsic flaws. As previously explained, these types of flaws are located in the bulk of the material and arise from cullet contamination, such as adhesive or coating residues, or from poorly homogenised batches containing stones. These various contaminants and stones have different thermal expansion properties and melting points compared to glass, resulting in hard, rock-like inclusions within the glass composition. This leads to stress areas around the glass. Further details on this can be found in paragraph 8.3, "Stress in flaw categories."

During microscopic tests, two types of inclusions were often observed in the material composition: ceramic and silicone. Silicone forms small white rocks (silica) when subjected to high temperatures. Ceramic inclusions have very high stress levels and are transparent or translucent. They are the most common type of stones, frequently causing glass breakage issues. Glass ceramics form glassy knots in the oven because they do not melt completely. When heated to glass-melting temperatures, glass ceramics can recrystallise into opaque or milky white masses of microscopic zirconia crystals. In contrast, silica inclusions are opaque stones with low to moderate stress levels.

The flaw category, inclusions, was prevalent in the initial batches, including during Fire Rounds 1A and 2A. The material compositions used in these beams contained the entire batch without any pollutants removed. Consequently, the Fire Round 1A batch with HR glass for the homogeneous beams contained many ceramic inclusions (Figure 108). Due to these inclusions, all the beams failed the structural feasibility tests. Similarly, the material composition of CSP Pollutants in the beams also contained large inclusions. However, two beams with the CSP Pollutant composition did not fail the structural feasibility tests. Despite this, these beams had very low structural performance, with their flexural strength being the lowest compared to all the other C&D waste beams. Figure 109 shows an inclusion in a homogeneous beam with CSP Pollutants.

Multiple flaw categories are often found together. An inclusion can severely undermine a beam's structural integrity, resulting in existing damage, surrounding cracks, or breakage during the polishing process.

Composite beams, consisting of a surface of Float glass and a bulk of CSP pollutants, occasionally exhibited inclusions (Figure 110). However, these inclusions were typically located within the bulk of the composite compositions and not on the surface. Despite the presence of these inclusions, these composite beams demonstrated higher structural performance and greater flexural strength compared to homogeneous beams containing inclusions. Importantly, the cracks and fractures in these composite beams did not originate from these inclusions but from other flaws on the surface. This underscores that inclusions situated at the surface are more likely to lead to catastrophic failures compared to those embedded within the bulk. This finding emphasises that enhancing the purity of glass at the surface can indeed improve structural performance.

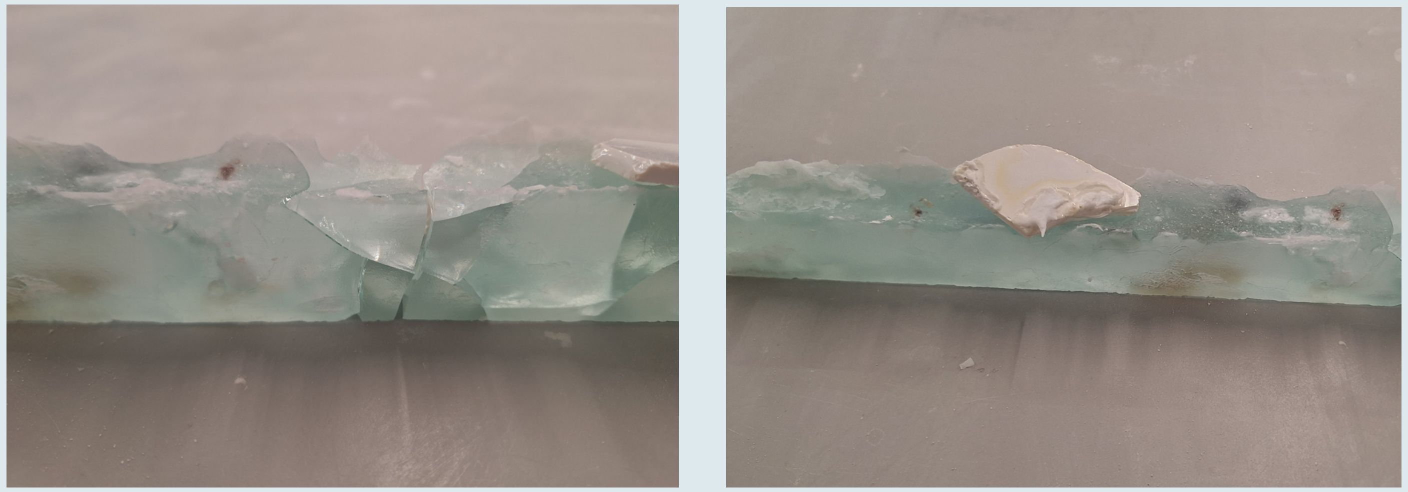

Figure 108: Ceramic inlcusions in a homogeneous beam with HR glass (a) Glassy knots and (b) White opaque mass

Beam V-1A-H-HR-2

Beam V-1A-H-HR-2

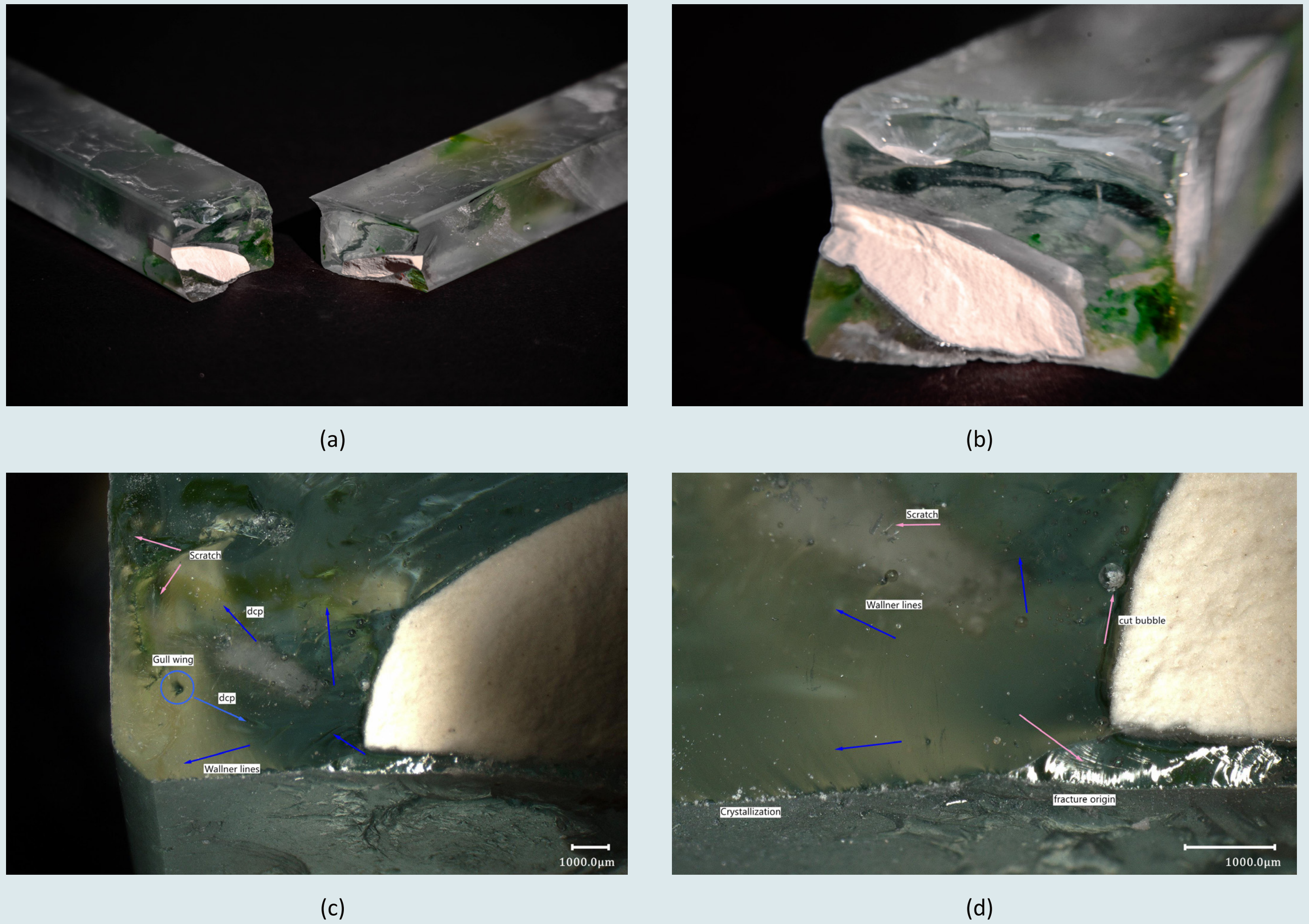

Figure 109: Microscopic photos of the flaw type, inclusions from beam V-1A-H-C-2, (a) Location of crack, (b) Zoomed-in location of the crack (c) location of the fracture and (d) Zoomed-in photoof the fracture

Figure 110: Inclusion in a composite beam in the bulk, Beam V-2B-C8-C-3 (a) location of the crack, (b) side view and (c) front view

08 | MICROSCOPIC VALIDATION

Infolds

Infolds are intrinsic flaws that manifest during the glass manufacturing process and are highly influenced by the temperature schedule. They occur when cullets fail to completely fuse together. This incomplete fusion leaves small gaps between cullets, significantly reducing the strength of the glass. Additionally, infolds can occur when there is insufficient fusion between the cullets and the surface composition, resulting in small air gaps.

These infolds are typically localised on the surface, creating tiny gaps where mould debris can concentrate. As the glass undergoes surface and edge treatments, these flaws can become more pronounced, allowing more debris to infiltrate these gaps and provoke stress concentrations in these areas. Unlike larger stone inclusions, which are visible and can be more easily detected, infolds create hidden stress points that can lead to structural weaknesses under loading conditions.

Figure 111 provides camera and microscopic images of this surface flaw, depicting infolds in a beam caused by inadequate cullet fusion.

Another type of infold arises from gas bubbles embedded in the glass surface. As previously discussed, the composition of 10 mm Float glass differs significantly from other thicknesses. Detailed microscopic analysis of the 10 mm glass surface reveals numerous visible air bubbles and signs of crystallization. This type of infolds is shown in Figure 112.

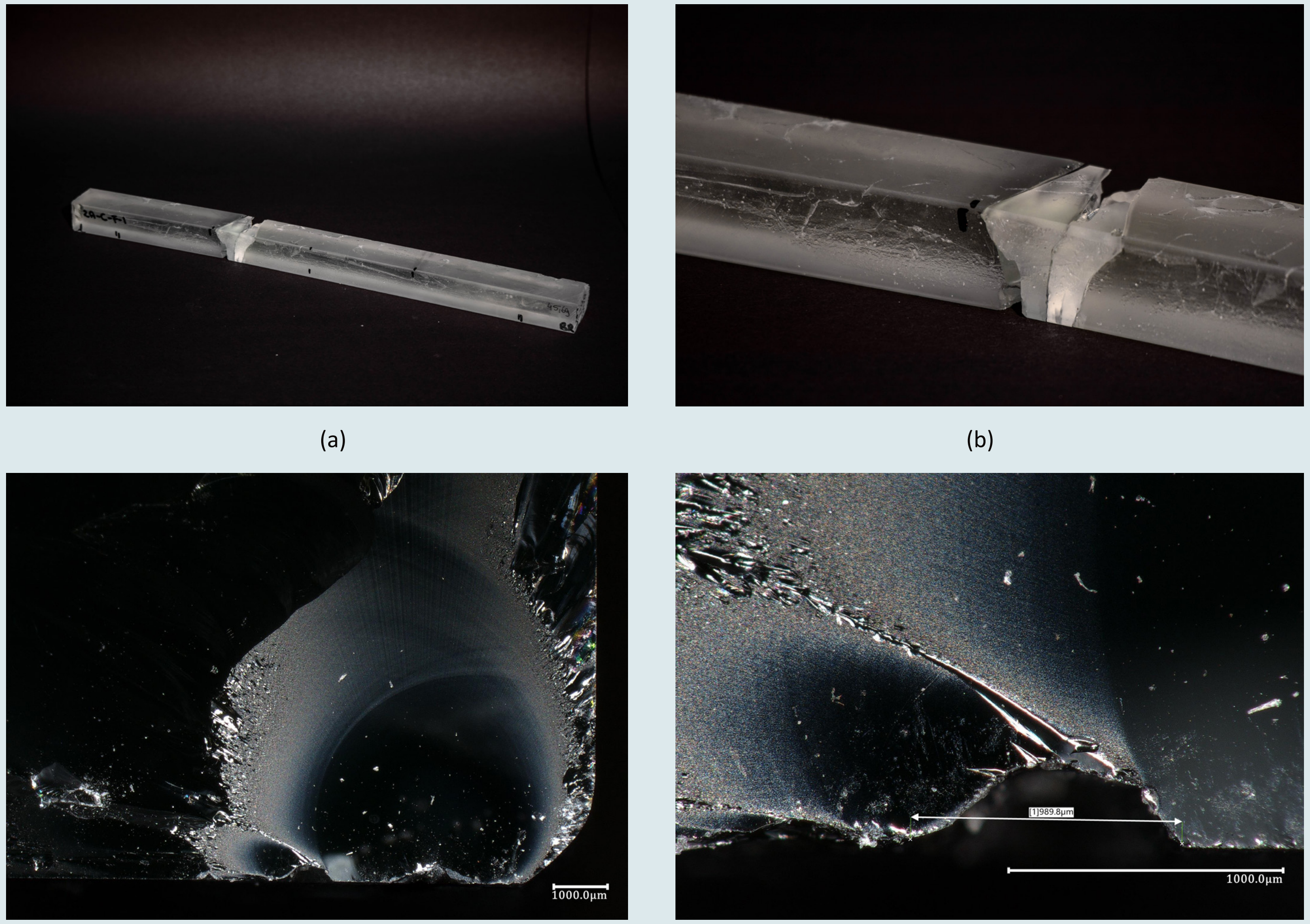

(a) (b) (c) (d)

Figure 111: Microscopic photos of the flaw type, infolds from beam V-2A-C8-F-1, (a) Location of the crack, (b) Zoomed-in image of the crack, (c) Overview of the fracture and (d) Zoomed in photo of the infold

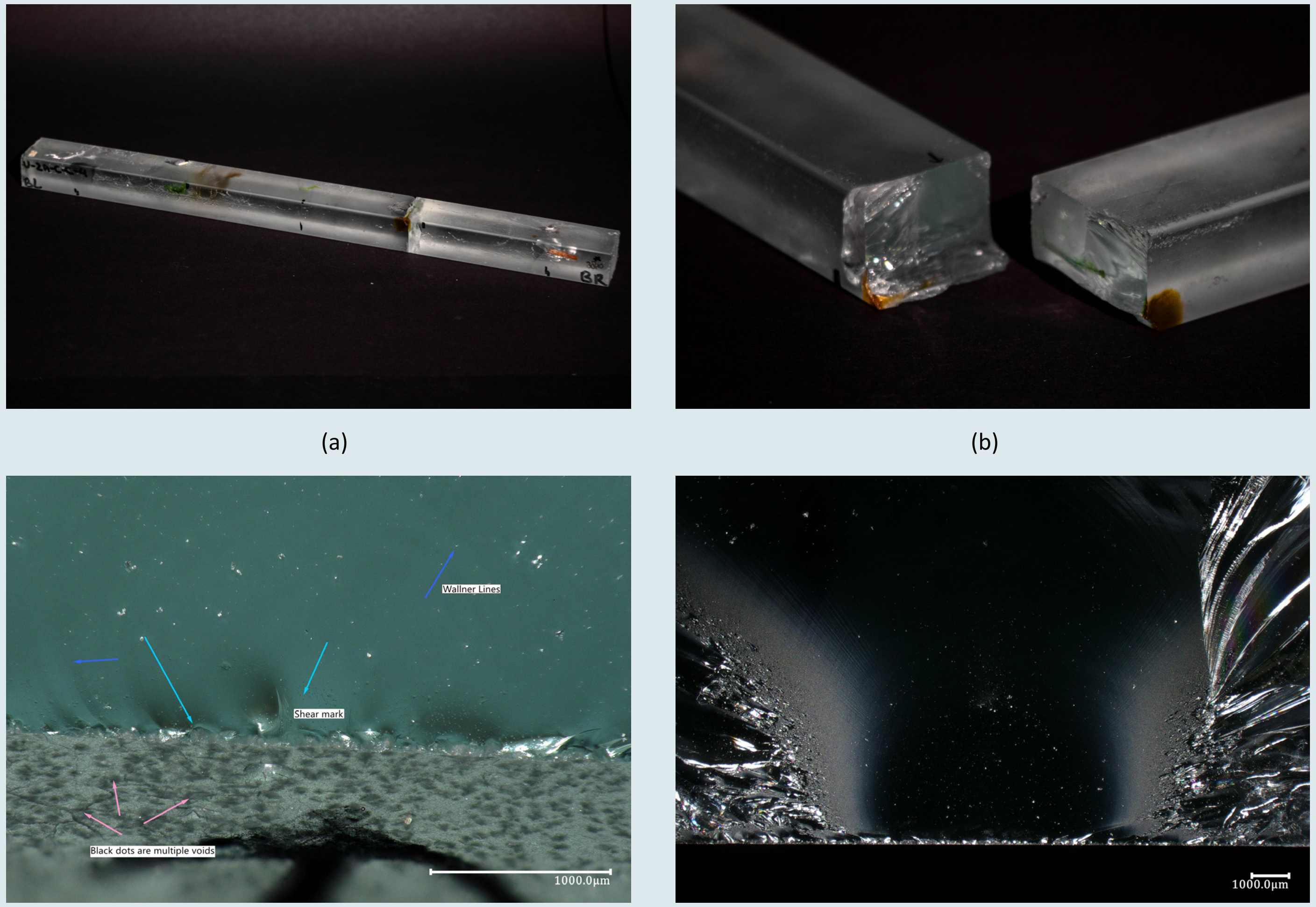

(a) (b) (c) (d)

Figure 112: Microscopic photos of the flaw type, infolds from beam V-2A-C10-C-1, (a) Location of the crack, (b) Zoomed-in image of the crack, (c) Overview of the fracture and (d) Zoomed in photo of the infold

Crystallization

To understand the behaviour of the cast glass specimens, various temperature schedules are employed, and the firing and cooling speeds are adjusted accordingly. When glass is formed at temperatures just below its crystallization range and then cooled slowly, there is a risk of crystallization occurring. To mitigate this risk, the heating ramp is set to a gradual 50 degrees per hour during the firing process.

The scheduled fire rounds involve manually quenching the glass below its softening point to prevent crystallization, which is considered a surface imperfection (one of the flaw categories). Crystallization can occur when components are formed at temperatures lower than the liquidus point or within the crystallization peak zone. Subtle variations in thermal history related to these processes are typically undetectable without detailed analysis. These variations can influence the material composition of the glass, potentially affecting its structural properties. However, noticeable defects such as bubble veils or crystallization, which arise due to specific thermal profiles during manufacturing, can have a pronounced impact on the glass's strength. If these defects are visible on the surface or within the glass, they can create stress concentrations that compromise its structural integrity and increase the likelihood of failure. This phenomenon is shown in the beams containing 10 mm Float glass during Fire Round 2C, which will be further discussed in the next chapter.

As mentioned earlier, crystallization is an intrinsic surface flaw in glass that occurs due to specific temperature-dependent melting reactions. It typically occurs at temperatures higher than the glass's melting point. Therefore, beams produced at 1120 degrees have a higher chance to crystallization compared to composite beams processed at 1070 degrees. Specifically, beams from Fire Rounds 1A and 1B were subjected to the 1120 degrees temperature schedule.

Interestingly, Fire Round 2C also utilised the 1120 degrees temperature schedule for a batch of composite beams, which will be discussed further in Chapter 9: Mechanical behaviour optimisation.

To prevent crystallization, the scheduled firing rounds involve manually quenching the glass below its softening point. Crystallization is considered a surface imperfection that can occur if glass components are formed at temperatures lower than the liquidus point or within the crystallization peak zone. While subtle variations in thermal history affecting the glass network are usually imperceptible, visible defects such as bubble veils or crystallization, resulting from specific thermal profiles, can significantly compromise the glass's strength and durability. An example of a beam with crystallization as a surface flaw is provided in Figure 113.

Machining (cutting and grinding)

One of the most common intrinsic flaws in cast glass specimens is machining errors, which occur during post-treatment processes such as cutting and grinding of cast glass beams. These processes can introduce imperfections on the surface of the beam. Many specimens fracture at the edges or surface of the beam, with machining errors being the most prevalent type of flaw, as evidenced by the tables in Appendix G: Microscopic analysis.

Lower strength specimens often fail due to the presence of stones or crystalline interfaces, whereas higher strength specimens typically fail more frequently due

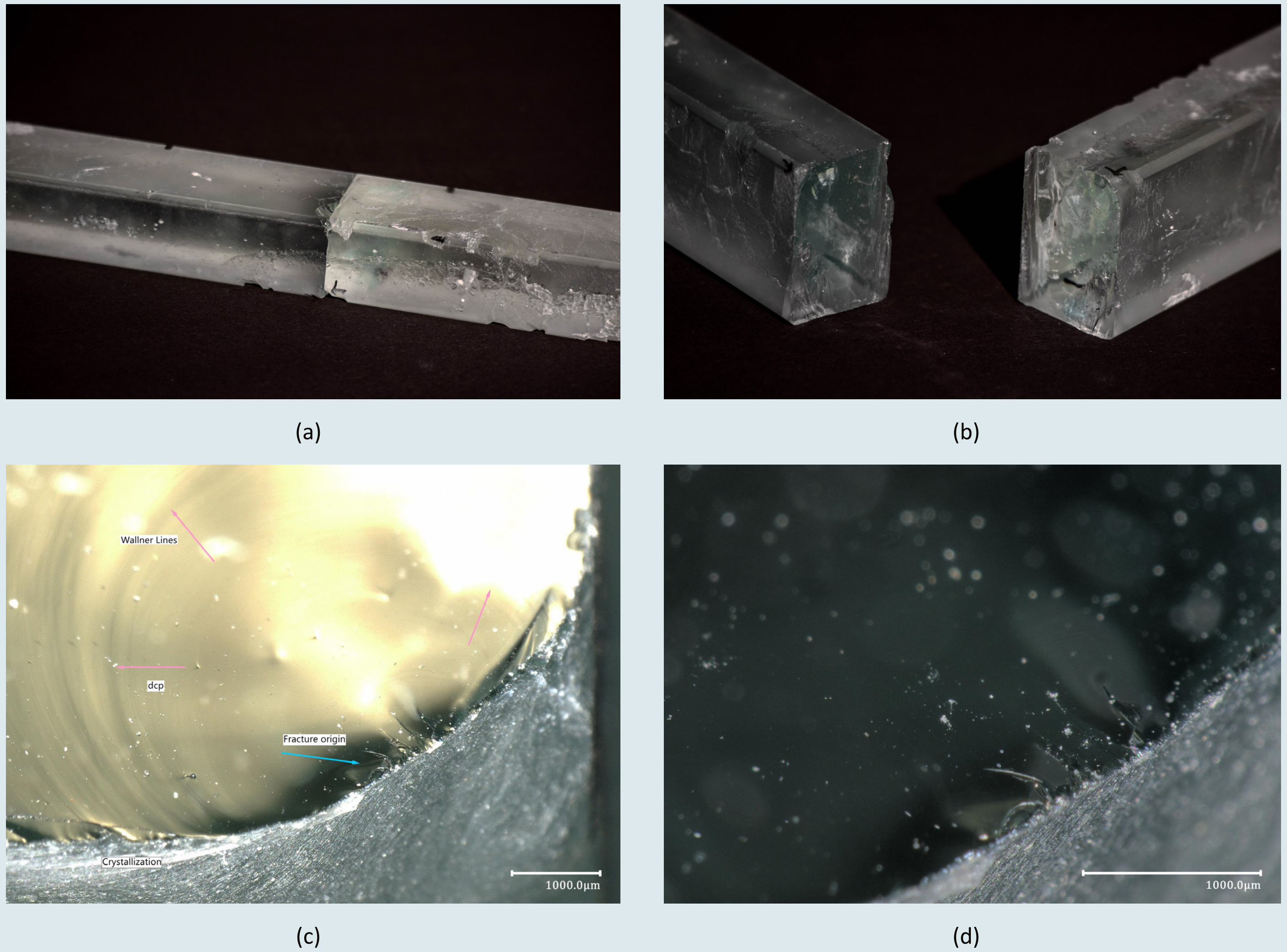

Figure 113: Microscopic photos of the flaw type, crystallization from beam V-1B-H-HR-1, (a) Location of the crack, (b) Zoomed-in image of the crack, (c) Overview of the fracture and (d) Zoomed in photo of the area with crystallization

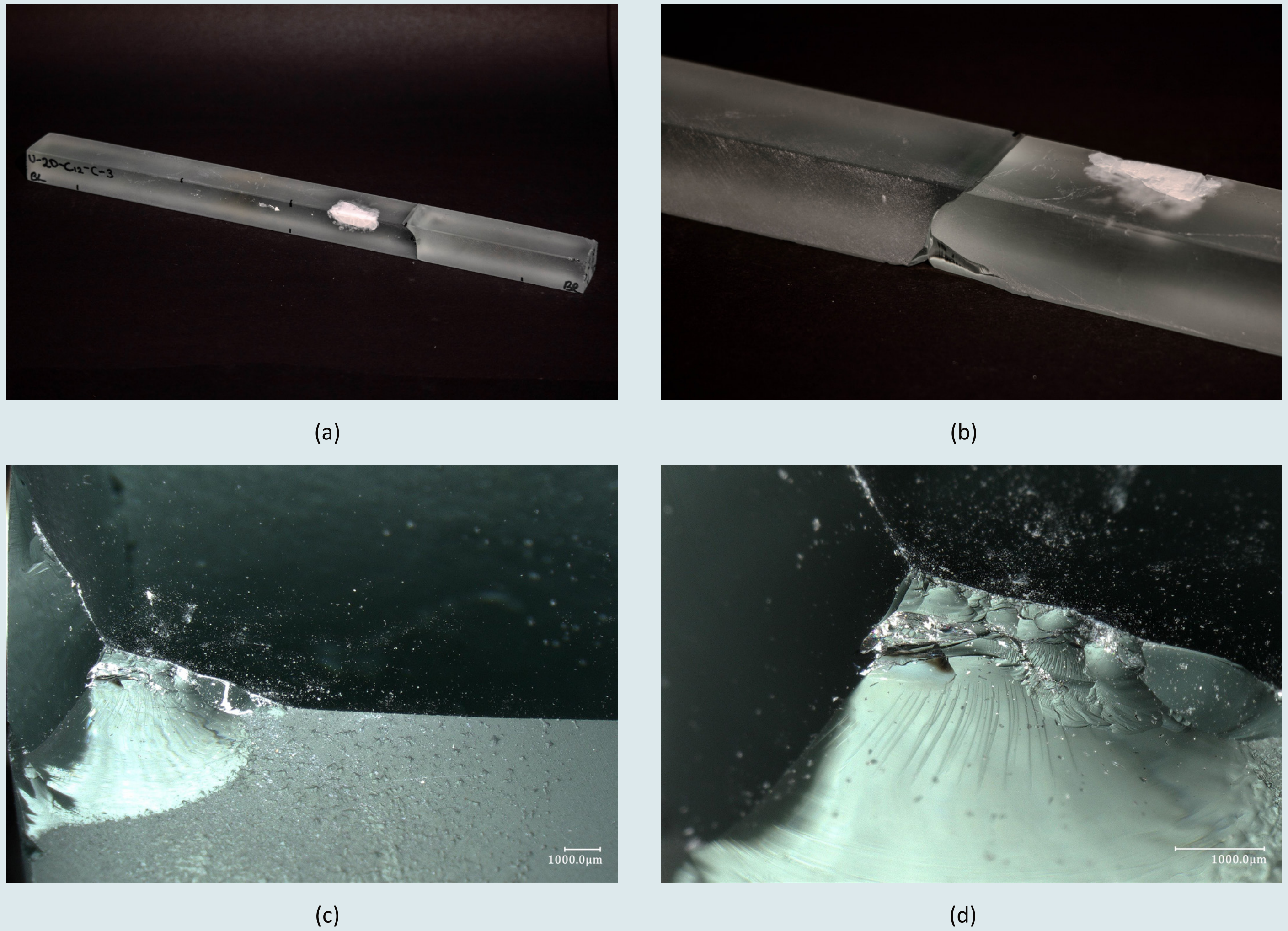

Figure 114: Microscopic photos of the flaw type, machining from beam V-2D-C12-C-3, (a) Location of the crack, (b) Zoomed-in image of the crack, (c) Overview of the fracture and (d) Zoomed in photo of the area with scratches

to machining errors. However, the exact reasons why certain glass samples exhibit lower strength cannot be fully explained solely by the type, size, quantity, and position of these surface faults.

Machining can intensify other types of defects, including inclusions or infolds. The excessive stress applied during grinding can cause some beams to crack. Inadequate annealing during cutting and grinding processes can lead to infolds (chips) and cleavage (debris) damage, which may only become apparent during polishing. Due to more pronounced machining imperfections on the surface compared to the bulk, increased stress and machining errors contribute to fractures at lower strength levels, resulting in multiple beam failures during surface treatment.

Figure 114 shows a beam that failed due to machining flaws, featuring numerous scratches on its surface from the grinding process. An interesting aspect of this machining failure from beam V-2D-C12-C-3 is the presence of a significant inclusion, identified as the white stone embedded in the beam. Despite this large inclusion located within the bulk of the glass, the beam ultimately failed at the surface due to the machining errors. This highlights how surface defects introduced during machining can be more detrimental to the overall structural performance of the beam than internal inclusions.

8.3 Stress in flaw categories

To analyse whether certain flaws lead to internal stresses, several beams with typical flaws were tested using cross-polarised light microscopy. The stresses were examined for inclusions, infolds, crystallisation, and machining flaws.

08 | MICROSCOPIC VALIDATION

For a clearer understanding of stress distribution in the beams, four images were provided per beam. The first image provides an overview, indicating the location of the crack and distinguishing between high and low energy failures. A zoomed-in photo of the crack pattern follows. Beams with compression curls, indicative of low energy failure, exhibit large, reflective surfaces known as "big mirrors." In contrast, beams with double compression curls, indicative of high energy failure, show small, compact mirrors.

As previously explained, cracks resulting from high energy failures display more localised stress, resulting in a clear mirror with distinct boundaries, whereas low energy failures show a large mirror with lower stress and less defined boundaries where the mist stops. An overview of the fracture origin is presented in the third image, followed by a zoomed-in photo of the fracture in the fourth picture.

Inclusions

Figure 115 displays polarised microscopic photos of a beam containing an inclusion. In this fracture, the inclusion (white spot) itself does not exhibit stress, but stress is localised around it, contributing to the beam's failure.

Infolds

Figure 116 shows polarised microscopic photos of a beam with an infold. Stress is localised around the gap caused by the infold. Figure 116d illustrates that stress distribution around the infold is less pronounced compared to an inclusion, where a distinct colour streak around the flaw indicates concentrated stress.

Crystallization

Figure 117 presents polarised microscopic photos of a beam containing crystallisation. Stress is visibly localised around the crystallisation, as depicted in Figure 117d.

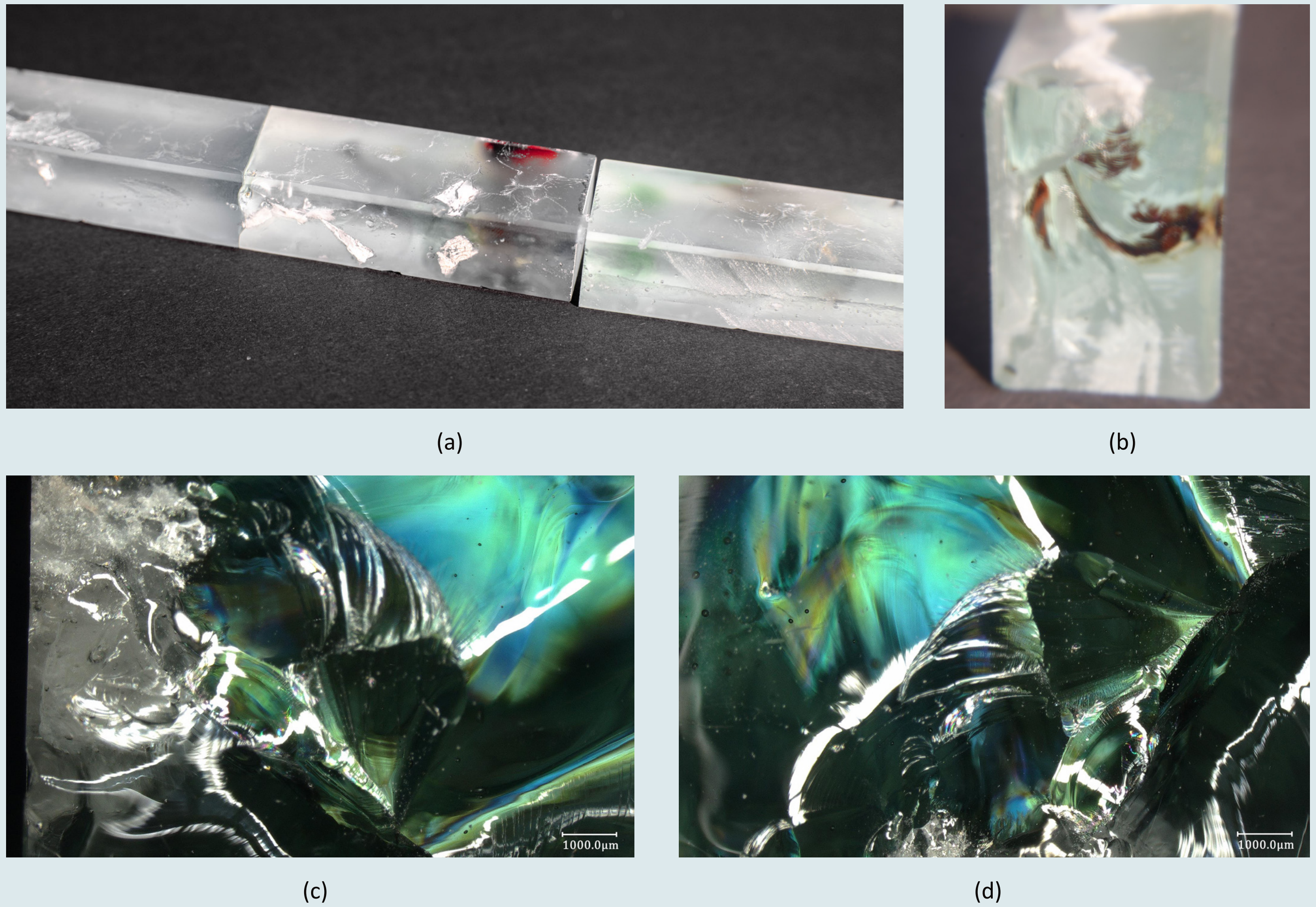

Figure 115: Microscopic cross polarised photos of the flaw type, inclusions from beam V-1A-H-C-1, (a) Location of the crack, (b) Zoomed-in image of the crack, (c) Overview of the fracture and (d) Zoomed in photo of the area with the inclusion

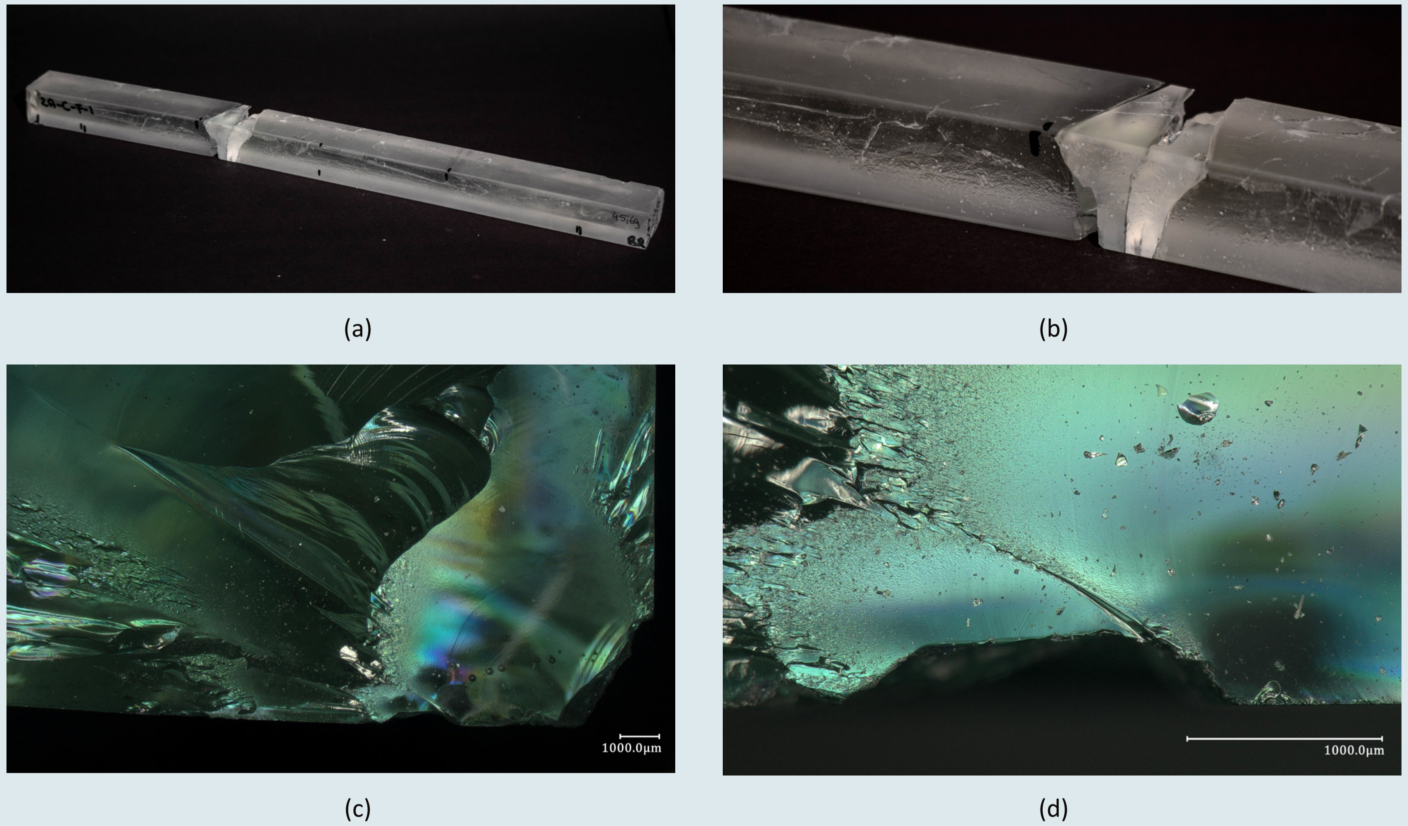

Figure 116: Microscopic cross polarised photos of the flaw type, infolds from beam V-2A-C8-F-1, (a) Location of the crack, (b) Zoomed-in image of the crack, (c) Overview of the fracture and (d) Zoomed in photo of the area with infolds

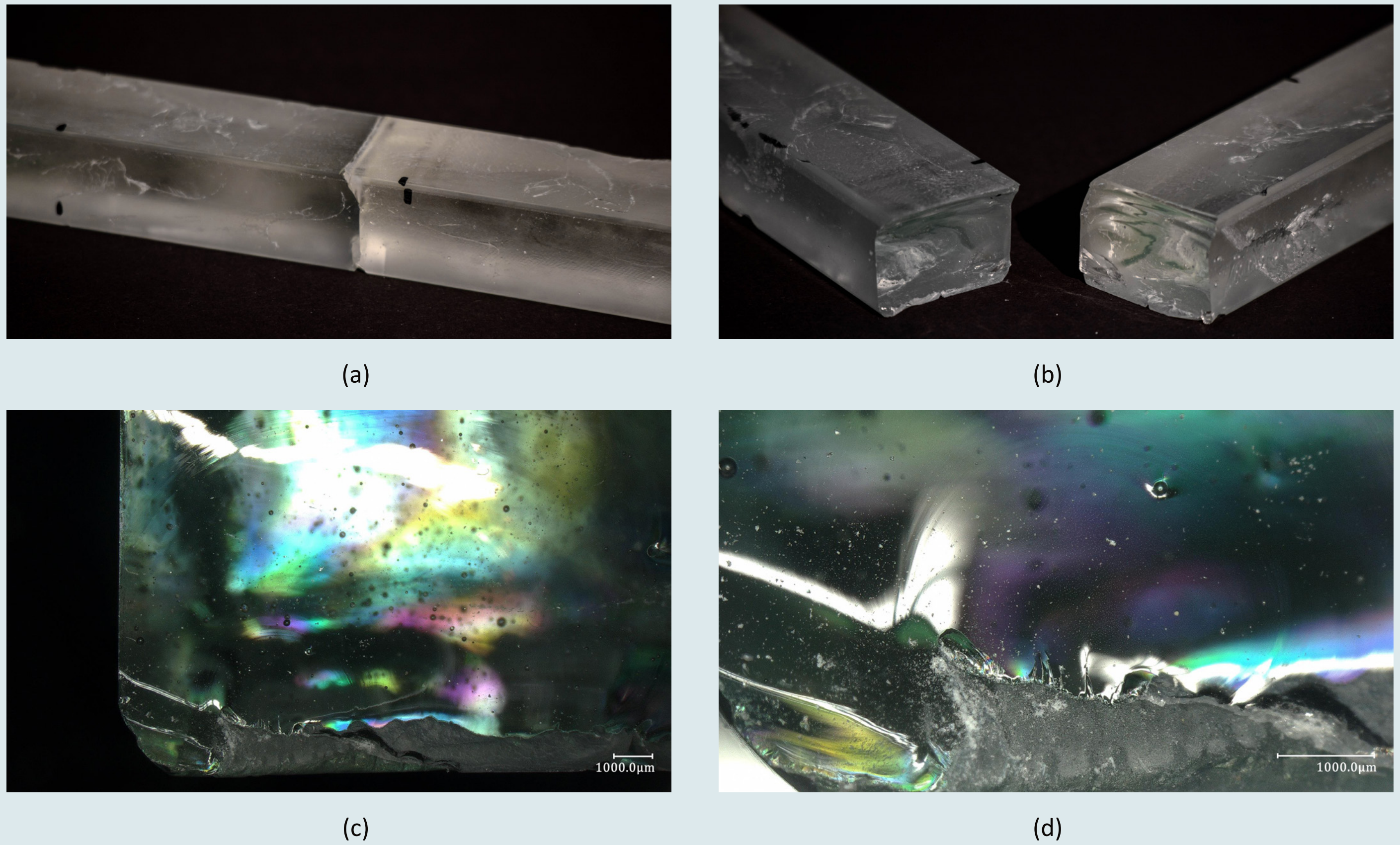

Figure 117: Microscopic cross polarised photos of the flaw type, crystallization from beam V-1B-H-F-2, (a) Location of the crack, (b) Zoomed-in image of the crack, (c) Overview of the fracture and (d) Zoomed in photo of the area with crystallization

08 | MICROSCOPIC VALIDATION

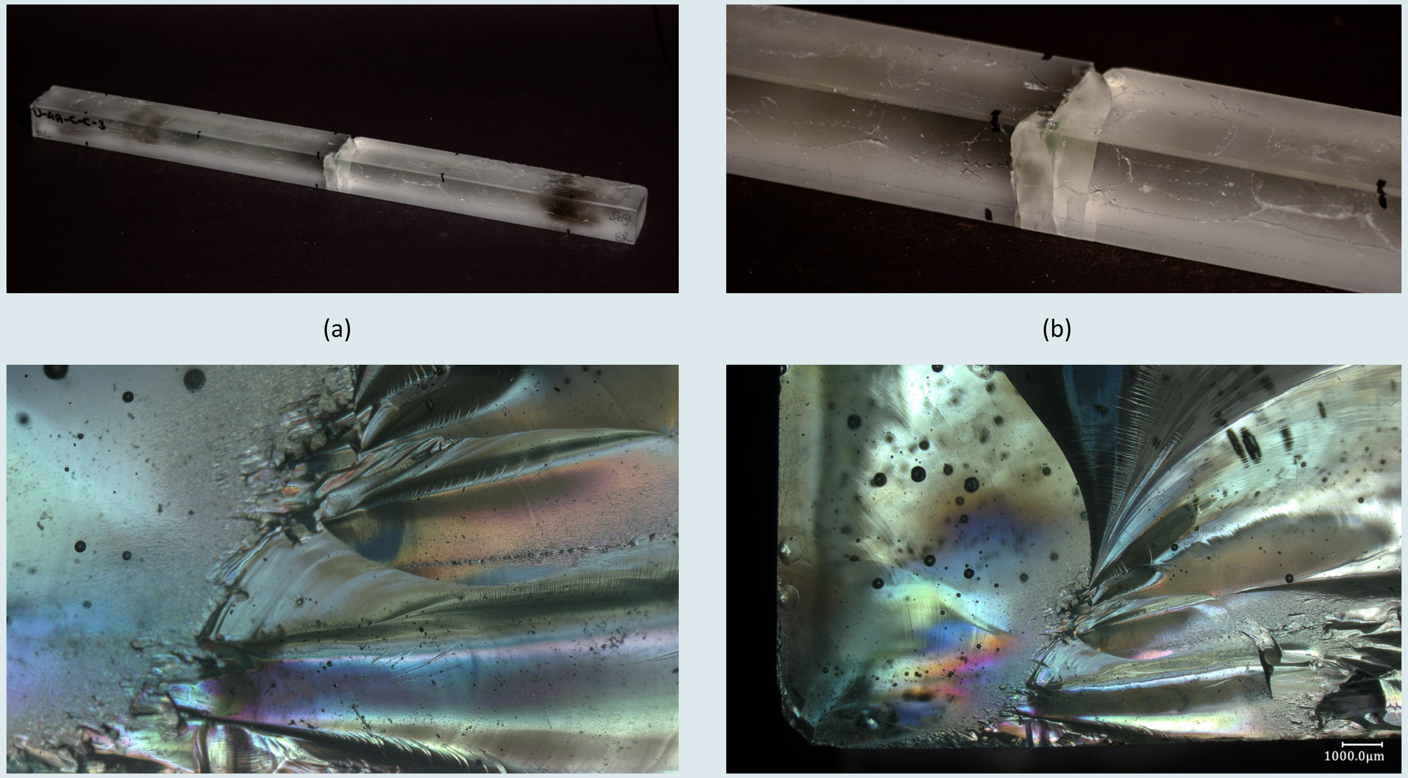

(a) (b) (c) (d)

Figure 118: Microscopic cross polarised photos of the flaw type, machining from beam V-4A-CR8-C-3, (a) Location of the crack, (b) Zoomed-in image of the crack, (c) Overview of the fracture and (d) Zoomed in photo of the area with scratches

Machining

Figure 118 displays polarised microscopic photos of a beam with machining flaws from surface and edge treatments. Interestingly, stress around the scratches from machining is not notably pronounced. However the mirror shows some colour streaks of stress.

8.4 Discussion and conclusion

8.4.1 Crack patterns

Appendix F, "Overview beams with failure analysis," provides a comprehensive analysis of all beams tested in the four-point bending tests. It includes details on the location of failure along the beams—whether under a load point (left, right, or centre at distances of -175 mm to 0 mm to 175 mm), the vertical position of the fracture origin (0 mm to 21 mm from bottom to top), and the horizontal position of the fracture on the beam's surface (0 mm to 28 mm from the edges to the centre). And provides an image of the crack.

Since failures occur at various locations and not exclusively under load points, the results are applicable. If failures were concentrated solely under load points, it would suggest potential misalignments.

Upon reviewing Appendix F, it is evident that some beams exhibit such misalignments. It is crucial to consider twisting or misalignments during the analysis.

The beams that contain possible misalignments are

Homogeneous beams:

- V-1B-H-F-1
- V-1C-H-M-3

Composite beams: relation between surface and bulk:

- V-2A-C10-C-1
- V-2C-C12-C-1
- V-2D-C12-C-3

Composite beams: influence of bulk material:

- V-3A-C10-M-3

The failure analysis will be discussed per Experiment Type.

Experiment type 1: Homogeneous beams

- A high energy failure is experienced for all the homogeneous beams with A cullet grade.
- A medium-high energy failure is typically experienced by homogeneous beams with a B cullet grade.
- The stress fracture of homogeneous beams with a C cullet grade is low.
- As a result of the ceramic being removed, the beam with the HR glass is now an exception and exhibits a high energy failure.
- Regardless of energy level, homogeneous beams with type B and C cullet exhibit a compression curl upon failure.

Experiment type 2: Composite beams: influence of ratio between surface and bulk

- Composite beams with Float glass and CSP Pollutants have in general a high energy failure
- Beam V-2B-C10-C-2 is an irregularity; this indicates a low stress fracture of that kind. Furthermore, low energy failure also occurs in beams V-2D-C8-C-1 and V-2D-C10-C-1. These are an additional exemption. A large surface imperfection caused these beams to break. The Float glass in each of these beams was split in half and arranged sequentially. As a result of this experiment, the impact of the Float glass sides was seen. In the tension area, it produced an open perpendicular area. This defect is so strong that it greatly reduces the strength. This demonstrates how surface imperfections can significantly reduce flexural strength.

Experiment type 3: Composite beams: influence of the material composition of the bulk

- Beams with Metallic Pollutants in the bulk show most of the time a low energy failure. Beam V-3A-C-M8-2 and V-3A-C8-M-3 are exceptions.
- There is an intriguing double compression curl in Beam V-3A-C8-M-2. The split occurs nearly at the top of the very long perpendicular line.

Experiment type 4: Composite beams: influence of the material composition of the surface

- Beams focusing on surface material, incorporating Fritted glass, exhibit a diverse array of crack patterns.
- Beams with CSP Pollutants in the bulk and Fritted glass on the surface show both low and high energy failures, yet exhibit low flexural strength overall. Remarkably, beam V-4A-CR8-C-3 displays a double compression curl.
- Beams with Metallic Pollutants in the bulk and Fritted glass on the surface demonstrate low energy failures and exhibit compression curls.

8.4.2 Flaw types

Appendix G: "Overview beams with microscopic analysis" provides a comprehensive review of the research conducted at the microscopic level. Each beam tested in the four-point bending test undergoes detailed microscopic analysis, capturing surface conditions (tensile area), fracture locations, and close-ups of fractures.

Defect categories such as inclusions, infolds, crystallization, and machining (surface and edge treatment) are examined and correlated with the crack patterns (fracture origins) and the structural performance (flexural strength) of the beams. Additionally, these defect types are analysed under polarised light to assess internal stresses.

Graph 20 uses the tables from Appendix G to visualise the relationship between different flaw types and the flexural strength of each beam. This graph aims to bring light to any correlations between specific flaw types and the occurrence of beam failures.

It's important to note that this graph includes only the beams tested in the four-point bending tests. Beams that failed the structural feasibility assessment are not represented in this graph, although they were also investigated. The most common flaw in these excluded beams was an inclusion (ceramic or silica).
Using this graph, each flaw type will be discussed and the following conclusions can be drawn:

Inclusions

- The most destructive types of flaws to the beams are inclusions. Most of the time, a localised inclusion in a beam is a significant failure to the beam. Due to excessive inclusions, a total of 13 beams fractured before the structural performance test either when they were taken out of the oven or during the surface treatment process while the beams were being polished.

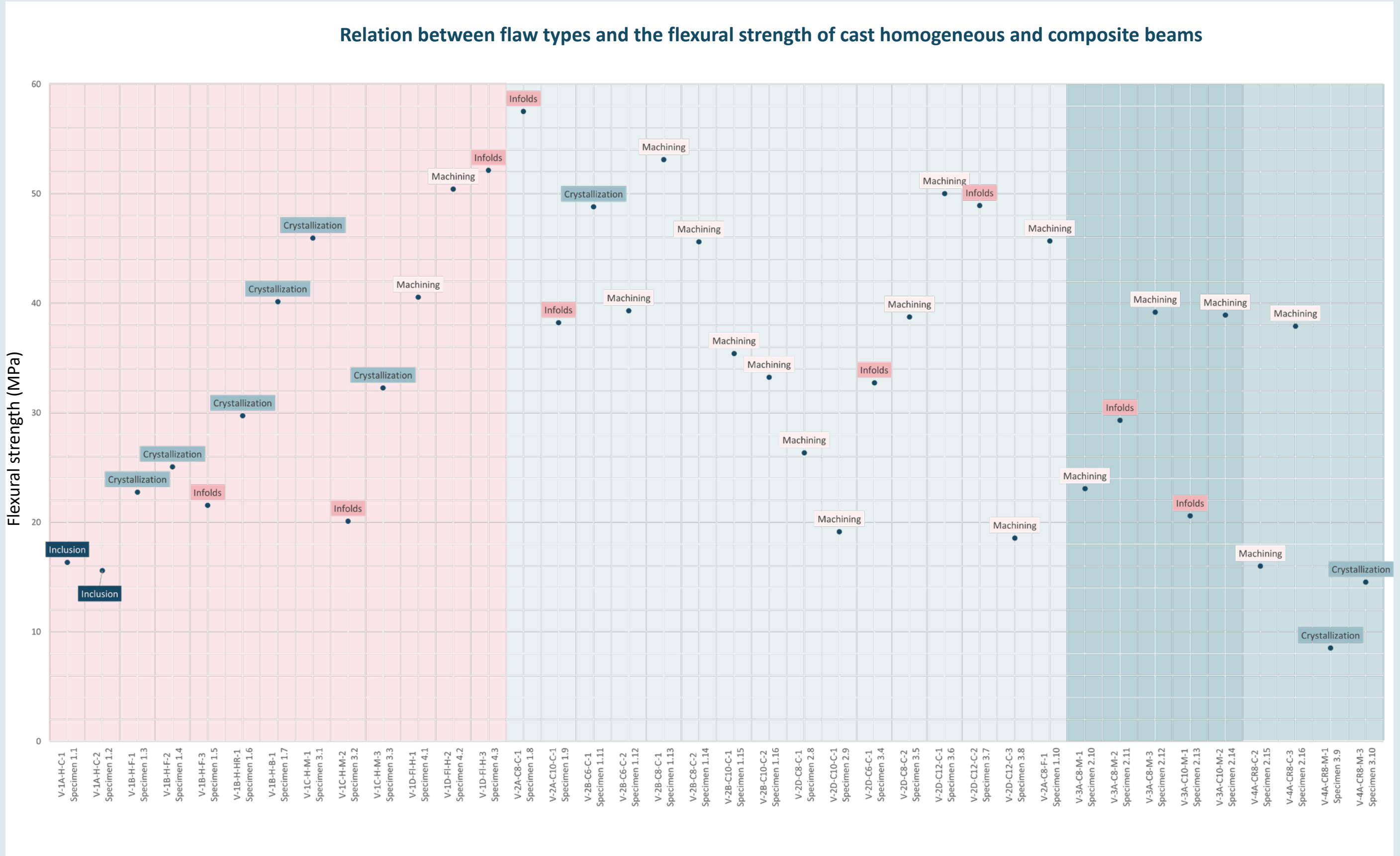

Graph 20: Flaw types compared with the structural performance of cast C&D beams

The results from Fire Round 2C are not integrated in this graph, these will be explained in Chapter 9

Experiment type 1: (Pink)
Homogeneous beams
Glass with A cullet

Float glass	V-1D-H-Fl-1, V-1D-H-Fl-2 and V-1D-H-Fl-3

Glass with B cullet

Fritted glass	V-1B-H-F-1, V-1B-H-F-2 and V-1B-H-F-3
Soft coating	V-1B-H-B-1

Glass with C cullet

CSP	V-1A-H-C-1 and V-1A-H-C-2
HR glass	V-1B-H-HR-1
Metallic	V-1C-H-M-1, V-1C-H-M-2 and V-1C-H-M-3

Experiment type 2: (Light blue)
Composite beams: Surface + Bulk
Float glass + CSP pollutants

6 mm + 15 mm	V-2B-C6-C-1 and V-2B-C6-C-2
8 mm + 13 mm	V-2A-C8-C-1, V-2B-C8-C-1, V-2B-C8-C-2, V-2D-C8-C-1 and V-2D-C8-C-2
10 mm + 11 mm	V-2A-C10-C-1, V-2B-C10-C-1, V-2B-C10-C-2, and V-2D-C10-C-1
12 mm + 9 mm	V-2D-C12-C-1, V-2D-C12-C-2 and V-2D-C12-C-3

Experiment type 3: (Dark blue)
Composite beams: Surface + Bulk
Float glass + Fritted glass

8 mm + 13 mm	V-2A-C8-F-1

Float glass + Metallic pollutants

8 mm + 13 mm	V-3A-C8-M-1, V-3A-C8-M-2 and V-3A-C8-M-3
10 mm + 11 mm	V-3A-C10-M-1 and V-3A-C10-M-2

Experiment type 4: (Blue)
Composite beams: Surface + Bulk
Fritted glass + CSP Pollutants

8 mm + 13 mm	V-4A-CR8-C-2 and V-4A-CR8-C-3

Fritted glass + Metallic Pollutants

8 mm + 13 mm	V-4A-CR8-M-1 and V-4A-CR8-M-3

Infolds

- This type of surface flaw have tiny gaps or chips in the surface. Due to infolds in the surface the strength of the specimen (beam) will reduced. Infolds happen when cullets did not probably interfere with each other. As a result, these tiny spaces allow debris to enter and the growth of mould. Infolds occur in each experiment type and do not correlate with a specific strength for the beams in which these flaws are present.

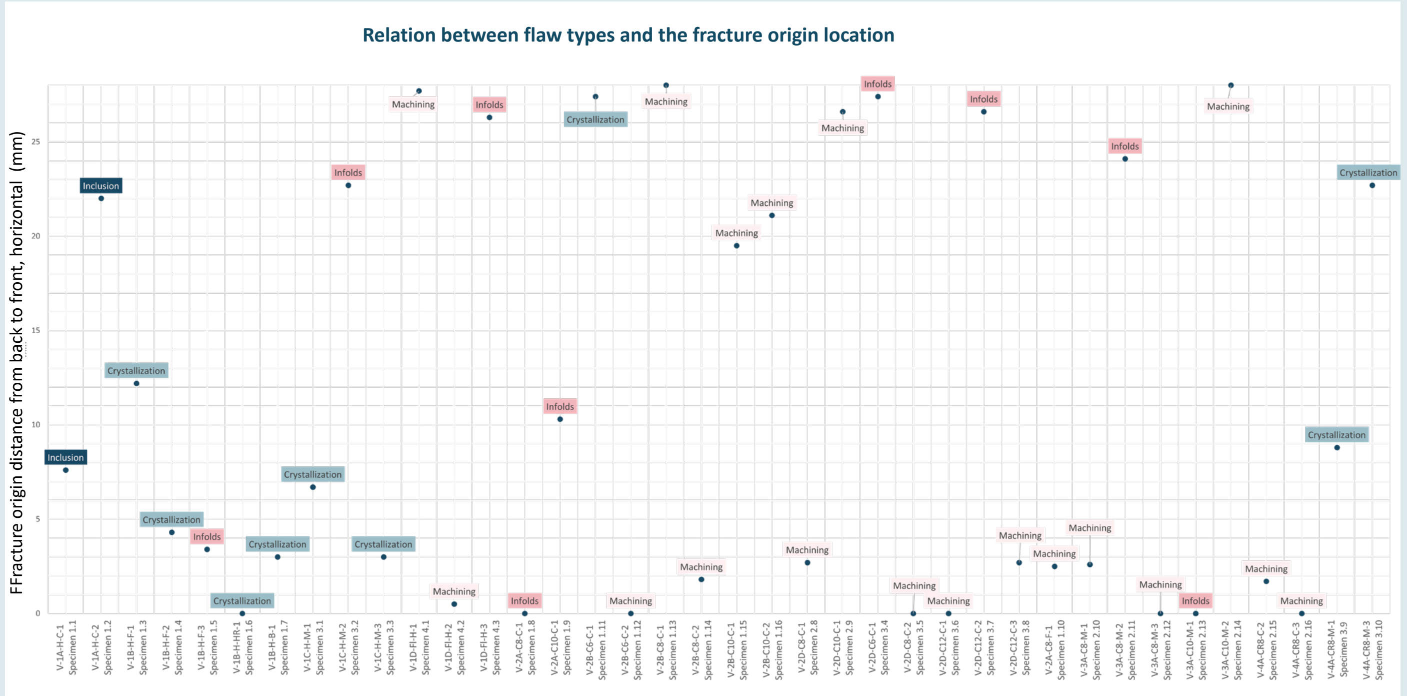

Graph 21: Flaw categories compared with the location of the fracture of cast C&D beams

The results from Fire Round 2C are not integrated in this graph, these will be explained in Chapter 9

The width of a beam is 28 mm. The back of the beam is set on 0 mm and the front is set on 28 mm.

Crystallization

- As Graph 20 displays is that crystallization most often is for homogeneous beams, which is due to the higher temperature schedule used for two fire rounds of these beams : Fire Round 1A and Fire Round 1B. Crystallisation is the most impactive flaw category after inclusions. Crystallisation happens while the oven is operating (intrinsic flaw). Formation processes occurring in the crystallisation peak zone and at temperatures below the liquidus point may lead to partially crystallised components.

Machining

- The most common defect for cast glass is machining due to surface and edge treatment. This is a superficial error. When surface cracks develop, the beams' strength will decrease. Fractures with lower strength were produced by greater stress and machining errors because the surface of the material had more severe defects than the bulk. This type of flaw is most common for the higher performance cast glass beams

Another analysis conducted examines the relationship between the flaw type and the location of the fracture origin, as shown in Graph 21. This analysis utilises data from Appendix F: Overview beams with failure analysis and Appendix G: Overview beams with microscopic analysis.

- Inclusions are localised in the middle of the material compositions. Those inclusions that failed before the structural performance test were found on the edge of the surface, indicating that surface flaws at an edge are more critical than surface flaws in the middle of the surface.

- Infolds are surface flaws typically located around the edges. However, they can also occur in the middle of the beam, as shown by specimen 1.9 Beam V-2A-C10-C-1.

- Crystallization is another type of surface flaw commonly found at the edges, but these flaws can also be present in the middle of the beam.

- Machining flaws are usually confined to the edges. However, beams V-2B-C10-C-1 and V-2B-C10-C-1 show exceptions to this pattern.

09 | MECHANICAL BEHAVIOUR OPTIMISATION

To enhance the mechanical behaviour of cast glass beams, several adjustments were implemented. This chapter outlines these strategies with the aim of creating beams that exhibit higher structural performance in four-point bending tests, while also ensuring high recyclability.

9.1 Influence of cullet selection

9.1.1 Contaminants on the cullets

The cullets used in the experiments are stored in large buckets filled with sand and soil. Figure 119 provides an impression of the cullets' appearance before the selection and removal of harmful pollutants. Initially, the cullets needed to be washed with water, followed by the removal of harmful pollutants. Numerous contaminants can adversely affect the beam's performance. To ensure clearer findings, it is crucial to identify the characteristics of pollutants in this batch, as a single pollutant can significantly influence the overall material composition.

After the initial firing rounds, Fire Rounds 1A and 2A, it became evident that many beams broke. Those that did not fail had an unknown material composition. Therefore, it is important to precisely control the pollutants added to the material composition to achieve more consistent results.

To isolate the characteristics of CSP pollutants in the composite beams of Experiment Type 2, "Influence of the ratio between surface and bulk in composite beams," CSP pollutants needed to be completely separated from other contaminants. Therefore, the following pollutants were manually selected and removed from the overall CSP batch (Figure 120).

- Silicone
- Ceramic
- Metal traces
- Yellow tinted glass
- Dark tinted glass
- Plastics
- Papers
- Mirror

For compositions containing Metallic Pollutants, all the previously mentioned contaminants, including the cullets containing CSP pollutants, are removed from the buckets. This ensures a focused investigation into metallic contaminations, ensuring any flaws are solely attributed to Metallic Pollutants and no other contaminants.

9.1.2 Tiles with contaminants

To evaluate the effects of these individual pollutants, contaminants are initially assessed in tiles. However, since the goal is to produce beams with specific structural performance, different dimensions of tiles may yield results differing from those of beams. Therefore, when considering overall structural performance, it is important to acknowledge that these findings may not directly apply to beams.

Nevertheless, for a deeper understanding of these pollutants and their impact on overall performance, harmful pollutants on the tiles are investigated using cross-polarised light and microscopic research, which will be further discussed in paragraph 9.1.4: Stress in pollutants.

Figure 119: Cullets with CSP Pollutants before the seletion of removing other contaminants

Figure 120: Overview of contaminants in the buckets with CSP Pollutants

Given the significant number of beams that broke during the initial firing rounds, Fire Round 1A (homogeneous beams) and Fire Round 2A (composite beams), it was informative to explore the types of pollutants contributing to these fractures and those potentially used in the composition. Consequently, specific pollutants were intentionally placed in two corners of the tiles, with the remaining tiles containing clear glass. The contaminants listed in 9.1.1 were observed:

- Tile 1 contained cullets with silicone and metal contaminants.
- Tile 2 included cullets made of plastic and yellow-tinted glass.
- Tile 3 featured glass fragments with a dark tint on one side and mirror cullets.

The objective of these tiles was to identify the types of cullets responsible for the damage observed in previous firing rounds. The arrangement of the firing rounds is illustrated in Figure 121, while the placement of the tiles within the oven can be seen in Figure 122. The tiles were placed in the oven for several hours, not for 100 hours like the beams produced.

9.1.3 Feasibility evaluation – Tiles

Figure 123 depicts the tiles as they emerged from the oven, each evaluated for its structural integrity. It is noteworthy that none of the tiles cracked. However, it is likely that some of these same pollutants would fracture if they were incorporated into a beam especially the tile including silicone.

Tile 1 reveals an intriguing pattern with metallic and silicone pollutants. At 1070 degrees Celsius, the metallic pollutants melted and began to interact with the glass. White markings indicative of a reaction with the mould are visible where the metal traces are present. Similarly, clear white traces are evident in areas where silicone is located.

Under high temperatures, silicone undergoes transformation into various byproducts such as silicon dioxide (silica). However, the silicone does not completely convert into silica during this process, as evidenced by pink/white traces of silicone. This suggests that silica formation requires a longer duration in the oven.

Tile 2, featuring cullets containing plastic and tinted glass, demonstrates that these contaminants do not compromise structural integrity. The plastic melts completely, becoming invisible at 1070 degrees. The behaviour of the tinted glass at this temperature is particularly noteworthy, especially compared to how clear glass cullets react. Surprisingly, the piece of tinted glass remained in place without causing significant disturbance. Some minor signs of mould reaction are visible.

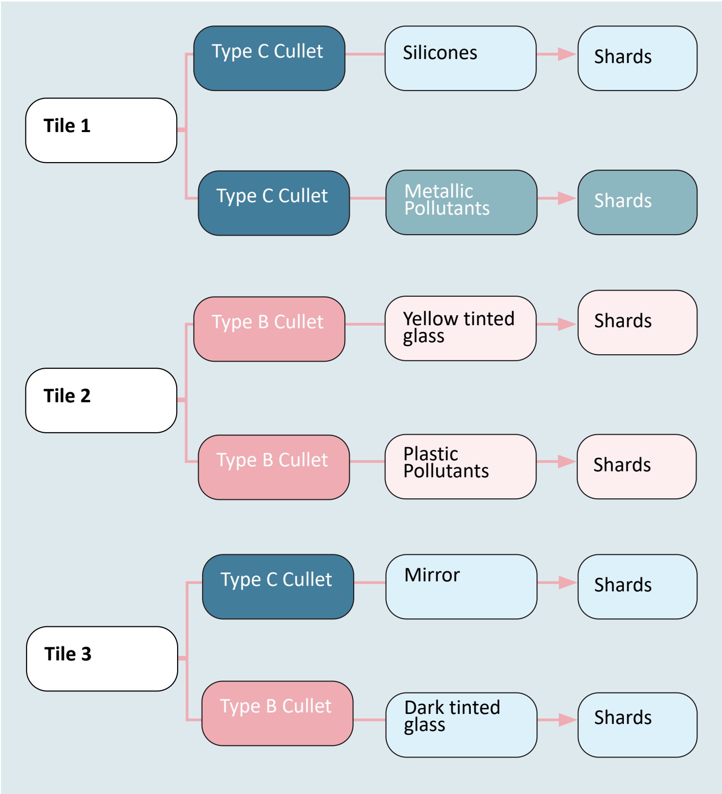

Figure 121: Illustratic diagram - Tiles

Figure 122: Tiles are placed in the oven

Tile composition with pollutants

	Tile 1 **Material characteristics**	Tile 2 **Material characteristics**	Tile 3 **Material characteristics**
The product:	Combi Mag Float (Maltha)	Combi CSP Float (Maltha)	Combi Mag Float (Maltha)
Cullet grade:	Class C	Class B	Class B + C
Contamination:	Silicone + Metal Pollutants	Yellow tinted glass + Plastic	Small Metal Pollutants + Dark tinted glass
Cullet Type:	Small shards	Small shards	Small shards
Forming temperature:	1070 °C	1070 °C	1070 °C

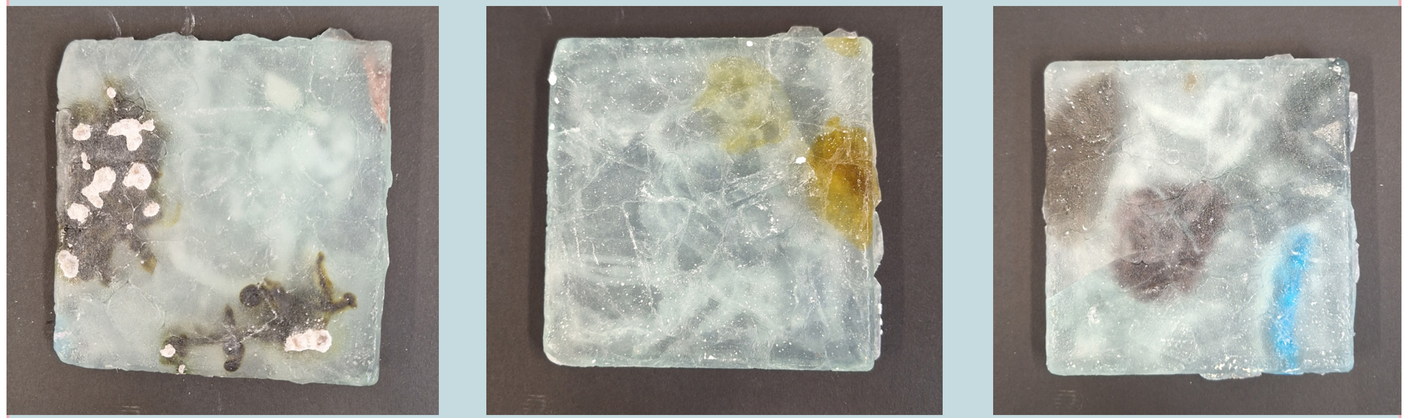

(a) (b) (c)

	Feasibility characteristics	**Feasibility characteristics**	**Feasibility characteristics**
Compatibility:	high	medium	high
Transparency:	translucent	translucent	translucent
Mould reaction:	present	absent	absent
Cracks presence:	present	present	absent
Breakage:	absent	absent	absent
Bubbles level:	low	low	low
Structural performance:	succeeded	succeeded	succeeded

Figure 123: Feasibility validation of tiles for understanding the characteristcs of specific contaminants. (a) Tile 1 with silicone and metallic pollutants, (b) Tile 2 with yellow tinted glass and plastics and (c) Tile 3 with cullets with mirror and dark tinted glass

Tile 3, featuring cullets containing dark-tinted glass and mirror fragments, shows interesting behaviour. The mirror-fused cullet turned blue and contained some trapped white bubbles. The dark-tinted glass behaves similarly to the yellow-tinted glass in Tile 2; it melts but does not blend with the translucent cullets. Overall, the compatibility across all tiles is medium to high, as the different cullets remain distinguishable from one another. While they may have started to merge at higher temperatures, they have not fully fused.
To better understand the effect of each individual pollutant, the tiles are analysed and checked for internal stresses. To visualise these stresses more clearly, microscopic photos are taken with and without polarised light. Figure 124 displays these results.

9.1.3 Stress in pollutants

The microscopic photos reveal that metallic pollutants, shown in Figures 124a and 124b, cause noticeable internal stress around the affected areas. In contrast, silicone pollutants, displayed in Figures 124c and 124d, do not allow any light to pass through. While some internal stress is present around the silicone, it is not significant.

Cullets containing plastic, depicted in Figures 124e and 124f, show no visible internal stresses. This indicates that the plastic has been completely removed during this short temperature schedule and does not pose any harm. The cullets with tinted glass, visualised in Figures 124g and 124h, also exhibit minimal internal stresses. However, the dark tinted glass in Figures 124i and 124j contains slightly more internal stress compared to the lighter tinted glass.

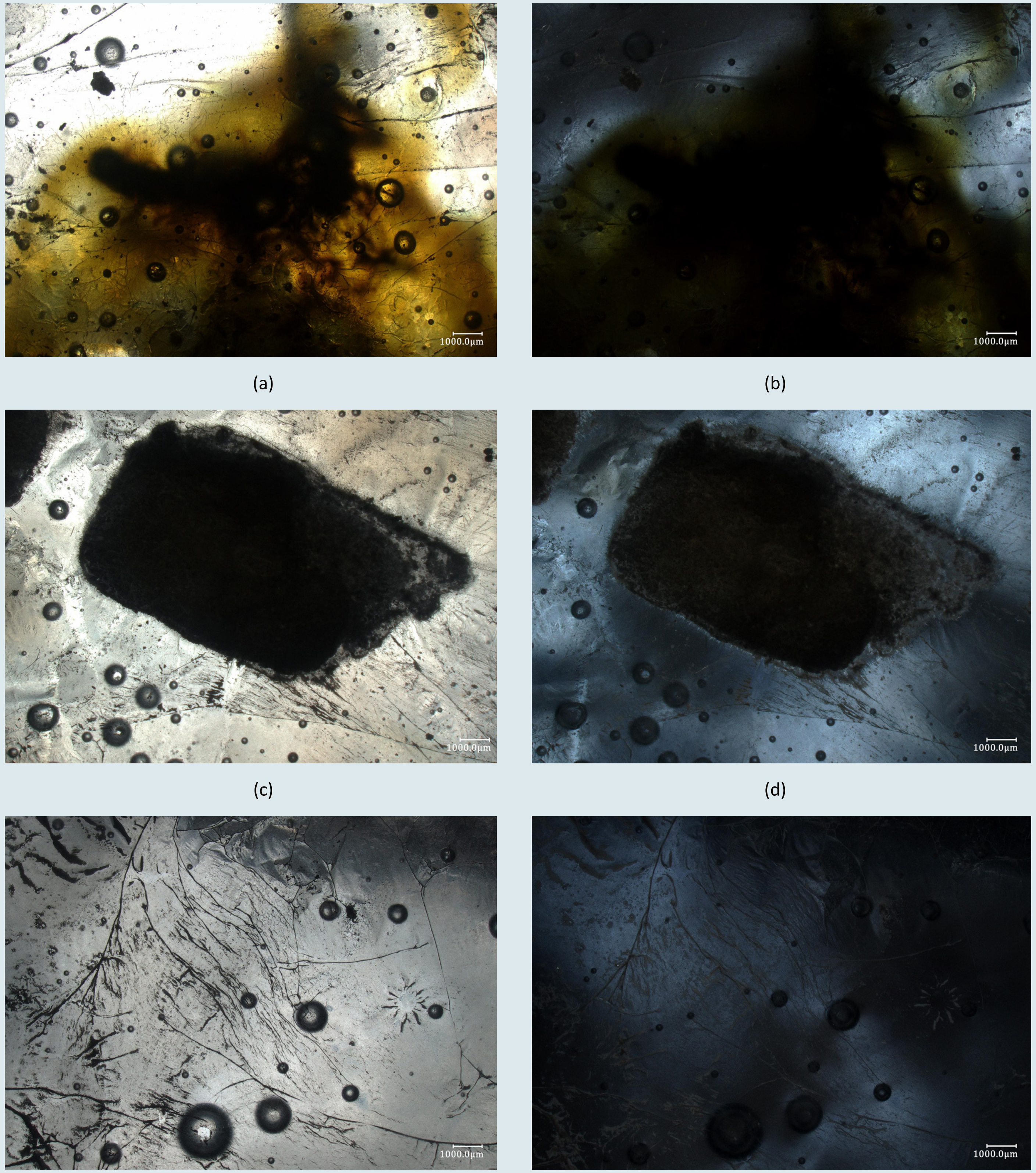

(a) (b) (c) (d) (e) (f)

Lastly, the cullets containing mirror material, shown in Figures 124k and 124l, display some internal stresses.

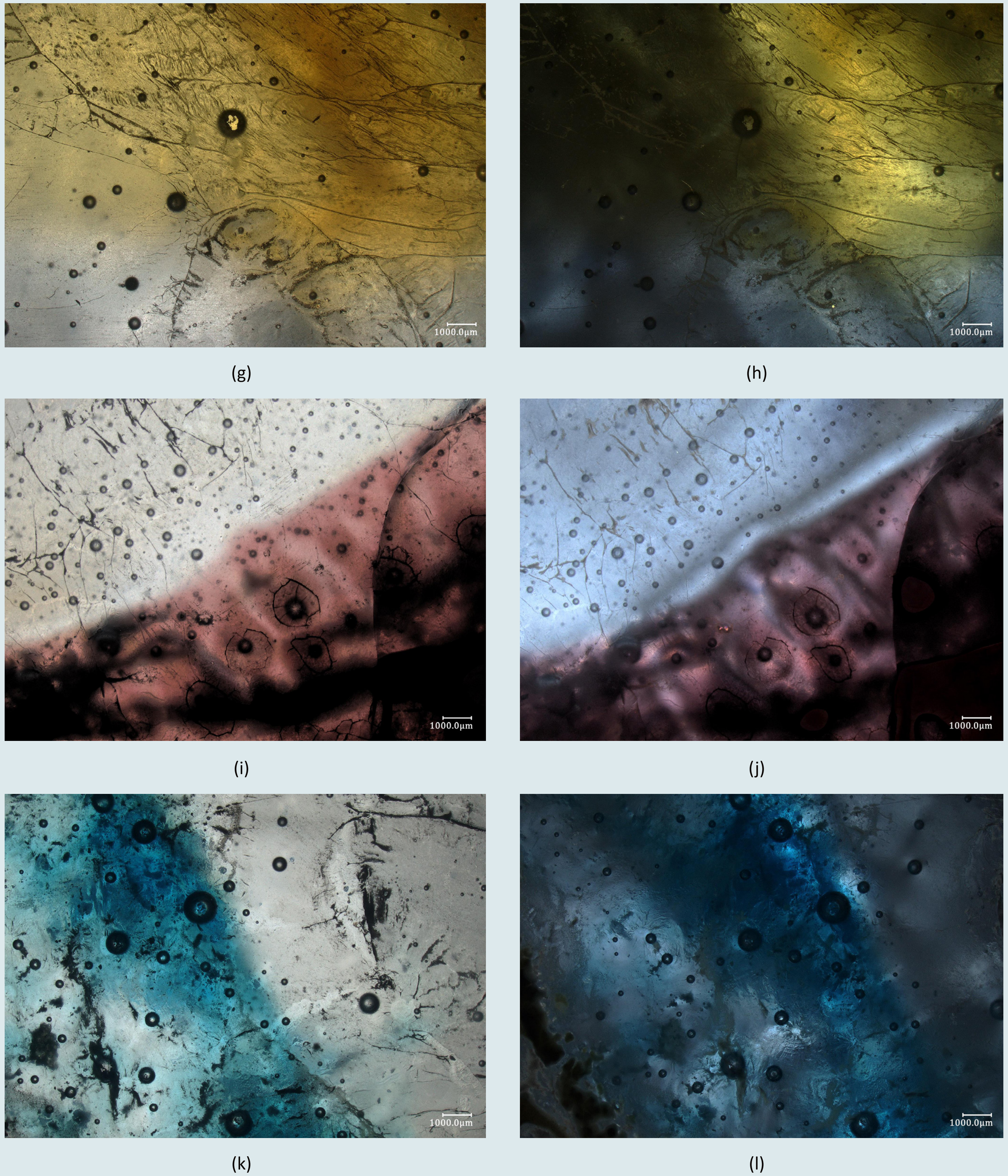

Figure 124: Microscopic photos with cross polarised light to show the internal stresses per pollutant. (a) Metallic Polllutant, (b) Polarised Metallic Polllutant, (c) Sillicone, (d) Polarised Sillicone, (e)Plastics, (f) Polarised Plastics, (g) Yellow tinted glass, (h) Polarised Yellow tinted glass, (i) Dark tinted glass, (j) Polarised Dark tinted glass, (k) Mirror and (l) Polarised Mirror

9.2 Influence of a higher temperature schedule

9.2.1 Fire Round 2C, Composite beams, Influence of the ratio between surface and bulk with a higher temperature schedule

Experiment type 2: Composite beams, this experiment investigates the influence of the ratio between surface and bulk materials. The initial fire round was conducted at a temperature of 1070 degrees. However, an alternative fire round, Fire Round 2C, was performed using the same material compositions as Fire Round 2B, but with a higher temperature schedule. Specifically, Fire Round 2C included a four-hour period at 1120 degrees. This adjustment was made to examine the impact on glass behaviour and to determine if the higher temperature would influence the outcomes of the structural performance tests. The rationale behind the higher temperature schedule was to create beams with greater compatibility, where cullets would interact more closely with each other, reducing surface flaws: infolds.

For this fire round, eight beams were created, all containing CSP pollutants in the bulk and Float glass on the surface. The compositions were distributed as follows: two beams with composition 2A, two with composition 2B, two with composition 2C, and two with composition 2D.

The primary objective of this fire round was to investigate how varying temperatures affected the bond between the bulk and surface and whether increased homogeneity/ higher compatibility would enhance structural performance. The organisation of the fire round is depicted in the diagram in Figure 125. An illustration of the beam placement in the oven can be found in Figure 126.

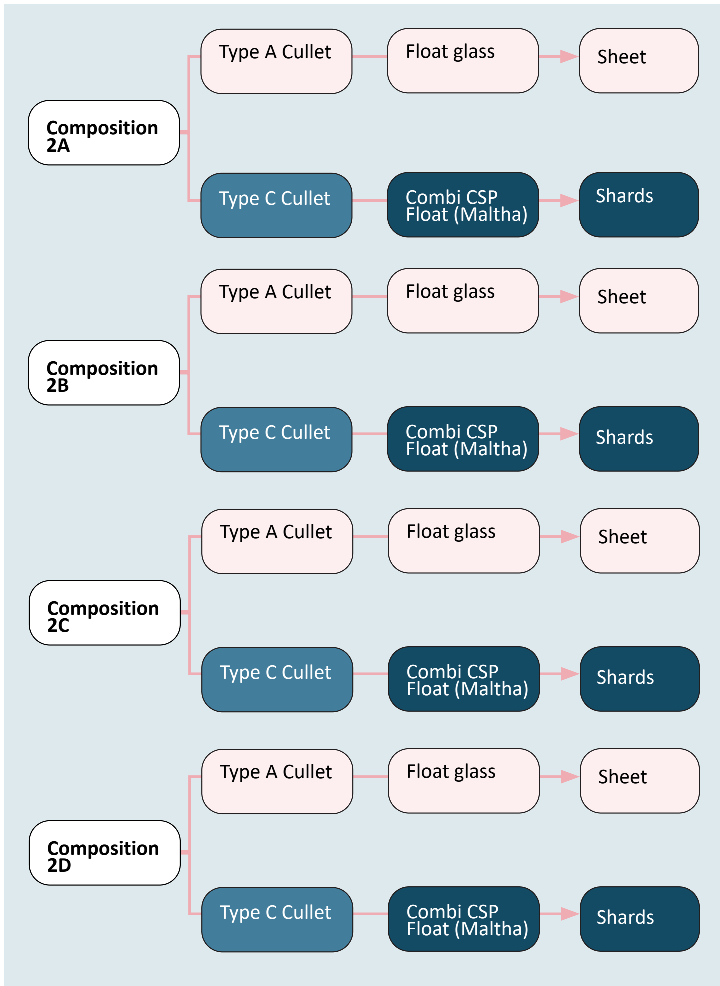

Figure 125: Illustratic overview of Fire Round 2C

Figure 126: Fire Round 2C placed in the oven

9.2.2 Feasibility evaluation - Fire Round 2C

- Composite beams: Surface 6 mm and Bulk 15 mm (Figure 127)
- Composite beams: Surface 8 mm and Bulk 13 mm (Figure 128)
- Composite beams: Surface 10 mm and Bulk 11 mm (Figure 129)
- Composite beams: Surface 20 mm and Bulk 9 mm (Figure 130)

From the eight beams created for Fire Round 2C, one beam, V-2C-C8-C-1, failed due to a machining error during polishing. The beam contained an inclusion that was exposed during grinding, causing it to break immediately.

It was anticipated that the compositions' homogeneity would be higher and that the surface and bulk layers would mix more compared to Fire Rounds 2A, 2B, and 2D.

A noteworthy finding in every beam was the significant mould reaction, which was more pronounced than in earlier fire rounds (Experiment Type 2). It is hypothesised that mould reactions become more reactive at higher temperatures. Another effect of the high temperature was the appearance of tiny surface cracks on the beams. For instance, Beam V-2C-C8-C-1 exhibited serious cracks in the middle.

The beams with the 10 mm Float glass were particularly interesting. This type of Float glass showed many trapped bubbles beneath the surface, forming a pattern visible in Figure 131. Microscopic examination revealed that the 10 mm Float glass had numerous tiny spaces on its surface. The creation of microcracks and trapped bubbles beneath the surface is attributed to a different material composition, as confirmed by an XRF test.

Based on validation, Beams V-2C-C6-C-1, V-2C-C6-C-2, and V-2C-C12-C-1 had the highest structural feasibility scores overall.

Table 36 provides an overview of the feasibility validations of the beams from Fire Round 2C.

Composite beams: Surface: Float 6 mm, Bulk: CSP | *Composite beams: Surface: Float 8 mm, Bulk: CSP*

	Beam V-2C-C6-C-1	**Beam V-2C-C6-C-2**	**Beam V-2C-C8-C-1**
	Material characteristics	**Material characteristics**	**Material characteristics**
The product:	Float glass + Combi CSP Float (Maltha)	Float glass + Combi CSP Float (Maltha)	Float glass + Combi CSP Float (Maltha)
Cullet grade:	Class A + Class C	Class A + Class C	Class A + Class C
Contamination:	Float glass + CSP Pollutants	Float glass + CSP Pollutants	Float glass + CSP Pollutants
Cullet Type:	Sheet + Small shards	Sheet + Small shards	Sheet + Small shards
Forming temperature:	1070 °C and 1120°C	1070 °C and 1120°C	1070 °C and 1120°C

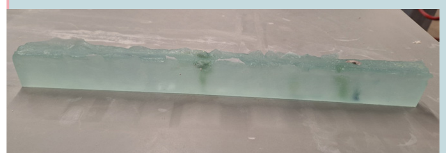
(a)

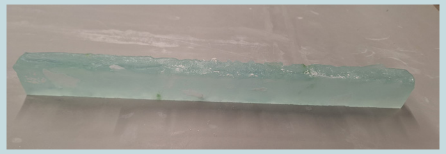
(b)

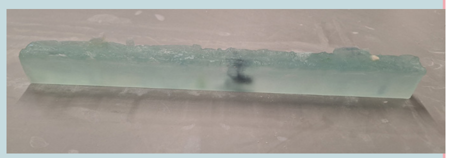
(a)

	Feasibility characteristics	**Feasibility characteristics**	**Feasibility characteristics**
Compatibility:	high	high	high
Transparency:	translucent	translucent	translucent
Mould reaction:	present	absent	present
Cracks presence:	absent	present	present
Breakage:	absent	absent	present
Bubbles level:	low	low	low
Structural performance:	succeeded	succeeded	failed

Figure 127: Feasibility validation of Fire Round 2C, (a) Beam V-2C-C6-C-1 and (b) Beam V-2C-C6-C-2

Composite beams: Surface: Float 10 mm, Bulk: CSP

	Beam V-2C-C8-C-2	**Beam V-2C-C10-C-1**	**Beam V-2C-C10-C-2**
	Material characteristics	**Material characteristics**	**Material characteristics**
The product:	Float glass + Combi CSP Float (Maltha)	Float glass + Combi CSP Float (Maltha)	Float glass + Combi CSP Float (Maltha)
Cullet grade:	Class A + Class C	Class A + Class C	Class B + Class C
Contamination:	Float glass + CSP Pollutants	Float glass + CSP Pollutants	Float glass + CSP Pollutants
Cullet Type:	Sheet + Small shards	Sheet + Small shards	Sheet + Small shards
Forming temperature:	1070 °C and 1120°C	1070 °C and 1120°C	1070 °C and 1120°C


(b)

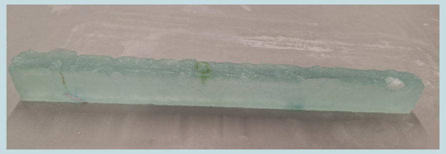
(a)

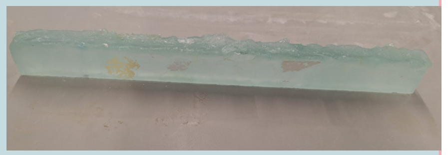
(b)

	Feasibility characteristics	**Feasibility characteristics**	**Feasibility characteristics**
Compatibility:	high	medium	medium
Transparency:	translucent	translucent	translucent
Mould reaction:	absent	present	present
Cracks presence:	present	present	present
Breakage:	absent	absent	absent
Bubbles level:	medium	high	high
Structural performance:	succeeded	succeeded	succeeded

Figure 128: Feasibility validation of Fire Round 2C, (a) Beam V-2C-C-C8-1 and (b) Beam V-2C-C8-C-2

Figure 129: Feasibility validation of Fire Round 2C, (a) Beam V-2C-C10-C-1 and (b) Beam V-2C-C10-C-2

Composite beams: Surface: Float 12 mm, Bulk: CSP

	Beam V-2C-C12-C-1	**Beam V-2C-C12-C-2**
	Material characteristics	**Material characteristics**
The product:	Float glass + Combi CSP Float (Maltha)	Float glass + Combi CSP Float (Maltha)
Cullet grade:	Class B + Class C	Class B + Class C
Contamination:	Float glass + CSP Pollutants	Float glass + CSP Pollutants
Cullet Type:	Sheet + Small shards	Sheet + Small shards
Forming temperature:	1070 °C and 1120°C	1070 °C and 1120°C

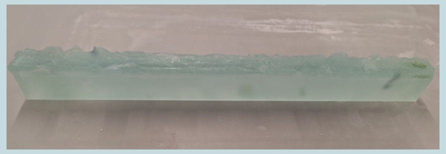
(a)

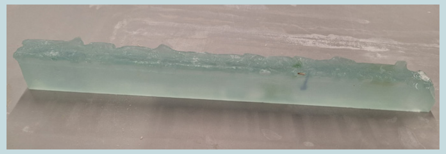
(b)

	Feasibiliy characteristics	**Feasibility characteristics**
Compatibility:	high	high
Transparency:	translucent	translucent
Mould reaction:	present	present
Cracks presence:	absent	present
Breakage:	absent	present
Bubbles level:	low	low
Structural performance:	succeeded	succeeded

Figure 130: Feasibility validation of Fire Round 2C, (a) Beam V-2C-C12-C-1 and (b) Beam V-2C-C12-C-2

Beam information						Feasibility characteristics						
Beam Name	The product	Cullet grade	Contamination	Cullet type	Forming temperature	Compatibility	Transparency	Mould reaction	Cracks	Breakage	Bubbles level	Structural performance
Composite beams - Ratios - Influence of temperature												
V-2C-C6-C-1	Float glass 6 mm + Combi CSP Float (Maltha)	Class A + Class C	Float glass + CSP Pollutants	Sheet + Small Shards	1070 °C + 1070 °C	+++	++	++	+++	+++	+++	+++
V-2C-C6-C-2	Float glass 6 mm + Combi CSP Float (Maltha)	Class A + Class C	Float glass + CSP Pollutants	Sheet + Small Shards	1070 °C + 1070 °C	+++	++	+++	++	+++	+++	+++
V-2C-C8-C-1	Float glass 8 mm + Combi CSP Float (Maltha)	Class A + Class C	Float glass + CSP Pollutants	Sheet + Small Shards	1070 °C + 1070 °C	+++	++	++	-	-	+++	-
V-2C-C8-C-2	Float glass 8 mm + Combi CSP Float (Maltha)	Class A + Class C	Float glass + CSP Pollutants	Sheet + Small Shards	1070 °C + 1070 °C	+++	++	+++	++	+++	++	+++
V-2C-C10-C-1	Float glass 10 mm + Combi CSP Float (Maltha)	Class A + Class C	Float glass + CSP Pollutants	Sheet + Small Shards	1070 °C + 1070 °C	++	++	++	++	+++	+	+++
V-2C-C10-C21	Float glass 10 mm + Combi CSP Float (Maltha)	Class A + Class C	Float glass + CSP Pollutants	Sheet + Small Shards	1070 °C + 1070 °C	++	++	+	++	+++	+	+++
V-2C-C12-C-1	Float glass 12 mm + Combi CSP Float (Maltha)	Class A + Class C	Float glass + CSP Pollutants	Sheet + Small Shards	1070 °C + 1070 °C	+++	++	++	+++	+++	+++	+++
V-2C-C12-C-2	Float glass 12 mm + Combi CSP Float (Maltha)	Class A + Class C	Float glass + CSP Pollutants	Sheet + Small Shards	1070 °C + 1070 °C	+++	++	+++	+++	+	+++	+++

Table 36: Overview feasibility validation of Fire Round 2C

Structural feasibility - Influence of a higher temperature schedule

The structural feasibility is divided into seven categories. For each category, the influence of a higher temperature schedule compared to a standard 1070-degree temperature schedule will be explained. These comparisons are made using the overview in Tables 16 and 36.

Compatibility: This category examines how the cullets interact/ interfere with each other and with the surface (Float glass). There is barely any difference between the two temperature schedules, both showing good compatibility. To determine if compatibility has indeed increased, microscopic research will be conducted. If the cullets interact more effectively with each other, there should be fewer infolds and bubbles on the surface. This will be further discussed in paragraph 9.2.4, "Microscopic validation of Fire Round 2C."

Transparency: Both the beams with the 1070 degrees temperature schedule and the higher temperature schedule show translucency for all the beams.

Mould reaction: The beams produced with a higher temperature schedule show more mould reaction.

Cracks: Less beams contained cracks for the higher temperature schedule compared with the lower temperature schedule. However the beams with the 10 mm Float glass beam V-2C-C10-C-1 and beam V-2C-C10-C-2 seem to contain many microcracks under the Float glass. This needed to be further investigated under the microscope. This will further explained in section 9.2.4. Beam V-2C-C8-C-1 contained severe cracks in the middle, which led to its breakage.

Breakage: During Fire Round 2C, one beam broke, beam V-2C-C-C-3. This beam broke during the polishing process. Furthermore one beam contains some breakage at the compression zone, beam V-2C-C12-C-2. At the lower temperature schedule more beams contained breakages

Bubbles level: In general the bubbles level is for all the beams quit similar. With the exception of the beams with the 10 mm Float glass during Fire round 2C. These beams seems to have a lot trapped air bubbles under the surface.

Structural performance: The beams produced during Fire Round 2C seem to have a higher feasibility for structural performance than the beams with a lower temperature schedule (Fire Round 2A, 2B and 2D)

9.2.3 Structural performance - Fire Round 2C

General overview

- **Cullet Type A** (dark pink): Homogeneous beams with Float glass (specimens 4.1-4.3)
- **Composite beams** (dark blue): Composite beams with 12 mm Float glass and 9 mm bulk material with CSP Pollutants (specimens 2.6 and 2.7)
- **Composite beams** (light blue): Composite beams with 10 mm Float glass and 11 mm bulk material with CSP Pollutants (specimens 2.4 and 2.5
- **Composite beams** (blue): Composite beams with 8 mm Float glass and 13 mm bulk material with CSP Pollutants (specimen 2.3)
- **Composite beams** (lightest blue): Composite beams with 6 mm Float glass and 15 mm bulk material with CSP Pollutants (specimens 2.1 and 2.2)
- **Cullet Type C** (light pink): Homogeneous beams with CSP Pollutants (specimens 1.1 and 1.2)

In Chapter 7: Mechanical tests, the expected curve for the relationship between composite and homogeneous beams was introduced (Graph 07). Subsequently, the actual relationship between composite beams with CSP pollutants in the bulk and Float glass on the surface, and homogeneous beams containing CSP pollutants, was presented (Graph 08).

The following graph, Graph 22, shows the relationship between composite beams with CSP pollutants in the bulk and Float glass on the surface, and homogeneous beams with CSP pollutants. In this case, the composite beams were made with a higher temperature schedule, as discussed earlier. As in Graph 08, homogeneous beams with Float glass are also included in Graph 22 to visualise the relationship between the higher temperature composite beams and the homogeneous beams with Float glass. The shape of the curve in Graph 22 is more comparable to the expected curve in Graph 07.

The following conclusions can already made with the help of Graph 22.

The following conclusions can already be drawn from Graph 22. Homogeneous beams containing Float glass perform slightly better than the other types in this comparison. Composite beams with 12 mm, 8 mm, and 6 mm Float glass show similar results in the structural performance test, all outperforming homogeneous beams with CSP pollutants. Since composite beams with 6 mm Float glass perform similarly to those with 12 mm Float glass, it is more sustainable to choose the 6 mm Float glass composite beams. This allows for more Class Cullet C to be used in the bulk, meaning that more material can be recycled.

Lastly, the composition with 10 mm Float glass performs the worst, particularly beam V-2C-C10-C-2. This beam even performs worse than the homogeneous beams with CSP pollutants. As noted in the structural feasibility overview, beams containing 10 mm Float glass have many trapped bubbles and micro cracks beneath the surface. These surface flaws significantly reduce the overall structural performance.

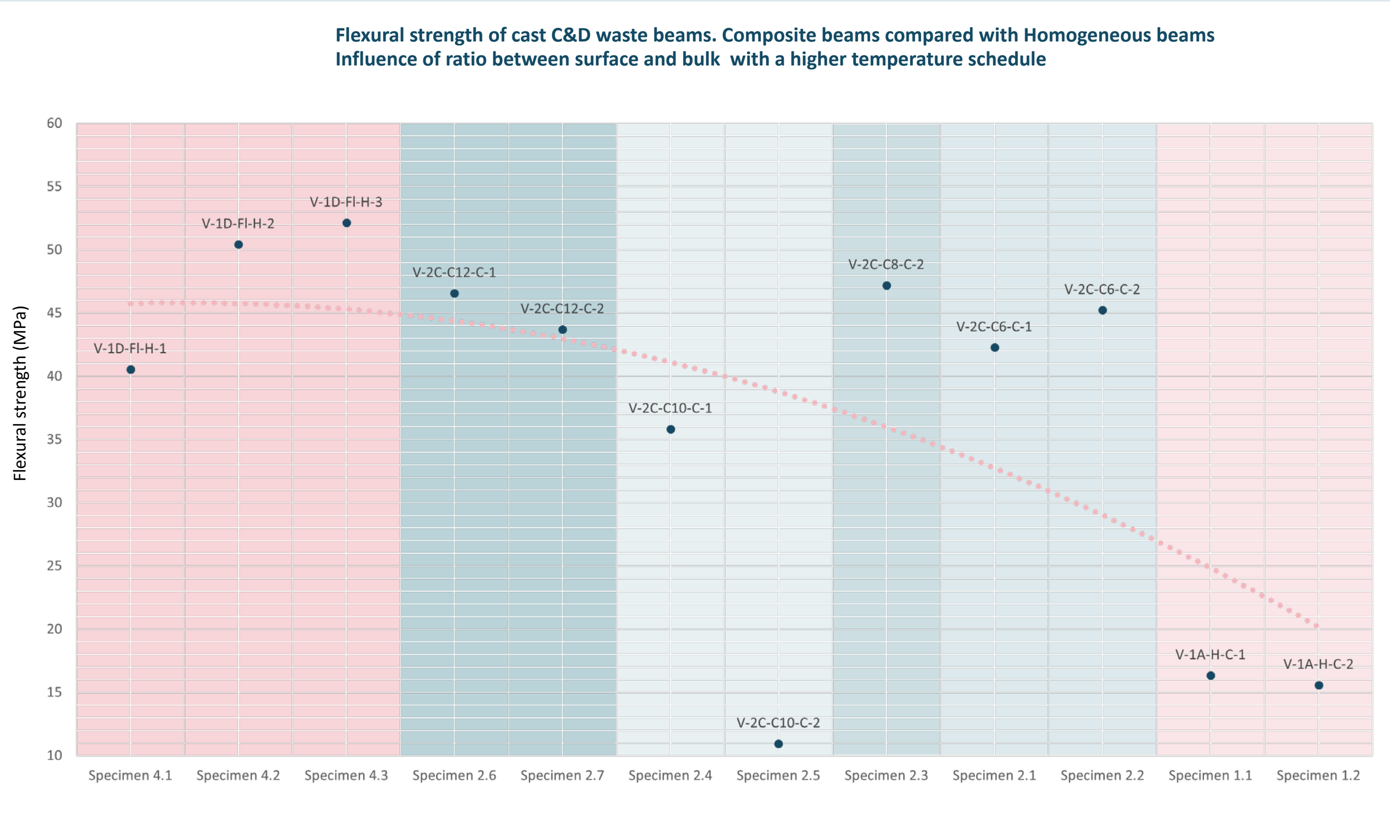

Graph 22: Relationship between homogeneous beams and composite beams with a higher temperature schedule

Experiment type 1:
Homogeneous beams
Glass with A cullet
Float glass V-1D-H-Fl-1, V-1D-H-Fl-2 and V-1D-H-Fl-3
Glass with C cullet
CSP V-1A-H-C-1 and V-1A-H-C-2

Experiment type 2:
Composite beams: Surface + Bulk
Float glass + CSP pollutants

6 mm + 15 mm	V-2C-C6-C-1 and V-2C-C6-C-2
8 mm + 13 mm	V-2C-C8-C-2
10 mm + 11 mm	V-2C-C10-C-1 and V-2C-C10-C-2
12 mm + 9 mm	V-2C-C12-C-1 and V-2C-C12-C-2

Influence of a higher temperature schedule

To understand the influence of a higher temperature schedule, a separate graph is shown for each material composition in Experiment Type 2, comparing the standard 1070-degree schedule with the higher temperature schedule.

Graph 23 presents the comparison for composite beams containing 6 mm Float glass. Similarly, Graph 24 illustrates the performance of beams with 8 mm Float glass. For the composite beams with 10 mm Float glass, see Graph 25. Lastly, Graph 26 showcases the comparison for beams containing 12 mm Float glass.

- In terms of flexural strength, Graph 23 demonstrates that there are hardly any variations between the composite compositions with 6 mm Float glass as surface material.
- The summary for the 8 mm surface material compositions is displayed in Graph 24. Since only one beam with an 8 mm composition passed the structural feasibility test, no definitive conclusions can be drawn from this graph. This result appears to be invalid.
- The results for the 10 mm Float glass in Fire Round 2C appear to be somewhat inconsistent (Graph 25). The difference between V-2C-C10-C-1 and V-2C-C10-C-2 is too significant to draw reliable conclusions. Due to this discrepancy, it is difficult to compare these results with those of the 10 mm compositions under the 1070-degree temperature schedule.
- The beams with 12 mm Float glass generally exhibit similar results, with the exception of beam V-2D-C12-C-3, which shows significantly lower flexural strength compared to the other 12 mm compositions. As noted in Appendix G, this beam had a severe edge flaw (see Table 34). Comparing these beams to those in Fire Round 2C, they generally perform slightly worse than beams V-2D-C12-C-1 and V-2D-C12-C-2.

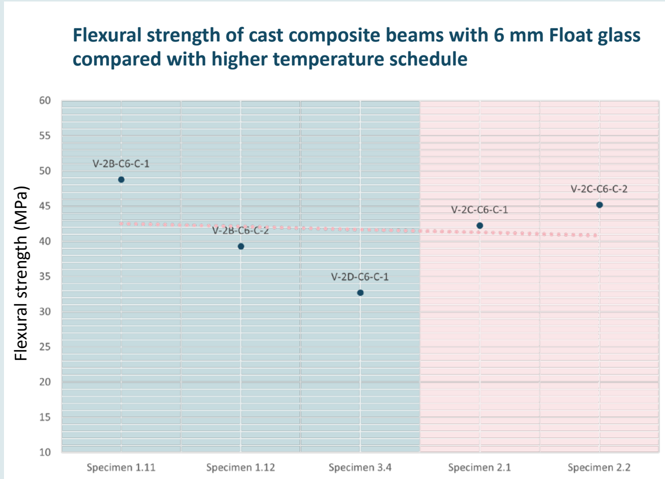

Graph 23: Relationship between a composite with 6 mm Float glass (1070 degrees) 6 mm Float glass with a higher temperature schedule

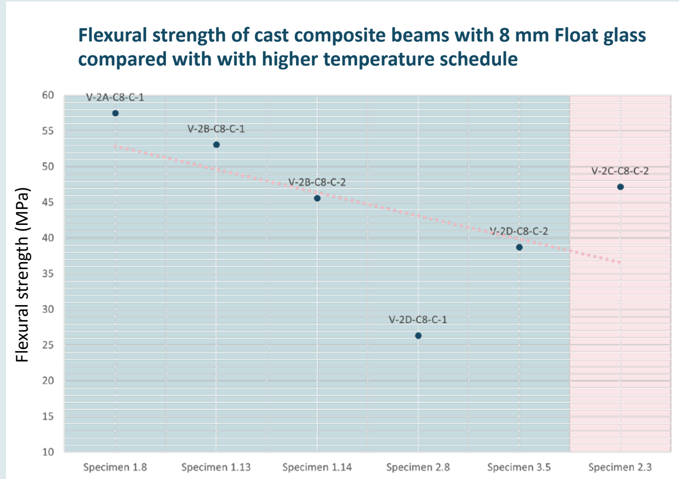

Graph 24: Relationship between a composite with 8 mm Float glass (1070 degrees) 8 mm Float glass with a higher temperature schedule

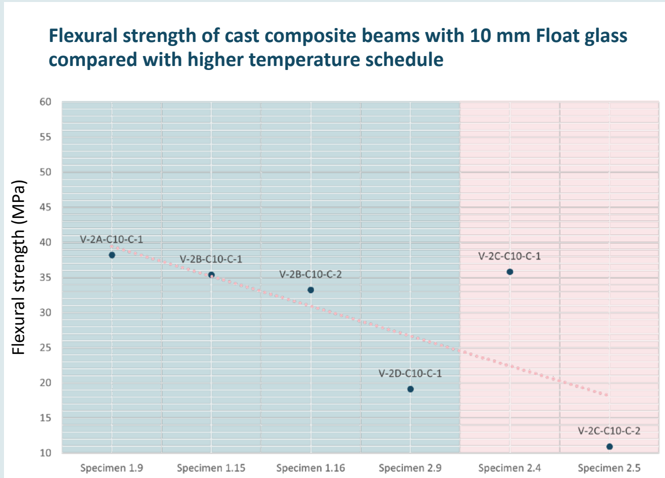

Graph 25: Relationship between a composite with 10 mm Float glass (1070 degrees) 10 mm Float glass with a higher temperature schedule

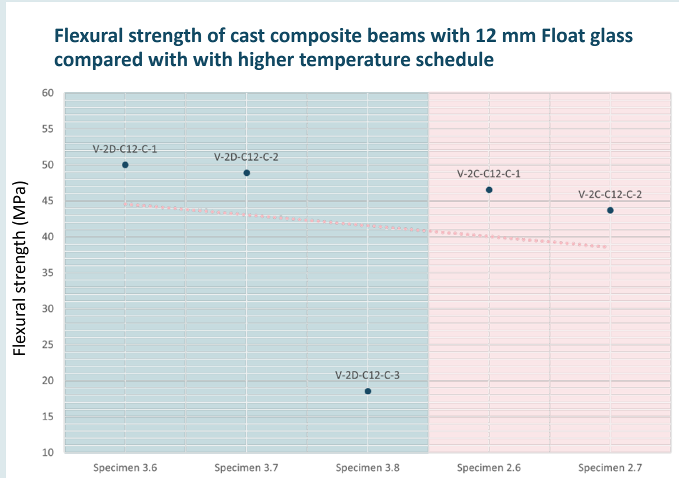

Graph 26: Relationship between a composite with 12 mm Float glass (1070 degrees) 12 mm Float glass with a higher temperature schedule

Experiment type 2: 1070 temperature schedule
Composite beams: Surface + Bulk
Float glass + CSP pollutants

6 mm + 15 mm	V-2B-C6-C-1,V-2B-C6-C-2 and V-2D-C6-C-1
8 mm + 13 mm	V-2A-C8-C-1, V-2B-C8-C-1, V-2B-C8-C-2, V-2D-C8-C-1 and V-2D-C8-C-2
10 mm + 11 mm	V-2A-C10-C-1, V-2B-C10-C-1, V-2B-C10-C-2, and V-2D-C10-C-1
12 mm + 9 mm	V-2D-C12-C-1, V-2D-C12-C-2 and V-2D-C12-C-3

Experiment type 2: Higher temperature schedule
Composite beams: Surface + Bulk
Float glass + CSP pollutants

6 mm + 15 mm	V-2C-C6-C-1 and V-2C-C6-C-2
8 mm + 13 mm	V-2C-C8-C-2
10 mm + 11 mm	V-2C-C10-C-1 and V-2C-C10-C-2
12 mm + 9 mm	V-2C-C12-C-1 and V-2C-C12-C-2

9.2.4 Microscopic validation of Fire Round 2C

To better understand the structural feasibility and mechanical behaviour results of the four-point bending test, microscopic research was conducted. As previously mentioned, it was anticipated that beams from Fire Round 2C would exhibit fewer infolds because the cullets would interfere more effectively at higher temperatures.

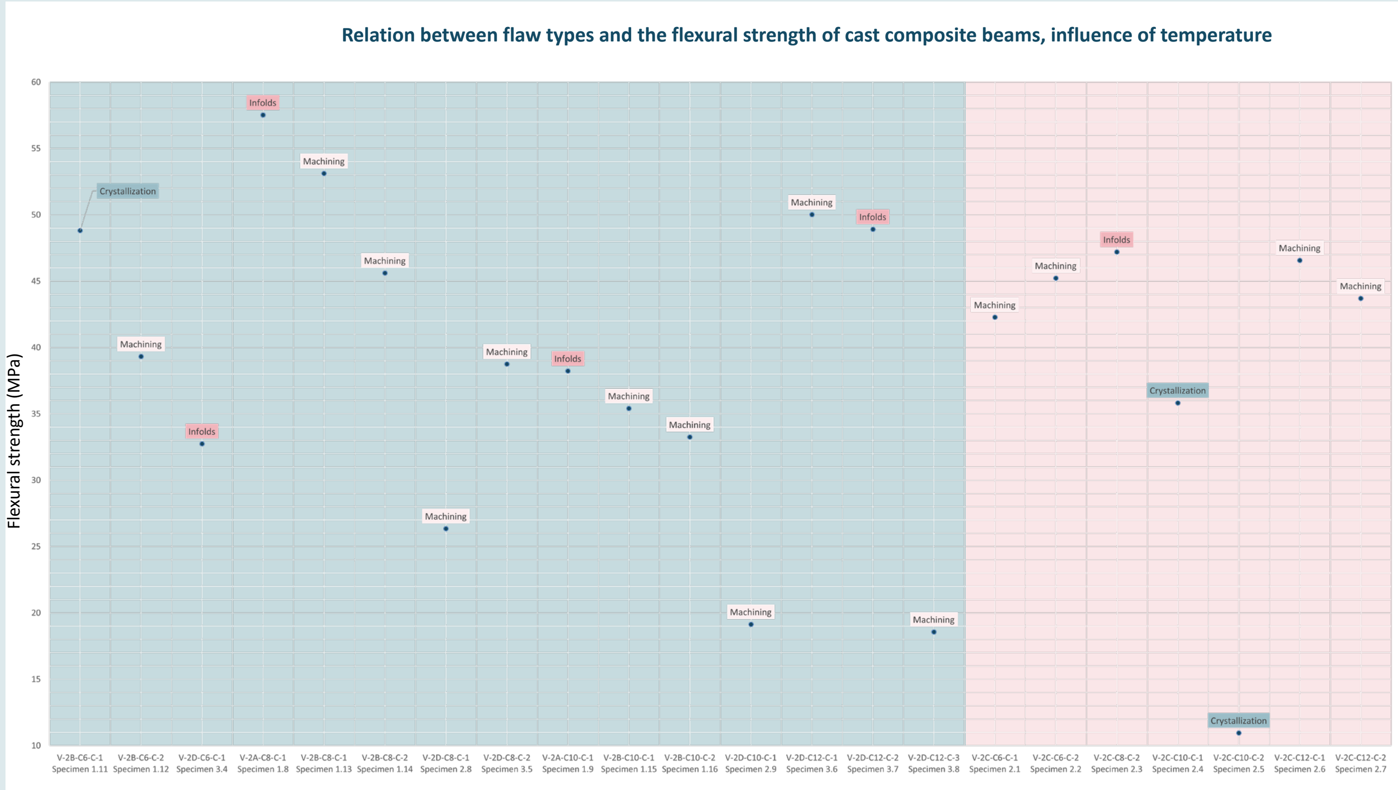

Graph 27: Flaw types compared with the structural performance of cast C&D beams, influence of temperature

Experiment type 2: 1070 temperature schedule (Blue)
Composite beams: Surface + Bulk
Float glass + CSP pollutants

6 mm + 15 mm	V-2B-C6-C-1,V-2B-C6-C-2 and V-2D-C6-C-1
8 mm + 13 mm	V-2A-C8-C-1, V-2B-C8-C-1, V-2B-C8-C-2, V-2D-C8-C-1 and V-2D-C8-C-2
10 mm + 11 mm	V-2A-C10-C-1, V-2B-C10-C-1, V-2B-C10-C-2, and V-2D-C10-C-1
12 mm + 9 mm	V-2D-C12-C-1, V-2D-C12-C-2 and V-2D-C12-C-3

Experiment type 2: Higher temperature schedule (Pink)
Composite beams: Surface + Bulk
Float glass + CSP pollutants

6 mm + 15 mm	V-2C-C6-C-1 and V-2C-C6-C-2
8 mm + 13 mm	V-2C-C8-C-2
10 mm + 11 mm	V-2C-C10-C-1 and V-2C-C10-C-2
12 mm + 9 mm	V-2C-C12-C-1 and V-2C-C12-C-2

Using a microscope, the beams were thoroughly examined to identify the types of flaws that could cause significant damage. Appendix G provides a comprehensive summary of all beams and the microscopic analysis conducted on them. Based on the insights from this chapter and Appendix G, Graph 27 was created. This graph provides an overview of flaw categories for Experiment Type 2 (1070 temperature schedule) compared to the higher temperature schedule.

Graph 27 illustrates that compatibility did indeed improve, as fewer composite beams exhibit infolds, indicating increased interference among cullets at higher temperatures. Additionally, the graph clearly shows that machining is the most prevalent flaw in composite beams. Finally, the graph highlights that surface crystallization significantly decreases structural performance.

Since beam V-2C-C10-C-2 exhibited the poorest performance overall, it was intriguing to investigate the defects and flaws that contributed to its subpar results. Figure 131 provides an overview of surface and microscopic images of this beam. During the structural feasibility tests, it was observed that the Float glass exhibited several surface flaws. There is localised crystallization between the cullets, resembling the glass has fractured into multiple pieces. Additionally, numerous black spots, indicative of trapped bubbles, are visible. The presence of elements such as MgO in the cast glass material compositions significantly influences these occurrences. Specifically, the 10 mm compositions contain less MgO than the others, making the effect more noticeable at this temperature.

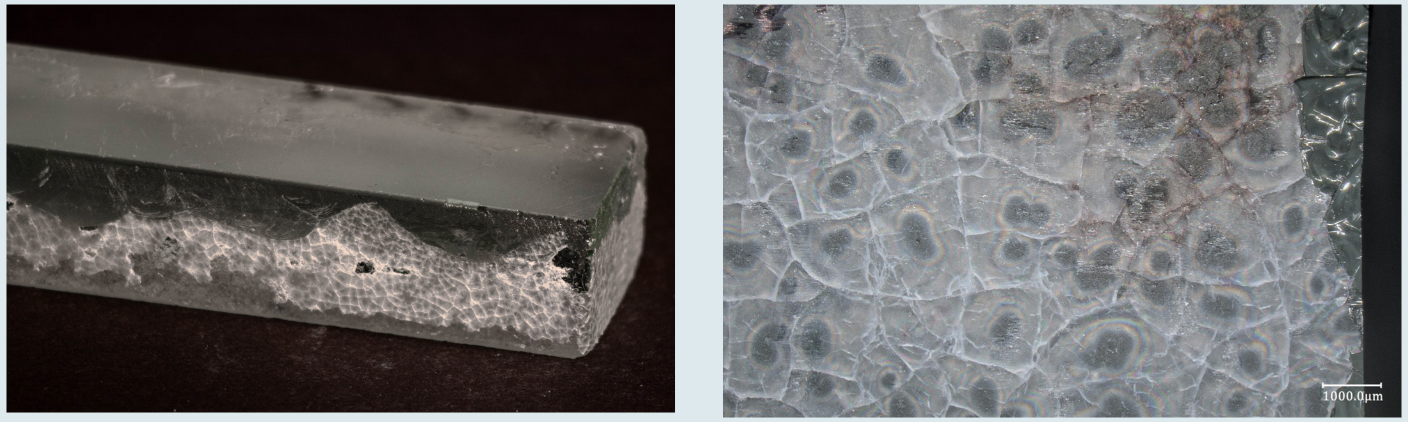

(a) (b)

Figure 131: Surface flaw analysis of beam V-2C-C10-C-2. (a) Overview surface and (b) Microscopic view

9.3 Discussion and conclusion

To optimise the mechanical behaviour of the cast glass composite beams and ensure fewer beams would fail during structural feasibility, two methods were applied. The first was to investigate the influence of specific pollutants, and the second was to explore the impact of a higher temperature schedule, aiming to achieve a more beams with a higher compatibility.

Influence of cullet selection

- To better understand the outcomes of the cast glass beams, the compositions were refined by focusing on a single type of pollutant instead of multiple. In Experiment 2, only cullets with CSP pollutants were used, and all others were removed. In Experiment 3, only cullets with metallic pollutants were used, and the rest were removed.
- Because the silicone and ceramic impurities were removed, less beams contained cracks and severe breakage. However removing these pollutants is a difficult task. So on a bigger scale this will cause logistical problems.

Tiles containing specific pollutants are manufactured to study internal stresses and their impact on structural feasibility.

- White traces are the result of silicones converting to silica. These regions have modest to moderate levels of localised stress.
- When metallic contaminants come into contact with mould, the metal "eats" the mould. Furthermore, the metallic pollutants melted and began to interact with the glass. The area around these particles have some noticeable stress.
- Both yellow tinted and dark tinted glass demonstrates that the colour does not noticeably affect the tiles. The dark tinted glass exhibits slightly more internal stress compared to the yellow tinted glass.
- The plastic has completely disappeared from the tiles, indicating that these pollutants do not affect the beams. Minimal internal stresses are localised in this area.
- The mirror on the cullets, turned blue (meaning that it contains Copper). It shows some internal stresses.

Influence of a higher temperature schedule

- A higher temperature schedule results in more mould reaction between the glass and the mould
- Composite beams with 6 mm, 8 mm, and 12 mm Float glass demonstrate similar flexural strength results at this higher temperature schedule.
- There is minimal difference in flexural strength between composite beams with 6 mm and 12 mm Float glass surfaces at 1070 degrees and those at a higher temperature schedule.
- A higher temperature schedule resulted in an increased presence of trapped bubbles in the 10 mm Float glass compositions. These beams exhibit numerous surface flaws that diminish their structural performance.
- In terms of flaw categories, beams created using a higher temperature schedule show fewer infolds, indicating improved compatibility.

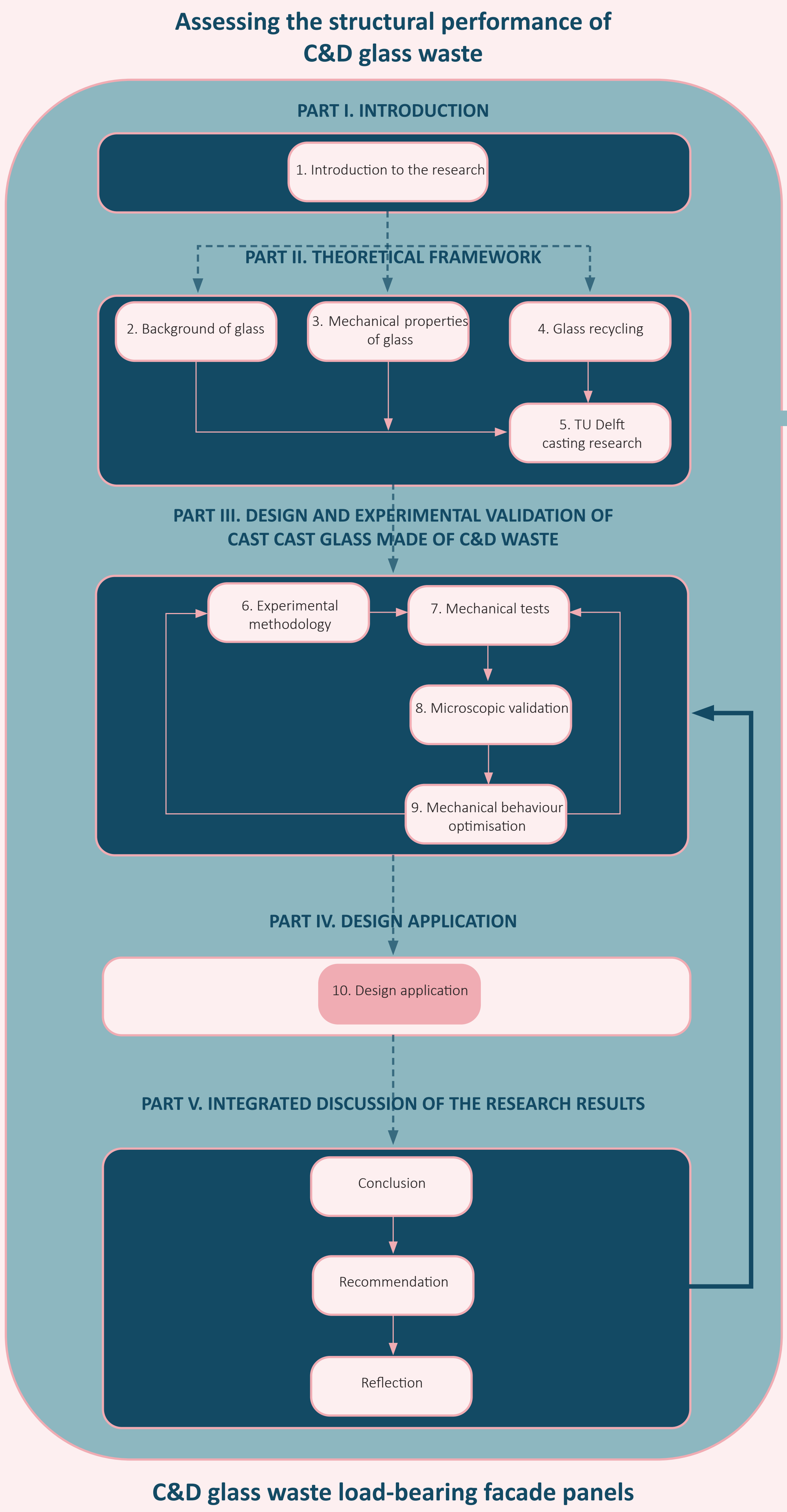

PART 4

DESIGN APPLICATION

10 | DESIGN APPLICATION

10.1 Introduction to the design application

The majority of glass used in the built environment ends up in landfills in our contemporary economy. However, with the help of modern technologies, we may strive to meet EU requirements and increase the amount and quality of glass recycling. Glass companies have set goals to become carbon neutral by 2050 (Rijksoverheid, 2023a, 2023b; Schuttelaar & Partners, 2018). However, obstacles like logitsics, different glass compositions, and degradation of thin-walled glass products during recycling still need to be addressed (Bristogianni & Oikonomopoulou, 2010). It is clear that circularity is essential to the manufacture of glass. Reusing post-consumer glass shows promise, especially when it comes to high-quality surfaces (Rota et al., 2023). as previously discussed in this thesis's literature.

Glass is completely recyclable in theory, but its widespread usage in construction is limited by difficult disassembly processes and adhesive and coating contamination. Furthermore, most facilities only handle container glass, leaving Float glass in need of proper infrastructure for collection and treatment. Although glass may be recycled indefinitely in theory without losing quality, this is not always the case in practice. Recyclers mostly come from specialised businesses and only a tiny portion gets recycled. Because cast glass units can handle greater impurities and use waste glass as a raw material, they provide a solution (Bristogianni et al., 2019). With the help of this innovative technology, we can recycle glass that has been contaminated while still using it, preventing the majority of building and demolition debris from ending up in landfills.

10.1.1 Introduction to the case study

Nowadays architectural claddings for facades are made of plastics and concrete. Producing these panels generates a significant amount of CO2, and they ultimately end up in landfills. This is problematic, as the volume of C&D waste in landfills continues to grow with the use of these panels. Additionally, these panels are made from raw materials, and recycling is not currently implemented.

Trespa is the firm selected for the case study. For more than 60 years, Trespa® products have been used by architects and builders worldwide in a wide range of construction projects, from apartment buildings to private homes. Most cladding panels today are made from Trespa (panels of resin, glue, and fibers pressed together) or Ethernit (concrete panels).

10.1.2 Introduction to the Recycled Composite Cast Glass Panels made of C&D waste

For these reasons, there is a pressing need to develop more sustainable cladding materials that reduce landfill waste, minimise CO2 emissions, and eliminate the need for raw materials.

Recycled Composite Cast Glass Panels made from C&D waste offer a compelling solution, especially considering the widespread use of Trespa cladding in various structures. These innovative panels can effectively replace traditional claddings.

Unlike Trespa and Eternit panels, which contribute to increasing C&D waste and require raw materials with high CO2 production costs, Recycled Composite Panels help alleviate C&D waste issues. These panels are crafted entirely from 100% recycled materials and are fully recyclable themselves. Moreover, their substructure, whether metal or wood, can be easily replaced, ensuring the panels remain truly eco-friendly.

10.2 The design application

10.2.1 Design principle

The recycled composite panel is made of C&D and when the panel is not longer used it can be recycled into another product. The goal with this application was to use a closed loop methodology. based on the structural performance of the recycled cast glass beams and experimental study conducted at the departments of Mechanical and Civil engineering. The panels will feature a structure comprising a purer cullet layer on the surface and a layer with more impurities within the bulk, as depicted in Figure 40. This will form a three-layered system: surface - bulk - surface. The outermost surface will have a slightly thicker glass layer compared to the inner surface.

10.2.2 Manufacturing of the panels

With the aim of utilising the casting process, this cladding panel has been developed using glass waste sourced from the building and demolition industry.

In the initial research, disposable moulds were employed, but for larger-scale production, permanent moulds will be created to expedite panel manufacturing. The first step in this process is the creation of permanent moulds.

For this thesis and subsequent research, a single panel (350 x 350 mm) was created using a silica plaster mould.

The following steps outline the manufacturing process for this panel (see Figure 132):

1. **Mould creation**: The first step involves creating the mould.
2. **Placement of surface layer:** Next, an 8 mm thick Float glass surface layer is placed in the mould, ensuring a small offset of 5 mm to facilitate fitting.
3. Cullet placement: An 8 mm layer of cullets, including class C cullets, is then placed.
4. Placement of top surface: Finally, a 6 mm thick Float glass top surface is placed.
5. After assembly, the panel is placed in the oven.

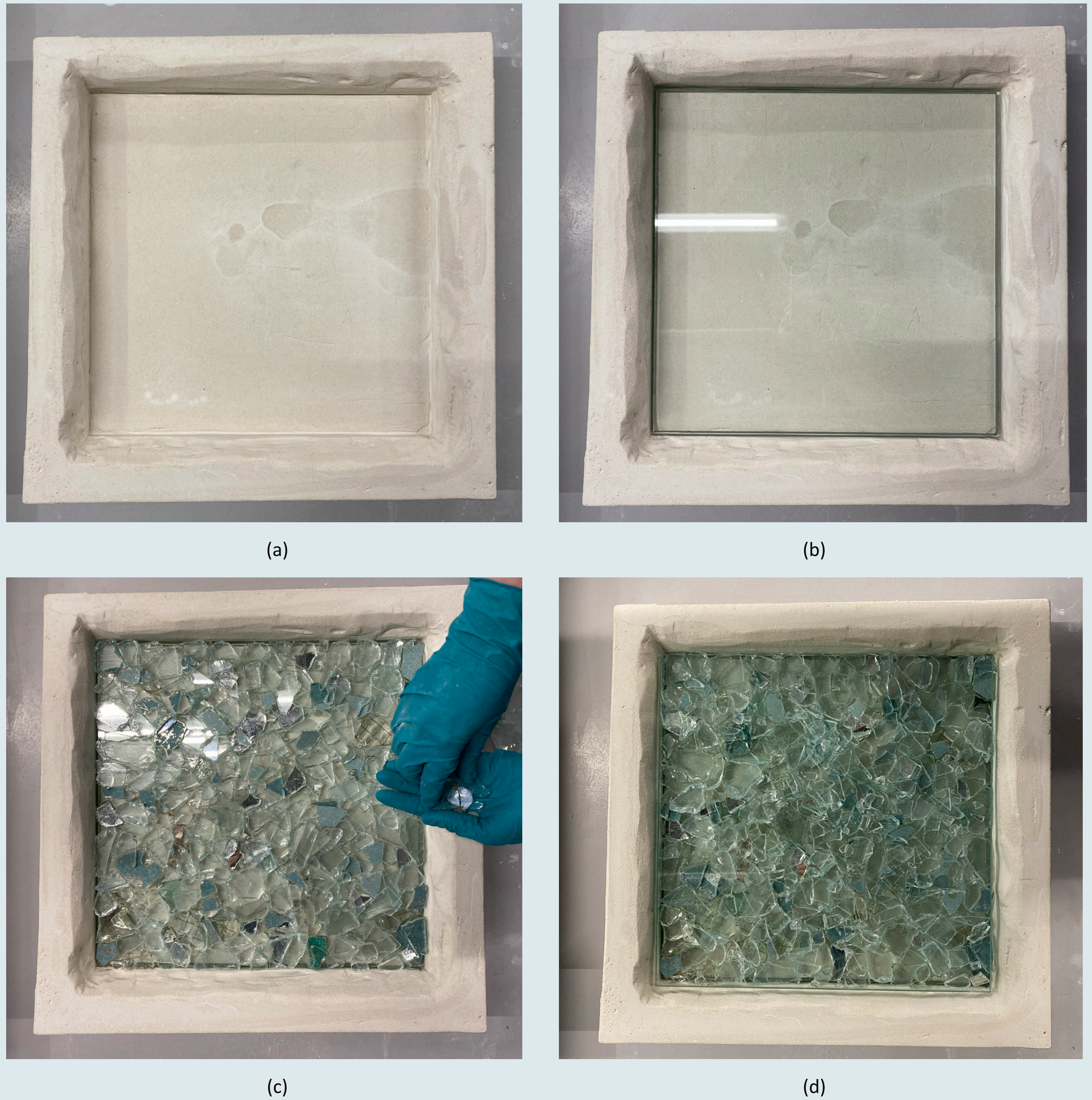

Figure 132: Manufacturing steps of the recycled composite cast glass panel. (a) Mould, (b) Placement of the surface, (c) Placement of the cullets and (d) placement of the top surface

10 | DESIGN APPLICATION

The production of these panels presents logistical challenges. Each panel requires 100 hours at 1070 degrees Celsius, making it a lengthy and intensive process that must be carefully planned logistically. When scaling up production, it's essential to determine the size of ovens needed.

Permanent moulds offer the advantage of minimising post-processing requirements, which significantly reduces production time. This contrasts with the time-consuming tasks involved in creating beams during this research phase.

10.2.3 Aesthetics of the panels

The primary aim of this project was to develop recycled components suitable for building façades. These components offer similar capabilities to regular Float glass but provide a more recyclable and translucent alternative suitable for a wider range of outdoor applications. It's important to note that the appearance of this glass differs significantly. Instead of being transparent, it becomes translucent and exhibits colour streaks due to varying compositions.

While the idea of transparent cladding is appealing, it isn't practical. The reality is that we must increase recycling of C&D waste to align with EU goals. Each panel will have a unique appearance because the material compositions, influenced by varying ratios of contaminants, result in distinctive patterns that foster imaginative designs (Figure 133 and Figure 134).

Due to its unique properties, heavily influenced by the diverse composition of cullet placed in the central layer of the composite, no two panels are alike. The mixed cullet yields distinctive colour properties, creating an intriguing visual effect. Uneven cullet distribution contribute to allow light to pass through these translucent panels. Recycled glass, being less transparent than Float glass, effectively disperses light across spaces.

10.2.4 Connections and details

This innovative glass panel opens up intriguing possibilities for building applications. The glass façade panels come in various sizes, including strips and rectangles, and can also vary in thickness. However, focusing on achieving the maximum possible thickness for the cladding would enable greater recycling of materials, contributing to the reduction of enormous landfill volumes generated by the building and demolition industry.

Currently, the panels are targeted to have a thickness of around 2 cm, but exploring thicker options is feasible. Concrete panels, for instance, can be as thick as 10 cm, suggesting that similar thicknesses could be achieved for glass panels with appropriate substructures. This approach aims to significantly reduce landfill contributions from the construction sector.

One of the advantages of these panels is that new details are not necessary; the existing connections for Trespa and Eternit can be used for these panels (Figure 135 and Figure 136). There should not be any screws in the cladding

(a) (b)

Figure 133: From Eternit facade panels to recycled glass panels. (a) Building with Eternit panels, (b) Building with recycled composite panels

Figure 134: Render of Recycled composite panels on a building

where it connects to the load-bearing part. Instead, it should be attached to the rear of the component. Blind connections are problematic for Trespa panels because they require more material, leading to higher CO2 production costs and more waste. However, for the Reycled Composite panels, a blind connection is not an issue at all. This allows the panels to be made thicker, meaning more glass waste is recycled (Figure 137).

Other potential connections could involve using a clamp on the outer edge of the entire panel (Figure 138a and Figure 138c)or embedding the clamp into the bulk layer for a few centimetres (Figure 138b). Creating this groove is straightforward using a diamond saw to make a small cut in the panel.

The glass used for the facade panels is exceptionally weather-resistant and durable. These panels are also easily replaceable and recyclable for making new facade panels. Further research is needed to ensure safety measures, but potential ideas include using lamination. Previous tests indicated that plastic completely melts without showing internal stresses under a microscope, making it recyclable for reapplication in laminations. Another method could involve chemical treatment of the panels, with a maximum thickness of 2 cm.

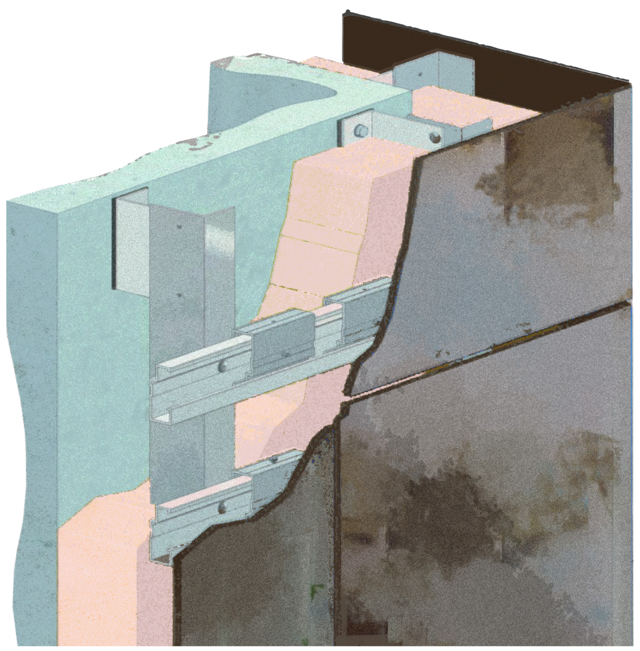

Figure 135: 3D image of the connection of the Recycled Composite panel

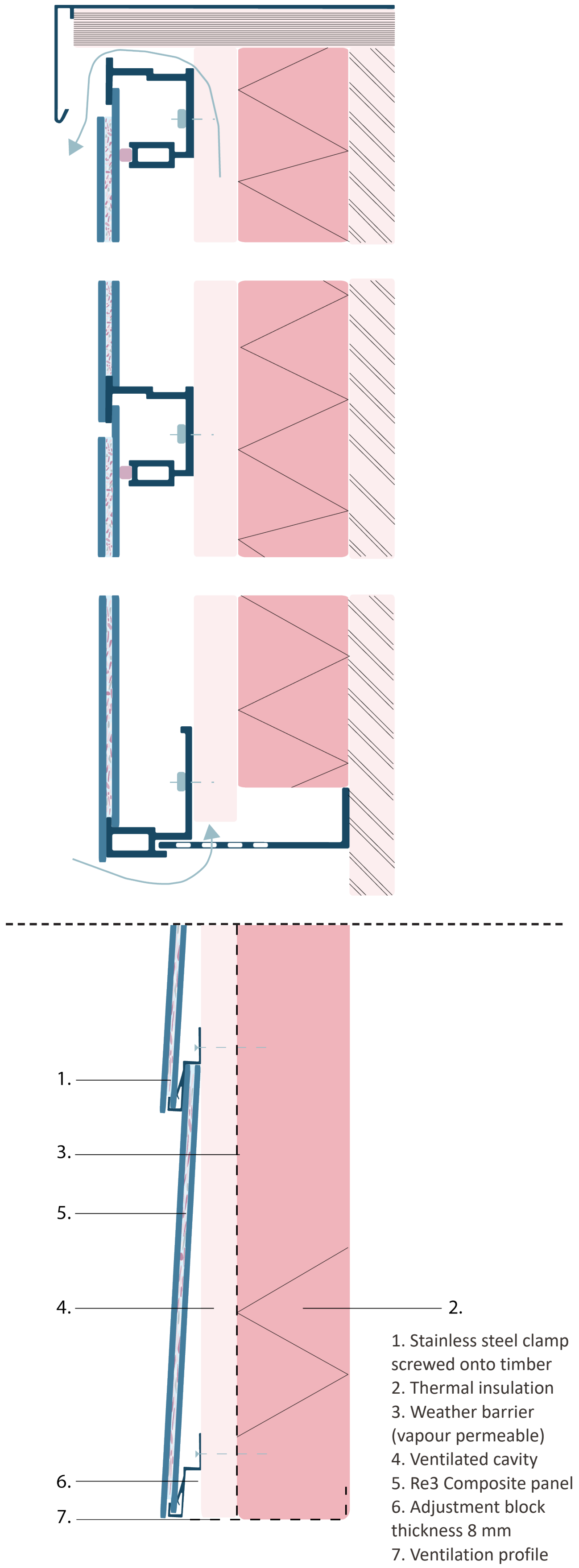

Figure 136: Connection methods for the Recycled Composite Panels

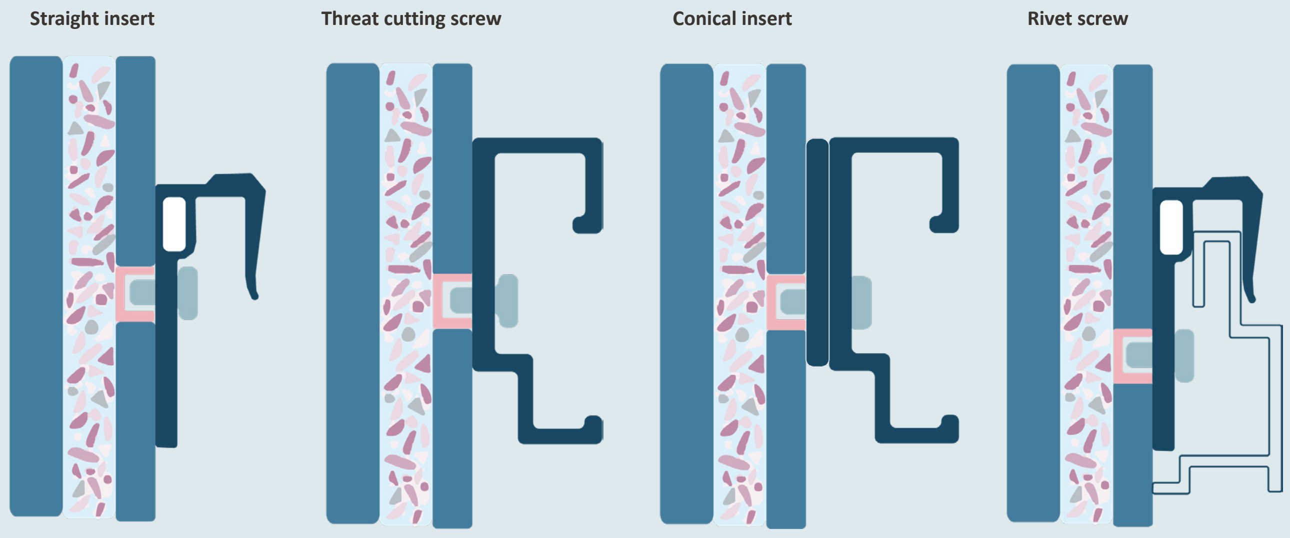

Figure 137: Diagrams for possible bolt connections of the Recycled Composite Panel

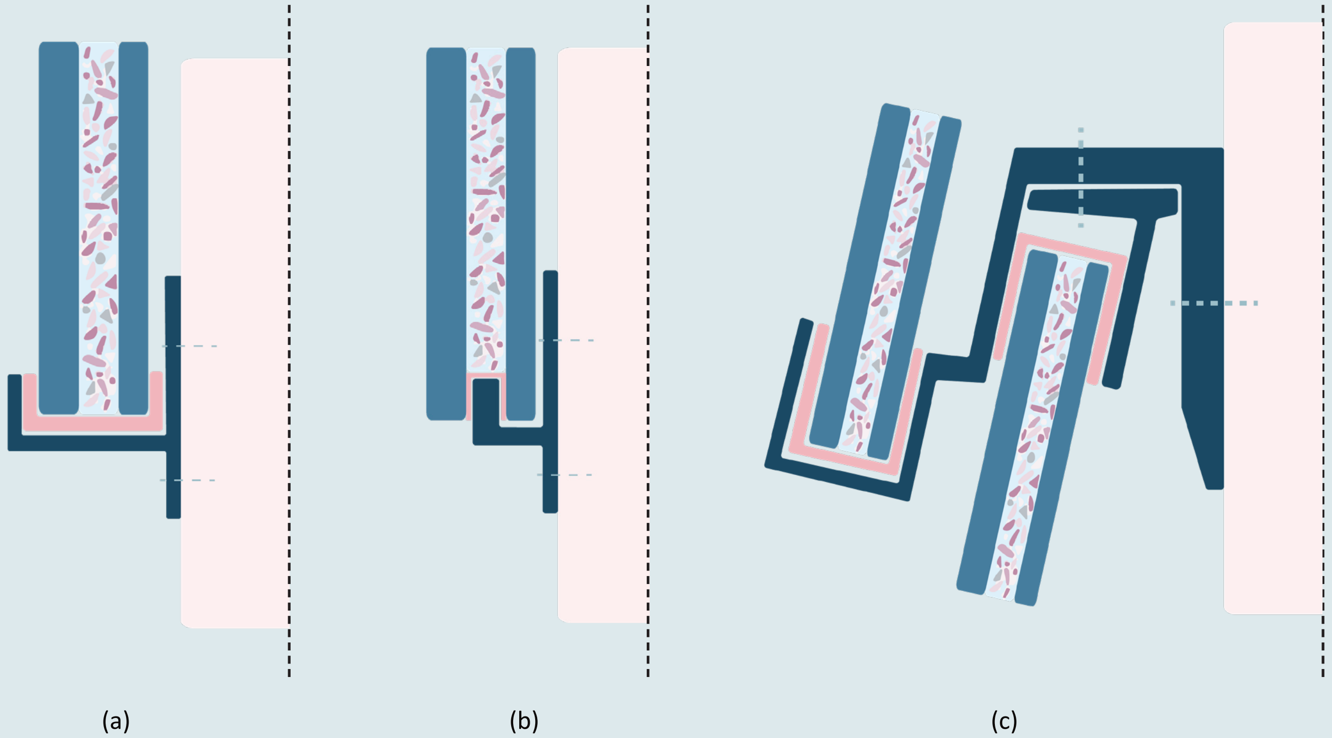

Figure 138: Diagrams for possible clamp connections. (a) Clamp on the outer edge, (b) Clamp in the bulk layer and (c) Clamp on the outer edge on an angle

The Recycled Composite Panels offer a straightforward solution for durable facade construction. Often, simplicity is key in engineering solutions. Further research is essential for these panels, yet they represent a promising step towards a more circular approach.

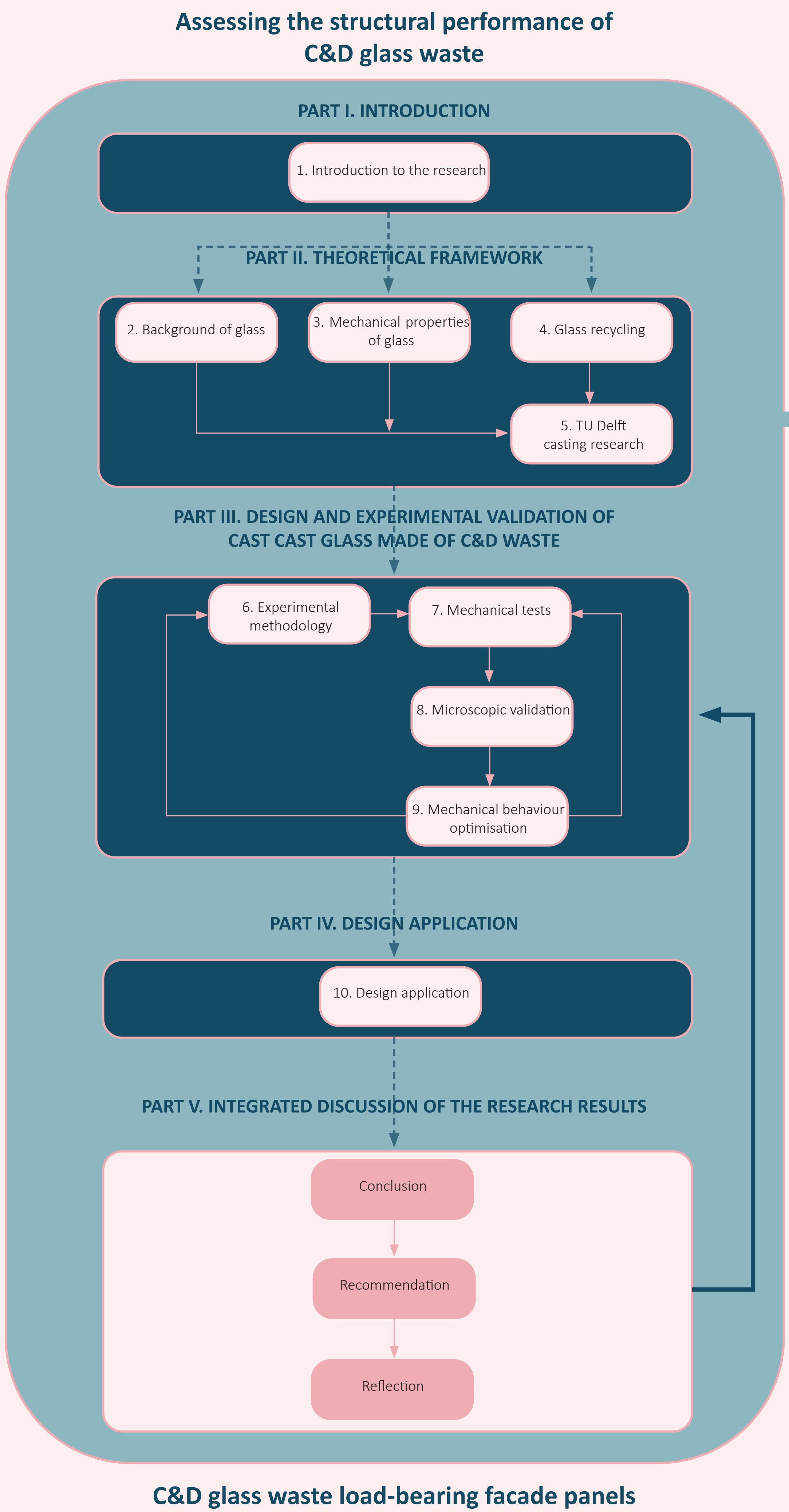

PART 5

INTEGRATED DISCUSSION OF THE RESEARCH RESULTS

CONCLUSION

An overview of the major conclusions drawn from different parts of the experimental design, mechanical testing, microscopic analysis, and mechanical optimisation is given in this chapter. It also answers the main research question and the related sub questions. After that, an analysis of the conclusions made by this thesis will take place.

The primary objective of this thesis was to advance sustainable construction practices by effectively utilising C&D waste glass, which currently does not return to architectural glass, in the production of structural glass panels. Architectural glass waste from C&D currently operates in an open loop system. Introducing new innovative panel manufacturing processes can transition this system to a closed loop approach, emphasising circularity.

Aligned with EU circular economy regulations, this project aimed to maximise the potential of recycled glass, particularly flat glass commonly found in construction materials. By reducing energy consumption and CO2 emissions, this project supports the EU's objectives of achieving zero waste and promoting a circular economy.

In recent years, there has been significant advancement in the production and recycling of glass, particularly in the realm of cast glass panels. Researchers from TU Delft have played a pivotal role in these developments. When inspecting cast glass components for quality control using a microscope, common flaws identified include inclusions, crystallized interfaces, bubbles, infolds, and surface damage resulting from machining, post-processing. The severity of these defects varies depending on their location within the cast component, whether on the surface or within the bulk.

Flaws within the bulk of the glass panels are often tolerated. However, when these flaws manifest on the surface and interact with other defects, they can diminish the glass's strength. This underscores the concept of using a composite panel approach, where glass with higher purity and fewer contaminants should be positioned on the surface, while glass with lower purity and more contaminants should be placed within the bulk (Bristogianni, 2023).

Bristogianni and Oikonomopoulou (2023) emphasise that surface imperfections and flaws are often the primary causes of failure in Float glass and large cast glass components. Therefore, by using higher-quality glass on the surface to counterbalance the weaker quality of glass in the bulk, this composite structure aims to enhance the strength and durability of the glass.

Studies from TU Delft have explored this topic to some extent. However, much remains unknown about the optimal geometry and parameters of these composite panels. The ideal ratio of low-quality cullet in the bulk to high-quality cullet at the surface is yet to be determined. Additionally, the specific material compositions for the low-quality bulk and high-quality surface are also unknown. To address this gap, the main research question was formulated:

"What is the effect of the different parameters in respect to the geometry and glass composition of composite cast glass beams to their overall structural performance made out of C&D flat glass waste?"

To assess the structural feasibility of these recycled panels, multiple beams were created to examine their mechanical and microscopic behaviour. Once the material compositions and beam geometries are thoroughly understood, this information can aid in the development of recycled composite cast glass panels.

For the setup of this research, four types of experiments are outlined, as depicted in Figure 42.

- **Experiment Type 1: Homogeneous beams:** These beams served as a reference group for comparison with the composite beams. They allowed for an investigation into the influence of employing a composite strategy with higher quality glass on the surface.
- **Experiment Type 2: Composite beams with different surface-bulk ratios:** These experiments aimed to find the optimal ratio between the surface and bulk materials and to observe how this ratio affects structural performance.
- **Experiment Type 3: Composite beams with different bulk materials:** These tests explored the impact of various bulk materials on the overall structural performance.
- **Experiment Type 4: Composite beams with different surface materials:** These experiments analysed how different surface materials affect the overall structural performance.

In order to provide a more comprehensive understanding of the outcomes for both homogeneous and composite beams, several sub questions were formulated.

1. *What are the main practical implications and limitations of recycling C&D glass elements?*

The primary challenge is the inability to fully separate glass from foreign matter, particularly contaminants embedded in the glass, such as ceramic frit, lamination, and adhesives. A more thorough separation process of IGUs could enhance the purity of the cullet, significantly reducing traces of metal.

To be recycled, flat glass must be free of impurities such as metals, organic compounds, stones, porcelain (CSP), glass ceramics, and hazardous elements. These contaminants often originate from IGU components or other building materials used during renovation or demolition. According to DeBrincat et al. (2018), even minimal pollution levels in a furnace can lead to several days of production loss, negating the financial and environmental benefits of recycling. This contamination can cause significant harm (Geboes et al., 2023).

Another issue is recipe incompatibility. It is very difficult to verify whether a glass is soda-lime or borosilicate, complicating the recycling process.

2. *How can casting be utilised in the manufacturing of glass panels for built environment applications, specifically in transforming C&D glass waste into reusable cast glass products for facade envelopes, and what are the advantages and limitations of this method?*

The current method for producing architectural glass is the Float glass process, which creates thin-walled flat glass. However, altering the recipes in the Float line is challenging, and Float glass must be free of impurities. Consequently, most Float glass ends up in landfills.

Recent studies from TU Delft have proposed an alternative approach: casting architectural glass. Casting allows for the creation of volumetric shapes and offers flexible design possibilities. It works well with mixed or imperfect glass and, importantly, enables the reuse of cullet, reducing the amount of material that ends up in landfills. A key advantage of casting is its ability to produce volumetric glass components that can tolerate more contamination in the bulk, as these are less likely to affect structural integrity compared to surface impurities.

This tolerance is due to the fact that glass strength is significantly influenced by its surface and edge quality. Littleton (1942) observed that "we never test the strength of glass; all we test is the weakness of its surface." Float glass typically breaks from its surface, so in theory, a stronger surface is more crucial than the bulk. This leads to the concept of composite panels, where purer cullet is used on the surface and lower-purity cullet in the bulk. This bulk layer can contain more impurities and contaminants without compromising the overall strength.

There is an urgent need for innovative, flexible glass recycling techniques that can handle variations in glass composition and tolerate higher levels of contamination in the final products. One such innovative approach is casting volumetric glass components from glass waste.

Advantages of casting:

- Flexibility in design: The casting process allows for a wide range of design possibilities, enabling the creation of various shapes.
- Reduced waste: Since cullet can be reused, less material ends up in landfills.
- Tolerance for impurities: Casting can accommodate mixed glass properties and higher levels of contamination.

Limitations of casting:

- Novelty: As a new glass production process, casting is still in the early stages of research. Further investigation is needed to determine its viability for large-scale glass recycling.

3. *Which glass composition family group is the most promising in the creation of recycled glass beams?*

Soda-lime silica glass was selected for the manufacturing of the cast glass beams in this research because it is the most cost-efficient option and is widely used in the building sector. This type of glass is commonly found in C&D waste. Soda-lime glass has a lower melting point compared to borosilicate glass, making it more affordable. Additionally, it is in higher demand and more readily available than borosilicate glass.

CONCLUSION

4. *How does a composite C&D beam compare with a homogeneous C&D beam of similar external glass quality in terms of structural performance?*

To address this question, it was essential to first understand the structural performance characteristics of homogeneous beams. Beams containing Class A cullet (Float glass compositions) exhibited the highest structural performance. Beams with B cullet generally performed better structurally than those with C cullet. This difference can be attributed to the higher degree of contamination often present in C cullet beams compared to B cullet beams, a finding consistent with existing literature.

B cullet can be more easily cleaned of contaminants, such as coatings or frit, at temperatures of 1070 degrees and above. In contrast, C cullet beams face greater challenges because the inclusions have different thermal expansion characteristics from the glass, leading to trapped stress within the beam.

Considering the structural performance outcomes of the composite beams, experiment type 2 was compared with experiment type 1. The composite beams had Float glass on the surface and CSP pollutants in the bulk, allowing for a comparison with homogeneous beams made entirely of Float glass (Type A) and those containing CSP pollutants (Type C).

All the composite beams with Float glass (6 mm, 8 mm, 10 mm and 12 mm) on the surface and CSP pollutants in the bulk showed an improvement in structural performance compared to homogeneous beams with CSP pollutants.

Homogeneous beams made of Float glass performed similarly to composite beams with 12 mm Float glass and CSP pollutants in the bulk. This indicates that creating a composite structure facilitates the recycling of type C cullet, as the structural performance of homogeneous Float glass beams matches that of composite beams with 12 mm Float glass.

5. *How do variations in geometrical parameters, specifically the surface-bulk thickness, affect the structural performance of recycled composite C&D cast beams?*

To address this question, the outcomes of Experiment 2, encompassing compositions 2A, 2B, 2C, and 2D, were compared.

All compositions demonstrated an increase in structural performance compared to homogeneous beams with CSP pollutants (Graph 08).

The composite beams with 8 mm Float glass exhibited the highest structural performance, although there were some variations among these beams. Following closely were the beams with 12 mm Float glass. Two of these beams, V-2D-C12-C-1 and V-2D-C12-C-2, performed almost as well as pure Float glass. However, the third beam, 2D-C12-C-3, showed significantly lower structural performance due to a substantial edge flaw.

The beams with 6 mm Float glass also performed well, though not as highly as the 8 mm and 12 mm compositions. The worst performance was observed in the composite beams with 10 mm Float glass. XRF analysis revealed that this composition contained less MgO, resulting in a different material composition. Consequently, the 10 mm Float glass beams did not provide an accurate basis for comparison.

6. *How does temperature affect the homogeneity and structure of the composite panel, particularly regarding the viscosity of molten glass, the cooling process, and the annealing schedule?*

To assess the influence of a higher temperature schedule, Experiment Type 2 involved composite beams with Float glass on the surface and CSP pollutants in the bulk, produced initially at 1070 degrees. These were compared with beams of the same compositions processed at 1070 degrees followed by four hours at 1120 degrees, known as Fire Round 2C, comprising 8 beams.

Comparing the feasibility validation of Fire Round 2C beams with those from Fire Rounds 2A, 2B, and 2D reveals a notable effect of the higher temperature schedule on the structural appearance of the beams. Fire Round 2C produced beams with improved compatibility, confirmed through microscopic examination which revealed fewer infolds, indicating enhanced structural consistency.

However, every beam from Fire Round 2C also exhibited a low to medium level of mould reaction, higher than observed in fire rounds processed solely at 1070 degrees. Additionally, nearly all beams displayed noticeable microcracks, particularly prominent in beams with 10 mm Float glass where numerous bubbles formed beneath the surface. Ultimately, it is evident that temperature significantly impacts the uniformity and structural integrity of composite beams.

Regarding mechanical performance, the flexural strength of composite beams treated at 1070 degrees versus those exposed to the higher temperature schedule showed minimal differences for beams with 6 mm, 8 mm, and 12 mm Float glass on the surface. However, the 10 mm Float glass compositions exhibited increased bubble formation at higher temperatures, severely compromising the beams' structural integrity due to these surface flaws.

7. *How do different flaws/defects in glass, such as inclusions, crystallization, infolds and machining manifest in the beams created from recycled glass, and how do they impact the structural performance?*

For the microscopic validation, the focus was on four types of flaws: inclusions, infolds, crystallization, and machining.

Graph 20 utilises data from Appendix G to illustrate the relationship between different flaw types and the flexural strength of each beam. This graph aims to reveal any correlations between specific flaw types and beam failures.

From the encountered flaws, inclusions are the most destructive flaws for the beams (extrinsic flaw). Localised inclusions often lead to significant beam failures. Due to excessive inclusions, a total of 13 beams fractured either during removal from the oven or during surface treatment while being polished.

Composite beams, with Float glass on the surface and CSP pollutants in the bulk, occasionally exhibited inclusions (Figure 110). These inclusions were typically found within the bulk of the composite compositions rather than on the surface. Despite these inclusions, the composite beams demonstrated overall good structural performance and higher flexural strength compared to homogeneous beams with similar inclusions. Importantly, cracks and fractures observed in these composite beams did not originate from these inclusions but from other surface flaws. This underscores that inclusions on the surface are more likely to cause catastrophic failures than those embedded within the bulk, highlighting the importance of improving surface glass purity for enhanced structural integrity.

Infolds (intrinsic flaw) are small gaps or chips on the surface that reduce specimen (beam) strength. Infolds occur when cullets do not properly interfere with each other, allowing debris to enter and mould growth. Infolds were observed in all experiment types but did not correlate with specific beam strengths.

After inclusions, crystallization is the next critical concern (intrinsic flaw). Graph 20 indicates that crystallization predominantly affects homogeneous beams, likely due to the higher temperature schedules used in Fire Rounds 1A and 1B. Crystallization occurs during oven operations and can lead to partially crystallized components at temperatures below the liquidus point.

Finally, machining is the most common defect for cast glass (intrinsic flaw) due to surface and edge treatments. Surface cracks from machining reduce beam strength, with severe defects on the surface impacting strength more than those in the bulk. This flaw is most prevalent in high-performance cast glass beams.

Inclusions are the most harmful flaws, originating from material compositions. However, cullet selection and removal of pollutants like ceramic and silicone can mitigate their impact. In composite beams, inclusions are less harmful compared to surface flaws. Crystallization is influenced by temperature and can be minimised by optimising temperature schedules. Infolds can also be minimised by adjusting temperature schedules; higher temperatures reduce infolds but may increase crystallization. Machining flaws are challenging to eliminate and significantly affect structural performance, highlighting intrinsic flaws as the most detrimental to overall beam integrity.

8. *What information does the crack pattern provide about the properties of the glass beam?*

As mentioned in paragraph 8.1: Crack patterns, insights into stress levels, fracture energies, and origins can be derived from observing general patterns of crack extension and branching.

Chapter 3: Mechanical tests, explored how stress distribution places the highest tensile stress at the bottom during bending loads. The equilibrium between tensile and compressive forces can be disrupted by minor misalignments in elastic properties, potentially leading to fractures.

Fracture locations reveal stress levels through fracture mirrors, typically 10 to 13 times larger than the original flaw. Well-defined fracture mirror boundaries suggest high-energy fractures for composite beams, whereas indistinct boundaries indicate low-energy fractures such

CONCLUSION

as homogeneous beams. Compression curls on fracture surfaces, like cantilever curls, indicate low bending loads. Double compression curls indicate a high flexural strength. Secondary fractures often result from stress reverberations and reflections, typically occurring at non-perpendicular angles to the specimen axis.

9. *How can recycled C&D waste beams be optimised using experimental research?*

To understand the behaviour of cast glass C&D waste beams, an investigation into their geometrical and material compositions is conducted through a setup involving four types of experiments.

Experiment type 1: homogeneous beams, focussed on a comprehensive analysis of three different type of homogeneous beams, type A cullet, type B cullet and type C cullet. In this test the beams containing class A performed the best, followed by B and as last type C

Experiment type 2: composite beams, focussing on analysing the optimal ratio between surface and bulk. Different ratios were being used. These beams all contained Class A cullet at the surface (Float glass) and Class B cullet in the bulk (CSP Pollutants). The following ratios were being used:

- Surface: 6 mm and Bulk: 15 mm
- Surface: 8 mm and Bulk: 13 mm
- Surface: 10 mm and Bulk: 11 mm
- Surface: 12 mm and Bulk 9 mm

For these compositions the beams containing 8 mm Float glass performed the best, followed by the beams containing 12 mm, then 6 mm and as last the beams with 10 mm Float glass.

Experiment type 3: composite beams, focussing on the material composition of the bulk. Different material for in the bulk are applied (Fritted glass and Metallic Pollutants) to see the influence of another material in the compression zone of the beam.

Given that 8 mm Float glass showed the best performance and 10 mm Float glass showed the worst, it was intriguing to investigate whether introducing a different bulk material would influence structural performance and potentially increase flexural strength. Interestingly, beams containing CSP pollutants performed better than those containing Fritted glass or Metallic Pollutants in the bulk.

Experiment type 4: composite beams, focussing on the material composition of the surface. Fritted glass was being used instead of Float glass to assess the impact of switching from an A class cullet to a B class cullet in the tensile area. These beams are compared with those from experiment types 2 and 3, where beams containing Float glass showed better performance.

Overall, this indicates that a composite beam with 8 mm Float glass and 13 mm CSP Pollutants in the bulk exhibits the highest structural performance. The quality of this beam is comparable to that of a homogeneous type A cullet beam, marking a significant improvement from using type C cullet to type A cullet.

Furthermore, additional strategies were implemented to optimise the mechanical behaviour. The first approach involved examining the influence of cullet selection. This experiment specifically introduced pollutants into tiles to assess their impact on structural performance. It was found that silicone and ceramic inclusions had the most detrimental effect among all pollutants tested. Removing these impurities resulted in an increase in the beam's flexural strength.

The second strategy investigated the impact of higher temperature schedules on composite beams, aiming to reduce infolds and enhance compatibility between cullets and Float glass. Structural feasibility research, as detailed in overview tables 36 and 16, compared the effects of these schedules across seven categories.

Cullets and Float glass exhibit good compatibility across both temperature ranges. At 1070 degrees and the higher schedule (1070 degrees with four hours at 1120 degrees), all beams demonstrate translucency. Higher temperature schedules result in increased mould reaction but fewer fractures. Beams featuring 10 mm Float glass display numerous microcracks. Conversely, lower temperature schedules show more instances of breakage. Bubbles levels are comparable except for beams with 10 mm Float glass at 1120 degrees, which exhibit a high number of trapped air bubbles. Beams produced at higher temperatures show greater potential for structural performance. Microscopically, they exhibit fewer surface flaws such as infolds.

10. *Is there an optimum balance between class B and C waste for achieving structural performance while maximising material recyclability?*

Yes! Composite beams significantly enhance the structural performance of recycled C&D glass beams.

Regarding the beams subjected to the higher temperature schedule, it's important to note that compositions with 12 mm, 8 mm, and 6 mm all demonstrated excellent structural performance. Notably, the 12 mm composition utilised 9 mm of bulk material, whereas the 6 mm Float composition used 15 mm. This suggests that grade C cullet was employed for the 6 mm Float compositions, maximising the use of recycled material. However, the higher temperature schedule also implies increased energy consumption during production, which impacts sustainability negatively. Moreover, since the differences between the higher temperature schedule and the normal schedule (1070 degrees) are minimal, opting for the normal temperature schedule is more sustainable.

Following the four four-point bending tests, beam V-2A-C8-C-1 exhibited the best performance. This beam featured class A cullet on the surface (Float glass) and class C cullet with CSP Pollutants in the bulk.

11. *How should a created panel be reintegrated into the building market after its production from recycled materials?*

The decision was made to utilise the findings of this research to develop a new building application, a cladding. Currently, these claddings are typically made from harmful materials such as plastics and concrete, contributing significantly to CO2 emissions during manufacturing and often ending up in landfills. Utilising these C&D waste panels could reduce CO2 emissions and decrease the amount of C&D waste in landfills.

Cast glass, capable of handling impurities and utilising waste glass, is essential for reintroducing panels composed of recycled materials into the building market while diverting C&D waste from landfills. These panels should be designed with a closed-loop process to ensure complete recyclability at the end of their life cycle. They offer similar functionality to Float glass but are more recyclable, making them suitable for building façades. Each panel is unique due to variations in cullet composition, providing diverse visual effects.

Recycled Composite Cast Glass Panels made from C&D waste, constructed entirely from recycled materials and designed for infinite recycling cycles, can significantly reduce C&D waste and CO2 emissions.

No additional installation instructions are necessary as these panels are compatible with current connection methods. They should be fastened to the back of the load-bearing portion rather than using screws on the cladding, ensuring secure and blind connections. The thicker panels allow for more material usage, thereby utilising more C&D waste. This ensures easy integration into existing building methods, making them an eco-friendly and practical choice for sustainable development.

To enhance panel safety, lamination could be considered, though this adds some additional contaminants. Microscopic tests conducted in Chapter 9 investigated the influence of plastics and found minimal internal stresses, suggesting that lamination might be a viable option. Another safety enhancement could involve chemical treatment, feasible for panels up to a maximum thickness of 2 cm, which is also suitable for the recycled composite panels.

Investigating the mechanical and microscopic differences in the structural behaviour of composite cast glass C&D waste beams constituted the primary objective of this thesis. The ultimate aim of the project was to introduce a novel application: the Recycled Composite Cast Glass cladding system made from C&D waste. This innovative architectural solution provided valuable insights into enhancing the feasibility of recycled cast glass panels for load-bearing façade applications.

To address these objectives, the following main research question guided the study:

"What is the effect of the different parameters in respect to the geometry and glass composition of composite cast glass beams to their overall structural performance made out of C&D flat glass waste?"

Material compositions of the surface and the bulk: The placement of higher purity glass on the surface (Cullet A) and lower purity glass (Cullet C) in the bulk significantly influences structural performance. High-quality Float glass on the surface enhances strength by minimising surface flaws that can lead to failure, while glass with impurities or contaminants in the bulk area tolerates higher levels of imperfections without compromising overall strength.

CONCLUSION

Material composition of the bulk

The type of material used in the bulk (such as Fritted glass or metallic pollutants) impacts structural integrity. Beams containing CSP pollutants in the bulk have shown better performance compared to those with other types of contaminants. This suggests that careful selection and understanding of bulk material properties are critical to achieving desired structural outcomes.

Material composition of the surface

The type of material used at the surface impacts structural integrity. Beams containing Float glass at the surface have a higher structural performance than beams with Fritted glass.

Ratio between surface and bulk: Experimentation with different ratios of surface-to-bulk materials has shown that an optimal balance is crucial. Beams with configurations where Float glass thickness varies from 6 mm to 12 mm on the surface and corresponding bulk thicknesses have demonstrated varying levels of structural performance. Generally, configurations with thicker Float glass on the surface exhibit improved strength. However the beam with 8 mm Float glass performs in the end the best.

Impact of cullet selection: Conscious consideration of cullet placement in the compositions plays a crucial role in optimising overall structural performance. By eliminating harmful pollutants such as ceramic and inclusions, the performance can be significantly enhanced.

Impact of temperature schedules: Temperature variations during casting and annealing significantly affect the structural integrity of composite panels. Higher temperature schedules have been observed to reduce flaws like infolds and enhance compatibility between different glass compositions. However, this temperature can lead to issues like increased microcracks and bubble formation, thereby compromising structural performance.

Microscopic analysis of defects: Microscopic flaws such as inclusions, infolds, crystallization, and machining defects have a profound impact on structural performance. Inclusions, especially those on the surface, are particularly detrimental and can cause catastrophic failures. Crystallization, influenced by temperature, infolds, and machining defects are also critical factors that must be carefully managed to ensure structural reliability.

This thesis demonstrates that by optimising material compositions and geometries, composite cast glass beams made from recycled C&D flat glass waste can achieve exceptional structural performance. Enhanced surface cullet quality and effective management of bulk materials contribute to increased strength and durability of the beams. These recycled panels not only have the potential to significantly reduce environmental impact but also integrate into existing building systems.

Moreover, this innovative approach not only offers a cost-effective solution for recycling unwanted flat glass but also is the start of practical applications in building façades. By diverting waste from landfills and promoting environmentally responsible building practices, this technique supports sustainable construction methods.

Figure 139: My first created cast glass C&D glass beam and I

RECOMMENDATION

A number of recommendations for additional research can be made in light of the primary conclusions of this thesis as well as the challenges faced, particularly during the experimental phase. These options are covered in this chapter's recommendations. All of the recommendations are aimed at developing a façade application that prioritises structural performance. The content focuses on C&D waste, with an emphasis on developing a building application that can be utilised to redirect glass waste from landfills and towards closed-loop systems. The casting technique is the main subject of the investigation.

This research is just getting started, and further studies should be conducted to ensure that glass can be recycled more effectively and that there is less glass C&D waste dumped in landfills. Since it hasn't been thoroughly studied, research and development on creating architectural thick-walled glass components using the casting process to withstand the high contamination rates of undefined composition recycled cullet is still in its early stages. This study outlines the preliminary findings on the viability of a recycled panel. While the recyclability and structural performance of the composite panel design are highly promising, further research is still needed.

1. Sufficient beams were created during this research to allow for an assessment of the microscopic and mechanical validity. To ensure the impact of each contamination, additional beams must be produced in order to do a more accurate statistical analysis. If there had been more data to consider, a couple of the findings drawn during this thesis would have been different. Generally speaking, some outcomes could be the consequence of pure randomness. In summary, which beams require additional analysis:

- **Experiment type 1: Homogeneous beams**
  - **Class B Cullet:**
  - Beams with Fritted glass: Although this thesis uses black Fritted glass, it could be worthwhile to assess the impact of other coloured frits as well.
  - Beams with a soft coating: Two different kinds of soft coatings were applied in this thesis. But since there wasn't enough material, it would be wise to test a number of additional beams with soft coatings. It would also be crucial to determine where and how much silicone is tolerated before removing the silicone.
  - **Class C Cullet:**
  - Beams with CSP Pollutants: Here, emphasis should be placed on the various contaminations, with less randomisation.
  - Beams with HR glass: Care should be taken to adjust the ceramics slightly, as well as the amount and location of the permitted ratio of ceramics before the beam breaks.
  - Beams with Metallic Pollutants: To investigate the occurrence of metal contaminants and the locations of mould reactions.
- **Experiment type 2: Composite beams, influence of ratio between surface and bulk.**

  Containing Float glass at the surface and CSP Pollutants in the bulk.

  - Beams with 2 mm Float and 19 mm bulk
  - Beams with 4 mm Float and 17 mm bulk
  - Beams with 6 mm Float and 15 mm bulk
  - Beams with 8 mm Float and 13 mm bulk
  - Beams with 10 mm Float and 11 mm bulk
  - Beams with 12 mm Float and 9 mm bulk
- **Experiment type 3: Composite beams, influence of the bulk material.**

  Comparing all of the beams with various ratios to beams with a different bulk materials could be a fascinating experiment. To observe that the influence between bulk and surface would remain unchanged or change in the presence of another type of bulk. A bulk may contain a class B cullet such as Fritted glass or soft coated glass or a type C cullet such as HR glass or Metallic Pollutants

  - Beams with 2 mm Float and 19 mm bulk
  - Beams with 4 mm Float and 17 mm bulk
  - Beams with 6 mm Float and 15 mm bulk
  - Beams with 8 mm Float and 11 mm bulk
  - Beams with 10 mm Float and 11 mm bulk
  - Beams with 12 mm Float and 9 mm bulk
- **Experiment type 4: Composite beams, influence of the surface material.**

  Type B cullet, such as Fritted glass and soft-coated glass, requires further investigation. If these materials demonstrate structural performance comparable to beams with Float glass on the surface, it would allow for the increased recycling of materials, including the use of contaminated cullet as surface material.

  - Beams with 2 mm glass with contamination and 19 mm bulk
  - Beams with 4 mm glass with contamination and 17 mm bulk
  - Beams with 6 mm glass with contamination and 15 mm bulk
  - Beams with 8 mm glass with contamination Float and 11 mm bulk
  - Beams with 10 mm glass with contamination Float and 11 mm bulk
  - Beams with 12 mm glass with contamination Float and 9 mm bulk

2. There is just one length (350 mm) used for the beam. To compare the outcomes, it could be interesting to test various lengths. For example a beam of 500 mm and a beam of 200 mm. The width and the height of the beam remains the same. A shorter beam will have fewer contaminants than a longer beam, which will have more contaminants. It will be intriguing to investigate other forms as well. Only beams were created in this thesis. On the façade, nevertheless, a tile would be utilised. Thus, it is also useful to produce and test tiles.

3. The way the composite beams behave in relation to their structural performance is rather intriguing. Additional studies, including ones using a thermal shock, could be beneficial to do in order to better understand how the beams behave under stress.

4. The safety requirements for recycled glass panels are a significant concern. Further assessment is necessary to identify the most viable and promising options, even if a coating is applied to enhance the resistance and strength of the component—something that has been shown to be achievable. Additionally, to ensure glass can be recycled back into the closed loop of glassmaking at the end of its useful life, the safety strategy should focus on the reversibility or recyclability of the selected material or technology. This means conducting safety tests and exploring alternative methods for producing safety glass.

5. Further research could investigate the design and development of reversible connections for attaching panels in various applications. Key questions include: How is the cladding application connected to the wall? Can these connections withstand maximum stress? Are the connections visible or concealed? Which types of connections are suitable for use?

6. Further design is needed for the application of cast glass cladding. Key considerations include: What is the largest tile that can be produced, what size oven is required, and are such ovens currently available? Can these panels be made thicker? Thicker panels could not only recycle more material but also increase the weight when installed on the façade. Is there an optimal combination of thickness and weight for these panels?

7. Conducting further microscopic studies is an excellent method for gaining a deeper understanding of the behaviour of cast glass. These studies can help evaluate the beam's break patterns and identify which types of inclusions in the compositions are detrimental to the beam and which are not. Once this knowledge is established, it will be possible to create more effective beams by avoiding components that degrade the beam's performance.

8. The original plan for this thesis included using a Finite Element Model (FEM) to do a mechanical analysis of the beams. Unfortunately, there was not time for this throughout this thesis due to lab issues and delays. The investigation of every beam and attempt to use a FEM model to discover an optimal value for glass recycling and structural beam performance, however, may still be a highly fascinating aspect of this study.

REFLECTION

1. *What is the relation between your graduation project topic, your master track (A, U, BT, LA, MBE), and your master programme (MSc AUBS)?*

To reduce the amount of construction and demolition (C&D) glass waste that ends up in landfills, this thesis, "Recycled Composite Cast Glass Panels made of C&D Waste: Assessing the Structural Performance," explores the potential of recycling C&D glass for innovative façade cladding applications. The research involves collaboration between the chairs of structural design and mechanics, and building product innovation within the Building Technology master's program.

The chair of structural design and mechanics provides essential information on glass behaviour, glass casting methods, and the potential for recycling architectural flat glass. This thesis advocates for the closed-loop recycling of flat glass and demonstrates how glass casting can help mitigate waste problems. The research investigates recycling options for glass through mechanical tests, microscopic validation, and the optimisation of mechanical behaviour using laboratory experiments.

Conversely, the chair of building product innovation offers insights into contemporary manufacturing techniques and methods for reusing (glass) waste materials in innovative building design applications. The production of recycled glass cladding materials focuses on optimising waste usage and recycling processes while ensuring good structural performance. The ultimate goal of this research is to develop a circular, sustainable product that contributes to reducing C&D glass waste in landfills.

2. *How did your research influence your design/ recommendations and how did the design/ recommendations influence your research?*

Influence of research on design / recommendation

For my thesis, I investigated the potential for recycling glass waste in new building applications. Reusing cullet in the glass casting process minimises waste. Due to the diverse material compositions of glass waste, each new application of repurposed glass results in a unique composition, enabling the creation of innovative and aesthetic compositions. To explore the possibilities of recycled glass, I produced multiple beams and tested their flexural strength.

To understand the casting process and the influence of individual contaminants on structural performance, I first created homogeneous beams. Since glass typically fails at its surface, it is beneficial for the surface to have a stronger material composition while the bulk can be of a less strong composition, forming composite beams. I researched the material compositions of both the surface and the bulk, as well as the optimal ratio between them, aiming to balance waste recovery and structural optimisation.

However, testing these qualities presented several challenges in the lab, requiring resource adaptation under stringent time constraints. The methodology of the thesis needed to be adjusted weekly to accommodate time planning, supplier issues, and setbacks in the lab. For instance, when the oven was non-operational for several weeks, significant time pressure necessitated quick decisions and adaptations to the methodology.

Influence of design/ recommendation on the research

My original design idea was to create a panel that could serve as an alternative to end-of-life architectural glass. However, my mentor highlighted a significant challenge in recycling glass: the presence of contaminants such as glues, sealants, plastics, and CSP pollutants. He questioned the rationale of adding a new glass structure to an existing window, as it would reintroduce these contaminants, which have complicated glass recycling efforts. This insight prompted me to explore various glass recycling strategies, focusing on developing a product that maximises the use of C&D waste, thereby reducing the percentage of material sent to landfills.

3. *How do you assess the value of your way of working (your approach, your used methods, used methodology)?*

My research consists of five main parts:

Part 1: Introduction
This section introduces the research, outlining the problem statement and explaining the methodology used.

Part 2: Theoretical framework
This section focuses on the behaviour of glass and its production methods, highlighting the differences between Float glass and cast glass, the mechanical behaviour of glass, its recyclability, and the current open-loop recycling system. It also explores the potential of using cast glass for recycling and reviews previous research from TU Delft, which forms the basis for this study.

Part 3: Experimental fethodologies
This section details the design concept of the beams and the four types of experiments conducted:

- Homogeneous beams
- Composite beams focusing on the ratio between surface and bulk materials
- Composite beams focusing on the material composition of the bulk
- Composite beams focusing on the material composition of the surface

It includes structural feasibility validation of the beams, examining factors such as compatibility, transparency, mould reaction, cracks, breakage, bubbles levels, and overall structural performance. Mechanical testing was performed using a four-point bending machine to assess flexural strength. Post-testing, the cracks were examined, and the origin of the fractures was explored under a microscope. Structural behaviour optimisation was then conducted based on experimental testing.

Part 4: Design application
This part focuses on the creation of the design application.

Part 5: Integrated discussion
This section integrates and discusses the research results, reflecting on the main question and outcomes.

Although my approach is methodical, there are areas for improvement. Currently, I can only test three beams per type, but for statistically feasible results, testing at least thirty beams of each kind is necessary. Time constraints make achieving this level of thoroughness challenging. Additionally, the laboratory setting presents many unknowns, requiring patience and flexibility during the research process.

4. *How do you assess the academic and societal value, scope and implication of your graduation project, including ethical aspects?*

The research holds high academic value, particularly within TU Delft's ongoing efforts to integrate waste materials into construction practices. This effort, along with lowering CO_2 emissions and promoting a circular economy, is in line with the EU's objective of reaching zero waste in building by 2050.

Glass's expanding social relevance is reflected in its increased application in structural designs. Glass has changed from being thought of as opaque and brittle to offering structural integrity, durability, and optical clarity. This change establishes glass as a developing material in the construction sector and represents a substantial shift in architectural and structural applications.

To reduce construction waste, ethical issues must be taken into account, especially with regard to recycling glass. Glass recycling helps the environment by lowering the amount of waste that ends up in landfills, but it's important to consider the environmental effects of glass compositions at every stage of their lifespan, taking into account the energy and resource consumption involved in manufacture and recycling. When incorporating recycled glass items into architectural projects, it's critical to be transparent about their origins, composition, and any drawbacks. This way, consumers will be aware of any performance or aesthetic deviations from regular glass products.

5. *How do you assess the value of the transferability of your project results?*

To facilitate comparisons with current data and to make my research setup available to future students, I'm using comparable settings. To be more precise, I'm using Isidora Matskidou's material settings, adopting her test setup for beam manufacturing and testing, and deciding which defects to pay attention to base on Dr. Telesilla Bristogianni's publications on flexural strength. Regretfully, time restrictions prevent me from testing every element I would like to investigate. But I think changing the beam lengths might provide important information on surface imperfections and structural performance. Furthermore, investigating the production of panels rather than beams may prove to be a fascinating topic for additional study.

6. *To what extent are the results of this thesis applicable in the practice in the built environment?*

The purpose of the manufactured beams is to explore the potential of transforming C&D glass waste into a new architectural product. The results from the mechanical and microscopic tests on both homogeneous and composite beams serve as a foundation for developing a future strategy aimed at creating more closed-loop, circular building applications. One promising application for the newly developed composite material is its integration into cladding systems. Current cladding materials, typically made of plastics and concrete, have a high CO_2 footprint during manufacturing. Utilising C&D glass waste for cladding materials would reduce the overall C&D waste sent to landfills, contributing to more sustainable construction practices.

REFLECTION

7. *To what extent is this research innovative?*

The research exhibits innovation in several key ways. Firstly, it explores new methods of recycling glass for building applications by using casting and analysing the structural behaviour of glass, ultimately creating a composite panel to increase material recycling. This approach seeks to transition from the current open-loop system to a closed-loop recycling process for glass waste management.

Secondly, by developing a closed-loop application, the research contributes to a more circular and sustainable approach in the construction industry.

Thirdly, while current glass production primarily involves Float glass for architectural purposes, this research demonstrates the potential of using casting as a another main production method, thereby expanding the range of building applications for recycled glass.

Fourthly, the creation of composite panels from C&D glass waste results in unique material compositions and appearances for each panel. The variability in contamination rates among different batches leads to the production of beautiful, highly aesthetic, innovative panels.

8. *How does this thesis helps with creating a circular economy in the future?*

This research significantly advances the concept of a circular economy by establishing sustainable methods that minimise C&D waste and optimise resource efficiency in building construction applications. One of the key aspects of this thesis is the investigation of glass casting, which transforms leftover glass (cullets) into useful structural elements. This method promotes a circular approach to material consumption, facilitating a shift from an open-loop to a closed-loop strategy.

Practically, the study demonstrates how recycled glass can be effectively integrated into new architectural applications, providing scalable solutions to reduce the demand for raw materials and divert waste from landfills. Additionally, the thesis supports the implementation of closed-loop systems, where recycled materials are continuously reintegrated into production processes, enhancing sustainability and resource management.

Figure 141: The first day in the lab with the Glass team

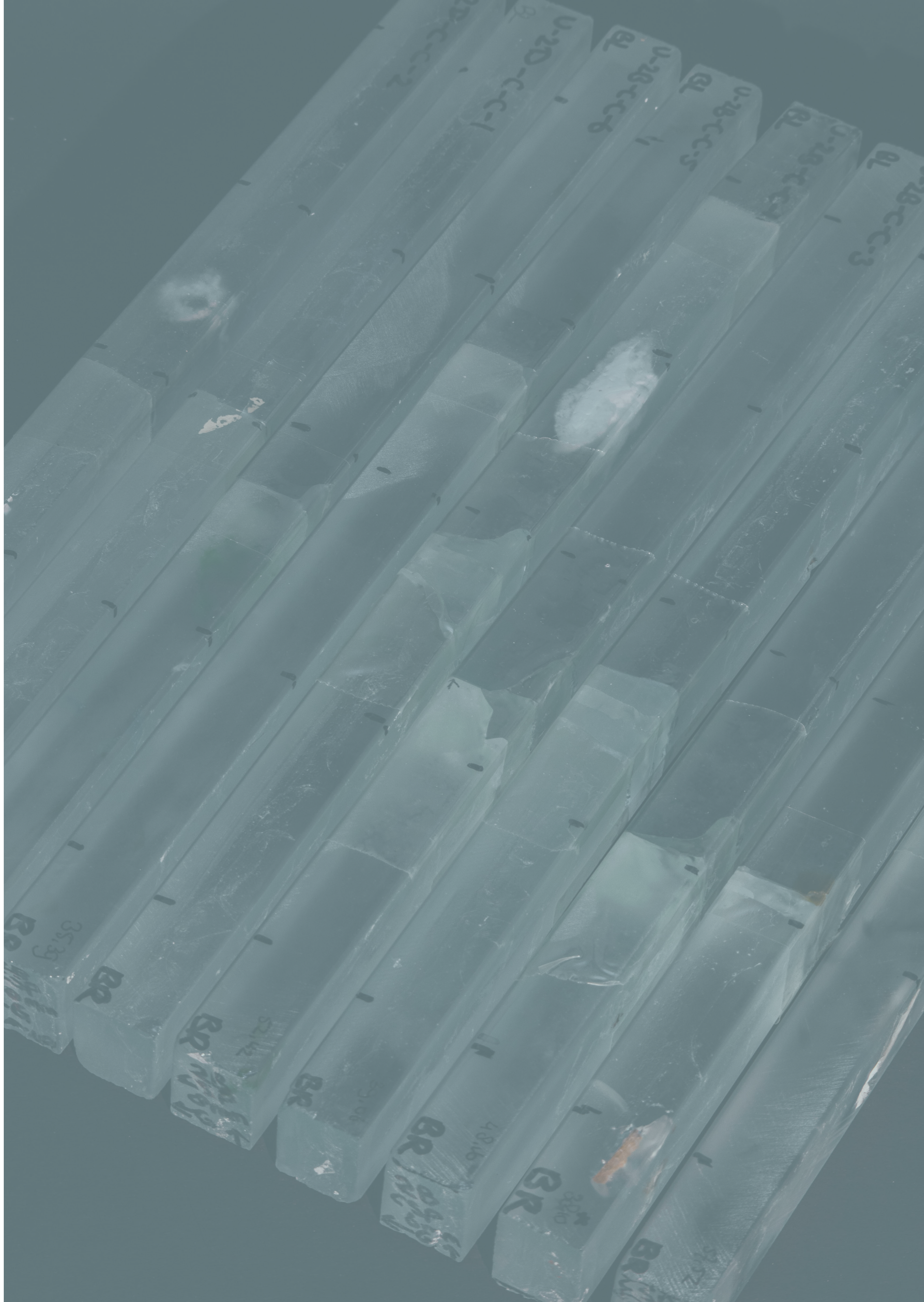

REFERENCES

Abrisa Technologies. (2024). Glass Chemical Strengthening. Retrieved from https://abrisatechnologies.com/glass-fabrication/chemical-strengthening/

Achintha, M. (2016). 5 - Sustainability of glass in construction. In Woodhead Publishing Series in Civil and Structural Engineering.

AGC Glass Europe. (2024). Glass Recycling. Retrieved from https://www.agc-glass.eu/en/sustainability/decarbonisation/recycling

Aldinger, B. S., & K., C. B. (2016). Color Atlas of Stones in Glass: American Glass Research

Anagnia, G. M., Bristogiannia, T., Oikonomopouloua, F., Rigoneb, P., & Mazzucchelli, E. S. (2020). Recycled Glass Mixtures as Cast Glass Components for Structural Applications, Towards Sustainability. Challenging Glass, 7.

ARUP, & Saint-Gobain. (2023). Understanding the carbon footprint of facades and the role of glass.

Ashby, M., Shercliff, H., & Cebon, D. (2013). Materials, Engineering, Science, Processing and Design (Vol. third edition): Elsevier.

Bedon, C., Zhang, X., Santos, F., Honfi, D., Kozłowski, M., Arrigoni, M., . . . Lange, D. (2018). Performance of structural glass facades under extreme loads – Design methods, existing research, current issues and trends. Construction and Building Materials, 163, 921-937. doi:https://doi.org/10.1016/j.conbuildmat.2017.12.153

Bergmann, G. (2020). VDMA: Recycling flat glass – circular economy with potential. Retrieved from https://www.glassonweb.com/article/vdma-recycling-flat-glass-circular-economy-with-potential

Bray, C. (2001). Dictionary of Glass. Materials and Techniques (second ed.): A&C Black Limited.

Bregroup. (2023). BREEAM Refurbishment and fit-out. Retrieved from https://bregroup.com/products/breeam/breeam-technical-standards/breeam-refurbishment-and-fit-out/

Bricknell, D. J. (2009). Float: Pilkingtons' Glass Revolution: Crucible.

Bristogianni, T. (2022). Anatomy of cast glass
The effect of casting parameters on the meso-level structure and macro-level structural
performance of cast glass components. (Doctor of Philosophy). Delft University of Technology, TU Delft Repisotory. Retrieved from https://repository.tudelft.nl/islandora/object/uuid%3A8a12d0b1-fee2-47f1-9fa9-ff56ab2e84c1

Bristogianni, T., & Oikonomopoulou, F. (2023a). Glass up-casting: a review on the current challenges in glass recycling and a novel approach for recycling "as-is" glass waste into volumetric glass components. Glass Structures & Engineering, 8(2), 255-302. doi:10.1007/s40940-022-00206-9

Bristogianni, T., & Oikonomopoulou, F. (2023b). Re3 Glass: A new generation of Recyclable, Reducible and Reusable cast glass components for structural and architectural applications. . Retrieved from https://www.restructgroup-tudelft.nl/re3

Bristogianni, T., Oikonomopoulou, F., Barou, L., Veer, F., Nijsse, R., Jacobs, E., . . . Rutecki, K. (2019). Re3 Glass: a Reduce/Reuse/Recycle Strategy. SPOOL, 6(2), 37-40. doi:10.7480/spool.2019.2.4372

Bristogianni, T., Oikonomopoulou, F., Justino de Lima, C., Veer, F., & Nijsse, R. (2018a). Cast Glass Components out of Recycled Glass: Potential and Limitations of Upgrading Waste to Load-bearing Structures. Challenging Glass, 6. doi:10.7480/cgc.6.2130

Bristogianni, T., Oikonomopoulou, F., Justino de Lima, C., Veer, F., & Nijsse, R. (2018b). Structural cast glass components manufactured from waste glass

Diverting everyday discarded glass from the landfill to the building industry. Retrieved from http://resolver.tudelft.nl/uuid:f4e41fb0-13b3-4f70-9195-fea304e3f06e

Bristogianni, T., Oikonomopoulou, F., & Veer, F. (2021b). On the flexural strength and stiffness of cast glass. Glass Structures & Engineering, 6(2), 147-194. doi:10.1007/s40940-021-00151-z

Bristogianni, T., Oikonomopoulou, F., Veer, F., & Nijsse, R. (2021a). Exploratory Study on the Fracture Resistance of Cast Glass. International Journal of Structural Glass and Advanced Materials Research, 5(1). doi:10.3844/sgamrsp.2021.195.225

Bristogianni, T., Oikonomopoulou, F., Yu, R., Veer, F., & Nijsse, R. (2020). Investigating the flexural strength of recycled cast glass. Glass Structures & Engineering, 5(3), 445-487. doi:10.1007/s40940-020-00138-2

Britannica, T. E. o. E. (2023). Glass. Retrieved from https://www.britannica.com/technology/glass

British Glass. (2023). British Glass. Retrieved from https://www.britglass.org.uk/

Buildings Department. (2018). Code of Practice for Structural Use of Glass2018. Retrieved from https://www.bd.gov.hk/doc/en/resources/codes-and-references/code-and-design-manuals/SUG2018e.pdf

Cwyl, M., Garbacz, A., Michalczyk, R., & Grzegorzewska, N. (2017). Predicting Performance of Aluminum - Glass Composite Facade Systems Based on Mechanical Properties of the Connection. Periodica Polytechnica Civil Engineering, 62. doi:10.3311/PPci.9988

Damen, W., Oikonomopoulou, F., Bristogianni, T., & Turrin, M. (2022). Topologically optimized cast glass: a new design approach for loadbearing monolithic glass components of reduced annealing time. Glass Structures & Engineering, 7(2), 267-291. doi:10.1007/s40940-022-00181-1

DeBrincat, G., & Babic, E. (2023). Re-thinking the life-cycle of architectural glass. Retrieved from https://www.arup.com/perspectives/publications/research/section/re-thinking-the-life-cycle-of-architectural-glass

del Valle-Zermeño, R., Gómez-Manrique, J., Giro-Paloma, J., Formosa, J., & Chimenos, J. (2017). Material characterization of the MSWI bottom ash as a function of particle size. Effects of glass recycling over time. Science of The Total Environment, 581, 897-905.

Devlin, K. (2022). Flat glass recycling. Retrieved from https://www.glassmagazine.com/article/flat-glass-recycling

Dodd, G., & Vinson, J. (2023). Carbon footprint of façades: significance of glass.

Ecofys. (2009). Methodology for the free allocation of emission allowances in the EU ETS post 2012

Sector report for the glass industry Retrieved from https://climate.ec.europa.eu/system/files/2016-11/bm_study-glass_en.pdf

Edgar, R. (2008). UK Glass Manufacture.

FEVE. (2021). Record collection of glass containers for recycling hits 78% in the EU. Retrieved from https://feve.org/glass_recycling_stats_2019/

Galle, W., Debacker, W., & Weerdt, Y. (2019). The Flemish living lab on circular construction, from transition thinking to policy design.

Geboes, E., Galle, W., & De Temmerman, N. (2023). Make or break the loop: a cross-practitioners review of glass circularity. Glass Structures & Engineering, 8(2), 193-210. doi:10.1007/s40940-022-00211-y

Glass Academy. (2023). Heat Strengthened Glass. Retrieved from https://glass-academy.com/heat-strengthened-glass/#:~:text=Overview%20of%20Heat%20Strengthened%20Glass%3A&text=Annealed%20glass%20is%20heated%20to,the%20same%20size%20and%20thickness.

Glass for Europe. (2013). Recycling of end-of-life building glass. Retrieved from https://glassforeurope.com/recycling-of-end-of-life-building-glass/

Glass for Europe. (2014). EU waste legislation & building glass recycling. Adapting the Waste Framework and Landfill Directives to increase glass recycling. Retrieved from https://glassforeurope.com/eu-waste-legislation-building-glass-recycling/

Glass for Europe. (2020). 2050 Flat glass in climate neutral europe, triggering a virtuous cycle of decarbonisation. Retrieved from https://glassforeurope.com/2050-flat-glass-in-a-climate-neutral-europe/

Glass packaging institute. (2023). Why Recycle Glass? Retrieved from https://www.gpi.org/why-recycle-glass

Guardian Glass. (2024a). SunGuard® eXtraSelective SNX 60/28. Retrieved from https://www.guardianglass.com/eu/en/our-glass/sunguard-extraselective/snx-60-28

Guardian Glass. (2024b). SunGuard® Solar Light Blue 52. Retrieved from https://www.guardianglass.com/ap/en/our-glass/sunguard-solar/light-blue-52

Gubberman, R. (2021). The Complete Glass Recycling Process. Retrieved from https://www.rts.com/blog/the-complete-glass-recycling-process/

Guberman, R. (2021). The Complete Glass Recycling Process. Retrieved from https://www.rts.com/blog/the-complete-glass-recycling-process/

Haldimann, M., Luible, A., & Overend, M. (2008). Structural use of Glass.

Hartwell, R., Coult, G., & Overend, M. (2022). Mapping the flat glass value-chain: a material flow analysis and energy balance of UK production. Glass Structures & Engineering, 8(2), 167-192. doi:10.1007/s40940-022-00195-9

REFERENCES

Hubert, M. (2019). Industrial Glass Processing and Fabrication. In J. D. Musgraves, J. Hu, & L. Calvez (Eds.), Springer Handbook of Glass (pp. 1195-1231). Cham: Springer International Publishing.

Inano, H., Akemoto, Y., & Asakura, K. (2023). Upcycling of fluorescent light tube glass via kiln-casting using its properties. Glass Structures & Engineering, 8(2), 303-314. doi:10.1007/s40940-022-00199-5

Jury, G. (2023). What Ceramics (CSP) Does To The Glass Circular Economy. Retrieved from https://bottlecycler.com/what-ceramics-csp-does-to-the-glass-circular-economy/

Justino de Lima, C., Veer, F., Çopuroglu, O., & Nijsse, R. (2018). Innovative Glass Recipes Containing Industrial Waste Materials. 6. doi:10.7480/cgc.6.2175

Kozłowski, M., Akmadzic, V., Malewski, A., Vrdoljak, A. . (2019). Glass in structural applications. E-Zbornik elektronički zbornik radova Građevinskog fakulteta.

Lendager, A. (2020). Upcycle Windows. Solution Circular Buildings, 152-203.

Maltha. (2024). Glas, eindeloos en 100% recyclebaar. Retrieved from https://www.maltha-glassrecycling.com/nl-nl/

Martlew, D. (2005). Viscosity of Molten Glasses. In.

Matskidou, I. (2022). Re-Facade Glass Panels. (Master). Delft University of Technology, TU Delft Repisotory. Retrieved from https://repository.tudelft.nl/islandora/object/uuid%3Ae804092c-5006-428f-b8b7-fce799f4a32b

McLellan, J. (2023). Glass Recycling Process. Retrieved from https://www.generalkinematics.com/blog/glass-recycling-process/

Mohajerani, A., Vajna, J., Cheung, T. H. H., Kurmus, H., Arulrajah, A., & Horpibulsuk, S. (2017). Practical recycling applications of crushed waste glass in construction materials: A review. Construction and Building Materials, 156, 443-467.

Mohamed, J. (2020). The re-seal window: a redesign of the edge seals of insulated glass units to facilitate easy and fast re-manufacturing. (Master). Delft University of Technology, TU Delft Repisotory. Retrieved from http://resolver.tudelft.nl/uuid:90a3a7c6-3952-42b0-b26b-0ac63d7726b2

O'Regan, C. (2014). Structural use of glass in buildings (second ed.). London: IStructE Ltd.

Oikonomopoulou, F. (2019). Unveiling the third dimension of glass. Solid cast glass components and assemblies for structural applications. (Doctor of Philosophy). Delft University of Technology, TU Delft Repisotory. Retrieved from https://repository.tudelft.nl/islandora/object/uuid%3A16f1560f-1739-492c-bd95-3f47bf096182

Oikonomopoulou, F., Bhatia, I. S., van der Weijst, F. A., Damen, J. T. W., & Bristogianni, T. (2020). Rethinking the Cast Glass Mould

An Exploration on Novel Techniques for Generating Complex and Customized Geometries. Challenging Glass Conference: Conference on Architectural and Structural Applications of Glass, CGC 7. doi:https://doi.org/10.7480/cgc.7.4662

Oikonomopoulou, F., Bristogianni, T., Barou, L., Veer, F., & Nijsse, R. (2018). The potential of cast glass in structural applications. Lessons learned from large-scale castings and state-of-the art load-bearing cast glass in architecture. Journal of Building Engineering, 20, 213-234. doi:https://doi.org/10.1016/j.jobe.2018.07.014

Oikonomopoulou, F., DeBrincat, G., & Fuhrmann, S. (2023). Glass and circularity. Glass Structures & Engineering, 8(2), 165-166. doi:10.1007/s40940-023-00230-3

Ortiz, C. (2007). Spectroscopy of Terbium doped Sol-gel Glasses.

Quinn, G. D. (2020). Fractography of Ceramics and Glasses (Third ed.): National Institute of Standards and Technology.

Quinn, G. D., Sparenberg, B. T., Koshy, P., Ives, L. K., Jahanmir, S., & Arola, D. D. (2009). Flexural Strength of Ceramic and Glass Rods. Journal of Testing and Evaluation, 37(3), 222-244. doi:10.1520/JTE101649

Rijksoverheid. (2023a). Klimaatbeleid. Retrieved from https://www.rijksoverheid.nl/onderwerpen/klimaatverandering/klimaatbeleid

Rijksoverheid. (2023b). Nederland circulair in 2050. Retrieved from https://www.rijksoverheid.nl/onderwerpen/circulaire-economie/nederland-circulair-in-2050

Rota, A., Zaccaria, M., & Fiorito, F. (2023). Towards a quality protocol for enabling the reuse of post-consumer flat glass. Glass Structures & Engineering, 8(2), 235-254. doi:10.1007/s40940-023-00233-0

Saint-Gobain. (2023a). Glass Recycling from Saint-Gobain. Retrieved from https://www.saint-gobain-glass.co.uk/en-gb/glass-recycling-saint-gobain

Saint-Gobain. (2023b). Mechanical Properties of Glass. Retrieved from https://www.saint-gobain-glass.co.uk/en-gb/architects/physical-properties

Saint-Gobain. (2023c). The UK's leading cullet return scheme offered by Saint-Gobain building glass. Retrieved from https://www.saint-gobain-glass.co.uk/en-gb/glass-recycling-saint-gobain

Schuttelaar & Partners. (2018). 'Circular Netherlands in 2050' – An Impetus for Secondary Raw Materials in the Construction Industry. Retrieved from https://vb.nweurope.eu/projects/project-search/seramco-secondary-raw-materials-for-concrete-precast-products/news/circular-netherlands-in-2050-an-impetus-for-secondary-raw-materials-in-the-construction-industry/

sds industries. (2023). Understanding Kiln Firing Schedules for Glass, Ceramics, Pottery, and Heat Treat. Retrieved from https://www.kilncontrol.com/blog/kiln-firing-schedules/

Shand, E. B. (1968). Engineering Glass, Modern Materials. 6.

Shelby, J. E. (2005). Introduction to Glass Science and Technology (second ed.): The Royal Society of Chemistry.

Statista. (2023). Production volume of glass containers and bottles worldwide in 2020 and 2023, with a forecast for 2028. Retrieved from https://www.statista.com/statistics/700260/glass-bottles-and-containers-production-volume-worldwide/

Surgenor, A., Holcroft, C., Gill, P., & DeBrincat, G. (2018). Building glass into the circular economy

How to guide. Retrieved from https://ukgbc.org/wp-content/uploads/2018/10/How-to-guide_Building-glass-into-CE.pdf

Trespa. (2024). Innovatieve Hoogwaardige Architectonische Oplossingen. Retrieved from https://www.trespa.com/nl_BE/

Uheida, K., Deng, Y., Zhang, H., Galuppi, L., Gao, J., Xie, L., . . . Mohamed, A. (2021). Evaluate equivalent-sectional shear modulus of laminated glass beams using torsion tests and photogrammetry methods.

Van Marcke de Lummen, G., & Schreuder, N. (2013). Recycling of Glass from Construction & Demolition Waste

Views from the flat glass industry. AGC Glass Europe.

Varshneya, A. K. (2013). Fundamentals of inorganic glasses (2nd ed.). Sheffield, UK: Society of Glass Technology.

Varshneya, A. K. (2016). Industrial glass. Retrieved from https://www.britannica.com/science/industrial-glass

Veer, F. (2007). The strength of glass, a nontransparent value. Heron, 52.

Veer, F., & Rodichev, Y. (2011). The structural strength of glass: Hidden damage. Strength of Materials, 43, 302-315. doi:10.1007/s11223-011-9298-5

Vlakglas Recycling Nederland. (2022). Vlakglas Recycling Nederland

Jaarverslag 2022. Retrieved from https://www.vlakglasrecycling.nl/uploads/jaarverslagen/Jaarverslag%202022_VRN_4.pdf

W&WGlass. (2023). The Future of Glass Architecture. Retrieved from https://www.wwglass.com/future-glass-architecture/#:~:text=The%20goal%20for%20the%20future,appear%20to%20be%20ultimate%20simplicity.

Warm glass. (2024). Kiln Firing Schedules.

Programme your kiln with confidence. Retrieved from https://warm-glass.co.uk/kiln-schedules-cms-74

Watson, D. M. (1999). Practical Annealing. 11th Biennial Ausglass Conference, Wagga Wagga 1999.

LIST OF FIGURES

PART 1: INTRODUCTION

Chapter 1 | Introduction to the research

Figure 01: Front page image, Photo of overview of beeams ..... Page 1

Figure 02: Photo of overview beams .... Page 4

Figure 03: Photo of overview beams .... Page 6

Figure 04: Illustration of the production and glass cullet in EU28 in 2017 (Bristogianni & Oikonomopoulou, 2023)............... Page 16

Figure 05: (a), (b) Glass waste from Octatube was being placed in a container .... Page 17

Figure 06: Wide range of kiln-cast glasses evolved from the recycling of various different glass waste streams. (Bristogianni & Oikonomopoulou, 2023).. Page 18

Figure 07: Composite kiln-cast components showing abrupt and gradient transitions between opaque or dark tinted and clear glass. (Bristogianni & Oikonomopoulou, 2023).................. Page 19

Figure 08: Tiles made of C&D waste during the thesis of Isidora Matskidou (Matskidou, 2022) .... Page 20

Figure 09: Design objectives: (a) creation of recycled glass panel, (b) Four-point bending tests on the manufactured C&D glass cast beams, (c) contributing to a more circular economy in glass recycling practices, (d) mechanical evaluation of the bending strength, (e)microscopic evaluation and (f) Overall goal, optimisation of the structural performance. .... Page 22

Figure 10: Illustrution of the research framework, the framework is devided into 5 parts .... Page 25

PART 2: THEORETICAL FRAMEWORK

Chapter 2 | Background of glass

Figure 11: Two molecule structures, left Crystalline SiO2 (Quartz), right Amorphous SiO2 (Glass) (Ortiz, 2007) .... Page 28

Figure 12: Glass production techniques. (Luible et al., 2008) .... Page 31

Figure 13: Production process for Float glass.(Luible et al., 2008) .... Page 32

Figure 14: Casting of soda-lime glass blocks at Poesia Factory in Italy. (Oikonomopoulou, 2019).. Page 34

Figure 15: Kiln-casting (Oikonomopoulou, 2019)........................ Page 34

Figure 16: Illustration of the most common mould types (Oikonomopoulou, 2019) .... Page 35

Chapter 3 | Mechanical behaviour of glass

Figure 17: (a) The Apple Store in New York by EOC Engineers (EOC Engineers, 2006), (b) The Crystal Houses façade in Amsterdam by MVRDV Architects, made of adhesively bonded glass blocks. (Scagliola & Brakke, 2016) and (c) Markthal in Rotterdam by Octatube (Octatube, 2014) .... Page 36

Figure 18: (a) Set-up for of 1st series of four-point bending experiment at the TU Delft, for investigating glass waste its flexural strength and (b) set up for 2nd series of four-point bending experiment at the TU Delft. (Bristogianni, et al., 2021b)........... Page 39

Figure 19: Tensile and compressive stress areas visualised in a beam .... Page 40

Figure 20: Classification of casting defects and assessment of their severity based on their characteristics and location in the glass specimen. (Bristogianni, 2022)... Page 41

Figure 21: Flaw categories in kiln-cast specimens. (a) Crystalline inclusions, (b) Glassy inhomogeneities and (c) Gaseous inhomogeneities (Bristogianni, et al., 2021b) .... Page 42

Figure 22: Post breakage behaviour of laminated glasss made of different glass types (Hubert, 2019) .... Page 42

Figure 23: Stress profile in tempered glass (Buildings Department, 2018) .... Page 43

Chapter 4 | Glass recycling

Figure 24: Facade Glass Removal & Replacements (Glass Hoppers, 2021) .... Page 44

Figure 25: Schematic representation of the excisting recovery routes for flat glass (FG), container glass (CG) and glass wool (GW) and glass wool (GW) in the UK. (Hartwell et al., 2022) ..... Page 46

Figure 26: Linear life-cycle of glass manufacturing and processing. (DeBrincat & Babic, 2023).. Page 47

Figure 27: Circular economy diagram adopted for glass industry. (DeBrincat & Babic, 2023) .... Page 47

Figure 28: Sankey diagram of the pre-consumer flat glass flow per origin, ownership, and application in Flanders, expressed in kilotonnes (reference year 2015). Results from and figure based on Debacker et al. (2021.). (Geboes et al., 2022)............ Page 48

Figure 29: Sankey Diagram of the post-consumer flat glass flow per origin, ownership, and application in Flanders, expressed in kilotonnes (reference year 2015). Results from and figure based on Debacker et al. (2021) . (Geboes et al., 2022)............ Page 48

Figure 30: Grades of cullet. (DeBrincat & Babic, 2023) and added illustrations of the classification types .... Page 50

Figure 31: Energy inputs and corresponding emissions associated with glass products including: raw material sourcing and processing (stage 1), primary glass production (stage 2-3) and secondary flat glass processing (stage 4). (Hartwell et al., 2022) .... Page 51

Figure 32: Schematic of emission savings potential from the use of cullet t each stage of flat glass production. (Hartwell et al., 2022) .... Page 51

Figure 33: Ranking of the impact each type of flaw may have on the hosting glass network (Bristogianni, 2022)..................... Page 52

Chapter 5 | TU Delft casting research

Figure 34: Restruct Group and their specification (Restruct TU Delft, 2024) .... Page 54

Figure 35: (a) Glass bricks used for the facade of Crystal Houses, (b) Mechanical tests conducted to verify the structural integrity of the building facade with glass bricks and (c) The final appearance of the glass brick facade. (Restruct TU Delft, 2024)............ Page 55

Figure 36: (a) Glass kiln-cast panels (350*350*10 mm) made at TU Delft from glass waste cullet, namely Cathode-Ray Tube (CRT) front screen, (b)transition Float glass from clear to blue, (c) CRT back screen and crystal coloured glass, (d) enamel Float glass, (e) automotive glass and (f) oven doors. (Bristogianni & Oikonomopoulou, 2023)... Page 56

Figure 37: (a) Interlocking waste glass component, (b) Interlocking waste glass component, (c) Structural cast glass components out of different glass waste streams, to be used in an interlocking wall system, (d) Structural cast glass components out of different glass waste streams, to be used in an interlocking wall system, (e) Re3 casted component and (f) Re3 casted component. (Restruct TU Delft, 2024) .... Page 56

Figure 38: Quality grading of tested glass waste types, based on the strength obtained for castings performed slightly above the glasses' liquidus point (Bristogianni & Oikonomopoulou, 2023).. Page 57

Figure 39: The extent of difference in thermal expansion in combination with the size of a contaminant play the most crucial role in the probability of fracture of the glass matrix (Bristogianni, 2022)... Page 58

Figure 40: Ilustration of the principle of a composite cast glass panel .... Page 58

LIST OF FIGURES

PART 3: DESIGN AND EXPERIMENTAL VALIDATION OF CAST C&D WASTE

Chapter 6 | Experimental methodology

Figure 41: Parameters affecting the quality grade of the recycled kiln-cast glass component. (Bristogianni & Oikonomopoulou, 2023) ....
Page 62

Figure 42: Experimental setup, (a) homogeneous beams with cullet type A, (b) homogeneous beams with cullet type B, (c) homogeneous beams with cullet type C , (d) composite beams ratio between surface and bulk variant A (6 mm Float glass), (e) composite beams ratio between surface and bulk variant B (8 mm Float glass), (f) composite beams ratio between surface and bulk variant C (10 mm Float glass), (g) composite beams ratio between surface and bulk variant D (12 mm Float glass), (h) composite beams with different bulk material variant A (8 mm Float glass), (i) composite beams with different bulk material variant B (10 mm Float glass), (j) composite beams with different surface material variant A (CSP Pollutants), (k) composite beams with different surface material variant B (Metallic Pollutants) ....
Page 64

Figure 43: Preparation of the crystal silica moulds for the beams. (a) step 1, (b) step 5, (c) step 6,(d) step 7 and (e) step 8
Page 67

Figure 44: llustratic diagram of Fire Round 1A....................
Page 69

Figure 45: Fire Round 1A placed in the oven ....
Page 69

Figure 46: Illustratic diagram of Fire Round 1B....................
Page 69

Figure 47: Fire Round 1B placed in the oven ....
Page 69

Figure 48: Illustratic diagram of Fire Round 1C ....
Page 70

Figure 49: Fire Round 1C placed in the oven ....
Page 70

Figure 50: Illustratic diagram of Fire Round 1D....................
Page 70

Figure 51: Fire Round 1D placed in the oven ....
Page 70

Figure 52: Illustratic diagram of Fire Round 2A....................
Page 71

Figure 53: Fire Round 2A placed in the oven ....
Page 71

Figure 54: Illustratic diagram of Fire Round 2B ....
Page 71

Figure 55: Fire Round 2B placed in the oven ....
Page 71

Figure 56: Illustratic diagram of Fire Round 2D....................
Page 73

Figure 57: Fire Round 2D placed in the oven ....
Page 73

Figure 58: Illustratic diagram of Fire Round 3A....................
Page 73

Figure 59: Fire Round 3A placed in the oven ....
Page 73

Figure 60: Illustratic diagram of Fire Round 4A....................
74

Figure 61: Fire Round 4A placed in the oven, (a) CSP Pollutants, (b) Metallic Pollutants....................
Page 74

Figure 62: Feasibility validation of Fire Round 1A, Beams with CSP pollutants. (a) beam V-1A-H-C-1, (b) beam V-1A-H-C-2 and (c) beam V-1A-H-C-3 ....
Page 75

Figure 63: Feasibility validation of Fire Round 1A, Beams with HR glass. (a) Beam V-1A-H-HR-1, (b) beam V-1A-H-HR-2 and (c) Beam V-1A-H-HR-3....................
Page 75

Figure 64: Feasibility validation of Fire Round 1B, Beams Fritted glass. (a) Beam V-1B-H-F-1, (b) Beam V-1B-H-F-2 and (c) Beam V-1B-H-F-3....................
Page 77

Figure 65: Feasibility validation of Fire Round 1B, Beam V-1B-H-HR-1....................
Page 77

Figure 66: Feasibility validation of Fire Round 1B, Beam V-1B-H-S-1....................
Page 77

Figure 67: Feasibility validation of Fire Round 1B, Beam V-1B-H-B-1 ....
Page 77

Figure 68: Feasibilty validation of Fire Round 1C, Beams Metallic pollutants. (a) Beam V-1C-H-M-1, (b) Beam V-1C-H-M-2 and (c) Beam V-1C-H-M-3....................
Page 78

Figure 69: Feasibilty validation of Fire Round 1D, Beams with Float glass. (a) Beam V-1D-H-FL-1, (b) Beam V-1D-H-FL-2 and (c) Beam V-1D-H-FL-3 ....
Page 78

Figure 70: Feasibility validation of Fire Round 2A, (a) Beam V-2A-C8-C-1, (b) Beam V-2A-C8-C-2 and (c) Beam V-2A-C8-C-3..
Page 79

Figure 71: Feasibility validation of Fire Round 2A, (a) Beam V-2A-C10-C-1, (b) Beam V-2A-C10-C-2 and (c) Beam V-2A-C10-C-3 ....
Page 79

Figure 72: Feasibility validation of Fire Round 2A, beam V-2A-C8-F-1....................
Page 80

Figure 73: Feasibility validation of Fire Round 2B, (a) Beam V-2B-C6-C-1 and (b) Beam V-2B-C6-C-2 ....
Page 81

Figure 74: Feasibility validation of Fire Round 2B, (a) Beam V-2B-C8-C-1 and (b) Beam V-2B-C8-C-2 ....
Page 81

Figure 75: Feasibility validation of Fire Round 2B, (a) Beam V-2B-C10-C-1 and (b) Beam V-2B-C10-C-2 ....
Page 81

Figure 76: Feasibility validation of Fire Round 2D, Beam V-2D-C6-C-1....................
Page 82

Figure 77: Feasibility validation of Fire Round 2D, (a) Beam V-2D-C8-C-1 and (b) Beam V-2D-C8-C-2 ....
Page 82

Figure 78: Feasibility validation of Fire Round 2D, (a) Beam V-2D-C10-C-1 ....
Page 82

Figure 79: Feasibility validation of Fire Round 2D, (a) Beam V-2D-C12-C-1, (b) Beam V-2D-C12-C-2 and (c) Beam V-2D-C12-C-3 ....
Page 83

Figure 80: Feasibility validation of Fire Round 3A, (a) Beam V-3A-C8-M-1, (b) Beam V-3A-C8-M-2 and (c) Beam V-3A-C8-M-3 ....
Page 84

Figure 81: Feasibility validation of Fire Round 3A, (a) Beam V-3A-C10-M-1, (b) Beam V-3A-C10-M-2 and (c) Beam V-3A-C10-M-3 ....
Page 84

Figure 82: Feasibility validation of Fire Round 4A,(a) Beam V-4A-CR8-C-1, (b) Beam V-4A-CR8-C-2 and (c) Beam V-4A-CR8-C-3 ....
Page 85

Figure 83: Feasibility validation of Fire Round 4A, (a) Beam V-4A-CR8-M-1, (b) Beam V-4A-CR8-M-2 and (c) Beam V-4A-CR8-M-3 ....
Page 85

Chapter 7 | Mechanial tests

Figure 84: Ceramic traces on cullets ....
Page 86

Figure 85: Illustration how to prepare the beams for structural analysyis ....
Page 94

Figure 86: Cutting the beams with a diamond saw ....
Page 94

Figure 87: Polishing beams....................
Page 95

Figure 88: Illustration how to identify each beam for the structral performance test....................
Page 95

Figure 89: Illustration how to measure each beam for the structural performance test....................
Page 95

Figure 90: Photo of the test set-up of a four-point bending test..
Page 96

Figure 91: Experiment Type 1: Homogeneous beams of Cullet Type A, Cullet Type B and Cullet Type C ....
Page 98

Figure 92: Experiment Type 2: Composite beams, focus on the optimal ratio between surface and bulk ....
Page 100

Figure 93: Experiment Type 3: Composite beams, focus on influence of the material composition of the bulk ....
Page 104

Figure 94: Experiment Type 4: Composite beams, focus on influence of the material composition of the surface ....
Page 106

Figure 95: Experiment Type 1: Homogeneous beams of Cullet Type A, Cullet Type B and Cullet Type B ....
Page 109

Figure 96: Experiment Type 2: Composite beams, focus on the optimal ratio between surface and bulk ....
Page 109

Figure 97: Experiment Type 3: Composite beams, focus on influence of the material composition of the bulk ....
Page 109

Figure 98: Experiment Type 4: Composite beams, focus on influence of the material composition of the surface ....
Page 109

LIST OF FIGURES

Chapter 8 | Microscopic validation

Figure 100: Beam with a high energy failure. This is a composite beam .... Page 110

Figure 101: Beam with a low energy failure. This is a homogeneous beam with Metallic Pollutants .... Page 110

Figure 99: Illustratic overview of the theory of crack patterns (Quinn, 2020) .... Page 111

Figure 102: Beam with a high energy failure. A small mirror located at the fracture. This is a composite beam. .... Page 112

Figure 103: Beam with a low energy failure. A big mirror located at the fracture. This is a compositie beam with Fritted glass. Page 112

Figure 104: A double compression curl, a typical crack for composite beams .... Page 112

Figure 105: A compression curl, a typical crack pattern for homogeneous beams .... Page 112

Figure 106: A non-perpendicular compression curl .... Page 113

Figure 107: A perpendiculair compression curl .... Page 113

Figure 108: Ceramic inlcusions in a homogeneous beam with HR glass (a) Glassy knots and (b) White opaque mass .... Page 114

Figure 109: Microscopic photos of the flaw type, inclusions from beam V-1A-H-C-2, (a) Location of crack, (b) Zoomed-in location of the crack (c) location of the fracture and (d) Zoomed-in photoof the fracture .... Page 115

Figure 110: Inclusion in a composite beam in the bulk, Beam V-2B-C8-C-3 (a) location of the crack, (b) side view and (c) front view .... Page 115

Figure 111: Microscopic photos of the flaw type, infolds from beam V-2A-C8-F-1, (a) Location of the crack, (b) Zoomed-in image of the crack, (c) Overview of the fracture and (d) Zoomed in photo of the infold .... Page 116

Figure 112: Microscopic photos of the flaw type, infolds from beam V-2A-C10-C-1, (a) Location of the crack, (b) Zoomed-in image of the crack, (c) Overview of the fracture and (d) Zoomed in photo of the infold .... Page 117

Figure 113: Microscopic photos of the flaw type, crystallization from beam V-1B-H-HR-1, (a) Location of the crack, (b) Zoomed-in image of the crack, (c) Overview of the fracture and (d) Zoomed in photo of the area with crystallization .... Page 118

Figure 114: Microscopic photos of the flaw type, machining from beam V-2D-C12-C-3, (a) Location of the crack, (b) Zoomed-in image of the crack, (c) Overview of the fracture and (d) Zoomed in photo of the area with scratches .... Page 119

Figure 115: Microscopic cross polarised photos of the flaw type, inclusions from beam V-1A-H-C-1, (a) Location of the crack, (b) Zoomed-in image of the crack, (c) Overview of the fracture and (d) Zoomed in photo of the area with the inclusion .... Page 120

Figure 116: Microscopic cross polarised photos of the flaw type, infolds from beam V-2A-C8-F-1, (a) Location of the crack, (b) Zoomed-in image of the crack, (c) Overview of the fracture and (d) Zoomed in photo of the area with infolds .... Page 121

Figure 117: Microscopic cross polarised photos of the flaw type, crystallization from beam V-1B-H-F-2, (a) Location of the crack, (b) Zoomed-in image of the crack, (c) Overview of the fracture and (d) Zoomed in photo of the area with crystallization .... Page 121

Figure 118: Microscopic cross polarised photos of the flaw type, machining from beam V-4A-CR8-C-3, (a) Location of the crack, (b) Zoomed-in image of the crack, (c) Overview of the fracture and (d) Zoomed in photo of the area with scratches..... Page 122

Chapter 9 | Mechanical validation

Figure 119: Cullets with CSP Pollutants before the seletion of removing other contaminants .... Page 126

Figure 120: Overview of contaminants in the buckets with CSP Pollutants .... Page 126

Figure 121: Illustratic diagram- Tiles .... Page 127

Figure 122: Tiles are placed in the oven .... Page 127

Figure 123: Feasibility validation of tiles for understanding the characteristcs of specific contaminants. (a) Tile 1 with silicone and metallic pollutants, (b) Tile 2 with yellow tinted glass and plastics and (c) Tile 3 with cullets with mirror and dark tinted glass .... Page 128

Figure 124: Microscopic photos with cross polarised light to show the internal stresses per pollutant. (a) Metallic Polllutant, (b) Polarised Metallic Polllutant, (c) Sillicone, (d) Polarised Sillicone, (e)Plastics, (f) Polarised Plastics, (g) Yellow tinted glass, (h) Polarised Yellow tinted glass, (i) Dark tinted glass, (j) Polarised Dark tinted glass, (k) Mirror and (l) Polarised Mirror... Page 130

Figure 125: Illustratic overview of Fire Round 2C .... Page 131

Figure 126: Fire Round 2C placed in the oven .... Page 131

Figure 127: Feasibility validation of Fire Round 2C, (a) Beam V-2C-C6-C-1 and (b) Beam V-2C-C6-C-2 .... Page 132

Figure 128: Feasibility validation of Fire Round 2C, (a) Beam V-2C-C-C8-1 and (b) Beam V-2C-C8-C-2 .... Page 133

Figure 129: Feasibility validation of Fire Round 2C, (a) Beam V-2C-C10-C-1 and (b) Beam V-2C-C10-C-2 .... Page 133

Figure 130: Feasibility validation of Fire Round 2C, (a) Beam V-2C-C12-C-1 and (b) Beam V-2C-C12-C-2 .... Page 133

Figure 131: Surface flaw analysis of beam V-2C-C10-C-2. (a) Overview surface and (b) Microscopic view .... Page 139

PART 4: DESIGN APPLICATION

Chapter 10 | DESIGN APPLICATION

Figure 132: Manufacturing steps of the recycled composite cast glass panel. (a) Mould, (b) Placement of the surface, (c) Placement of the cullets and (d) placement of the top surface . Page 143

Figure 133: From Eternit facade panels to recycled glass panels. (a) Building with Eternit panels, (b) Building with recycled composite panels .... Page 144

Figure 134: Render of Recycled composite panels on a building Page 145

Figure 135: 3D image of the connection of the Recycled Composite panel .... Page 146

Figure 136: Connection methods for the Recycled Composite Panels .... Page 146

Figure 137: Diagrams for possible bolt connections of the Recycled Composite Panel .... Page 147

Figure 138: Diagrams for possible clamp connections. (a) Clamp on the outer edge, (b) Clamp in the bulk layer and (c) Clamp on the outer edge on an angle .... Page 147

PART 5: INTEGRATED DISCUSSION OF THE RESEARCH RESULTS

CONCLUSION

Figure 139: My first created cast glass C&D glass beam and I...... Page 156

Figure 140: Photo of overview of the beams .... Page 157

REFLECTION

Figure 141: The first day in the lab with the Glass team .... Page 162

Figure 142: Photo of composite beams .... Page 163

LIST OF GRAPHS

PART 2: THEORETICAL FRAMEWORK

Chapter 2 | Background of glass

Graph 01: Effect of temperature on the enthalpy of glass forming melt (Shelby, 2005) .... Page 28

Graph 02: Typical curve for viscosity as a function temperature for a soda-lime-silica (Shelby, 2005) .... Page 32

Graph 03: Typical annealing scheme for commercial soda-lime glasses. (Oikonomopoulou, 2019) .... Page 32

Chapter 3 | Mechanical behaviour of glass

Graph 04: Stress-strain behaviour of glass, steel and aluminium alloy (Buildings Department, 2018)... Page 37

PART 3: DESIGN AND EXPERIMENTAL VALIDATION OF CAST C&D WASTE

Chapter 7 | Mechanial tests

Graph 05: General overview of the flexural strength of all the beams during four-point bending test I, II, III and IV .... Page 97

Graph 06: Flexural strength of all the homogeneous beams containing type A cullet, type B cullet and type C cullet .... Page 99

Graph 07: Expected curve for the relationship between composite beams and homogeneous beams .... Page 101

Graph 08: Composite beams relation between surface and bulk compared with homogeneous beams .... Page 101

Graph 09: Comparison between a composite with 6 mm Float glass and a homogeneous beam .... Page 103

Graph 10: Comparison between a composite with 8 mm Float glass and a homogeneous beam .... Page 103

Graph 11: Comparison between a composite with 10 mm Float glass and a homogeneous beam .... Page 103

Graph 12: Comparison between a composite with 12 mm Float glass and a homogeneous beam .... Page 103

Graph 13: Overview of the difference between bulk CSP Pollutants and Fritted glass with 8 mm Float glass .... Page 105

Graph 14: Overview of the difference between bulk CSP pollutants and bulk Metallic pollutants with 8 mm Float glass............ Page 105

Graph 15: Overview of the difference between bulk CSP pollutants and bulk Metallic pollutants with 10 mm Float glass.......... Page 105

Graph 16: Overview of the difference between Float glass of 8 mm and Fritted glass of 8 mm at the surface with a bulk of CSP pollutants .... Page 107

Graph 17: Overview of the difference between Float glass of 8 mm and Fritted glass of 8 mm at the surface with a bulk of Metallic pollutants .... Page 107

Graph 18: Overview of the difference between homogeneous beams with CSP Pollutants and composite beams with Fritted glass and CSP Pollutants in the bulk .... Page 107

Graph 19: Overview of the difference between homogeneous beams with Metallic Pollutants and composite beams with Fritted glass and Metallic Pollutants in the bulk .... Page 107

Chapter 8 | Microscopic validation

Graph 20: Flaw types compared with the structural performance of cast C&D beams... Page 124

Graph 21: Flaw categories compared with the location of the fracture of cast C&D beams... Page 125

Chapter 9 | Mechanical validation

Graph 22: Relationship between homogeneous beams and composite beams with a higher temperature schedule............. Page 136

Graph 23: Relationship between a composite with 6 mm Float glass (1070 degrees) 6 mm Float glass with a higher temperature schedule .... Page 137

Graph 24: Relationship between a composite with 8 mm Float glass (1070 degrees) 8 mm Float glass with a higher temperature schedule .... Page 137

Graph 25: Relationship between a composite with 10 mm Float glass (1070 degrees) 10 mm Float glass with a higher temperature schedule .... Page 137

Graph 26: Relationship between a composite with 12 mm Float glass (1070 degrees) 12 mm Float glass with a higher temperature schedule .... Page 137

Graph 27: Flaw types compared with the structural performance of cast C&D beams, influence of temperature................ Page 138

LIST OF TABLES

PART 1: INTRODUCTION

Chapter 1 | Introduction to the research

Table 01: Time planning ....
Page 178

PART 2: THEORETICAL FRAMEWORK

Chapter 2 | Background of glass

Table 02: Approximate chemical compositions and typical applications of the different glass types (Shand,Armistead 1958; Oikonomopoulou, 2019)...
Page 29

Table 03: Approximate properties of the different glass types of Table 02 based on (Shand, Armistead 1958)*. Mean Melting Point at 10 Pa.s as stated by (Martlew 2005)..............................
Page 30

Table 04: Typical annealing scheme for commercial soda-lime glass (Oikonomopoulou, 2019)..
Page 33

Table 05: Overview of existing glass fabrication methods for building components and their current size limitations. (Oikonomopoulou, 2019) ....
Page 34

Table 06: Characteristics of prevailing mould types for glass casting (Oikonomopoulou, 2019) ....
Page 35

Chapter 3 | Mechanical behaviour of glass

Table 07: Basic properties of soda-lime-silicate glass based on (Achintha, 2016) and (Kozłowski, 2019)......................................
Page 37

Table 08: Ultimate design strength (p_y) for different glass types under short-term load duration (Buildings Department, 2018)..
Page 43

Table 09: Characteristic bending strength of different glass types (Luible et al., 2008) ....
Page 43

Chapter 4 | Glass recycling

Table 10: Specifications for clear and mixed cullet: a comparative overview (Surgenor et al.,2018) ....
Page 50

Table 11: Principal recyclability streams of flat glass according to processing steps based on (Surgenor et al. 2018) and (Kasper 2006)...
Page 53

PART 3: DESIGN AND EXPERIMENTAL VALIDATION OF CAST C&D WASTE

Chapter 6 | Experimental methodology

Table 12: Overview of used cullets during experiments.............
Page 68

Table 13: Amount of glass weight per mould..............................
Page 179

Table 14: Grading system of the feasibility validation of the created beams ....
Page 86

Table 15: Overview structural feasibility validation of the homogeneous beams with cullet grade A, B and C.........................
Page 87

Table 16: Overview structural feasibility of the compostite beams, focus on ratio between surface and bulk ....
Page 91

Table 17: Overview structural feasibility of the compostite beams, focus on different bulk material ....
Page 92

Table 18: Overview structural feasibility of the compostite beams, focus on different surface material ....
Page 93

Chapter 7 | Mechanial tests

Table 19: Overview beams with dimensions of Four-point bending test I ....
Page 180

Table 20: Overview beams with dimensions of Four-point bending test II ....
Page 182

Table 21: Overview beams with dimensions of Four-point bending test III ....
Page 182

Table 22: Overview beams with dimensions of Four-point bending test IV..
Page 182

Table 23: Overview beams with photos of Four-point bending test I ....
Page 186

Table 24: Overview beams with photos of Four-point bending test II ....
Page 190

Table 25: Overview beams with photos of Four-point bending test III ....
Page 194

Table 26: Overview beams with photos of Four-point bending test IV ....
Page 194

Table 27: Overview beams with their structural performance during Fire Round I, II, III and IV ....
Page 198

Chapter 8 | Microscopic validation

Table 28: Overview beams with failure analysis for Four-point bending test I ....
Page 202

Table 29: Overview beams with failure analysis for Four-point bending test II ....
Page 206

Table 30: Overview beams with failure analysis for Four-point bending test III ....
Page 208

Table 31: Overview beams with failure analysis for Four-point bending test IV..
Page 210

Table 32: Overview beams with microscopic analysis for Four-point bending test I..
Page 216

Table 33: Overview beams with microscopic analysis of Four-point bending test II...
Page 224

Table 34: Overview beams with microscopic analysis of Four-point bending test III..
Page 228

Table 35: Overview beams with microscopic analysis of Four-point bending test IV ....
230

Chapter 9 | Mechanical validation

Table 36: Overview feasibility validation of Fire Round 2C.........
Page 134

APPENDIX A

A - Time planning for thesis

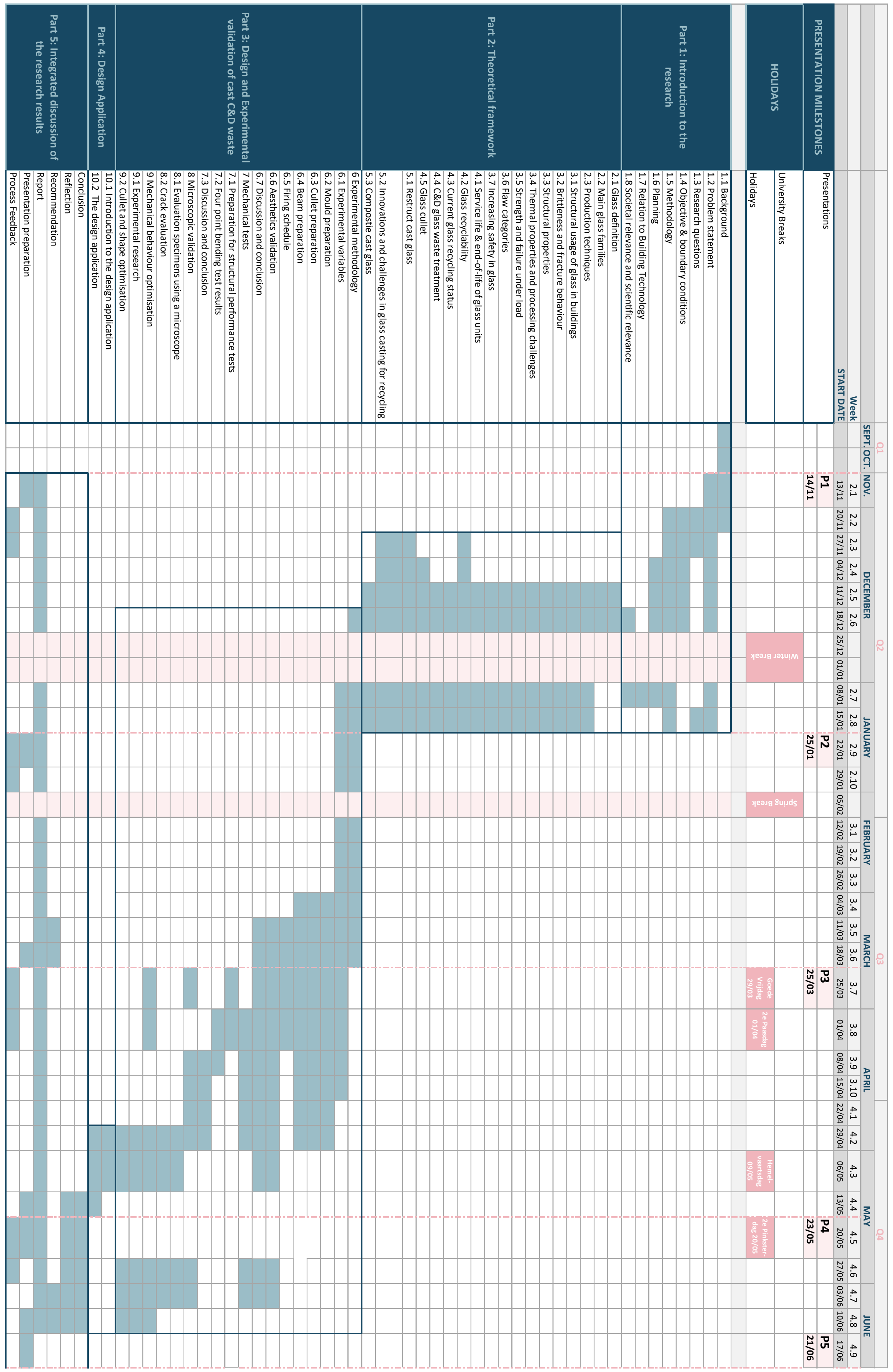

Table 01: Time planning

APPENDIX B

B - Amount of glass weight per mould

Beam of 21 mm x 28 mm x 350 mm = 205,8 mL	glass = (2,5 g/cm3)	514,5 g

Fire round 1A	Homogeneous beams	Amount of glass necessary (g per beam)	15% extra (g)
Cullet grade C			
3x	CSP Pollutants	514,5	**591,675**
	Total	1543,5	1775,025
3x	HR glass	514,5	**591,675**
	Total	1543,5	1775,025
Total: 6 beams			

Fire round 2A	Composite beams	Amount of glass necessary (g per beam)	15% extra (g)
Composition 2B (8 mm float glass and 13 mm bulk)			
3x	B: Float glass (8 mm)		
	C: CSP Pollutants (13 mm)	318,5	**366,275**
	Total	955,5	1098,825
Composition 2C (10 mm float glass and 11 mm bulk)			
3x	B: Float glass (10 mm)		
	C: CSP Pollutants (11 mm)	269,5	**309,925**
	Total	808,5	929,775
Composition 2B-I (8 mm float glass and 13 mm bulk)			
1x	B: Float glass (8 mm)		
	C: Fritted glass (13 mm)	318,5	**366,275**
	Total	318,5	366,275
Total: 7 beams			

Fire round 1B	Homogeneous beams	Amount of glass necessary (g per beam)	15% extra (g)
Cullet grade B			
3x	Lacobel LT (fritted glass)	514,5	**591,675**
	Total	1543,5	1775,025
1x	SNX 60/28 (Soft Coating)	514,5	**591,675**
	Total	514,5	591,675
1x	Solar Light Blue 52 (Soft Coating)	514,5	**591,675**
	Total	514,5	591,675
Cullet grade C			
1x	HR glass	514,5	**591,675**
	Total	514,5	591,675
Total: 6 beams			

Fire round 2B	Composite beams	Amount of glass necessary (g per beam)	15% extra (g)
Composition 2A (6 mm float glass and 15 mm bulk)			
2x	B: Float glass (6 mm)		
	C: CSP Pollutants (15 mm)	367,5	**422,625**
	Total	735	845,25
Composition 2B (8 mm float glass and 13 mm bulk)			
2x	B: Float glass (8 mm)		
	C: CSP Pollutants (13 mm)	318,5	**366,275**
	Total	637	732,55
Composition 2C (10 mm float glass and 11 mm bulk)			
2x	B: Float glass (10 mm)		
	C: CSP Pollutants (11 mm)	269,5	**309,925**
	Total	539	619,85
Total: 6 beams			

Fire round 2C	Composite beams	Amount of glass necessary (g per beam)	15% extra (g)
Composition 2A (6 mm float glass and 15 mm bulk)			
2x	B: Float glass (6 mm)		
	C: CSP Pollutants (15 mm)	367,5	**422,625**
	Total	735	845,25
Composition 2B (8 mm float glass and 13 mm bulk)			
2x	B: Float glass (8 mm)		
	C: CSP Pollutants (13 mm)	318,5	**366,275**
	Total	637	732,55

Fire round 2B	Composite beams	Amount of glass necessary (g per beam)	15% extra (g)
Composition 2C (10 mm float glass and 11 mm bulk)			
2x	B: Float glass (10 mm)		
	C: CSP Pollutants (11 mm)	269,5	**309,925**
	Total	539	619,85
Total: 6 beams			

Fire round 2C	Composite beams	Amount of glass necessary (g per beam)	15% extra (g)
Composition 2A (6 mm float glass and 15 mm bulk)			
2x	B: Float glass (6 mm)		
	C: CSP Pollutants (15 mm)	367,5	**422,625**
	Total	735	845,25
Composition 2B (8 mm float glass and 13 mm bulk)			
2x	B: Float glass (8 mm)		
	C: CSP Pollutants (13 mm)	318,5	**366,275**
	Total	637	732,55
Composition 2C (10 mm float glass and 11 mm bulk)			
2x	B: Float glass (10 mm)		
	C: CSP Pollutants (11 mm)	269,5	**309,925**
	Total	539	619,85
Composition 2D (12 mm float glass and 9 mm bulk)			
2x	B: Float glass (12 mm)		
	C: CSP Pollutants (9 mm)	220,5	**253,575**
	Total	441	507,15
Total: 8 beams			

Fire round 2D	Composite beams	Amount of glass necessary (g per beam)	15% extra (g)
Composition 2A (6 mm float glass and 15 mm bulk)			
1x	B: Float glass (6 mm)		
	C: CSP Pollutants (15 mm)	367,5	**422,625**
	Total	367,5	422,625
Composition 2D (12 mm float glass and 9 mm bulk)			
3x	B: Float glass (12 mm)		
	C: CSP Pollutants (9 mm)	220,5	**253,575**
	Total	661,5	760,725
Total: 4 beams			

Fire round 3A	Composite beams	Amount of glass necessary (g per beam)	15% extra (g)
Composition 3B (8 mm float glass and 13 mm bulk)			
3x	B: Float glass (8 mm)		
	C: Metallic Pollutants (13 mm)	318,5	**366,275**
	Total	955,5	1098,825
Composition 3C (10 mm float glass and 11 mm bulk)			
3x	B: Float glass (10 mm)		
	C: Metallic Pollutants (11 mm)	269,5	**309,925**
	Total	808,5	929,775
Total: 8 beams			

Fire round 4A	Composite beams	Amount of glass necessary (g per beam)	15% extra (g)
Composition 4B-I (8 mm fritted glass and 13 mm bulk)			
3x	B: Fritted glass (8 mm)		
	C: CSP Pollutants (13 mm)	318,5	**366,275**
	Total	955,5	1098,825
Composition 4B-II (8 mm fritted glass and 13 mm bulk)			
3x	B: Fritted glass (8 mm)		
	C: Metallic Pollutants (13 mm)	318,5	**366,275**
	Total	955,5	1098,825
Total: 6 beams			

Fire round 1C	Homogeneous beams	Amount of glass necessary (g per beam)	15% extra (g)
Cullet grade C			
3x	Metallic Pollutants	514,5	**591,675**
	Total	1543,5	1775,025
Total: 6 beams			

Table 13: Amount of glass weight per mould

APPENDIX C

C - Overview beams with dimensions - Four point bending test I

Number	Name beam	Fire round	Forming temperature (°C)	Type	Surface type: Float (Fl), Fritted (Fr)	Bulk type	Number of beam	Status before structural performance test	Mass (g)	Width (mm)					Height (mm)				
										Location 1	Location 2	Location 3	Location 4	Average	Location 1	Location 2	Location 3	Location 4	Average
	V-1A-H-HR-1	1A	1120	Homogeneous beam	x	HR glass	1	Failed	x										
	V-1A-H-HR-2	1A	1120	Homogeneous beam	x	HR glass	2	Failed	x										
	V-1A-H-HR-3	1A	1120	Homogeneous beam	x	HR glass	3	Failed	x										
1.1	V-1A-H-C-1	1A	1120	Homogeneous beam	x	CSP pollutants	1	Succeeded	536,85	29,27	28,44	28,54	28,34	**28,65**	20,96	21,17	20,97	20,98	**21,02**
1.2	V-1A-H-C-2	1A	1120	Homogeneous beam	x	CSP pollutants	2	Succeeded	531,46	29,02	29,39	28,71	28,62	**28,94**	21,25	20,90	20,86	20,80	**20,95**
	V-1A-H-C-3	1A	1120	Homogeneous beam	x	CSP pollutants	3	Failed	x										
1.3	V-1B-H-F-1	1B	1120	Homogeneous beam	x	Fritted glass	1	Succeeded	533,62	28,11	28,76	27,74	28,16	**28,19**	21,74	21,10	21,84	21,14	**21,46**
1.4	V-1B-H-F-2	1B	1120	Homogeneous beam	x	Fritted glass	2	Succeeded	535,30	28,85	29,09	28,96	28,54	**28,86**	20,99	21,25	20,82	20,99	**21,01**
1.5	V-1B-H-F-3	1B	1120	Homogeneous beam	x	Fritted glass	3	Succeeded	537,20	27,81	29,25	27,83	28,85	**28,44**	20,87	21,20	20,88	20,93	**20,97**
1.6	V-1B-H-HR-1	1B	1120	Homogeneous beam	x	HR glass	1	Succeeded	533,40	28,12	28,07	28,02	28,38	**28,15**	20,99	21,07	20,63	20,60	**20,82**
	V-1B-H-S-1	1B	1120	Homogeneous beam	x	SNX 60/26 Coated	1	Failed	527,08	28,00	27,29	28,90	28,42	**28,15**	20,98	21,02	21,06	21,24	**21,08**
1.7	V-1B-H-B-1	1B	1120	Homogeneous beam	x	Blue Solar light	1	Succeeded	535,77	28,17	27,93	29,02	28,68	**28,45**	20,97	20,84	20,95	21,20	**20,99**
1.8	V-2A-C8-C-1	2A	1070	Composite beam	Fl 8 mm	CSP pollutants	1	Succeeded	538,26	29,04	28,96	29,20	29,32	**29,13**	21,56	21,18	21,36	21,04	**21,29**
	V-2A-C8-C-2	2A	1070	Composite beam	Fl 8 mm	CSP pollutants	2	Failed	x										
	V-2A-C8-C-3	2A	1070	Composite beam	Fl 8 mm	CSP pollutants	3	Failed	x										
1.9	V-2A-C8-F-1	2A	1070	Composite beam	Fl 8 mm	Fritted glass	1	Succeeded	550,89	27,88	28,56	29,60	28,68	**28,68**	21,02	21,35	21,29	21,51	**21,29**
1.10	V-2A-C10-C-1	2A	1070	Composite beam	Fl 10 mm	CSP pollutants	1	Succeeded	547,57	29,06	28,32	28,81	28,58	**28,69**	21,03	21,19	21,09	21,38	**21,17**
	V-2A-C10-C-2	2A	1070	Composite beam	Fl 10 mm	CSP pollutants	2	Failed	x										
	V-2A-C10-C-3	2A	1070	Composite beam	Fl 10 mm	CSP pollutants	3	Failed	x										
1.11	V-2B-C6-C-1	2B	1070	Composite beam	Fl 6 mm	CSP pollutants	1	Succeeded	552,91	28,75	29,58	28,74	29,48	**29,14**	21,35	21,02	21,23	21,11	**21,18**
1.12	V-2B-C6-C-2	2B	1070	Composite beam	Fl 6 mm	CSP pollutants	2	Succeeded	549,01	29,14	29,15	28,85	28,56	**28,93**	20,71	20,86	20,87	20,97	**20,85**
1.13	V-2B-C8-C-1	2B	1070	Composite beam	Fl 8 mm	CSP pollutants	1	Succeeded	547,44	29,16	29,22	28,96	29,55	**29,22**	21,21	20,85	21,18	21,13	**21,09**
1.14	V-2B-C8-C-2	2B	1070	Composite beam	Fl 8 mm	CSP pollutants	2	Succeeded	546,17	29,69	29,13	28,47	28,42	**28,93**	21,11	21,08	21,07	21,19	**21,11**
1.15	V-2B-C10-C-1	2B	1070	Composite beam	Fl 10 mm	CSP pollutants	1	Succeeded	538,81	28,34	28,12	28,77	28,96	**28,55**	21,02	20,89	21,01	21,03	**20,99**
1.16	V-2B-C10-C-2	2B	1070	Composite beam	Fl 10 mm	CSP pollutants	2	Succeeded	534,90	28,35	27,77	28,39	27,35	**27,97**	21,03	21,04	20,94	21,01	**21,01**

Table 19: Overview beams with dimensions of Four-point bending test I

C - Overview beams with dimensions - Four point bending test II

Number	Name beam	Fire round	Forming temperature (°C)	Type	Surface type: Float (Fl), Fritted (Fr)	Bulk type	Number of beam	Status before structural performance test	Mass (g)	Width (mm)					Height (mm)				
										Location 1	Location 2	Location 3	Location 4	Average	Location 1	Location 2	Location 3	Location 4	Average
2.1	V-2C-C6-C-1	2C	1070 & 1120	Composite beam	Fl 6 mm	CSP pollutants	1	Succeeded	534,55	29,66	29,22	28,85	28,14	**28,97**	21,23	20,84	21,07	20,84	**21,00**
2.2	V-2C-C6-C-2	2C	1070 & 1120	Composite beam	Fl 6 mm	CSP pollutants	2	Succeeded	522,43	29,06	29,09	28,00	28,55	**28,68**	21,00	20,72	20,81	20,72	**20,81**
	V-2C-C8-C-1	2C	1070 & 1120	Composite beam	Fl 8 mm	CSP pollutants	1	Failed											
2.3	V-2C-C8-C-2	2C	1070 & 1120	Composite beam	Fl 8 mm	CSP pollutants	2	Succeeded	538,68	28,27	28,28	28,06	28,62	**28,31**	21,22	21,00	21,07	20,96	**21,06**
2.4	V-2C-C10-C-1	2C	1070 & 1120	Composite beam	Fl 10 mm	CSP pollutants	1	Succeeded	533,59	28,14	28,09	28,93	28,95	**28,53**	21,03	20,73	20,87	20,81	**20,86**
2.5	V-2C-C10-C-2	2C	1070 & 1120	Composite beam	Fl 10 mm	CSP pollutants	2	Succeeded	541,80	28,97	28,63	28,73	28,05	**28,60**	21,12	20,92	21,05	21,02	**21,03**
2.6	V-2C-C12-C-1	2C	1070 & 1120	Composite beam	Fl 12 mm	CSP pollutants	1	Succeeded	549,87	28,73	28,67	28,19	28,47	**28,52**	21,13	20,83	21,09	20,95	**21,00**
2.7	V-2C-C12-C-1	2C	1070 & 1120	Composite beam	Fl 12 mm	CSP pollutants	2	Succeeded	535,24	28,60	28,30	28,28	28,23	**28,35**	20,90	21,00	21,17	21,08	**21,04**
2.8	V-2D-C8-C-1	2D	1070	Composite beam	Fl 8 mm	CSP pollutants	1	Succeeded	496,38	27,92	27,74	26,78	26,70	**27,29**	21,01	21,32	20,94	21,04	**21,08**
2.9	V-2D-C10-C-1	2D	1070	Composite beam	Fl 10 mm	CSP pollutants	1	Succeeded	528,24	28,85	28,02	29,06	28,13	**28,52**	21,24	21,19	21,26	21,18	**21,22**
2.10	V-3A-C8-M-1	3A	1070	Composite beam	Fl 8 mm	Metallic pollutants	1	Succeeded	544,38	28,58	28,77	28,17	28,48	**28,50**	21,18	21,24	20,97	20,93	**21,08**
2.11	V-3A-C8-M-2	3A	1070	Composite beam	Fl 8 mm	Metallic pollutants	2	Succeeded	529,76	28,03	28,81	27,87	28,39	**28,28**	21,06	20,88	21,08	20,94	**20,99**
2.12	V-3A-C8-M-3	3A	1070	Composite beam	Fl 8 mm	Metallic pollutants	3	Succeeded	531,31	28,78	28,55	28,02	28,01	**28,34**	21,02	21,20	20,98	21,01	**21,05**
2.13	V-3A-C10-M-1	3A	1070	Composite beam	Fl 10 mm	Metallic pollutants	1	Succeeded	527,96	28,03	28,29	28,67	29,08	**28,52**	21,08	20,87	21,10	20,81	**20,97**
2.14	V-3A-C10-M-2	3A	1070	Composite beam	Fl 10 mm	Metallic pollutants	2	Succeeded	540,21	28,32	28,96	28,30	28,33	**28,48**	21,01	20,85	21,11	20,84	**20,95**
	V-3A-C10-M-3	3A	1070	Composite beam	Fl 10 mm	Metallic pollutants	3	Failed											

APPENDIX C

Number	Name beam	Fire round	Forming temperature (°C)	Type	Surface type: Float (Fl), Fritted (Fr)	Bulk type	Number of beam	Status before structural performance test	Mass (g)	Width (mm)					Height (mm)				
										Location 1	Location 2	Location 3	Location 4	Average	Location 1	Location 2	Location 3	Location 4	Average
	V-4A-CR8-C-1	4A	1070	Composite beam	Fr 8 mm	CSP pollutants	1	Failed											
2.15	V-4A-CR8-C-2	4A	1070	Composite beam	Fr 8 mm	CSP pollutants	2	Succeeded	530,06	28,26	28,11	28,72	28,59	**28,42**	20,70	20,83	20,74	21,03	**20,83**
2.16	V-4A-CR8-C-3	4A	1070	Composite beam	Fr 8 mm	CSP pollutants	3	Succeeded	535,36	28,63	28,25	28,19	28,48	**28,39**	20,92	20,92	20,94	21,08	**20,97**

Table 20: Overview beams with dimensions of Four-point bending test II

C - Overview beams with dimensions - Four point bending test III

Number	Name beam	Fire round	Forming temperature (°C)	Type	Surface type: Float (Fl), Fritted (Fr)	Bulk type	Number of beam	Status before structural performance test	Mass (g)	Width (mm)					Height (mm)				
										Location 1	Location 2	Location 3	Location 4	Average	Location 1	Location 2	Location 3	Location 4	Average
3.1	V-1C-H-M-1	1C	1070	Homogeneous beam	x	Metallic pollutants	1	succeeded	547,67	29,21	29,69	28,10	28,06	**28,77**	20,95	21,29	20,99	21,14	**21,09**
3.2	V-1C-H-M-2	1C	1070	Homogeneous beam	x	Metallic pollutants	2	succeeded	549,38	28,86	28,43	28,14	28,10	**28,38**	20,97	21,27	20,82	20,88	**20,99**
3.3	V-1C-H-M-3	1C	1070	Homogeneous beam	x	Metallic pollutants	3	succeeded	555,43	29,22	28,66	28,94	29,82	**29,16**	21,07	21,00	21,01	20,96	**21,01**
3.4	V-2D-C6-C-1	2D	1070	Composite beam	Fl 6 mm	CSP pollutants	1	succeeded	553,50	28,75	28,84	29,40	29,04	**29,01**	20,96	21,02	21,05	20,95	**21,00**
3.5	V-2D-C8-C-2	2D	1070	Composite beam	Fl 8 mm	CSP pollutants	2	succeeded	540,18	29,95	28,94	28,42	28,14	**28,86**	20,74	20,78	20,83	21,07	**20,86**
3.6	V-2D-C12-C-1	2D	1070	Composite beam	Fl 12 mm	CSP pollutants	1	succeeded	529,23	28,72	29,33	28,19	28,02	**28,57**	20,88	20,82	20,86	20,89	**20,86**
3.7	V-2D-C12-C-2	2D	1070	Composite beam	Fl 12 mm	CSP pollutants	2	succeeded	562,87	29,25	29,40	28,84	28,10	**28,90**	21,33	21,04	21,22	20,99	**21,15**
3.8	V-2D-C12-C-3	2D	1070	Composite beam	Fl 12 mm	CSP pollutants	3	succeeded	558,62	29,39	29,36	29,15	28,42	**29,08**	20,89	21,10	20,99	21,15	**21,03**
3.9	V-4A-CF8-M-1	4A	1070	Composite beam	Fr 8 mm	Metallic pollutants	1	succeeded	547,09	28,48	28,23	28,28	28,58	**28,39**	20,73	21,31	20,83	21,19	**21,02**
	V-4A-CF8-M-2	4A	1070	Composite beam	Fr 8 mm	Metallic pollutants	2	failed											
3.10	V-4A-CF8-M-3	4A	1070	Composite beam	Fr 8 mm	Metallic pollutants	3	succeeded	552,48	29,05	28,71	29,16	28,70	**28,91**	20,55	21,07	20,86	20,92	**20,85**

Table 21: Overview beams with dimensions of Four-point bending test III

C - Overview beams with dimensions - Four point bending test IV

Number	Name beam	Fire round	Forming temperature (°C)	Type	Surface type: Float (Fl), Fritted (Fr)	Bulk type	Number of beam	Status before structural performance test	Mass (g)	Width (mm)					Height (mm)				
										Location 1	Location 2	Location 3	Location 4	Average	Location 1	Location 2	Location 3	Location 4	Average
4.1	V-1D-H-FL-1	1D	1070	Homogeneous beam	Fl 6-8-6 mm	x	1	succeeded	539,08	28,75	28,79	28,64	28,51	**28,67**	21,12	21,10	21,26	21,31	**21,20**
4.2	V-1D-H-FL-2	1D	1070	Homogeneous beam	Fl 12-6 mm	x	2	succeeded	540,37	28,49	28,31	28,55	28,75	**28,53**	20,79	20,90	20,96	20,99	**20,91**
4.3	V-1D-H-FL-3	1D	1070	Homogeneous beam	Fl 6-8-6 mm	x	3	succeeded	538,44	28,73	28,51	28,73	28,50	**28,62**	21,00	20,92	21,12	20,95	**21,00**

Table 22: Overview beams with dimensions of Four-point bending test IV

APPENDIX D

D - Overview beams with photos - Four point bending test I

Number	Name beam	Fire round	Forming temperature (°C)	Type	Surface type: Float (Fl), Fritted (Fr)	Bulk type	Status before structural performance test	PHOTOS				
								Front view	Top view	Back view	Below view	Bird view
	V-1A-H-HR-1	1A	1120	Homogeneous beam	x	HR glass	Failed					
	V-1A-H-HR-2	1A	1120	Homogeneous beam	x	HR glass	Failed					
	V-1A-H-HR-3	1A	1120	Homogeneous beam	x	HR glass	Failed					
1.1	V-1A-H-C-1	1A	1120	Homogeneous beam	x	CSP pollutants	Succeeded					
1.2	V-1A-H-C-2	1A	1120	Homogeneous beam	x	CSP pollutants	Succeeded					
	V-1A-H-C-3	1A	1120	Homogeneous beam	x	CSP pollutants	Failed					
1.3	V-1B-H-F-1	1B	1120	Homogeneous beam	x	Fritted glass	Succeeded					
1.4	V-1B-H-F-2	1B	1120	Homogeneous beam	x	Fritted glass	Succeeded					
1.5	V-1B-H-F-3	1B	1120	Homogeneous beam	x	Fritted glass	Succeeded					
1.6	V-1B-H-HR-1	1B	1120	Homogeneous beam	x	HR glass	Succeeded					
	V-1B-H-S-1	1B	1120	Homogeneous beam	x	SNX 60/26 Coated	Failed					
1.7	V-1B-H-B-1	1B	1120	Homogeneous beam	x	Blue Solar light	Succeeded					
1.8	V-2A-C8-C-1	2A	1070	Composite beam	Fl 8 mm	CSP pollutants	Succeeded	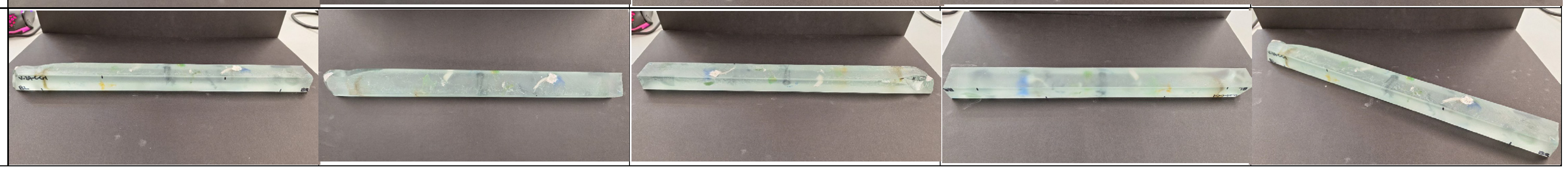				

APPENDIX D

Number	Name beam	Fire round	Forming temperature (°C)	Type	Surface type: Float (Fl), Fritted (Fr)	Bulk type	Status before structural performance test	PHOTOS				
								Front view	Top view	Back view	Below view	Bird view
	V-2A-C8-C-2	2A	1070	Composite beam	Fl 8 mm	CSP pollutants	Failed					
	V-2A-C8-C-3	2A	1070	Composite beam	Fl 8 mm	CSP pollutants	Failed					
1.9	V-2A-C10-C-1	2A	1070	Composite beam	Fl 10 mm	CSP pollutants	Succeeded	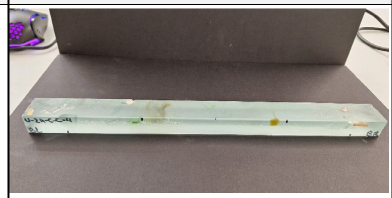		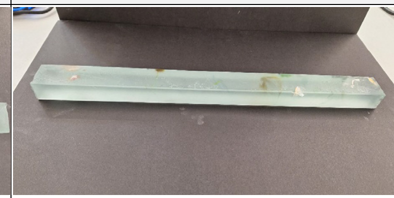		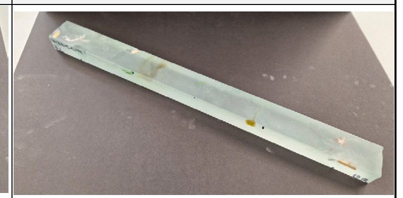
	V-2A-C10-C-2	2A	1070	Composite beam	Fl 10 mm	CSP pollutants	Failed					
	V-2A-C10-C-3	2A	1070	Composite beam	Fl 10 mm	CSP pollutants	Failed					
1.10	V-2A-C8-F-1	2A	1070	Composite beam	Fl 8 mm	Fritted glass	Failed			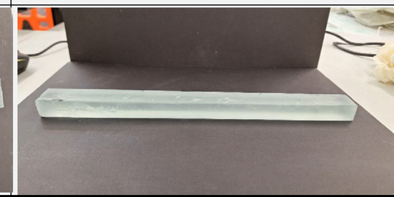		
1.11	V-2B-C6-C-1	2B	1070	Composite beam	Fl 6 mm	CSP pollutants	Succeeded	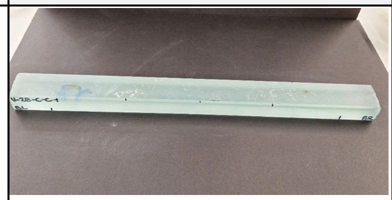				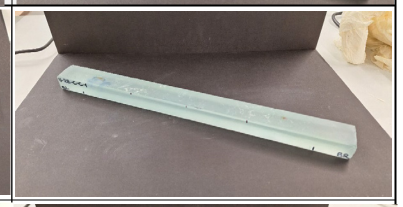
1.12	V-2B-C6-C-2	2B	1070	Composite beam	Fl 6 mm	CSP pollutants	Succeeded					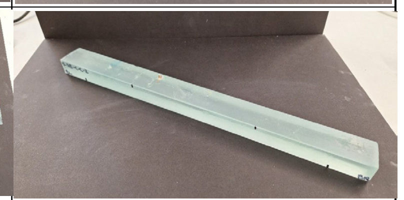
1.13	V-2B-C8-C-1	2B	1070	Composite beam	Fl 8 mm	CSP pollutants	Succeeded		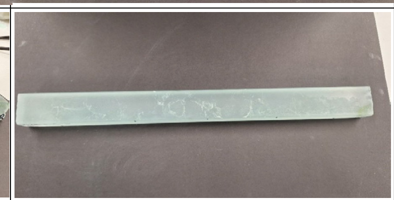			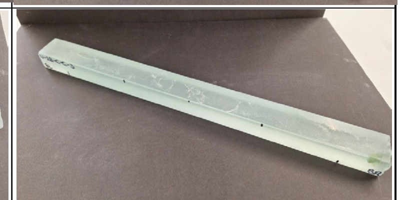
1.14	V-2B-C8-C-2	2B	1070	Composite beam	Fl 8 mm	CSP pollutants	Succeeded	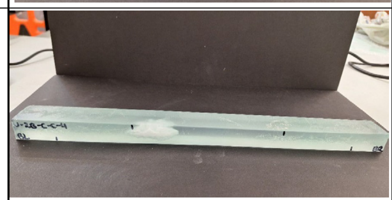	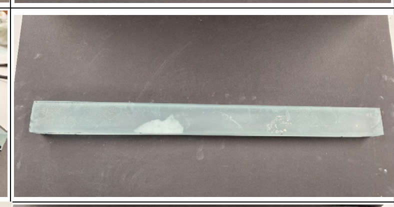	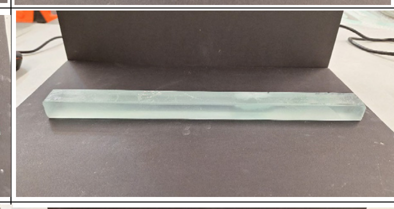		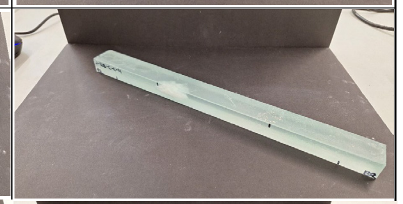
1.15	V-2B-C10-C-1	2B	1070	Composite beam	Fl 10 mm	CSP pollutants	Succeeded				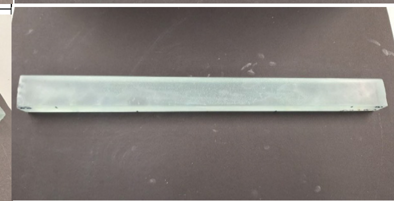	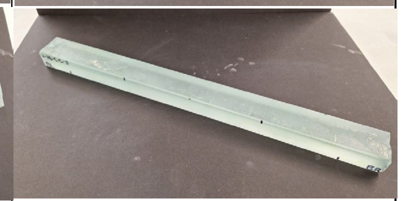
1.16	V-2B-C10-C-6	2B	1070	Composite beam	Fl 10 mm	CSP pollutants	Succeeded			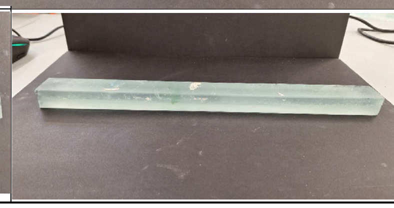		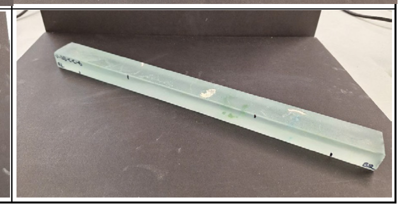

Table 23: Overview beams with photos of Four-point bending test I

APPENDIX D

D - Overview beams with photos - Four point bending test II

Number	Name beam	Fire round	Forming temperature (°C)	Type	Surface type: Float (Fl), Fritted (Fr)	Bulk type	Status before structural performance test	PHOTOS				
								Front view	Top view	Back view	Below view	Bird view
2.1	V-2C-C6-C-1	2C	1070 & 1120	Composite beam	Fl 6 mm	CSP pollutants	Succeeded					
2.2	V-2C-C6-C-2	2C	1070 & 1120	Composite beam	Fl 6 mm	CSP pollutants	Succeeded	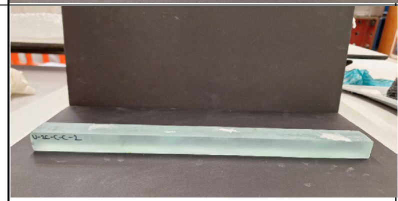		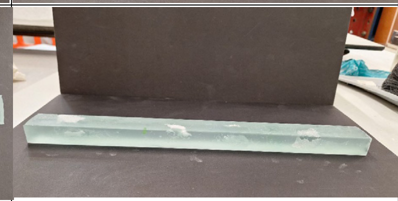		
	V-2C-C8-C-1	2C	1070 & 1120	Composite beam	Fl 8 mm	CSP pollutants	Failed					
2.3	V-2C-C8-C-2	2C	1070 & 1120	Composite beam	Fl 8 mm	CSP pollutants	Succeeded	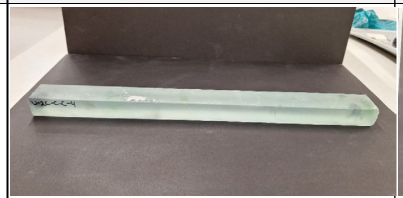				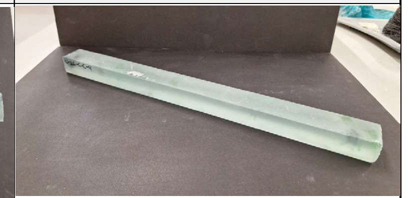
2.4	V-2C-C10-C-1	2C	1070 & 1120	Composite beam	Fl 10 mm	CSP pollutants	Succeeded			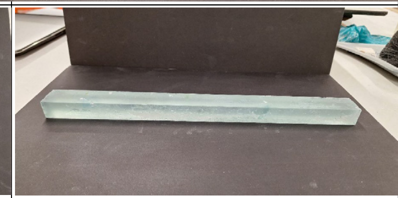	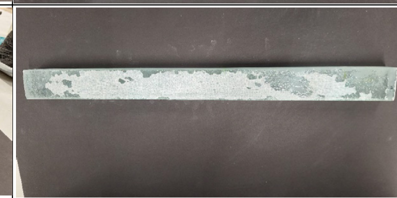	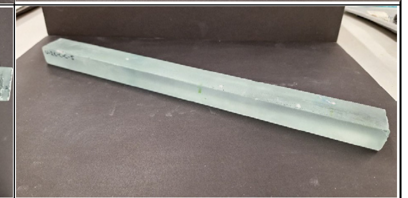
2.5	V-2C-C10-C-2	2C	1070 & 1120	Composite beam	Fl 10 mm	CSP pollutants	Succeeded	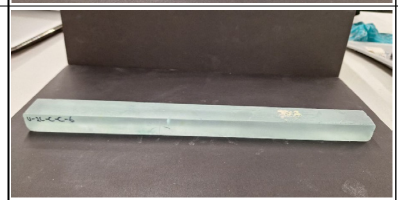	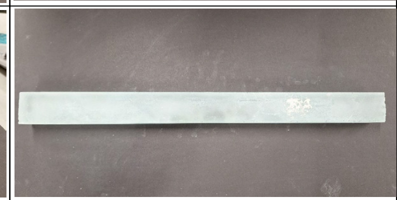			
2.6	V-2C-C12-C-1	2C	1070 & 1120	Composite beam	Fl 12 mm	CSP pollutants	Succeeded					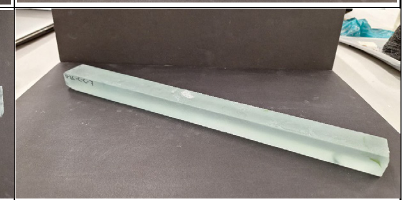
2.7	V-2C-C12-C-2	2C	1070 & 1120	Composite beam	Fl 12 mm	CSP pollutants	Succeeded			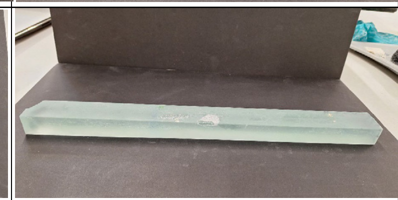		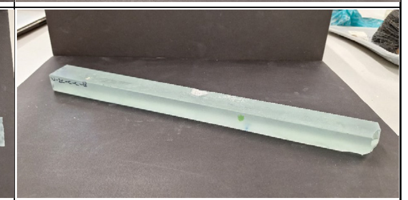
2.8	V-2D-C8-C-1	2D	1070	Composite beam	Fl 8 mm	CSP pollutants	Succeeded			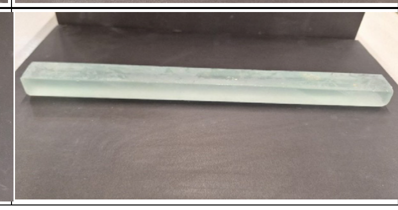		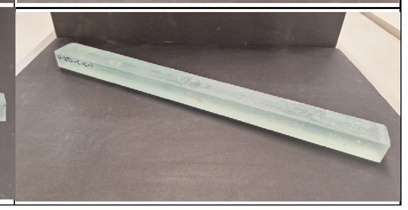

APPENDIX D

Number	Name beam	Fire round	Forming temperature (°C)	Type	Surface type: Float (Fl), Fritted (Fr)	Bulk type	Status before structural performance test	PHOTOS				
								Front view	Top view	Back view	Below view	Bird view
2.9	V-2D-C10-C-1	2D	1070	Composite beam	Fl 10 mm	CSP pollutants	Succeeded	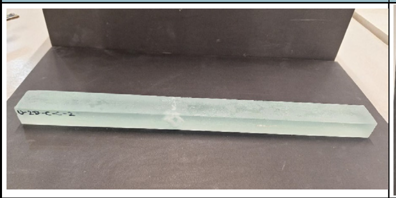		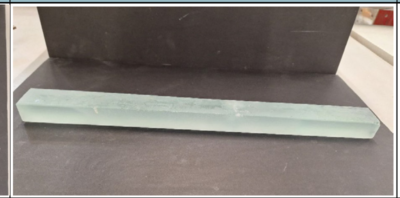		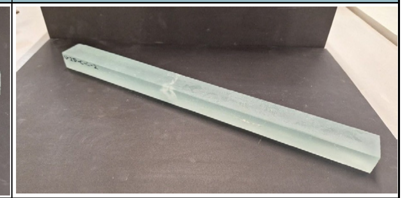
2.10	V-3A-C8-M-1	3A	1070	Composite beam	Fl 8 mm	Metallic pollutants	Succeeded	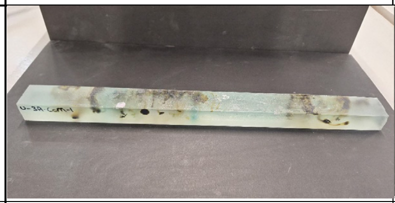		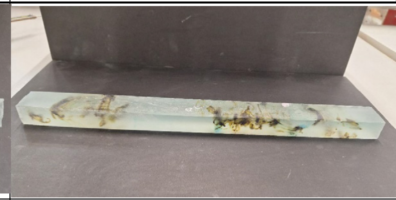		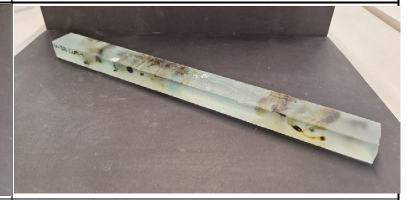
2.11	V-3A-C8-M-2	3A	1070	Composite beam	Fl 8 mm	Metallic pollutants	Succeeded			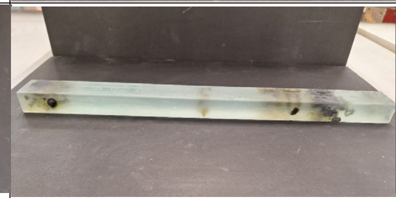		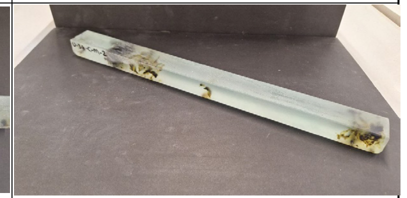
2.12	V-3A-C8-M-3	3A	1070	Composite beam	Fl 8 mm	CSP pollutants	Succeeded	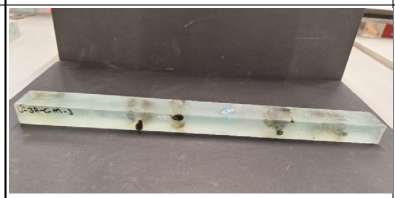				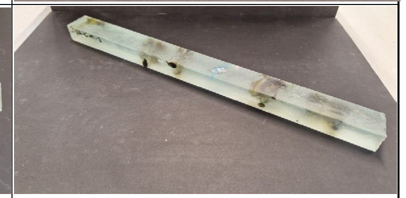
2.13	V-3A-C10-M-1	3A	1070	Composite beam	Fl 10 mm	Metallic pollutants	Succeeded	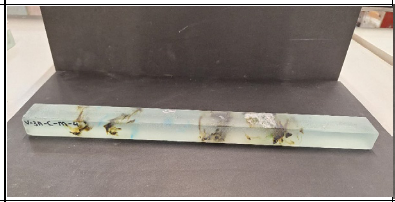		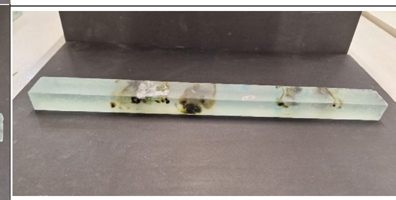		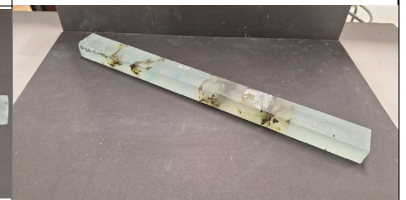
2.14	V-3A-C10-M-2	3A	1070	Composite beam	Fl 10 mm	Metallic pollutants	Succeeded	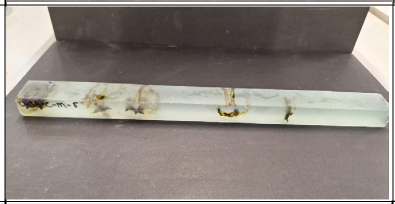		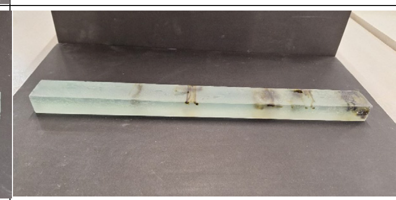		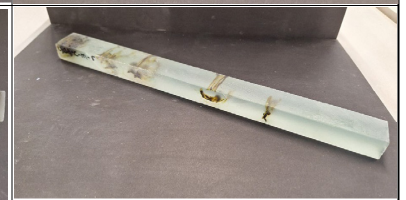
	V-3A-C10-M-3	3A	1070	Composite beam	Fl 10 mm	Metallic pollutants	Failed					
	V-4A-CR8-C-1	4A	1070	Composite beam	Fr 8 mm	CSP pollutants	Failed					
2.15	V-4A-CR8-C-2	4A	1070	Composite beam	Fr 8 mm	CSP pollutants	Succeeded	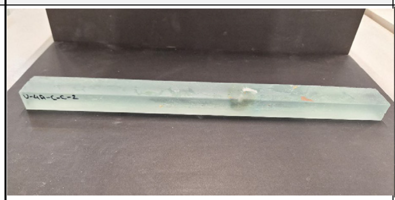				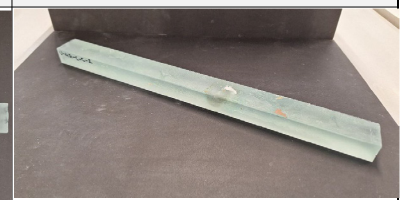
2.16	V-4A-CR8-C-3	4A	1070	Composite beam	Fr 8 mm	CSP pollutants	Succeeded	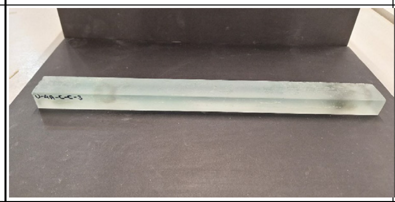		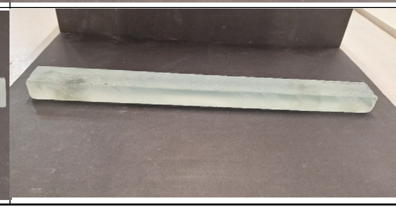	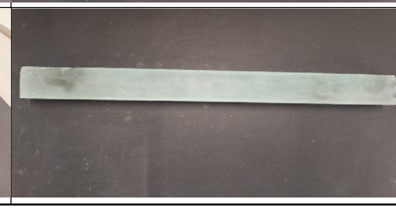	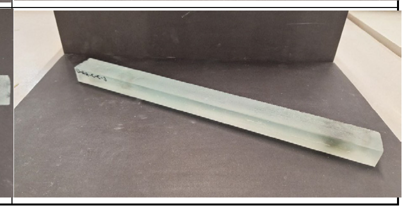

Table 24: Overview beams with photos of Four-point bending test II

APPENDIX D

D - Overview beams with photos - Four point bending test III

Number	Name beam	Fire round	Forming temperature (°C)	Type	Surface type: Float (Fl), Fritted (Fr)	Bulk type	Status before structural performance test	PHOTOS				
								Front view	Top view	Back view	Below view	Bird view
3.1	V-1C-H-M-1	1C	1070	Homogeneous beam	x	Metallic pollutants	succeeded					
3.2	V-1C-H-M-2	1C	1070	Homogeneous beam	x	Metallic pollutants	succeeded			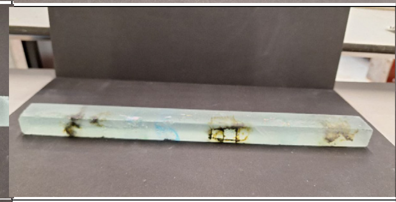		
3.3	V-1C-H-M-3	1C	1070	Homogeneous beam	x	Metallic pollutants	succeeded		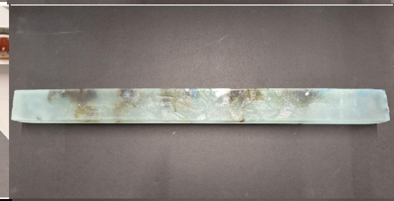			
3.4	V-2D-C6-C-1	2D	1070	Composite beam	Fl 6 mm	CSP pollutants	succeeded			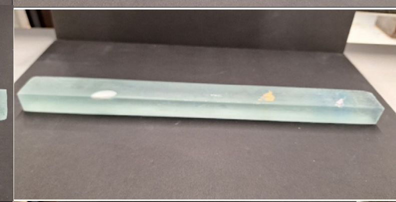		
3.5	V-2D-C8-C-2	2D	1070	Composite beam	Fl 8 mm	CSP pollutants	succeeded					
3.6	V-2D-C12-C-1	2D	1070	Composite beam	Fl 12 mm	CSP pollutants	succeeded					
3.7	V-2D-C12-C-2	2D	1070	Composite beam	Fl 12 mm	CSP pollutants	succeeded					
3.8	V-2D-C12-C-3	2D	1070	Composite beam	Fl 12 mm	CSP pollutants	succeeded			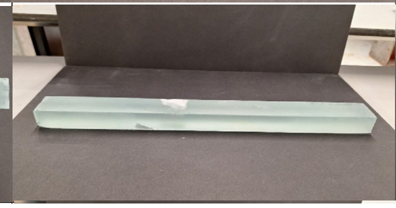		

APPENDIX D

Number	Name beam	Fire round	Forming temperature (°C)	Type	Surface type: Float (Fl), Fritted (Fr)	Bulk type	Status before structural performance test	PHOTOS				
								Front view	Top view	Back view	Below view	Bird view
3.9	V-4A-CR8-M-1	4A	1070	Composite beam	Fr 8 mm	Metallic pollutants	succeeded					
	V-4A-CR8-M-2	4A	1070	Composite beam	Fr 8 mm	Metallic pollutants	failed	Machining				
3.10	V-4A-CR8-M-3	4A	1070	Composite beam	Fr 8 mm	Metallic pollutants	succeeded	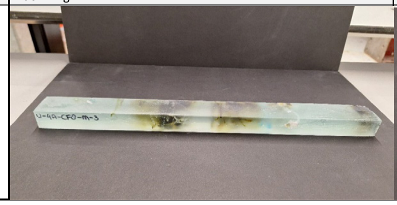		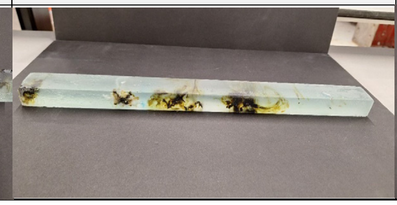		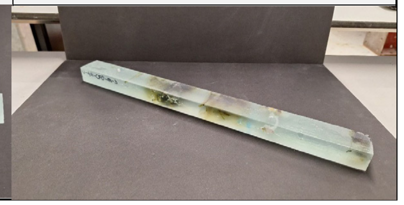

Table 25: Overview beams with photos of Four-point bending test III

D - Overview beams with photos - Four point bending test IV

Number	Name beam	Fire round	Forming temperature (°C)	Type	Surface type: Float (Fl), Fritted (Fr)	Bulk type	Status before structural performance test	PHOTOS				
								Front view	Top view	Back view	Below view	Bird view
4.1	V-1D-H-FL-1	1D	1070	Homogeneous beam	Fl 6-8-6 mm	x	succeeded			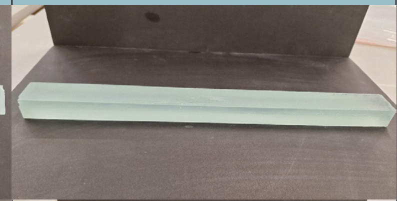		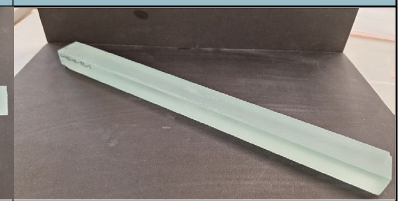
4.2	V-1D-H-FL-2	1D	1070	Homogeneous beam	Fl 12-6 mm	x	succeeded			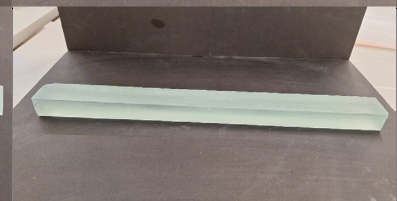		
4.3	V-1D-H-FL-3	1D	1070	Homogeneous beam	Fl 6-8-6 mm	x	succeeded	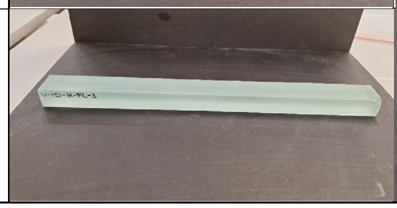				

Table 26: Overview beams with photos of Four-point bending test IV

APPENDIX E

E - Overview beams with structural performance - Four point bending test I, II, III and and IV

Beam information						Dimensions			F_{max}	Flexural strength (σ)	Flexural strength (incl. frictional constraint of	Moment of Inertia (I)	Strength at support (σ)
						Width (average)	Height (average)	h^3					
	Name	Forming temperature	Type	Surface type: Float (Fl), Fritted (Fr)	Bulk type	mm	mm	mm^3	N	Mpa	Mpa	mm^4	Mpa
Four-point bending test I													
Specimen 1.1	V-1A-H-C-1	1120	Homogeneous beam	x	CSP Pollutants	28,65	21,02	9287	985,10	**16,34**	**15,61**	**22172**	**16,34**
Specimen 1.2	V-1A-H-C-2	1120	Homogeneous beam	x	CSP Pollutants	28,94	20,95	9198	943,18	**15,59**	**14,89**	**22179**	**15,59**
Specimen 1.3	V-1B-H-F-1	1120	Homogeneous beam	x	Fritted glass	28,19	21,46	9876	1406,07	**22,75**	**21,71**	**23203**	**22,75**
Specimen 1.4	V-1B-H-F-2	1120	Homogeneous beam	x	Fritted glass	28,86	21,01	9278	1520,67	**25,06**	**23,93**	**22313**	**25,06**
Specimen 1.5	V-1B-H-F-3	1120	Homogeneous beam	x	Fritted glass	28,44	20,97	9221	1283,32	**21,55**	**20,58**	**21851**	**21,55**
Specimen 1.6	V-1B-H-HR-1	1120	Homogeneous beam	x	Heat resistant glass	28,15	20,82	9028	1727,66	**29,73**	**28,40**	**21177**	**29,73**
Specimen 1.7	V-1B-H-B-1	1120	Homogeneous beam	x	Soft coating	28,45	20,99	9248	2396,02	**40,14**	**38,34**	**21925**	**40,14**
Specimen 1.8	V-2A-C8-C-1	1070	Composite beam	Fl 8 mm	CSP Pollutants	29,13	21,29	9643	3614,51	**57,51**	**54,89**	**23409**	**57,51**
Specimen 1.9	V-2A-C10-C-1	1070	Composite beam	Fl 10 mm	CSP Pollutants	28,69	21,17	9491	2341,23	**38,23**	**36,49**	**22694**	**38,23**
Specimen 1.10	V-2A-C8-F-1	1070	Composite beam	Fl 8 mm	Fritted glass	28,68	21,29	9653	2828,71	**45,69**	**43,60**	**23072**	**45,69**
Specimen 1.11	V-2B-C6-C-1	1070	Composite beam	Fl 6 mm	CSP Pollutants	29,14	21,18	9498	3037,20	**48,81**	**46,59**	**23062**	**48,81**
Specimen 1.12	V-2B-C6-C-2	1070	Composite beam	Fl 6 mm	CSP Pollutants	28,93	20,85	9067	2354,92	**39,32**	**37,56**	**21856**	**39,32**
Specimen 1.13	V-2B-C8-C-1	1070	Composite beam	Fl 8 mm	CSP Pollutants	29,22	21,09	9384	3287,72	**53,11**	**50,71**	**22852**	**53,11**
Specimen 1.14	V-2B-C8-C-2	1070	Composite beam	Fl 8 mm	CSP Pollutants	28,93	21,11	9411	2800,59	**45,61**	**43,55**	**22686**	**45,61**
Specimen 1.15	V-2B-C10-C-1	1070	Composite beam	Fl 10 mm	CSP Pollutants	28,55	20,99	9244	2120,24	**35,41**	**33,82**	**21992**	**35,41**
Specimen 1.16	V-2B-C10-C-2	1070	Composite beam	Fl 10 mm	CSP Pollutants	27,97	21,01	9268	1953,31	**33,25**	**31,75**	**21597**	**33,25**
Four-point bending test II													
Specimen 2.1	V-2C-C6-C-1	1070 & 1120	Composite beam	Fl 6 mm	CSP pollutants	28,97	21,00	9261	2571,66	**42,27**	**40,37**	**22358**	**42,27**
Specimen 2.2	V-2C-C6-C-2	1070 & 1120	Composite beam	Fl 6 mm	CSP pollutants	28,68	20,81	9012	2674,86	**45,23**	**43,21**	**21538**	**45,23**
Specimen 2.3	V-2C-C8-C-2	1070 & 1120	Composite beam	Fl 8 mm	CSP pollutants	28,31	21,06	9341	2821,64	**47,19**	**45,06**	**22036**	**47,19**
Specimen 2.4	V-2C-C10-C-1	1070 & 1120	Composite beam	Fl 10 mm	CSP pollutants	28,53	20,86	9077	2118,06	**35,83**	**34,23**	**21581**	**35,83**
Specimen 2.5	V-2C-C10-C-2	1070 & 1120	Composite beam	Fl 10 mm	CSP pollutants	28,60	21,03	9301	659,67	**10,95**	**10,46**	**22167**	**10,95**
Specimen 2.6	V-2C-C12-C-1	1070 & 1120	Composite beam	Fl 12 mm	CSP pollutants	28,52	21,00	9261	2789,04	**46,57**	**44,47**	**22010**	**46,57**
Specimen 2.7	V-2C-C12-C-2	1070 & 1120	Composite beam	Fl 12 mm	CSP pollutants	28,35	21,04	9314	2611,49	**43,70**	**41,73**	**22004**	**43,70**
Specimen 2.8	V-2D-C8-C-1	1070	Composite beam	Fl 8 mm	CSP pollutants	27,29	21,08	9367	1521,46	**26,35**	**25,16**	**21303**	**26,35**
Specimen 2.9	V-2D-C10-C-1	1070	Composite beam	Fl 10 mm	CSP pollutants	28,52	21,22	9555	1170,20	**19,14**	**18,27**	**22709**	**19,14**
Specimen 2.10	V-3A-C8-M-1	1070	Composite beam	Fl 8 mm	Metallic pollutants	28,50	21,08	9367	1391,16	**23,07**	**22,03**	**22247**	**23,07**
Specimen 2.11	V-3A-C8-M-2	1070	Composite beam	Fl 8 mm	Metallic pollutants	28,28	20,99	9248	1738,97	**29,31**	**27,99**	**21794**	**29,31**
Specimen 2.12	V-3A-C8-M-3	1070	Composite beam	Fl 8 mm	Metallic pollutants	28,34	21,05	9327	2343,32	**39,19**	**37,42**	**22028**	**39,19**
Specimen 2.13	V-3A-C10-M-1	1070	Composite beam	Fl 10 mm	Metallic pollutants	28,52	20,97	9221	1228,95	**20,58**	**19,65**	**21916**	**20,58**
Specimen 2.14	V-3A-C10-M-2	1070	Composite beam	Fl 10 mm	Metallic pollutants	28,48	20,95	9195	2315,96	**38,91**	**37,16**	**21823**	**38,91**
Specimen 2.15	V-4A-CR8-C-2	1070	Composite beam	Fr 8 mm	CSP pollutants	28,42	20,83	9038	939,12	**15,99**	**15,28**	**21405**	**15,99**
Specimen 2.16	V-4A-CR8-C-3	1070	Composite beam	Fr 8 mm	CSP pollutants	28,39	20,97	9221	2253,66	**37,91**	**36,21**	**21816**	**37,91**
Four-point bending test III													
Specimen 3.1	V-1C-H-M-1	1070	Homogeneous beam	x	Metallic pollutants	28,77	21,09	9384	1361,93	**14,28**	**13,63**	**22494**	**14,28**
Specimen 3.2	V-1C-H-M-2	1070	Homogeneous beam	x	Metallic pollutants	28,38	20,99	9241	1195,99	**20,09**	**19,19**	**21857**	**20,09**
Specimen 3.3	V-1C-H-M-3	1070	Homogeneous beam	x	Metallic pollutants	29,16	21,01	9274	1977,97	**32,27**	**30,82**	**22536**	**32,27**
Specimen 3.4	V-2D-C6-C-1	1070	Composite beam	Fl 6 mm	CSP Pollutants	29,01	21,00	9254	1993,25	**32,74**	**31,26**	**22371**	**32,74**
Specimen 3.5	V-2D-C8-C-2	1070	Composite beam	Fl 8 mm	CSP Pollutants	28,86	20,86	9070	2315,91	**38,74**	**37,01**	**21816**	**38,74**
Specimen 3.6	V-2D-C12-C-1	1070	Composite beam	Fl 12 mm	CSP Pollutants	28,57	20,86	9080	2960,82	**50,01**	**47,78**	**21615**	**50,01**
Specimen 3.7	V-2D-C12-C-2	1070	Composite beam	Fl 12 mm	CSP Pollutants	28,90	21,15	9454	3009,14	**48,91**	**46,69**	**22767**	**48,91**
Specimen 3.8	V-2D-C12-C-3	1070	Composite beam	Fl 12 mm	CSP Pollutants	29,08	21,03	9304	1137,10	**18,56**	**17,73**	**22547**	**18,56**
Specimen 3.9	V-4A-CR8-M-1	1070	Composite beam	Fr 8 mm	Metallic pollutants	28,39	21,02	9281	508,20	**8,51**	**8,13**	**21959**	**8,51**
Specimen 3.10	V-4A-CR8-M-3	1070	Composite beam	Fr 8 mm	Metallic pollutants	28,91	20,85	9064	870,05	**14,54**	**13,89**	**21833**	**14,54**

APPENDIX E

Beam information						Dimensions			F_{max}	Flexural strength (σ)	Flexural strength (incl. frictional constraint of	Moment of Inertia (I)	Strength at support (σ)
						Width (average)	Height (average)	h^3					
	Name	Forming temperature	Type	Surface type: Float (Fl), Fritted (Fr)	Bulk type	mm	mm	mm^3	N	Mpa	Mpa	mm^4	Mpa
Four-point bending test IV													
Specimen 4.1	V-1D-Fl-H-1	1070	Homogeneous beam	Fl 6-8-6 mm	x	28,67	21,2	9528	2487,97	**40,55**	**38,71**	**22764**	**40,55**
Specimen 4.2	V-1D-Fl-H-2	1070	Homogeneous beam	Fl 12-6 mm	x	28,53	20,91	9142	2995,44	**50,43**	**48,17**	**21736**	**50,43**
Specimen 4.3	V-1D-Fl-H-3	1070	Homogeneous beam	Fl 6-8-6 mm	x	28,62	21	9261	3133,15	**52,13**	**49,78**	**22087**	**52,13**

Table 27: Overview beams with their structural performance during Fire Round I, II, III and IV

APPENDIX F

F - Overview beams with failure analysis - Four point bending test I

Number	Name beam	Fire round	Forming temperature (°C)	Type	Surface type: Float (Fl), Fritted (Fr)	Bulk type	Status before structural performance test	Reason	Flexural strength (σ) (Mpa)	Location of the failure (left, centre, right)	Fracture origin distance from middle, horizontal (mm) Left = - , Right = +	Fracture origin distance from botom, vertical (mm)	Fracture origin distance from back to front, horizontal (mm)	Type of crack: Stress level	Type of crack: Shape	Photo
	V-1A-H-HR-1	1A	1120	Homogeneous beam	x	HR glass	Failed	Ceramic inclusions								
	V-1A-H-HR-2	1A	1120	Homogeneous beam	x	HR glass	Failed	Ceramic inclusions								
	V-1A-H-HR-3	1A	1120	Homogeneous beam	x	HR glass	Failed	Ceramic inclusions								
1.1	V-1A-H-C-1	1A	1120	Homogeneous beam	x	CSP pollutants	Succeeded		16,34	Centre	4	8,4	7,6	Low energy failure	Compression curl	
1.2	V-1A-H-C-2	1A	1120	Homogeneous beam	x	CSP pollutants	Succeeded		15,57	Left	-57,6	0	22	Low energy failure	Compression curl	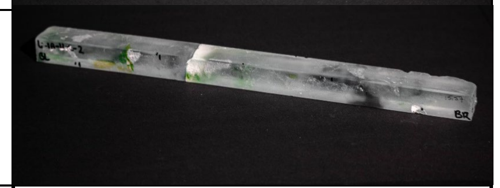
	V-1A-H-C-3	1A	1120	Homogeneous beam	x	CSP pollutants	Failed	Silicone inclusions								
1.3	V-1B-H-F-1	1B	1120	Homogeneous beam	x	Fritted glass	Succeeded		21,69	Right, Break at or near load pin, beware of misallignments or twisting errors	60	0	12,2	Medium - high energy failure	Compression curl	
1.4	V-1B-H-F-2	1B	1120	Homogeneous beam	x	Fritted glass	Succeeded		25,06	Right, primary - origin near, but not directly at load pin	60,8	0	4,3	Medium - high energy failure	Compression curl	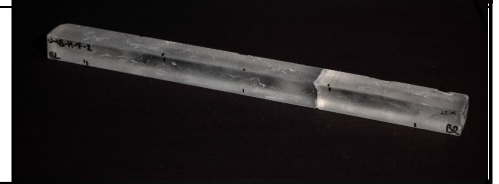
1.5	V-1B-H-F-3	1B	1120	Homogeneous beam	x	Fritted glass	Succeeded		21,55	Right	20,7	0	3,4	Low energy failure	Compression curl	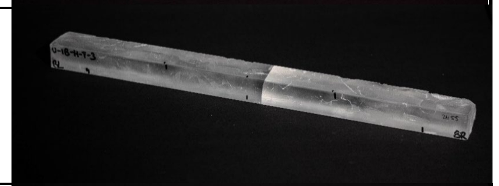
1.6	V-1B-H-HR-1	1B	1120	Homogeneous beam	x	HR glass	Succeeded		29,3	Left, primary - origin near, but not directly at load pin	-47,4	2,5	0	Medium - high energy failure	Compression curl	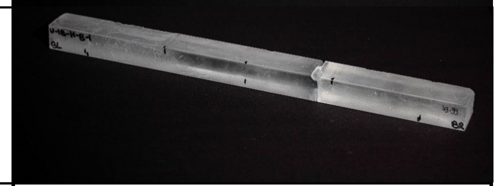
	V-1B-H-S-1	1B	1120	Homogeneous beam	x	SNX 60/26 Coated	Succeeded	Silicone inclusions								
1.7	V-1B-H-B-1	1B	1120	Homogeneous beam	x	Blue Solar light	Succeeded		40	Right, primary - origin near, but not directly at load pin	59	0	3	Medium - high energy failure	Compression curl	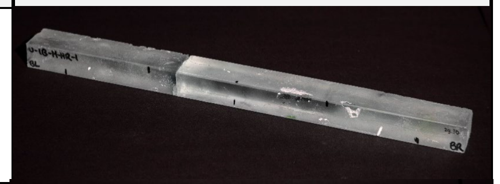
1.8	V-2A-C8-C-1	2A	1070	Composite beam	Fl 8 mm	CSP pollutants	Succeeded		57,51	Centre	-5,5	2	0	High energy failure	Double compression curl	
	V-2A-C8-C-2	2A	1070	Composite beam	Fl 8 mm	CSP pollutants	Failed	Silicone inclusions								
	V-2A-C8-C-3	2A	1070	Composite beam	Fl 8 mm	CSP pollutants	Failed	Silicone inclusions								

APPENDIX F

Number	Name beam	Fire round	Forming temperature (°C)	Type	Surface type: Float (Fl), Fritted (Fr)	Bulk type	Status before structural performance test	Reason	Flexural strength (σ) (Mpa)	Location of the failure (left, centre, right)	Fracture origin distance from middle, horizontal (mm)	Fracture origin distance from botom, vertical (mm)	Fracture origin distance from back to front, horizontal (mm)	Type of crack		Photo
											Left = - , Right = +			Stress level	Shape	
1.9	V-2A-C10-C-1	2A	1070	Composite beam	Fl 10 mm	CSP pollutants	Succeeded		38,09	Right, Break at or near load pin, beware of misallignments or twisting errors	60	0	10.3	Medium - high energy failure	Compression curl	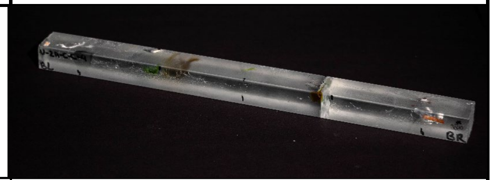
	V-2A-C10-C-2	2A	1070	Composite beam	Fl 10 mm	CSP pollutants	Failed	Silicone inclusions								
	V-2A-C10-C-3	2A	1070	Composite beam	Fl 10 mm	CSP pollutants	Failed	Silicone inclusions								
1.10	V-2A-C8-F-1	2A	1070	Composite beam	Fl 8 mm	Fritted glass	Succeeded		45,69	Left	-47,4	0	2,5	High energy failure	Double compression curl	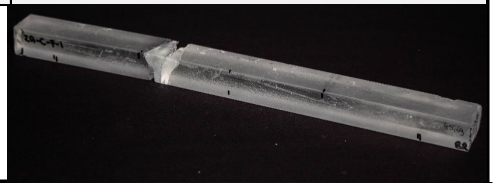
1.11	V-2B-C6-C-1	2B	1070	Composite beam	Fl 6 mm	CSP pollutants	Succeeded		48,16	Right	66,8	0	27,4	High energy failure	Double compression curl	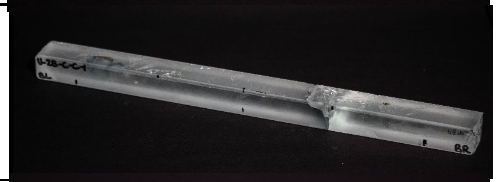
1.12	V-2B-C6-C-2	2B	1070	Composite beam	Fl 6 mm	CSP pollutants	Succeeded		39,06	Right	36	1,7	0	High energy failure	Double compression curl	
1.13	V-2B-C8-C-1	2B	1070	Composite beam	Fl 8 mm	CSP pollutants	Succeeded		52,42	Right	47,2	1,5	28	High energy failure	Double compression curl	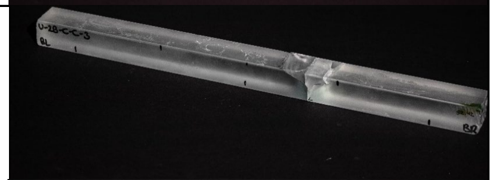
1.14	V-2B-C8-C-2	2B	1070	Composite beam	Fl 8 mm	CSP pollutants	Succeeded		45,61	Centre	-16,5	0	1,8	High energy failure	Double compression curl	
1.15	V-2B-C10-C-1	2B	1070	Composite beam	Fl 10 mm	CSP pollutants	Succeeded		35,39	Left	48,1	0	19,5	High energy failure	Double compression curl	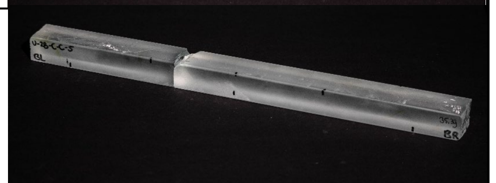
1.16	V-2B-C10-C-2	2B	1070	Composite beam	Fl 10 mm	CSP pollutants	Succeeded		31,91	Right	20,9	0	21,1	Low energy failure	Compression curl	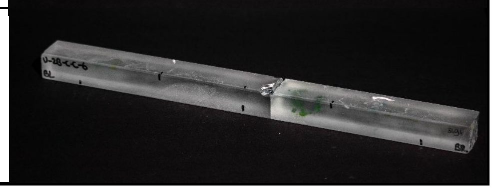

Table 28: Overview beams with failure analysis for Four-point bending test I

APPENDIX F

F - Overview beams with failure analysis - Four point bending test II

Number	Name beam	Fire round	Forming temperature (°C)	Type	Surface type: Float (Fl), Fritted (Fr)	Bulk type	Status before structural performance test	Reason	Flexural strength (σ) (Mpa)	Location of the failure (left, centre, right)	Fracture origin distance from middle, horizontal (mm)	Fracture origin distance from botom, vertical (mm)	Fracture origin distance from back to front, horizontal (mm)	Type of crack		Photo
											Left = - , Right = +			Stress level	Shape	
2.1	V-2C-C6-C-1	2C	1070 & 1120	Composite beam	Fl 6 mm	CSP pollutants	Succeeded		42,27	Right	31,4	1,3	28	High energy failure	Double compression curl	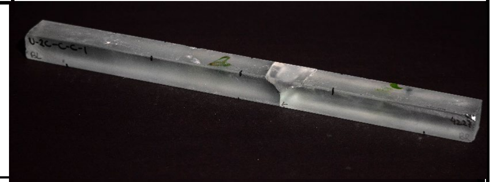
2.2	V-2C-C6-C-2	2C	1070 & 1120	Composite beam	Fl 6 mm	CSP pollutants	Succeeded		45,23	Left	-52,6	0	28	High energy failure	Double compression curl	
	V-2C-C8-C-1	2C	1070 & 1120	Composite beam	Fl 8 mm	CSP pollutants	Failed	Ceramic inclusion								
2.3	V-2C-C8-C-2	2C	1070 & 1120	Composite beam	Fl 8 mm	CSP pollutants	Succeeded		47,19	Right	57,3	0	27,5	High energy failure	Double compression curl	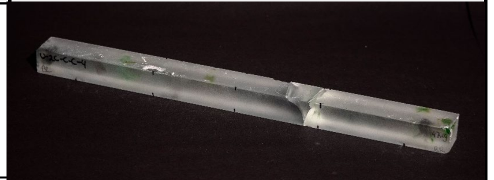
2.4	V-2C-C10-C-1	2C	1070 & 1120	Composite beam	Fl 10 mm	CSP pollutants	Succeeded		35,83	Right	51	0	25,7	Low energy failure	Compression curl	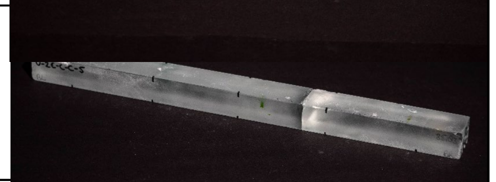
2.5	V-2C-C10-C-2	2C	1070 & 1120	Composite beam	Fl 10 mm	CSP pollutants	Succeeded		10,95	Left	-44,4	0	17,4	Low energy failure	Compression curl	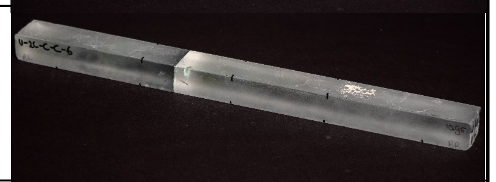
2.6	V-2C-C12-C-1	2C	1070 & 1120	Composite beam	Fl 12 mm	CSP pollutants	Succeeded		46,57	Right, Break at or near load pin, beware of misallignments or twisting	79,4	1,5	28	Medium - High energy failure	Compression curl	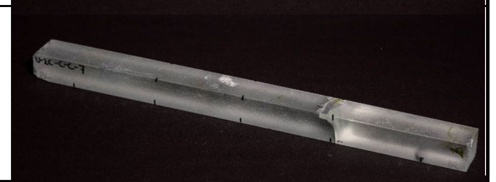
2.7	V-2C-C12-C-2	2C	1070 & 1120	Composite beam	Fl 12 mm	CSP pollutants	Succeeded		43,7	Right	22,8	0	0	High energy failure	Double compression curl	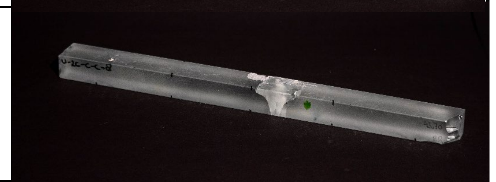
2.8	V-2D-C8-C-1	2D	1070	Composite beam	Fl 8 mm	CSP pollutants	Succeeded		26,35	Centre	-2,6	0	2,7	Low energy failure	Compression curl	
2.9	V-2D-C10-C-1	2D	1070	Composite beam	Fl 10 mm	CSP pollutants	Succeeded		19,14	Centre	4,3	0	26,6	Low energy failure	Compression curl	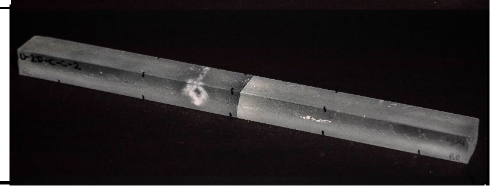

APPENDIX F

Number	Name beam	Fire round	Forming temperature (°C)	Type	Surface type: Float (Fl), Fritted (Fr)	Bulk type	Status before structural performance test	Reason	Flexural strength (σ) (Mpa)	Location of the failure (left, centre, right)	Fracture origin distance from middle, horizontal (mm)	Fracture origin distance from botom, vertical (mm)	Fracture origin distance from back to front, horizontal (mm)	Type of crack		Photo
											Left = - , Right = +			Stress level	Shape	
2.10	V-3A-C8-M-1	3A	1070	Composite beam	Fl 8 mm	Metallic pollutants	Succeeded		23,07	Left	-41,5	0	2,6	Low energy failure	Compression curl	
2.11	V-3A-C8-M-2	3A	1070	Composite beam	Fl 8 mm	Metallic pollutants	Succeeded		29,31	Right	50	0	24,1	Medium - High energy failure	Double compression curl with long perpendicular line	
2.12	V-3A-C8-M-3	3A	1070	Composite beam	Fl 8 mm	Metallic pollutants	Succeeded		39,19	Right	-39,5	1,4	0	High energy failure	Double compression curl	
2.13	V-3A-C10-M-1	3A	1070	Composite beam	Fl 10 mm	Metallic pollutants	Succeeded		20,58	Right	24,5	2	0	Low energy failure	Compression curl	
2.14	V-3A-C10-M-2	3A	1070	Composite beam	Fl 10 mm	Metallic pollutants	Succeeded		38,91	Left, Break at or near load pin, beware of misallignments or twisting	-71,8	1,4	28	Low energy failure	Compression curl	
	V-3A-C10-M-3	3A	1070	Composite beam	Fl 10 mm	Metallic pollutants	Failed	Ceramic inclusion								
	V-4A-CR8-C-1	4A	1070	Composite beam	Fr 8 mm	CSP pollutants	Failed	Ceramic inclusion								
2.15	V-4A-CR8-C-2	4A	1070	Composite beam	Fr 8 mm	CSP pollutants			15,99	Left	-80	0	1,7	Low energy failure	Compression curl	
2.16	V-4A-CR8-C-3	4A	1070	Composite beam	Fr 8 mm	CSP pollutants			37,91	Right	11,5	1,5	0	High energy failure	Double compression curl	

Table 29: Overview beams with failure analysis for Four-point bending test II

F - Overview beams with failure analysis - Four point bending test III

Number	Name beam	Fire round	Forming temperature (°C)	Type	Surface type: Float (Fl), Fritted (Fr)	Bulk type	Status before structural performance test	Reason	Flexural strength (σ) (Mpa)	Location of the failure (left, centre, right)	Fracture origin distance from middle, horizontal (mm)	Fracture origin distance from botom, vertical (mm)	Fracture origin distance from back to front, horizontal (mm)	Type of crack		Photo
											Left = - , Right = +			Stress level	Shape	
3.1	V-1C-H-M-1	1C	1070	Homogeneous beam	x	Metallic pollutants	succeeded		14,28	Right	18,1	0	6,7	Low energy failure	Compression curl	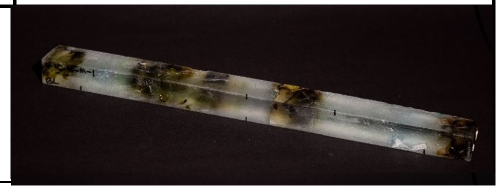

APPENDIX F

Number	Name beam	Fire round	Forming temperature (°C)	Type	Surface type: Float (Fl), Fritted (Fr)	Bulk type	Status before structural performance test	Reason	Flexural strength (σ) (Mpa)	Location of the failure (left, centre, right)	Fracture origin distance from middle, horizontal (mm) Left = - , Right = +	Fracture origin distance from botom, vertical (mm)	Fracture origin distance from back to front, horizontal (mm)	Type of crack		Photo
														Stress level	Shape	
3.2	V-1C-H-M-2	1C	1070	Homogeneous beam	x	Metallic pollutants	succeeded		20,09	Left	-24,1	5,5	22,7	Low energy failure	Compression curl	
3.3	V-1C-H-M-3	1C	1070	Homogeneous beam	x	Metallic pollutants	succeeded		32,27	Right, Break at or near load pin, beware of misallignments or twisting	62,2	0	3	Medium - High energy f	Double compression curl, with long perpendicular line	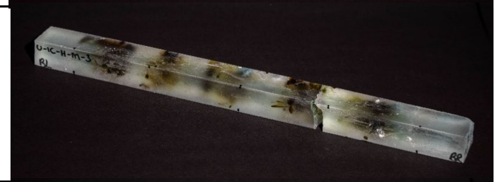
3.4	V-2D-C6-C-1	2D	1070	Composite beam	Fl 6 mm	CSP pollutants	succeeded		32,74	Right	9,3	0	27,4	Medium - High energy failure	Double compression curl, with long perpendicular line	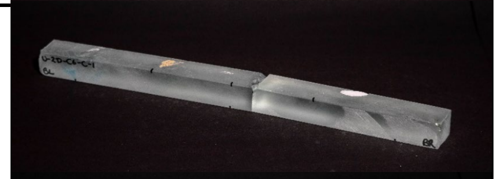
3.5	V-2D-C8-C-2	2D	1070	Composite beam	Fl 8 mm	CSP pollutants	succeeded		38,74	Right	11,4	1,4	0	High energy failure	Double compression curl	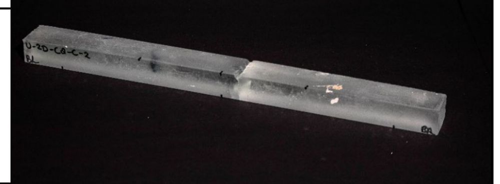
3.6	V-2D-C12-C-1	2D	1070	Composite beam	Fl 12 mm	CSP pollutants	succeeded		50,01	Centre	2,7	0	0	High energy failure	Double compression curl	
3.7	V-2D-C12-C-2	2D	1070	Composite beam	Fl 12 mm	CSP pollutants	succeeded		48,91	Right	41	0	26,6	High energy failure	Double compression curl	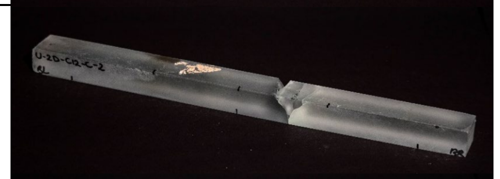
3.8	V-2D-C12-C-3	2D	1070	Composite beam	Fl 12 mm	CSP pollutants	succeeded		18,56	Right, Break at or near load pin, beware of misallignments or twisting	78,3	0	2,7	Low energy failure	Compression curl	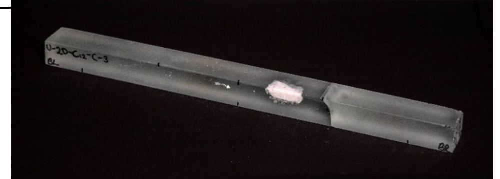
3.9	V-4A-CR8-M-1	4A	1070	Composite beam	Fr 8 mm	Metallic pollutants	succeeded		8,51	Right	39,4	0	8,8	Low energy failure	Compression curl	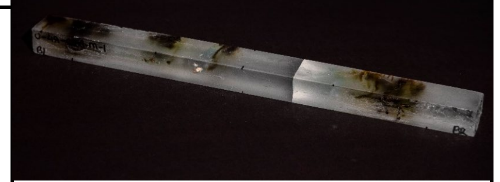
	V-4A-CR8-M-2	4A	1070	Composite beam	Fr 8 mm	Metallic pollutants	failed	Machining								
3.10	V-4A-CR8-M-3	4A	1070	Composite beam	Fr 8 mm	Metallic pollutants	succeeded		14,54	Left	-36,5	0	22,7	Low energy failure	Compression curl	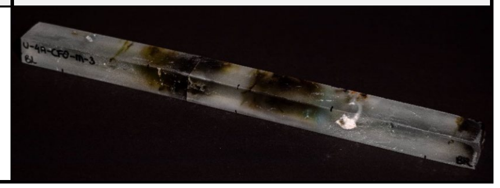

Table 30: Overview beams with failure analysis for Four-point bending test III

APPENDIX F

F - Overview beams with failure analysis - Four point bending test IV

Number	Name beam	Fire round	Forming temperature (°C)	Type	Surface type: Float (Fl), Fritted (Fr)	Bulk type	Status before structural performance test	Reason	Flexural strength (σ) (Mpa)	Location of the failure (left, centre, right)	Fracture origin distance from middle, horizontal (mm) Left = - , Right = +	Fracture origin distance from botom, vertical (mm)	Fracture origin distance from back to front, horizontal (mm)	Type of crack		Photo
														Stress level	Shape	
4.1	V-1D-H-FL-1	1D	1070	Homogeneous beam	Fl 6-8-6 mm	x	succeeded		40,55	Left	-52	0	27,7	High energy failure	Double compression curl	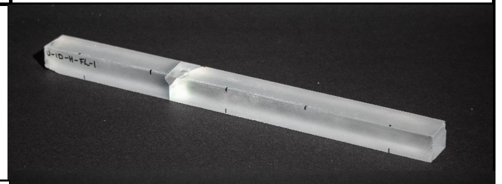
4.2	V-1D-H-FL-2	1D	1070	Homogeneous beam	Fl 12-6 mm	x	succeeded		50,43	Centre	-12	0	0,5	High energy failure	Double compression curl	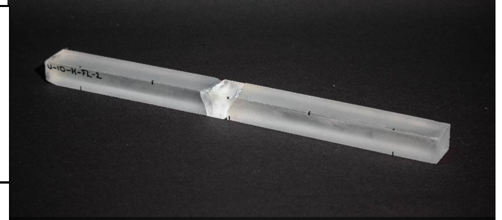
4.3	V-1D-H-FL-3	1D	1070	Homogeneous beam	Fl 6-8-6 mm	x	succeeded		52,15	Left	-37,9	0	26,3	High energy failure	Double compression curl	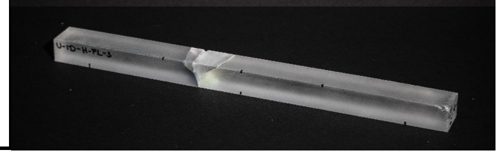

Table 31: Overview beams with failure analysis for Four-point bending test IV

APPENDIX G

G - Overview beams with microscopic analysis - Four point bending test I

Number	Name beam	Fire round	Forming temperature (°C)	Type	Surface type: Float (Fl), Fritted (Fr)	Bulk type	Observed defects	Microscopic photos		
								Close-up bottom view (on the side where the tension was located)	Location of fracture	Close-up fracture
	V-1A-H-HR-1	1A	1120	Homogeneous beam	x	HR glass	Ceramic inclusion			
	V-1A-H-HR-2	1A	1120	Homogeneous beam	x	HR glass	Ceramic inclusion			
	V-1A-H-HR-3	1A	1120	Homogeneous beam	x	HR glass	Ceramic inclusion			
1.1	V-1A-H-C-1	1A	1120	Homogeneous beam	x	CSP pollutants	Silicone inclusion			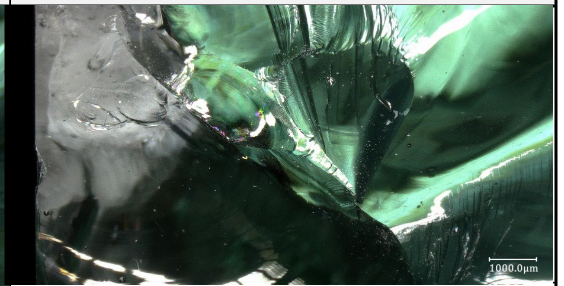
1.2	V-1A-H-C-2	1A	1120	Homogeneous beam	x	CSP pollutants	The fracture is located in the interface between the glass and the silicone			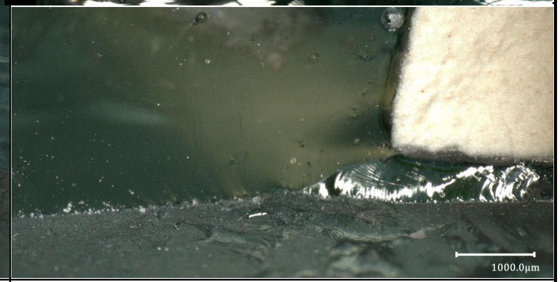
	V-1A-H-C-3	1A	1120	Homogeneous beam	x	CSP pollutants	Ceramic inclusion			
1.3	V-1B-H-F-1	1B	1120	Homogeneous beam	x	Fritted glass	Crystallization	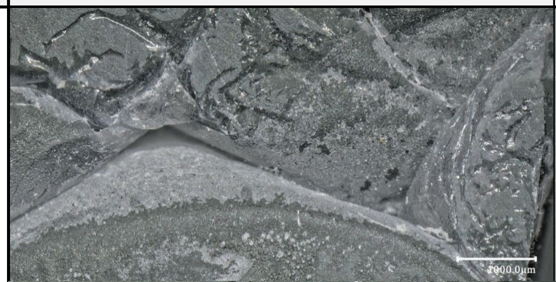		
1.4	V-1B-H-F-2	1B	1120	Homogeneous beam	x	Fritted glass	Crystallization			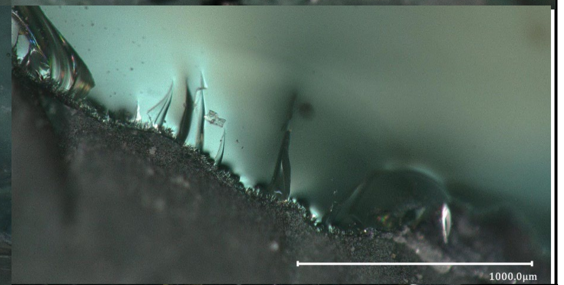
1.5	V-1B-H-F-3	1B	1120	Homogeneous beam	x	Fritted glass	Infolds (small gaps). The cullets did not fuse completely. Debris and mould content is located in the gap. Crytallization is also localised at the fracture	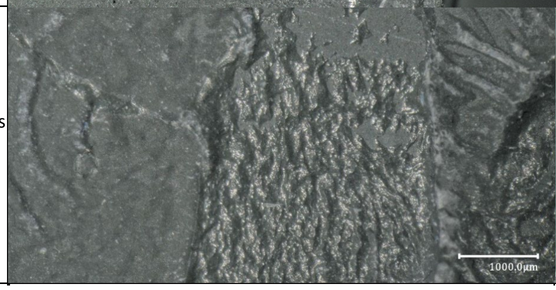	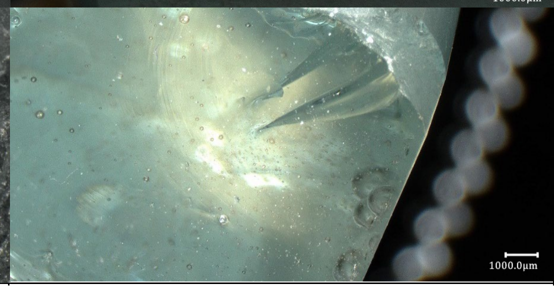	

APPENDIX G

Number	Name beam	Fire round	Forming temperature (°C)	Type	Surface type: Float (Fl), Fritted (Fr)	Bulk type	Observed defects	Microscopic photos		
								Close-up bottom view (on the side where the tension was located)	Location of fracture	Close-up fracture
1.6	V-1B-H-HR-1		1120	Homogeneous beam	x	HR glass	Crystallization	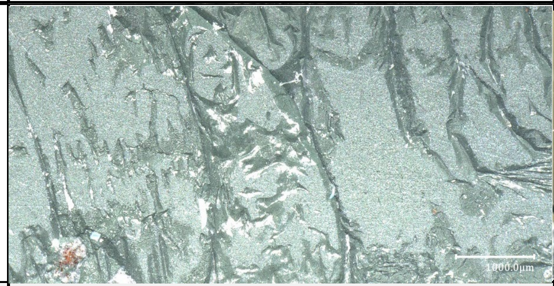	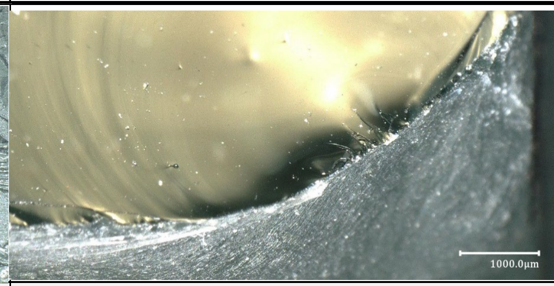	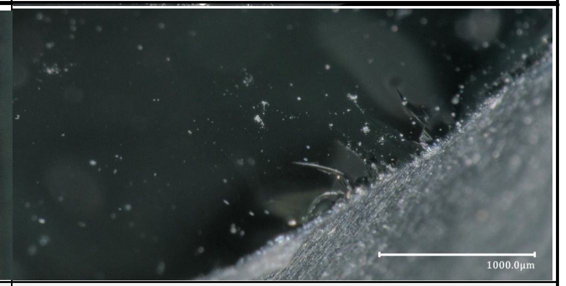
	V-1B-H-S-1	1B	1120	Homogeneous beam	x	SNX 60/26 Soft coating	Silicone inclusion			
1.7	V-1B-H-B-1	1B	1120	Homogeneous beam	x	Blue Solar light Soft coating	Crystallization	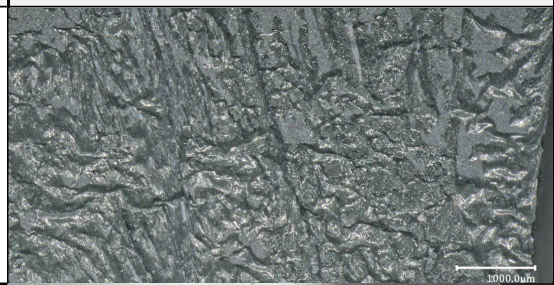	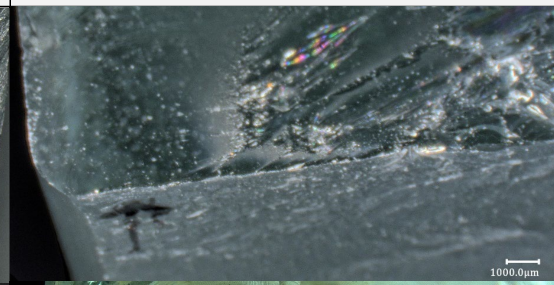	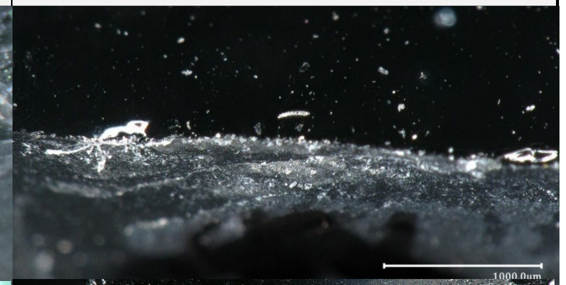
1.8	V-2A-C8-C-1	2A	1070	Composite beam	Fl 8 mm	CSP pollutants	Infolds, small gaps are located athe fracture. A shear mark is shown		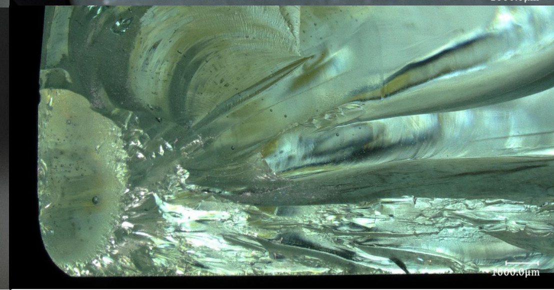	
	V-2A-C8-C-2	2A	1070	Composite beam	Fl 8 mm	CSP pollutants				
	V-2A-C8-C-3	2A	1070	Composite beam	Fl 8 mm	CSP pollutants				
1.9	V-2A-C8-F-1	2A	1070	Composite beam	Fl 8 mm	Fritted glass	Infolds (small gaps). The cullets did not fuse completely. Debris and mould content is located in the gap in the gap		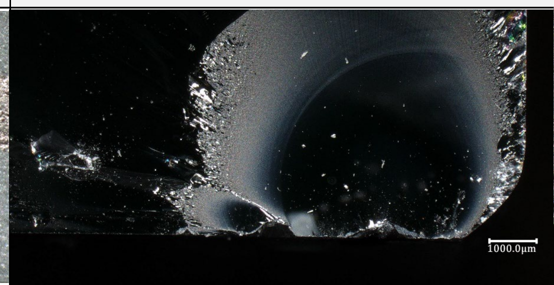	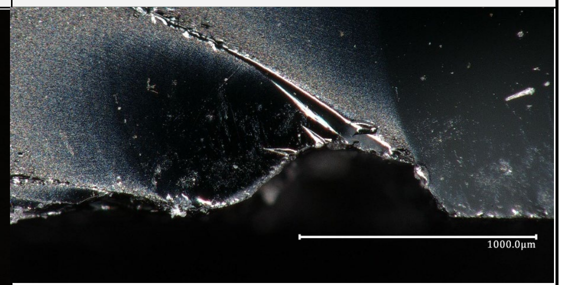
1.10	V-2A-C10-C-1	2A	1070	Composite beam	Fl 10 mm	CSP pollutants	Machining. The surface contains multiple voids	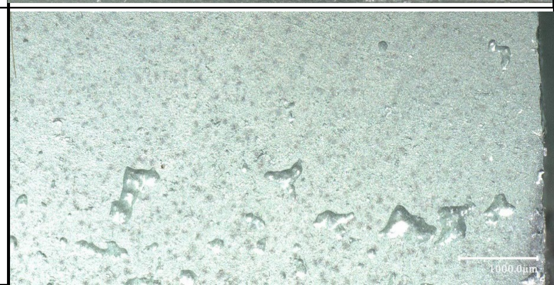		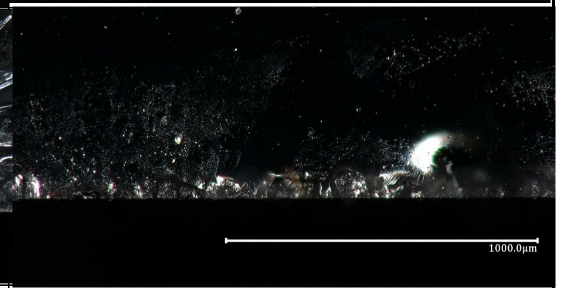
	V-2A-C10-C-2	2A	1070	Composite beam	Fl 10 mm	CSP pollutants				
	V-2A-C10-C-3	2A	1070	Composite beam	Fl 10 mm	CSP pollutants				

APPENDIX G

Number	Name beam	Fire round	Forming temperature (°C)	Type	Surface type: Float (Fl), Fritted (Fr)	Bulk type	Observed defects	Microscopic photos		
								Close-up bottom view (on the side where the tension was located)	Location of fracture	Close-up fracture
1.11	V-2B-C6-C-1	2B	1070	Composite beam	Fl 6 mm	CSP pollutants	Crystallization		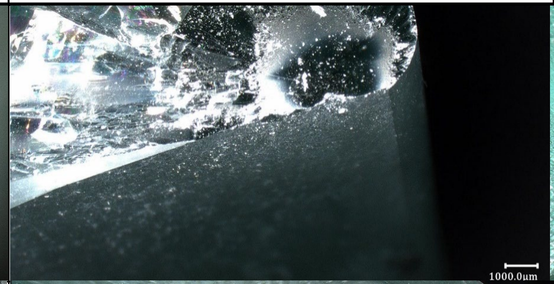	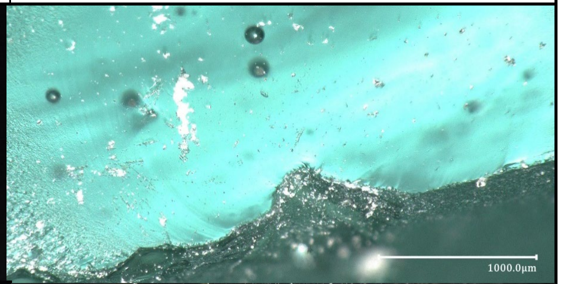
1.12	V-2B-C6-C-2	2B	1070	Composite beam	Fl 6 mm	CSP pollutants	Scratches, Machining (Polishing), Also infolds are visible at the location of the fracture			
1.13	V-2B-C8-C-1	2B	1070	Composite beam	Fl 8 mm	CSP pollutants	Scratches, Machining (Polishing), Also infolds are visible at the location of the fracture	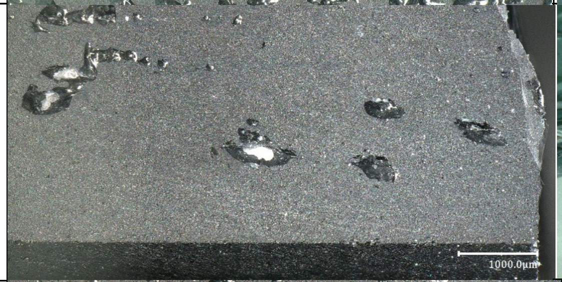		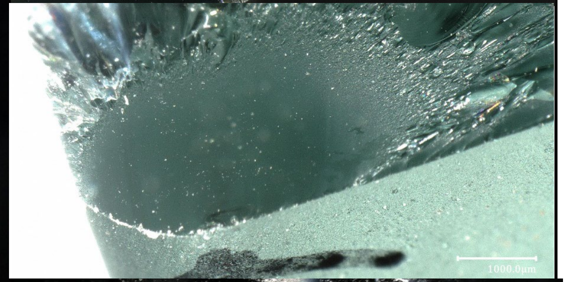
1.14	V-2B-C8-C-2	2B	1070	Composite beam	Fl 8 mm	CSP pollutants	Scratches, Machining (Polishing)		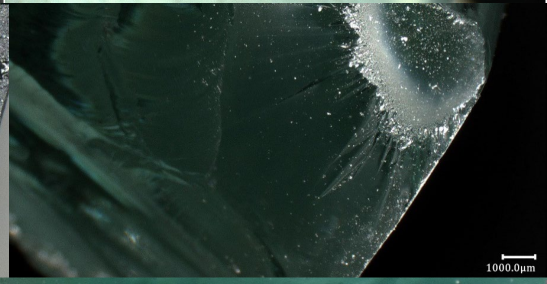	
1.15	V-2B-C10-C-1	2B	1070	Composite beam	Fl 10 mm	CSP pollutants	Scratches, Machining (Polishing)	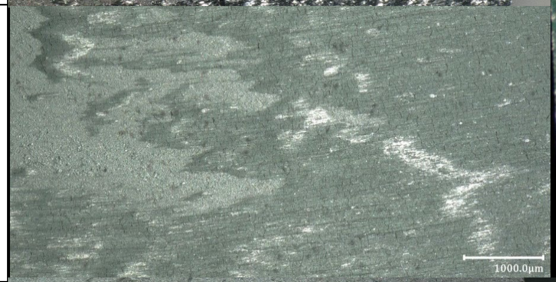		
1.16	V-2B-C10-C-2	2B	1070	Composite beam	Fl 10 mm	CSP pollutants	Machining (Polishing marks)			

Table 32: Overview beams with microscopic analysis for Four-point bending test I

APPENDIX G

G - Overview beams with microscopic analysis - Four point bending test II

Number	Name beam	Fire round	Forming temperature (°C)	Type	Surface type: Float (Fl), Fritted (Fr)	Bulk type	Observed defects	Microscopic photos		
								Close-up bottom view (on the side where the tension was located)	Location of fracture	Close-up fracture
2.1	V-2C-C6-C-1	2C	1070 & 1120	Composite beam	Fl 6 mm	CSP pollutants	Flaw origin starts at the polishing marks. Machining flaw		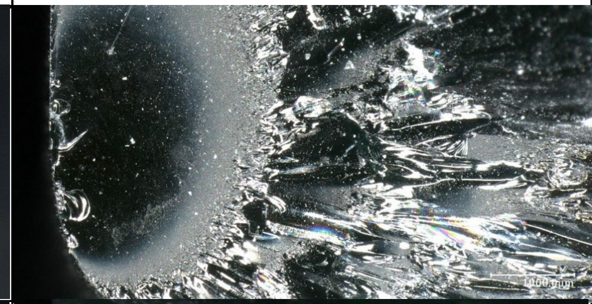	
2.2	V-2C-C6-C-2	2C	1070 & 1120	Composite beam	Fl 6 mm	CSP pollutants	Scratches. Machining flaw.			
	V-2C-C8-C-1	2C	1070 & 1120	Composite beam	Fl 8 mm	CSP pollutants				
2.3	V-2C-C8-C-2	2C	1070 & 1120	Composite beam	Fl 8 mm	CSP pollutants	Scratches. Machining flaw. Infolds	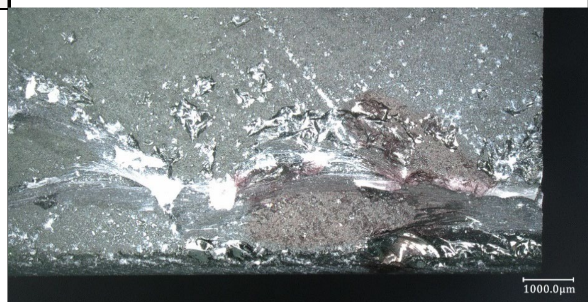	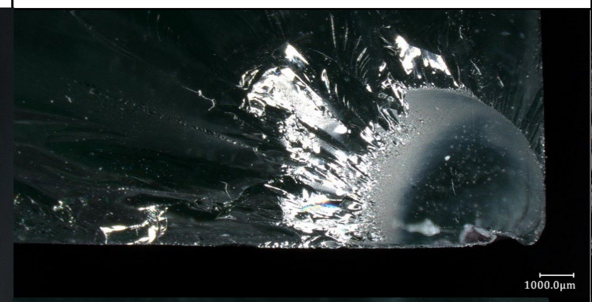	
2.4	V-2C-C10-C-1	2C	1070 & 1120	Composite beam	Fl 10 mm	CSP pollutants	Surface flaws. Crystallizations on the float glass			
2.5	V-2C-C10-C-2	2C	1070 & 1120	Composite beam	Fl 10 mm	CSP pollutants	Surface flaws. Crystallizations on the float glass	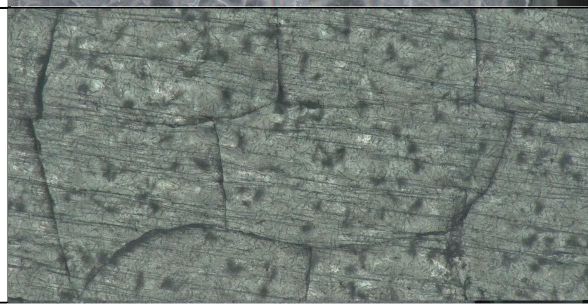	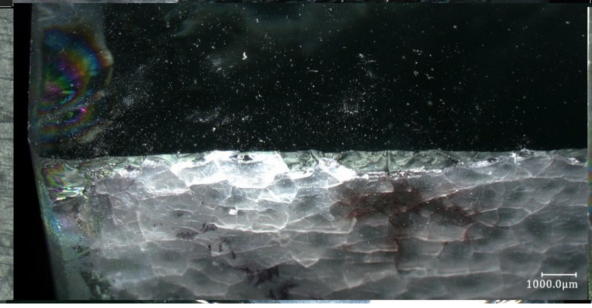	

APPENDIX G

Number	Name beam	Fire round	Forming temperature (°C)	Type	Surface type: Float (Fl), Fritted (Fr)	Bulk type	Observed defects	Microscopic photos		
								Close-up bottom view (on the side where the tension was located)	Location of fracture	Close-up fracture
2.6	V-2C-C12-C-1	2C	1070 & 1120	Composite beam	Fl 12 mm	CSP pollutants	Flaw origin starts at the polishing marks. Machining flaw. Scratches		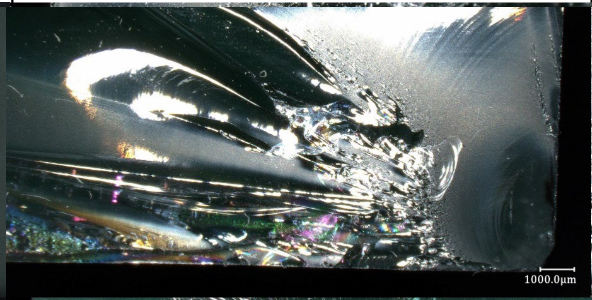	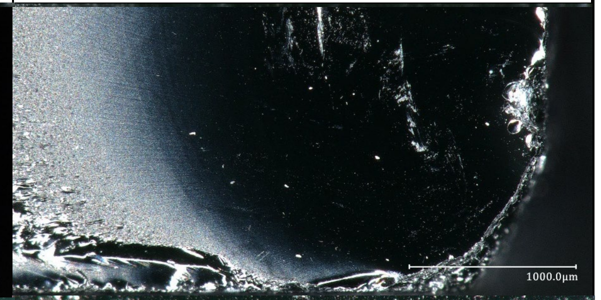
2.7	V-2C-C12-C-2	2C	1070 & 1120	Composite beam	Fl 12 mm	CSP pollutants	Flaw origin starts at the polishing marks. Machining flaw		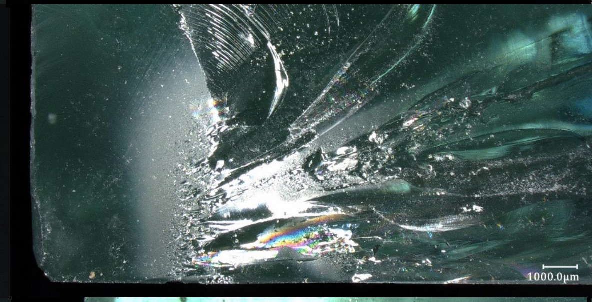	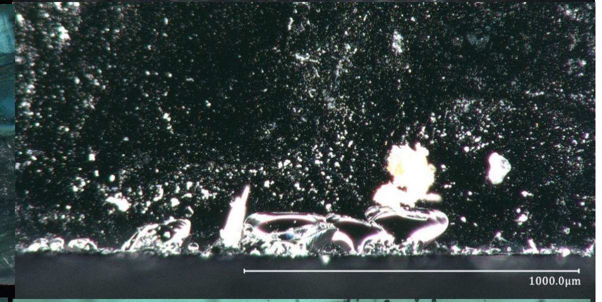
2.8	V-2D-C8-C-1	2D	1070	Composite beam	Fl 8 mm	CSP pollutants	Scratches. Machining flaw. Perpendiculair area is open. Powerful flaw.		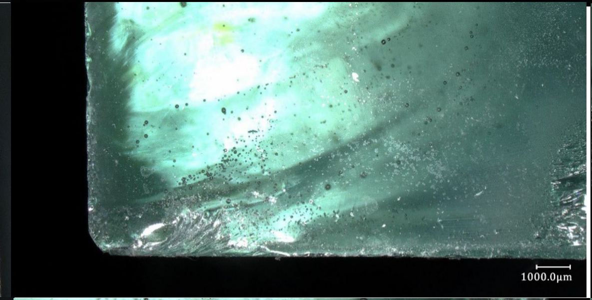	
2.9	V-2D-C10-C-1	2D	1070	Composite beam	Fl 10 mm	CSP pollutants	Flaw origin starts at the polishing marks. Machining flaw. Surface flaw. Perpendiculair area is open. Powerful flaw.	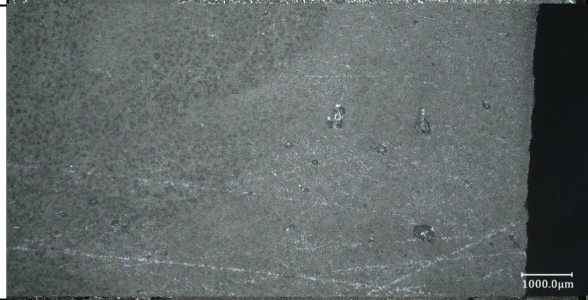		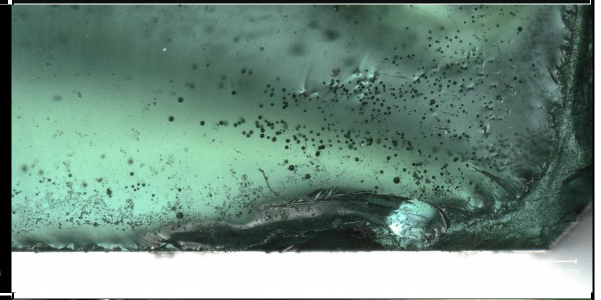
2.10	V-3A-C8-M-1	3A	1070	Composite beam	Fl 8 mm	Metallic pollutants	Flaw origin starts at the polishing marks. Machining flaw		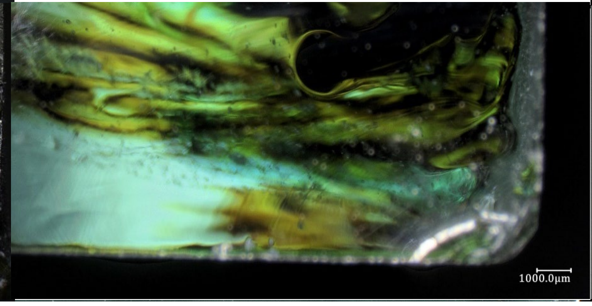	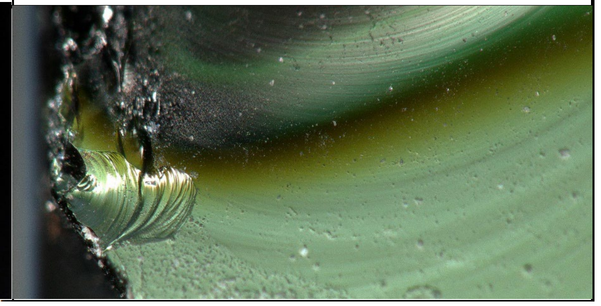

APPENDIX G

Number	Name beam	Fire round	Forming temperature (°C)	Type	Surface type: Float (Fl), Fritted (Fr)	Bulk type	Observed defects	Microscopic photos		
								Close-up bottom view (on the side where the tension was located)	Location of fracture	Close-up fracture
2.11	V-3A-C8-M-2	3A	1070	Composite beam	Fl 8 mm	Metallic pollutants	Infolds			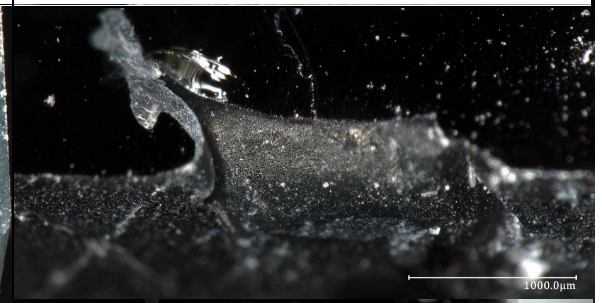
2.12	V-3A-C8-M-3	3A	1070	Composite beam	Fl 8 mm	Metallic pollutants	Flaw origin starts at the polishing marks. Machining flaw			
2.13	V-3A-C10-M-1	3A	1070	Composite beam	Fl 10 mm	Metallic pollutants	Infolds		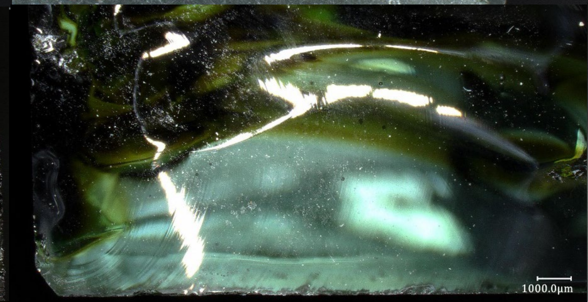	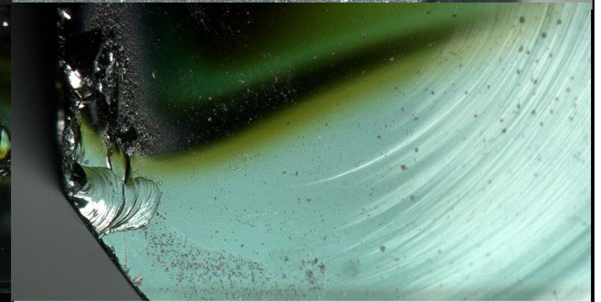
2.14	V-3A-C10-M-2	3A	1070	Composite beam	Fl 10 mm	Metallic pollutants	Cutting flaw. Scratches. Machining		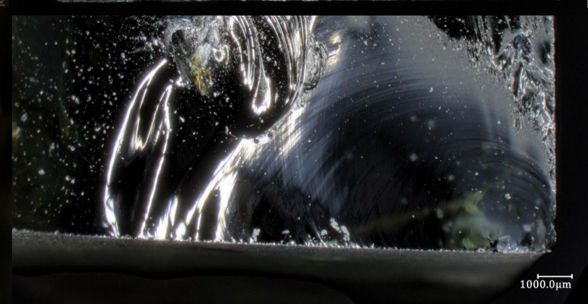	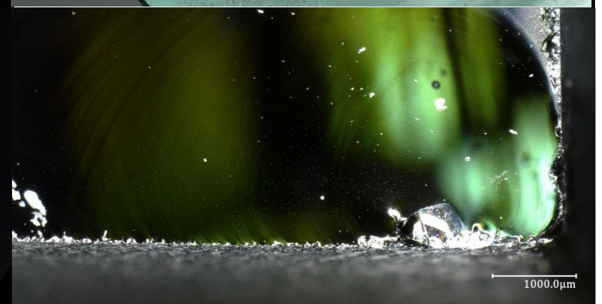
	V-3A-C10-M-3	3A	1070	Composite beam	Fl 10 mm	Metallic pollutants				
	V-4A-CR8-C-1	4A	1070	Composite beam	Fr 8 mm	CSP pollutants				
2.15	V-4A-CR8-C-2	4A	1070	Composite beam	Fr 8 mm	CSP pollutants	Machining. Polishing mark	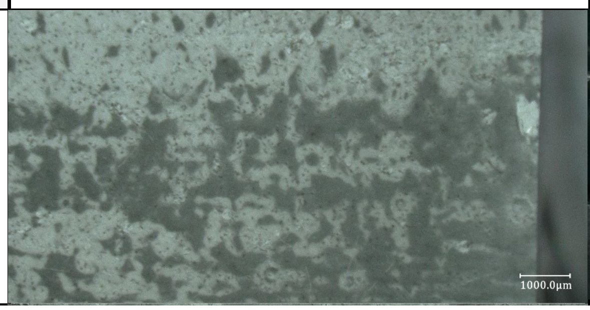	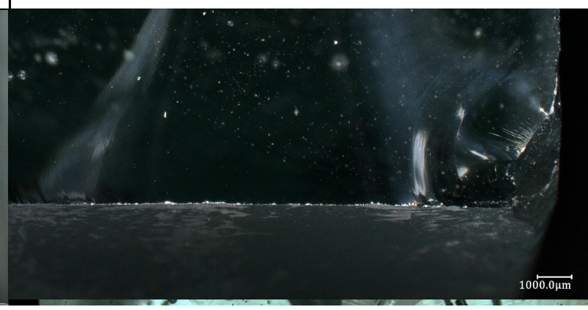	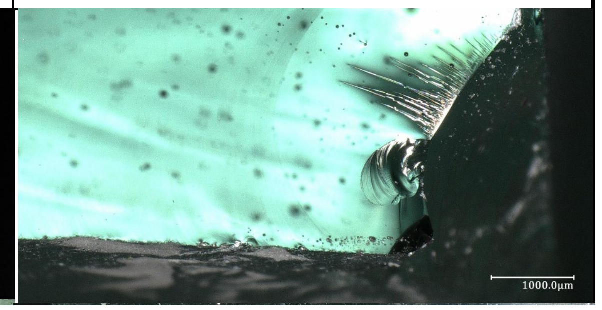

APPENDIX G

Number	Name beam	Fire round	Forming temperature (°C)	Type	Surface type: Float (Fl), Fritted (Fr)	Bulk type	Observed defects	Microscopic photos		
								Close-up bottom view (on the side where the tension was located)	Location of fracture	Close-up fracture
2.16	V-4A-CR8-C-3	4A	1070	Composite beam	Fr 8 mm	CSP pollutants	Machining. Polishing mark	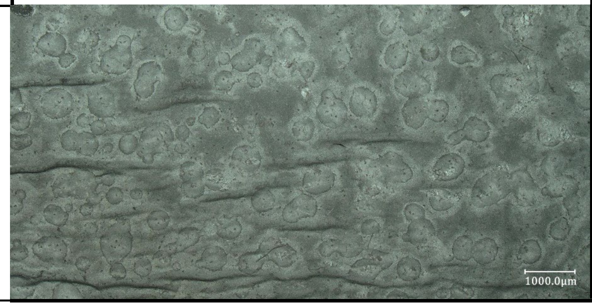	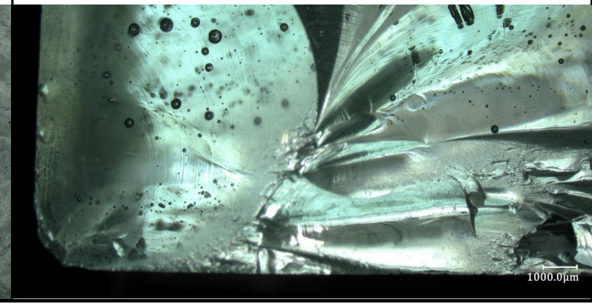	

Table 33: Overview beams with microscopic analysis of Four-point bending test II

G - Overview beams with microscopic analysis - Four point bending test III

Number	Name beam	Fire round	Forming temperature (°C)	Type	Surface type: Float (Fl), Fritted (Fr)	Bulk type	Observed defects	Microscopic photos		
								Close-up bottom view (on the side where the tension was located)	Location of fracture	Close-up fracture
3.1	V-1C-H-M-1	1C	1070	Homogeneous beam	x	Metallic pollutants	Crystallization			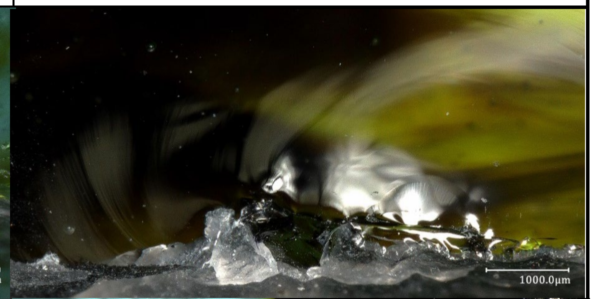
3.2	V-1C-H-M-2	1C	1070	Homogeneous beam	x	Metallic pollutants	Shear marks, cracks are starting to appear on the edge. Seems like infolds but due to machining they increased.		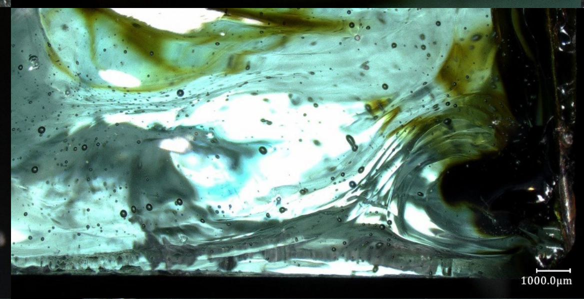	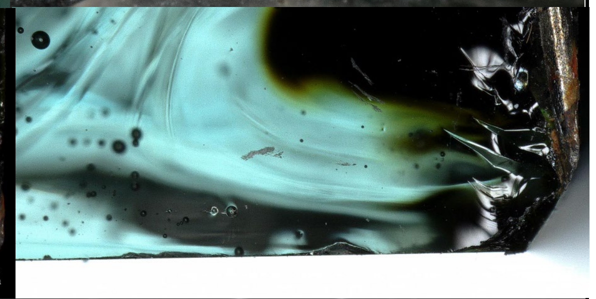
3.3	V-1C-H-M-3	1C	1070	Homogeneous beam	x	Metallic pollutants	Stress inducing. Under the syrface is debris localised. Crystallization			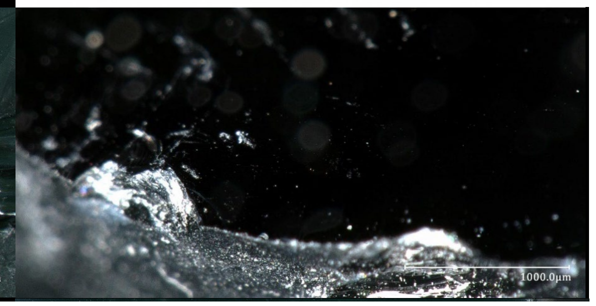

APPENDIX G

Number	Name beam	Fire round	Forming temperature (°C)	Type	Surface type: Float (Fl), Fritted (Fr)	Bulk type	Observed defects	Microscopic photos		
								Close-up bottom view (on the side where the tension was located)	Location of fracture	Close-up fracture
3.4	V-2D-C6-C-1	2D	1070	Composite beam	Fl 6 mm	CSP pollutants	Infolds	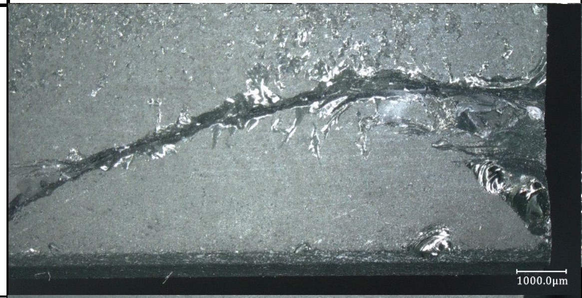	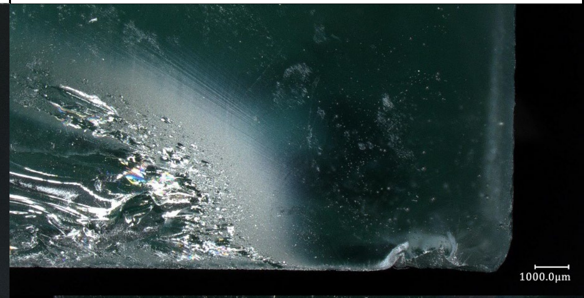	
3.5	V-2D-C8-C-2	2D	1070	Composite beam	Fl 8 mm	CSP pollutants	Machining			
3.6	V-2D-C12-C-1	2D	1070	Composite beam	Fl 12 mm	CSP pollutants	Machining. Scracthes are visible due to polishing	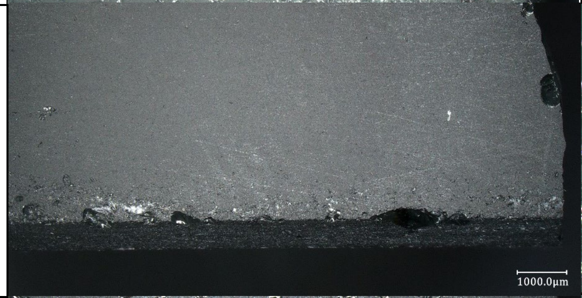		
3.7	V-2D-C12-C-2	2D	1070	Composite beam	Fl 12 mm	CSP pollutants	Machining. Scracthes are visible due to polishing. However infolds are also visible in the fracture started in an infold. Meaning that machining increased this surface flaw	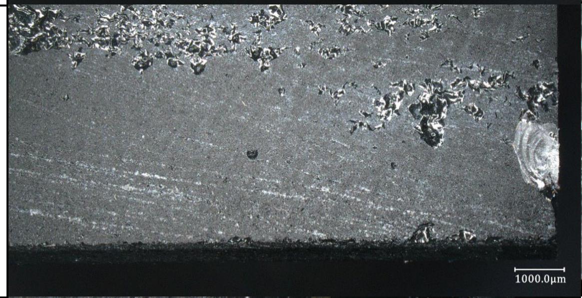	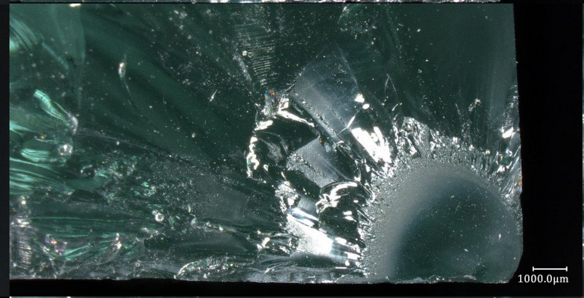	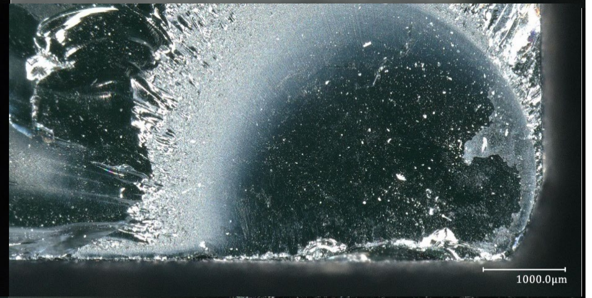
3.8	V-2D-C12-C-3	2D	1070	Composite beam	Fl 12 mm	CSP pollutants	This is a special type of fracture. The fracture started at an edge. Scracthes are visible so this means this is a machining flaw due to edge treatment.		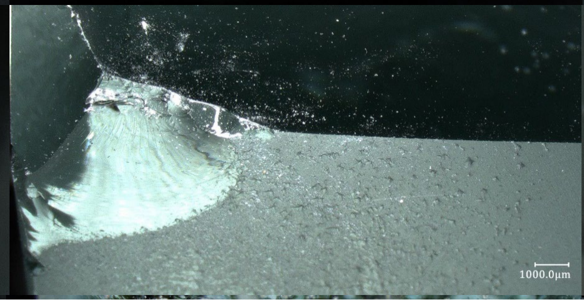	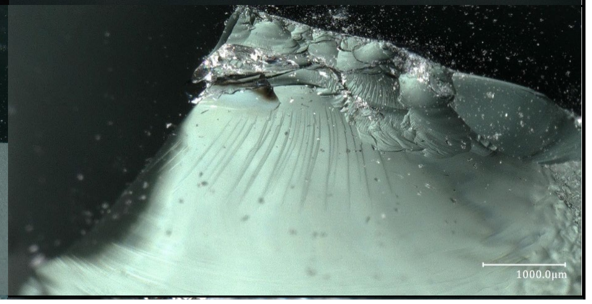

APPENDIX G

Number	Name beam	Fire round	Forming temperature (°C)	Type	Surface type: Float (Fl), Fritted (Fr)	Bulk type	Observed defects	Microscopic photos		
								Close-up bottom view (on the side where the tension was located)	Location of fracture	Close-up fracture
3.9	V-4A-CR8-M-1	4A	1070	Composite beam	Fr 8 mm	Metallic pollutants	Crystallization	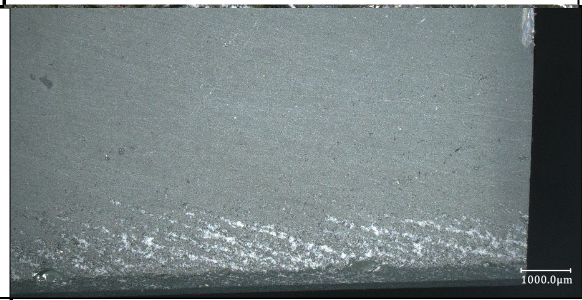		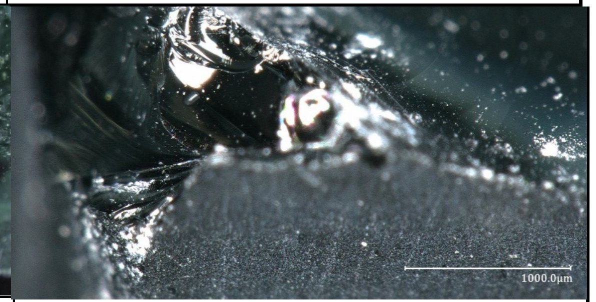
	V-4A-CR8-M-2	4A	1070	Composite beam	Fr 8 mm	Metallic pollutants				
3.10	V-4A-CR8-M-3	4A	1070	Composite beam	Fr 8 mm	Metallic pollutants	Crystallization	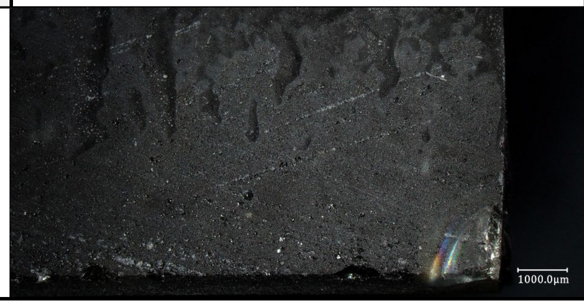	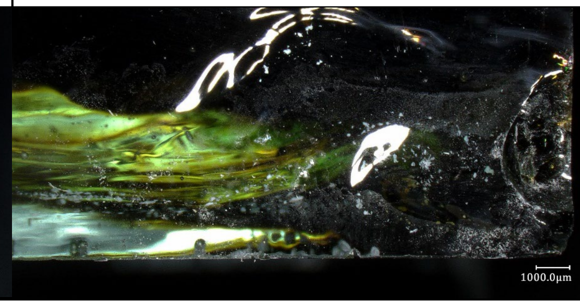	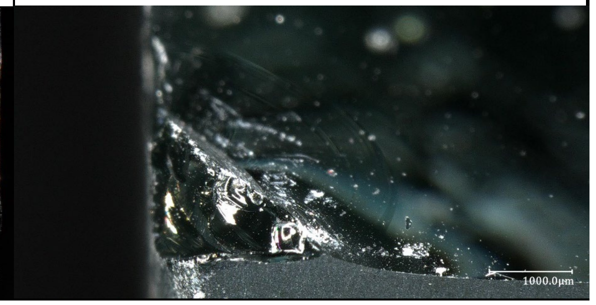

Table 34: Overview beams with microscopic analysis of Four-point bending test III

APPENDIX G

G - Overview beams with microscopic analysis - Four point bending test IV

Number	Name beam	Fire round	Forming temperature (°C)	Type	Surface type: Float (Fl), Fritted (Fr)	Bulk type	Observed defects	Microscopic photos		
								Close-up bottom view (on the side where the tension was located)	Location of fracture	Close-up fracture
4.1	V-1D-H-FL-1	1D	1070	Homogeneous beam	Fl 6-8-6 mm	x	Machining. Scratches are shown (Polishing marks). Furthermore also some crystalization is localised at the edges		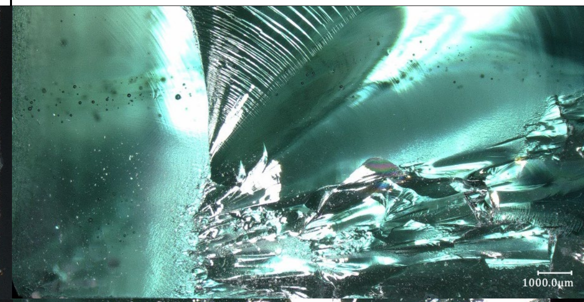	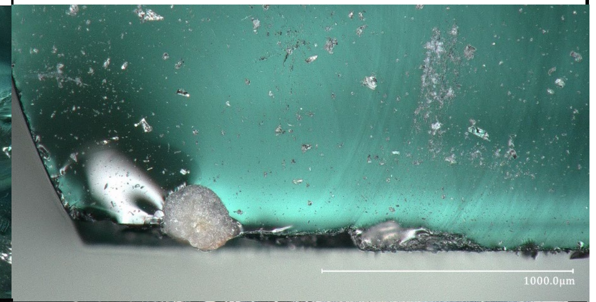
4.2	V-1D-H-FL-2	1D	1070	Homogeneous beam	Fl 12-6 mm	x	Machining. Scratches are shown (Polishing marks). Furthermore also some crystalization is localised at the edges	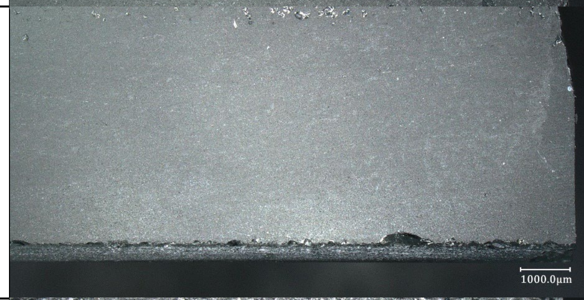	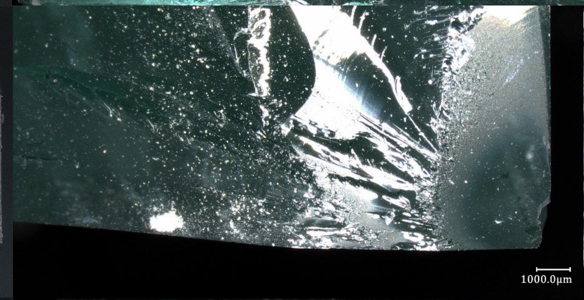	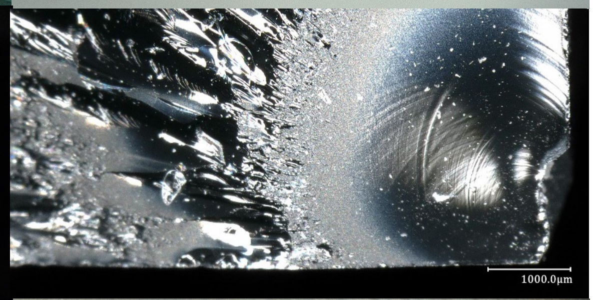
4.3	V-1D-H-FL-3	1D	1070	Homogeneous beam	Fl 6-8-6 mm	x	Infolds, Strength reducing		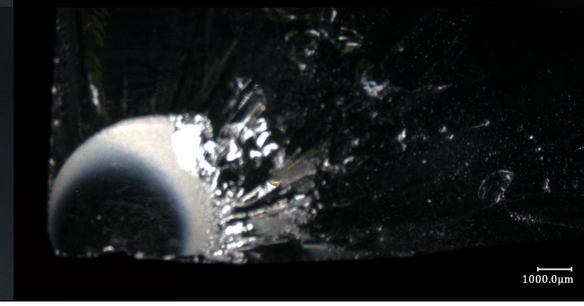	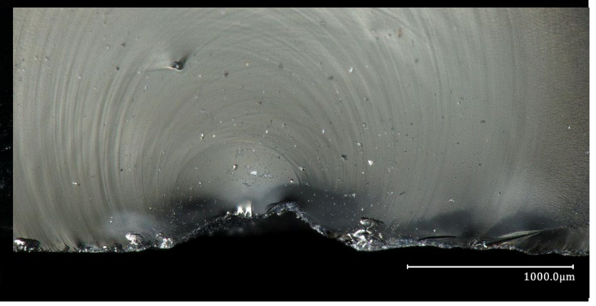

Table 35: Overview beams with microscopic analysis of Four-point bending test IV